APPLICATION OF THE CONTINUOUS *EUR* METHOD TO ESTIMATE RESERVES IN UNCONVENTIONAL GAS RESERVOIRS

A Thesis

by

STEPHANIE MARIE CURRIE

Submitted to the Office of Graduate Studies of
Texas A&M University
in partial fulfillment of the requirements for the degree of

MASTER OF SCIENCE

August 2010

Major Subject: Petroleum Engineering

Application of the Continuous *EUR* Method to Estimate Reserves in Unconventional Gas Reservoirs

APPLICATION OF THE CONTINUOUS *EUR* METHOD TO ESTIMATE RESERVES IN UNCONVENTIONAL GAS RESERVOIRS

A Thesis

by

STEPHANIE MARIE CURRIE

Submitted to the Office of Graduate Studies of
Texas A&M University
in partial fulfillment of the requirements for the degree of

MASTER OF SCIENCE

Approved by:

Chair of Committee,	Thomas A. Blasingame
Committee Members,	Maria A. Barrufet
	Walter B. Ayers, Jr.
Head of Department,	Stephen A. Holditch

August 2010

Major Subject: Petroleum Engineering

ABSTRACT

Application of the Continuous *EUR* Method to Estimate Reserves in Unconventional Gas Reservoirs.

(August 2010)

Stephanie Marie Currie

B.S., Texas A&M University

Chair of Advisory Committee: Dr. Thomas A. Blasingame

Reserves estimation in unconventional (low/ultra-low permeability) reservoirs has become a topic of increased interest as more of these resources are being developed, especially in North America. The estimation of reserves in unconventional reservoirs is challenging due to the long transient flow period exhibited by the production data. The use of conventional methods (*i.e.*, Arps' decline curves) to estimate reserves is often times inaccurate and leads to the overestimation of reserves because these models are only (theoretically) applicable for the boundary-dominated flow regime. The premise of this work is to present and demonstrate a methodology which continuously estimates the ultimate recovery during the producing life of a well in order to generate a time-dependent profile of the estimated ultimate recovery (*EUR*). The "objective" is to estimate the final *EUR* value(s) from several complimentary analyses.

In this work, we present the "Continuous *EUR* Method" to estimate reserves for unconventional gas reservoirs using a rate-time analysis approach. This work offers a coherent process to reduce the uncertainty in reserves estimation for unconventional gas reservoirs by quantifying "upper" and "lower" limits of *EUR* prior to the onset of boundary-dominated flow. We propose the use of traditional and new rate-time relations to establish the "upper" limit for *EUR*. We clearly demonstrate that rate-time relations which better represent the transient and transitional flow regimes (in particular the power law exponential rate decline relation) often lead to a more accurate "upper" limit for reserves estimates — earlier in the producing life of a well (as compared to conventional ("Arps") relations). Furthermore, we propose a straight line extrapolation technique to offer a conservative estimate of maximum produced gas which we use as the "lower" limit for *EUR*. The *EUR* values estimated using this technique continually increase with time, eventually reaching a maximum value.

We successfully demonstrate the methodology by applying the approach to 43 field examples producing from 7 different tight sandstone and shale gas reservoirs. We show that the difference between the "upper" and "lower" limit of reserves decreases with time and converges to the "true" value of reserves during the latter producing life of a well.

DEDICATION

This work is dedicated to my family and friends.

I also dedicate this work to Texas A&M University;
a place where I have met many lifelong friends and people that have an inspired me and will continue to inspire me for many years to come,
a place that has offered me so many great experiences and that has opened to door to many life changing opportunities,
and a place where I have experienced a spirit that can ne'er be told.

ACKNOWLEDGEMENTS

I would like to specifically thank the following people for their help during my graduate studies: Tom Blasingame, chair of my committee, for his unyielding demand for perfection and for his tough love; Dilhan Ilk, for being a great mentor and for his constant willingness to help; Dr. Ayers and Dr. Barrufet, for their support and service as committee members.

TABLE OF CONTENTS

Page

ABSTRACT iii

DEDICATION iv

ACKNOWLEDGEMENTS v

TABLE OF CONTENTS vi

LIST OF FIGURES viii

LIST OF TABLES xiii

CHAPTER

I INTRODUCTION 1

1.1 Statement of Problem 1
1.2 Objectives 2
1.3 Validation and Application 2

II LITERATURE REVIEW — PRODUCTION DATA ANALYSIS 10

2.1 Empirical, Semi-Analytical, and Analytical Production Data Analysis 12
2.2 Decline Type Curve Analysis 13
2.3 Diagnostic Methods 14

III DEVELOPMENT OF THE CONTINOUS *EUR* METHOD 16

3.1 Data Editing and Interval Selection 16
3.2 Rate-Time Analysis 16
3.3 Straight Line Extrapolation Technique 16
3.4 Continuous *EUR* Plots 20

IV APPLICATION OF THE METHOD TO FIELD EXAMPLES 21

4.1 Field Example 1: East Tx Tight Gas Well (SPE 84287) 21
4.2 Field Example 2: Tight Gas Well (Holly Branch Field) 28
4.3 Field Example 3: Shale Gas Well (Field A) 37
4.4 Field Example 4: Shale Gas Well (Field B) 46
4.5 Field Example 5: Shale Gas Well (Field C) 55
4.6 Field Example 6: Shale Gas Well (Field D) 64

V SUMMARY, CONCLUSIONS, AND RECOMMENDATIONS FOR FUTURE WORK 73

5.1 Summary 73
5.2 Conclusions 73
5.3 Recommendations for Future Work 74

NOMENCLATURE 75

Page

REFERENCES 76
APPENDIX A ARPS' HYPERBOLIC RATE DECLINE RELATION 81
APPENDIX B POWER LAW EXPONENTIAL RATE DECLINE RELATION 82
APPENDIX C EXAMPLES FROM HOLLY BRANCH FIELD 83
APPENDIX D EXAMPLES FROM FIELD A 133
APPENDIX E EXAMPLES FROM FIELD B 183
APPENDIX F EXAMPLES FROM FIELD C 223
APPENDIX G EXAMPLES FROM FIELD D 253
APPENDIX H EXAMPLE FROM FIELD E 263
VITA 268

LIST OF FIGURES

FIGURE Page

1.1 (Semi-log Plot): Production history plot for numerical simulation case — flow rate (q_g) and cumulative production (G_p) versus production time 3

1.2 (Log-log Plot): *qDb* plot — flow rate (q_g), *D*- and *b*-parameters versus production time and "hyperbolic" model matches for numerical simulation case 4

1.3 (Cartesian Plot): Hyperbolic *b*-parameter values obtained from model matches with production data for numerical simulation case 5

1.4 (Log-log Plot): *qDb* plot — flow rate (q_g), *D*- and *b*-parameters versus production time and power law exponential model matches for numerical simulation case 6

1.5 (Cartesian Plot): Rate Cumulative Plot — flow rate (q_g) versus cumulative production (G_p) and the linear trends fit through the data for numerical simulation case 7

1.6 (Cartesian Plot): *EUR* estimates from model matches and $G_{p,max}$ estimates from extrapolation technique for numerical simulation case 8

3.1 First step of the continuous *EUR* method: Data is reviewed and edited, and intervals are selected for individual analysis 17

3.2 Second step of the continuous *EUR* method: All previously specified intervals are evaluated and *EUR* values are obtained using the rate-time decline relations and a $G_{p,max}$ estimate is obtained using the straight line extrapolation technique 18

3.3 Final step of the continuous *EUR* method: All *EUR* and $G_{p,max}$ values are plotted versus time, and "upper" and "lower" limits for *EUR* are established. 19

4.1 (Semi-log Plot): Production history plot for field example 1 — flow rate (q_g) and cumulative production (G_p) versus production time 21

4.2 (Log-log Plot): *qDb* plot — flow rate (q_g), *D*- and *b*-parameters versus production time and "hyperbolic" model matches for field example 1 22

FIGURE Page

4.3 (Cartesian Plot): Hyperbolic *b*-parameter values obtained from model matches with production data for field example 1 23

4.4 (Log-log Plot): *qDb* plot — flow rate (q_g), *D*- and *b*-parameters versus production time and power law exponential model matches for field example 1 24

4.5 (Cartesian Plot): Rate Cumulative Plot — flow rate (q_g) versus cumulative production (G_p) and the linear trends fit through the data for field example 1 25

4.6 (Cartesian Plot): *EUR* estimates from model matches and $G_{p,max}$ estimates from extrapolation technique for field example 1 26

4.7 (Semi-log Plot): Production history plot for field example 2 — flow rate (q_g) and cumulative production (G_p) versus production time 28

4.8 (Log-log Plot): *qDb* plot — flow rate (q_g), *D*- and *b*-parameters versus production time and "hyperbolic" model matches for field example 2 29

4.9 (Cartesian Plot): Hyperbolic *b*-parameter values obtained from model matches with production data for field example 2 30

4.10 (Log-log Plot): *qDb* plot — flow rate (q_g), *D*- and *b*-parameters versus production time and power law exponential model matches for field example 2 31

4.11 (Cartesian Plot): Rate Cumulative Plot — flow rate (q_g) versus cumulative production (G_p) and the linear trends fit through the data for field example 2 32

4.12 (Cartesian Plot): *EUR* estimates from model matches and $G_{p,max}$ estimates from extrapolation technique for field example 2 33

4.13 (Cartesian Plot): Comparison of the hyperbolic *EUR* estimates for the tight gas wells producing from the Holly Branch field 35

4.14 (Cartesian Plot): Comparison of the power law exponential *EUR* estimates for the tight gas wells producing from the Holly Branch field 36

4.15 (Cartesian Plot): Comparison of the hyperbolic *b*-parameter for the tight gas wells producing from the Holly Branch field 36

FIGURE Page

4.16 (Semi-log Plot): Production history plot for field example 3 — flow rate (q_g) and cumulative production (G_p) versus production time 37

4.17 (Log-log Plot): *qDb* plot — flow rate (q_g), *D*- and *b*-parameters versus production time and "hyperbolic" model matches for field example 3 38

4.18 (Cartesian Plot): Hyperbolic *b*-parameter values obtained from model matches with production data for field example 3 39

4.19 (Log-log Plot): *qDb* plot — flow rate (q_g), *D*- and *b*-parameters versus production time and power law exponential model matches for field example 3 40

4.20 (Cartesian Plot): Rate Cumulative Plot — flow rate (q_g) versus cumulative production (G_p) and the linear trends fit through the data for field example 3 41

4.21 (Cartesian Plot): *EUR* estimates from model matches and $G_{p,max}$ estimates from extrapolation technique for field example 3 42

4.22 (Cartesian Plot): Comparison of the hyperbolic *EUR* estimates for the shale gas wells producing from field A 44

4.23 (Cartesian Plot): Comparison of the power law exponential *EUR* estimates for the shale gas wells producing from field A 45

4.24 (Cartesian Plot): Comparison of the hyperbolic *b*-parameter for the shale gas wells producing from field A 45

4.25 (Semi-log Plot): Production history plot for field example 4 — flow rate (q_g) and cumulative production (G_p) versus production time 46

4.26 (Log-log Plot): *qDb* plot — flow rate (q_g), *D*- and *b*-parameters versus production time and "hyperbolic" model matches for field example 4 47

4.27 (Cartesian Plot): Hyperbolic *b*-parameter values obtained from model matches with production data for field example 4 48

4.28 (Log-log Plot): *qDb* plot — flow rate (q_g), *D*- and *b*-parameters versus production time and power law exponential model matches for field example 4 49

FIGURE Page

4.29 (Cartesian Plot): Rate Cumulative Plot — flow rate (q_g) versus cumulative production (G_p) and the linear trends fit through the data for field example 4 50

4.30 (Cartesian Plot): *EUR* estimates from model matches and $G_{p,max}$ estimates from extrapolation technique for field example 4..... 51

4.31 (Cartesian Plot): Comparison of the hyperbolic *EUR* estimates for the shale gas wells producing from field B..... 53

4.32 (Cartesian Plot): Comparison of the power law exponential *EUR* estimates for the shale gas wells producing from field B..... 53

4.33 (Cartesian Plot): Comparison of the hyperbolic *b*-parameter for the shale gas wells producing from field B..... 54

4.34 (Semi-log Plot): Production history plot for field example 5 — flow rate (q_g) and cumulative production (G_p) versus production time 55

4.35 (Log-log Plot): *qDb* plot — flow rate (q_g), *D*- and *b*-parameters versus production time and "hyperbolic" model matches for field example 5 56

4.36 (Cartesian Plot): Hyperbolic *b*-parameter values obtained from model matches with production data for field example 5 57

4.37 (Log-log Plot): *qDb* plot — flow rate (q_g), *D*- and *b*-parameters versus production time and power law exponential model matches for field example 5 58

4.38 (Cartesian Plot): Rate Cumulative Plot — flow rate (q_g) versus cumulative production (G_p) and the linear trends fit through the data for field example 5 59

4.39 (Cartesian Plot): *EUR* estimates from model matches and $G_{p,max}$ estimates from extrapolation technique for field example 5..... 60

4.40 (Cartesian Plot): Comparison of the hyperbolic *EUR* estimates for the shale gas wells producing from field C..... 62

4.41 (Cartesian Plot): Comparison of the power law exponential *EUR* estimates for the shale gas wells producing from field C..... 62

FIGURE Page

4.42 (Cartesian Plot): Comparison of the hyperbolic *b*-parameter for the shale gas wells producing from field C 63

4.43 (Semi-log Plot): Production history plot for field example 6 — flow rate (q_g) and cumulative production (G_p) versus production time 64

4.44 (Log-log Plot): *qDb* plot — flow rate (q_g), *D*- and *b*-parameters versus production time and "hyperbolic" model matches for field example 6 65

4.45 (Cartesian Plot): Hyperbolic *b*-parameter values obtained from model matches with production data for field example 6 66

4.46 (Log-log Plot): *qDb* plot — flow rate (q_g), *D*- and *b*-parameters versus production time and power law exponential model matches for field example 6 67

4.47 (Cartesian Plot): Rate Cumulative Plot — flow rate (q_g) versus cumulative production (G_p) and the linear trends fit through the data for field example 6 68

4.48 (Cartesian Plot): *EUR* estimates from model matches and $G_{p,max}$ estimates from extrapolation technique for field example 6 69

4.49 (Cartesian Plot): Comparison of the hyperbolic *EUR* estimates for the shale gas wells producing from field D 71

4.50 (Cartesian Plot): Comparison of the power law exponential *EUR* estimates for the shale gas wells producing from field D 71

4.51 (Cartesian Plot): Comparison of the hyperbolic *b*-parameter for the shale gas wells producing from field D 72

LIST OF TABLES

TABLE		Page
1.1	Reservoir and fluid properties for numerical simulation case (single layer tight gas well with hydraulic fracture)	3
1.2	Analysis results for numerical simulation case — "hyperbolic" model parameters	8
1.3	Analysis results for numerical simulation case — power law exponential model parameters.	9
1.4	Analysis results for numerical simulation case — straight line extrapolation.	9
2.1	Categorization of production data analysis literature used for this work	10
2.2	Arps' rate-time and cumulative-time relations for production data analysis	14
4.1	Analysis results for field example 1 — "hyperbolic" model parameters	26
4.2	Analysis results for field example 1 — power law exponential model parameters.	27
4.3	Analysis results for field example 1 — straight line extrapolation.	27
4.4	Analysis results for field example 2 — "hyperbolic" model parameters	33
4.5	Analysis results for field example 2 — power law exponential model parameters.	34
4.6	Analysis results for field example 2 — straight line extrapolation.	34
4.7	Analysis results for field examples from the Holly Branch field	34
4.8	Analysis results for field example 3 — "hyperbolic" model parameters	42
4.9	Analysis results for field example 3 — power law exponential model parameters.	43
4.10	Analysis results for field example 3 — straight line extrapolation.	43
4.11	Analysis results for field examples from field A	44
4.12	Analysis results for field example 4 — "hyperbolic" model parameters	51
4.13	Analysis results for field example 4 — power law exponential model parameters.	52

TABLE Page

4.14 Analysis results for field example 4 — straight line extrapolation. 52

4.15 Analysis results for field examples from field B..... 52

4.16 Analysis results for field example 5 — "hyperbolic" model parameters 60

4.17 Analysis results for field example 5 — power law exponential model parameters. 61

4.18 Analysis results for field example 5 — straight line extrapolation. 61

4.19 Analysis results for field examples from field C..... 61

4.20 Analysis results for field example 6 — "hyperbolic" model parameters 69

4.21 Analysis results for field example 6 — power law exponential model parameters. 70

4.22 Analysis results for field example 6 — straight line extrapolation. 70

4.23 Analysis results for field examples from field D 70

CHAPTER I
INTRODUCTION

1.1 Statement of the Problem

Unconventional gas reservoirs, in particular tight sandstone and shale gas, exhibit extended periods of transient flow due to the low permeability nature of the reservoir rock. Conventional reserves estimation relations (*i.e.* Arps' decline curves) are only (theoretically) applicable for boundary-dominated flow. Rushing et al. (2007) showed and we also show in this work that the analysis of production data (particularly rate-time data) before the onset of boundary-dominated flow for unconventional gas reservoirs will often lead to significant overestimation of reserves. This issue is problematic for oil and gas operators producing from these unconventional gas reservoirs as they rely on accurate reserves estimates for field development and business planning.

We present the "Continuous *EUR* Method" as a consistent approach to reserves estimation for unconventional gas reservoirs. We developed this method to identify the error in estimating reserves at early times, especially prior to the onset of boundary-dominated flow. From this approach we are able to establish limits for *EUR* and quantify the change in these estimates as a function of time. We start by specifying intervals of the production data (*i.e.* flow rate versus time). We analyze each interval starting from the beginning of the production history (*i.e.* t = 0 days) using simple rate-time relations. Each interval of the data is matched with rate-time relations and an *EUR* value is obtained by extrapolating the relations to a specified time limit or an abandonment rate. Finally, the *EUR* values are plotted as a function of time. We observe that these estimates decrease with time and often stabilize prior to the onset of boundary-dominated flow.

For this work we demonstrate the "Continuous *EUR* Method" using the following rate-time relations:

- $q_g(t) = \dfrac{q_{gi}}{[1+bD_it]^{1/b}}$ ..... Arps' Hyperbolic Rate Decline Relation (Arps, 1945)
- $q_g(t) = \hat{q}_i \exp[-D_\infty t - \hat{D}_i t^n]$ ..... Power Law Exponential Rate Decline Relation (Ilk et al., 2008a)

Additional information about each relation is included in **Appendices A and B**.

This thesis follows the style and format of *SPE Journal*.

We show that the power law exponential rate decline relation is applicable in modeling the transient and transition flow regimes unlike the "hyperbolic" relation. The reserves estimates produced by the power law exponential relation are consistently more conservative and converge to a more accurate estimate of reserves earlier in the production history than the estimates given by the "hyperbolic" relation. At early times during transient and transition flow, the *EUR* values obtained by the power law exponential relation can be used as an "upper" limit for *EUR* for the particular well.

In addition we use a simple extrapolation technique to estimate a "lower" limit for *EUR*. We plot gas flow rate versus cumulative gas production for an individual well on a Cartesian scale and fit a straight line through the end part of the data for each interval of data previously specified. The *x*-axis intercept of the line yields an estimate for $G_{p,max}$. This method is commonly used to estimate oil-in-place for oil wells exhibiting boundary-dominated flow and is equivalent to forecasting production with an exponential decline. We found that applying this technique to analyze gas production yields a conservative estimate for $G_{p,max}$ and therefore a "lower" limit estimate for *EUR*. We observe that the $G_{p,max}$ estimates increase with time. The *EUR* values obtained from the extrapolation of the rate-time relations and the straight line extrapolation technique are plotted together as a function of time and provide a range for where the true *EUR* value should lie.

1.2 Objectives

The objectives of this work are to:

- *Compare* the applicability of simple rate-time relations as reserves estimation models for unconventional gas reservoirs.
- *Propose* the "Continuous *EUR* Method" as a coherent approach to reserves estimation.
- *Demonstrate* the applicability of the "Continuous *EUR* Method" by applying the approach to numerically simulated and field datasets from unconventional gas reservoirs.
- *Recommend* some best practices for the estimation of reserves for unconventional gas reservoirs.

1.3 Validation and Application

In this section we demonstrate our proposed "Continuous *EUR* Method" by applying the approach to a numerical simulation case.

Numerical Simulation Case: *East Tx Tight Gas Well* (*SPE* 84287)

In this case we consider a well model including a vertical fracture with finite conductivity producing from a tight gas reservoir. The model parameters including reservoir and fluid properties were obtained from the work by Pratikno et al. (2003) and are provided in **Table 1.1**. The synthetic flow rate data was generated using a numerical simulator by Ilk et al. (2008a). The flow rate data and cumulative production data which spans almost 6 years are presented in **Fig. 1.1**.

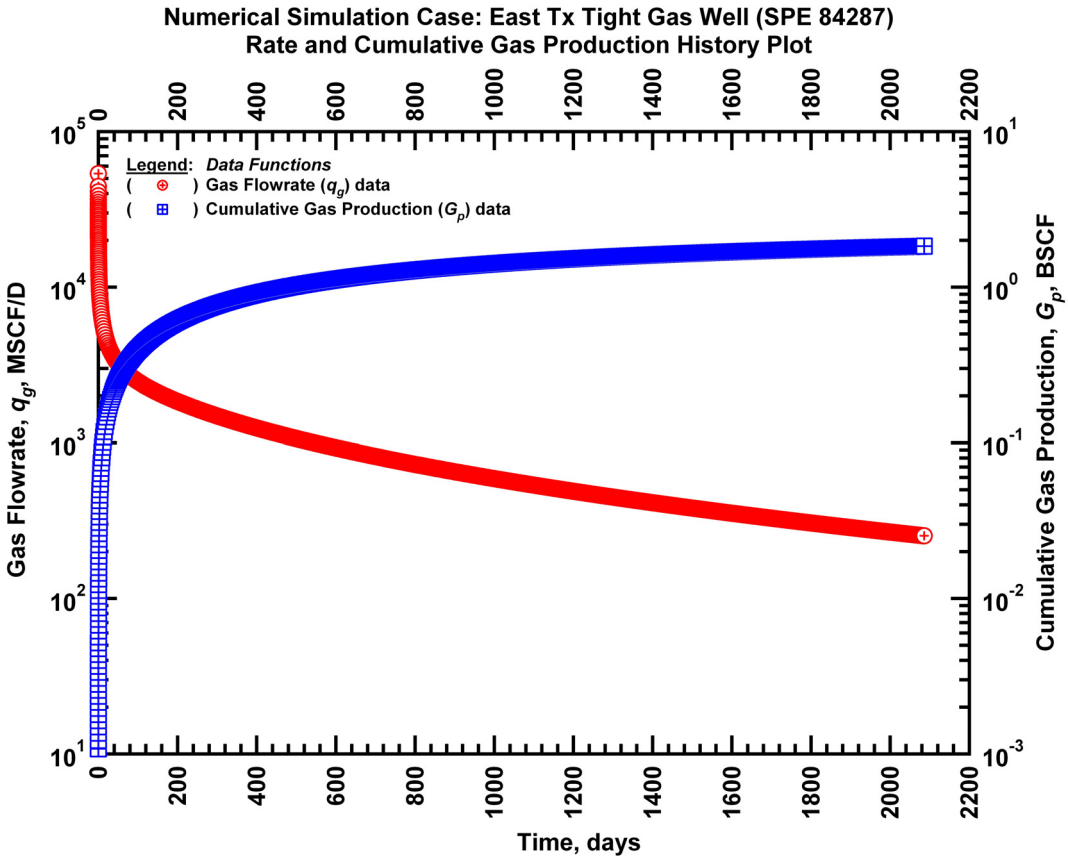

Figure 1.1 — (Semi-log Plot): Production history plot for numerical simulation case — flow rate (q_g) and cumulative production (G_p) versus production time. Tight gas well with a vertical hydraulic fracture (Ilk et al., 2008a).

Table 1.1 — Reservoir and fluid properties for numerical simulation case (single layer tight gas well with hydraulic fracture).

Reservoir Properties:		
Wellbore Radius, r_w	=	0.333 ft
Estimated net pay thickness, h	=	170 ft
Average porosity, ϕ	=	0.088 (fraction)
Average irreducible water saturation, S_{wirr}	=	0.131 (fraction)
Permeability, k	=	0.005 md
Fluid Properties:		
Gas formation volume factor at p_i, B_{gi}	=	0.5498 RB/MSCF
Gas viscosity at p_i, μ_{gi}	=	0.0361 cp
Gas compressibility at p_i, c_{gi}	=	5.1032×10^{-5} psi^{-1}
Production Parameters:		
Initial reservoir pressure, p_i	=	9,330 psia
Gas Produced at 30 years, $G_{p,\ 30\ years}$	=	2.42 BSCF
Original Gas In Place, *OGIP*	=	2.65 BSCF

Our first task is to match the subsets of the flow rate data with the "hyperbolic" rate decline relation. In **Fig. 1.2** we present the "hyperbolic" model matches imposed on the flow rate data, and the *D*- and *b*-parameter trends (see **Appendix A** for definitions of the *D*- and *b*-parameters). We fit the model with the entire dataset while the data exhibits transient flow (50 and 100 day intervals). For intervals where the transition and boundary-dominated flow regimes are observed, we fit the model to the late part of the data rather than fitting the equation to the entire interval as the "hyperbolic" relation is only valid for the boundary-dominated flow regime. Since the model for these intervals underestimates the flow rate profile, we correct the *EUR* by adding the cumulative production difference between the actual G_p value and the G_p value projected by the "hyperbolic" model. We calibrate the "hyperbolic" model parameters by hand and use regression to obtain the best match for each interval.

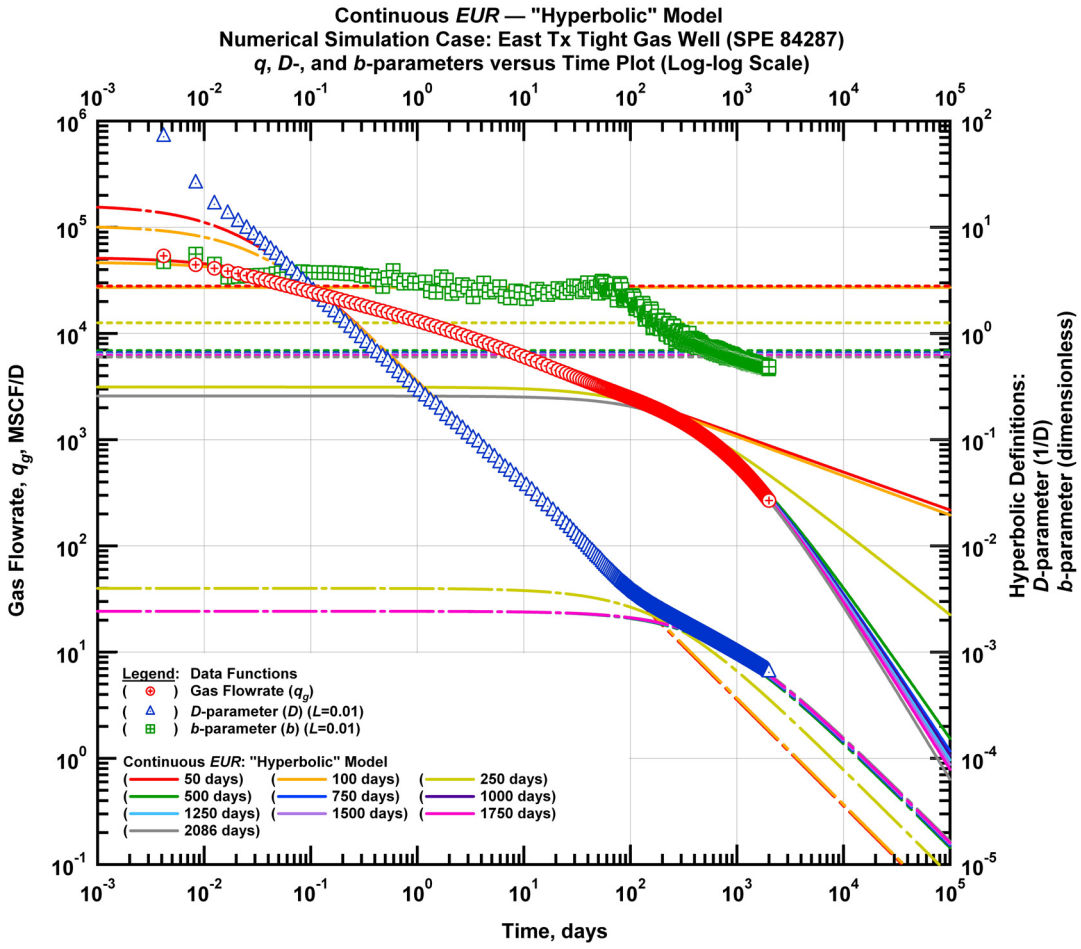

Figure 1.2 — (Log-log Plot): *qDb* plot — flow rate (q_g), *D*- and *b*-parameters versus production time and "hyperbolic" model matches for numerical simulation case.

In **Fig. 1.3** we observe the change in the *b*-parameter values over time; the *b*-parameter value decreases significantly at early times and begins to stabilize after about 500 days of production due to the onset of boundary-dominated flow. At early times (before 500 days) the data is matched with a "hyperbolic" *b*-parameter greater than 1 (*b* values greater than 1 may indicate the transient flow period).

In **Fig. 1.4** we present the simulated flow rate data and the calculated *D*- and *b*-parameters as well as the model matches obtained using the power law exponential model. We obtain identical matches for the 50 day and 100 day intervals. We expect this since the *D*-parameter trend exhibits almost perfect straight line behavior for the first 100 days of production. We observe the onset of transition and boundary-dominated flow after 100 days of production. The *D*-parameter trend begins to deviate from straight line behavior and approaches a constant value at late times. We match the production profile by including the boundary-dominated flow term, D_∞. The power law exponential rate decline relation matches the transient, transition, and boundary-dominated flow behavior very well.

We use the straight line extrapolation technique to estimate $G_{p,\,max}$. In **Fig. 1.5** we show the lines fit through the end portion of the data for each interval. The *x*-axis intercept of the lines increase with time resulting in an increasing estimate of $G_{p,max}$ or "lower" limit estimate of *EUR*.

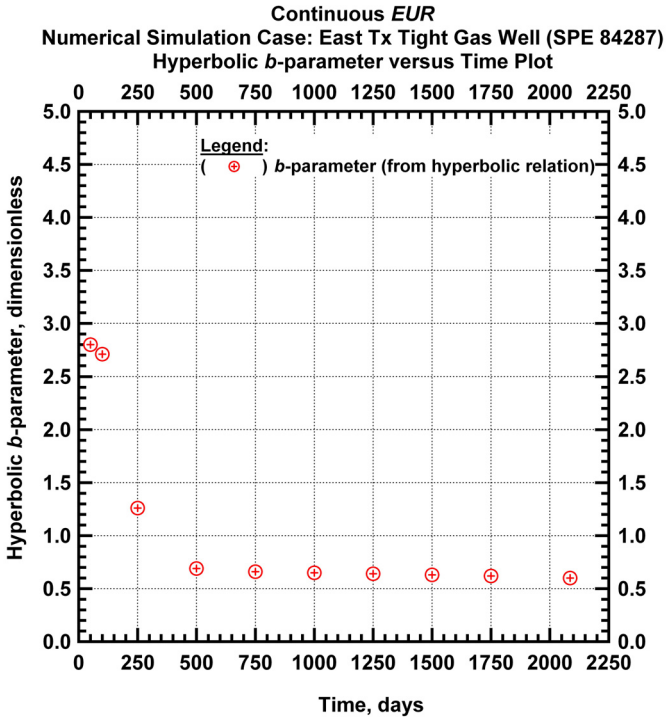

Figure 1.3 — (Cartesian Plot): Hyperbolic *b*-parameter values obtained from model matches with production data for numerical simulation case.

The last step in our workflow is to calculate the *EUR* based on the matches obtained with the "hyperbolic" and the power law exponential rate decline relations. In **Fig. 1.6** we present the calculated *EUR* values versus production time based on the model matches obtained using the "hyperbolic" and power law exponential rate decline relations as wells as the $G_{p,max}$ values estimated using the straight line extrapolation technique.

The *EUR* values obtained from the "hyperbolic" model matches decrease significantly at early times and then converge at late times to a value of 2.49 BSCF. The *EUR* values obtained from the power law exponential model matches are constant during the transient flow period and then decrease when boundary-dominated flow is established. The *EUR* become constant at a value of 2.40 BSCF after 250 days of production.

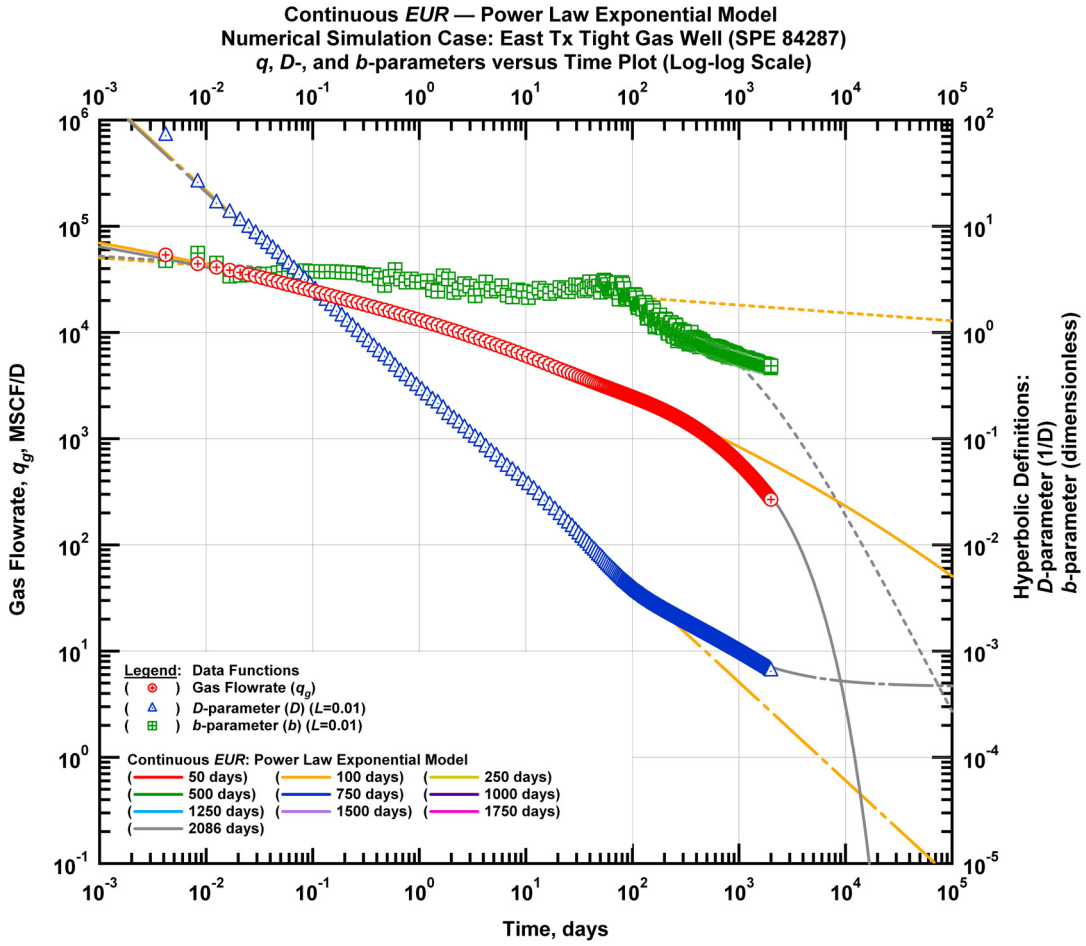

Figure 1.4 — (Log-log Plot): *qDb* plot — flow rate (q_g), *D*- and *b*-parameters versus production time and power law exponential model matches for numerical simulation case.

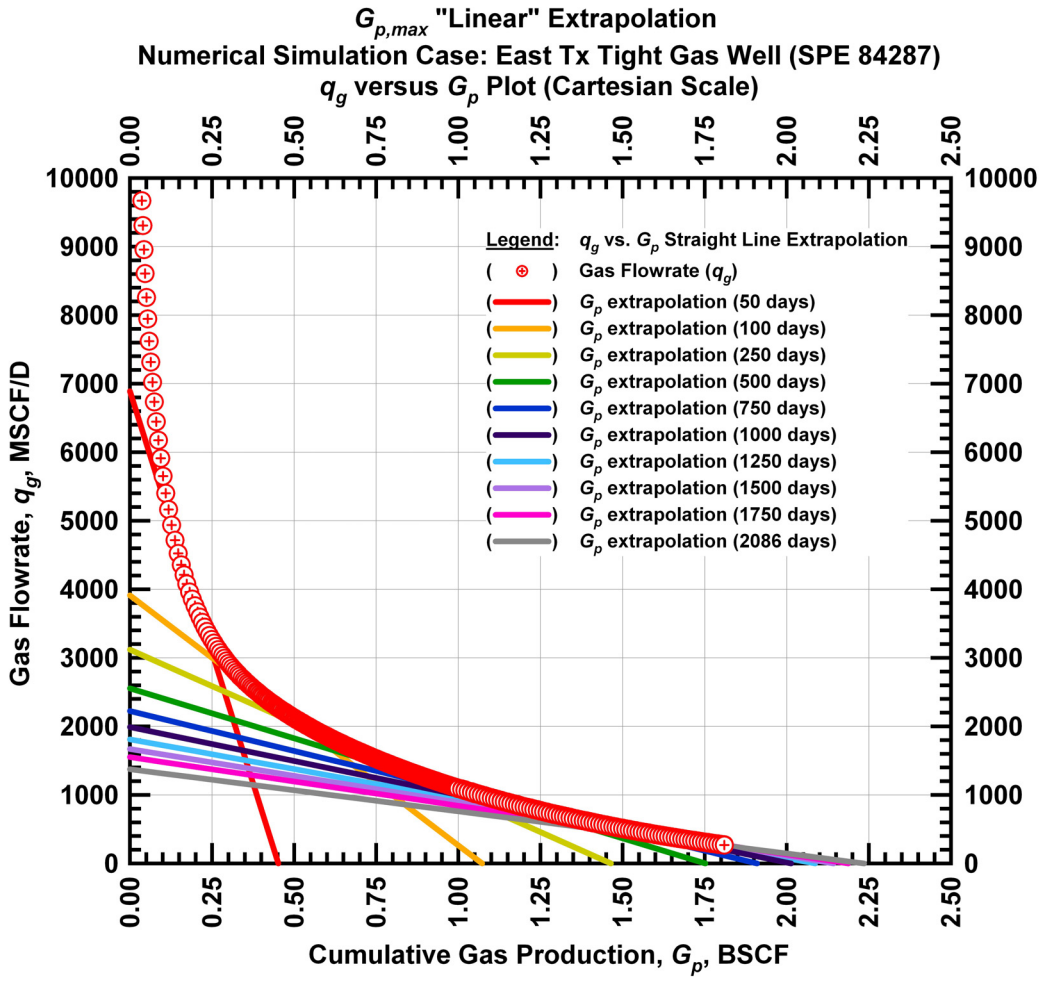

Figure 1.5 — (Cartesian Plot): Rate Cumulative Plot — flow rate (q_g) versus cumulative production (G_p) and the linear trends fit through the data for numerical simulation case.

From the reservoir simulation model, the gas produced at 30 years is 2.42 BSCF, which is consistent with the *EUR* obtained using the power law exponential model when boundary dominated flow is established. The *EUR* values obtained from the power law exponential model matches are more conservative the than values obtained from the hyperbolic model matches for each time interval analyzed. The *EUR* values from both models converge or become constant once boundary-dominated flow has been established.

The $G_{p,max}$ values obtained from the straight line extrapolation technique are shown to increase with time and never reach the actual cumulative production (G_p) value (2.42 BSCF) during the 2,086 days of production. This result confirms that the straight line technique may not be applicable for gas flow;

however, it can be used to provide a "lower" limit of *EUR* for practical purposes. Finally we present all of the model parameters and the *EUR* and $G_{p,max}$ values for each interval in **Tables 1.2, 1.3, and 1.4**.

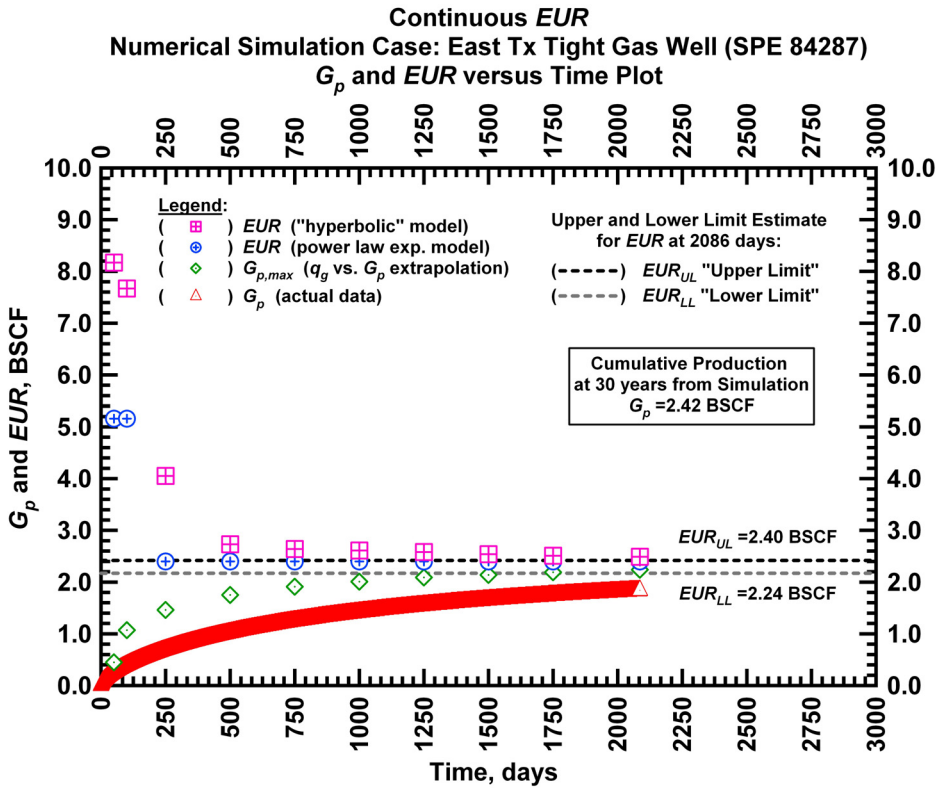

Figure 1.6 — (Cartesian Plot): *EUR* estimates from model matches and $G_{p,max}$ estimates from extrapolation technique for numerical simulation case.

Table 1.2 — Analysis results for numerical simulation case — "hyperbolic" model parameters.

Time Interval, days	q_{gi} (MSCFD)	D_i (D^{-1})	b (dimensionless)	EUR_{hyp} (BSCF)
50	51,846	16.16073	2.80	8.17
100	46,738	10.32035	2.71	7.67
250	3,130	0.003987	1.26	4.05
500	2,579	0.002423	0.69	2.73
750	2,579	0.002423	0.66	2.64
1,000	2,579	0.002423	0.65	2.61
1,250	2,579	0.002423	0.64	2.58
1,500	2,579	0.002423	0.63	2.54
1,750	2,579	0.002423	0.62	2.51
2,086	2,579	0.002423	0.60	2.49

Table 1.3 — Analysis results for numerical simulation case — power law exponential model parameters.

Time Interval, days	$\hat{q}_{gi}$ (MSCFD)	$\hat{D}_i$ (D^{-1})	n (dimensionless)	D_∞ (D^{-1})	EUR_{PLE} (BSCF)
50	835,453	4.142	0.074	0	5.16
100	835,453	4.142	0.074	0	5.16
250	812,662	4.117	0.070	0.000464	2.40
500	812,662	4.117	0.070	0.000464	2.40
750	812,662	4.117	0.070	0.000464	2.40
1,000	812,662	4.117	0.070	0.000464	2.40
1,250	812,662	4.117	0.070	0.000464	2.40
1,500	812,662	4.117	0.070	0.000464	2.40
1,750	812,662	4.117	0.070	0.000464	2.40
2,086	812,662	4.117	0.070	0.000464	2.40

Table 1.4 — Analysis results for numerical simulation case — straight line extrapolation.

Time Interval, days	Slope, 10^{-6} D^{-1}	Intercept, MSCF/D	$G_{p,max}$ (BSCF)
50	15,250	6,891	0.45
100	3,648	3,912	1.07
250	2,130	3,120	1.46
500	1,458	2,555	1.75
750	1,164	2,223	1.91
1,000	988	1,989	2.01
1,250	868	1,811	2.09
1,500	779	1,669	2.14
1,750	709	1,551	2.19
2,086	615	1,375	2.24

CHAPTER II
LITERATURE REVIEW — PRODUCTION DATA ANALYSIS

Many production data analysis methods have been developed to aid petroleum engineers in determining well behavior and production performance. This chapter reviews the petroleum engineering literature related to production data analysis. The literature is classified as shown by **Table 2.1** into three categories:

- Empirical, Semi-Analytical, and Analytical Production Data Analysis
- Decline Type Curve Analysis
- Diagnostic Methods

Table 2.1 — Categorization of production data analysis literature used for this work.

Empirical, Semi-Analytical, and Analytical Production Data Analysis

Author(s) (Year Published)	Production Data Analysis Topic
1. Cutler (1924)	Oil Reserves Estimation Using Production Type Curves
2. Johnson and Bollens (1927)	Extrapolating Oil Well Decline Curves Using the Loss Ratio Method
3. Arps (1945)	Analysis of Decline Curves
4. Maley (1985)	Analysis of Tight Gas Wells Using Conventional Decline Curve Analysis
5. Robertson (1988)	Hyperbolic and Exponential Rate-Time Relation
6. Camacho-V and Raghavan (1989)	Performance Prediction for Solution-Gas-Drive Reservoirs During Boundary-dominated Flow
7. Ansah et al. (1996)	Rate-Time Relation for Analysis of Gas Well Performance
8. Ansah (1996)	Production Data Analysis for Gas Reservoirs
9. Knowles (1999)	Semi-Analytical Methods to Analyze Gas Production Data
10. Buba (2003)	Production Data Analysis for Gas Reservoirs
11. El-Banbi and Wattenbarger (1998)	Analysis of Linear Flow Pressure and Production Data for Gas Wells
12. Rodriguez and Camacho (2005)	Decline Curve Analysis Considering Non-Darcy Flow Effects in Dual Porosity Systems
13. Li and Horne (2005)	Production Decline Curve Analysis for Naturally Fractured Reservoirs
14. Cox et al. (2003)	Production Analysis for Tight Gas Reservoirs
15. Rushing et al. (2007)	Production Analysis for Tight Gas Reservoirs

Table 2.1 — Continued.

Author(s) (Year Published)	Production Data Analysis Topic
16. Kupchenko et al. (2008)	Production Analysis for Tight Gas Reservoirs
17. Ilk et al. (2008a)	Production Analysis for Tight Gas Reservoirs
18. Cox et al. (2002)	Decline Curve Analysis for Multilayered Tight Gas Reservoirs
19. Cheng et al. (2007)	Decline Curve Analysis for Multilayered Tight Gas Reservoirs
20. Blasingame and Rushing (2005)	Method for Gas-in-Place and Reserves Estimation
21. Clarkson et al. (2007)	Production Data Analysis for Coalbed-Methane Wells
22. Clarkson et al. (2008)	Production Data Analysis for Coalbed-Methane Wells
23. Rushing et al. (2008)	Production Data Analysis for Coalbed-Methane Wells
24. Lewis and Hughes (2008)	Production Data Analysis for Shale Gas Wells
25. Mattar et al. (2008)	Production Data Analysis for Shale Gas Wells
26. Johnson et al. (2009)	Gas-in-Place and Reserves Estimation Using Rate-Time Data
27. Boulis et al. (2009)	New Rate Decline Relations for the Evaluation of Tight and Shale Gas Wells
Decline Type Curve Analysis	
28. Fetkovich (1980)	Type Curve Approach for Decline Curve Analysis
29. Fetkovich et al. (1987)	Application of Decline Type Curve Analysis
30. Carter (1985)	Finite Radial and Linear-Gas Flow Systems Type Curves
31. Fraim and Wattenbarger (1987)	Type Curves for Gas Reservoirs Using Real Gas Pseudopressure and Normalized Time
32. Fraim et al. (1986)	Finite Conductivity Vertical Fracture Type Curves
33. Palacio and Blasingame (1993)	Type Curves for Gas Wells
34. Doublet et al. (1994)	Type Curves for Oil Wells
35. Cox et al. (1996)	Type Curves for Hydraulically Fracture Gas Wells
36. Wattenbarger et al. (1998)	Type Curves for Fractured Tight Gas Wells
37. Agarwal et al. (1999)	Type Curves for Radial and Vertically Fracture Wells
38. Chen and Teufel (2000)	Type Curves Including Early-Time Linear Flow for Tight Gas Wells
39. Marhaendrajana and Blasingame (2001)	Type Curves for Evaluating a Well in a Multiwell System
40. Camacho-V et al. (2005)	Decline Curve Behavior of Naturally Fractured Vuggy Carbonate Reservoirs
41. Araya and Ozkan (2002)	Type Curve Analysis for Vertical, Fractured, and Horizontal Wells
42. Pratikno et al. (2003)	Type Curves for a Well with a Finite Conductivity Vertical Fracture

Table 2.1 — Continued.

Author(s) (Year Published)	Production Data Analysis Topic
43. Amini et al. (2007)	Type Curves for the Elliptical Flow of Hydraulically Fractured Wells in Tight Gas Reservoirs
Diagnostic Methods	
44. Mattar and Anderson (2003)	Overview of Production Data Analysis Methods
45. Anderson and Mattar (2004)	Practical Diagnostics for Production Data Analysis
46. Kabir and Izgec (2006)	Diagnosis of Reservoir Behavior using Pressure and Production Data
47. Anderson et al. (2006)	Production Data Diagnostics
48. Ilk et al. (2008b)	Production Data Analysis Techniques for Assessing Tight Gas Reserves

2.1 Empirical, Semi-Analytical, and Analytical Production Data Analysis

Cutler (1924) reviewed the methods used to analyze oil production using production-decline curves. Johnson and Bollens (1927) proposed the loss ratio and the loss ratio derivative which are the basis for the exponential and the hyperbolic rate decline relations respectively. The loss ratio is given by Eq. 1, and the loss ratio derivative is given by Eq. 2.

$$\frac{1}{D} = -\frac{q_g}{dq_g / dt} \quad \text{.....(1)}$$

$$b = \frac{d}{dt}\left[\frac{1}{D}\right] = -\frac{d}{dt}\left[\frac{q_g}{dq_g / dt}\right] \quad \text{.....(2)}$$

Arps (1945) presented an empirical method used to analyze rate-time data. This method includes the exponential, hyperbolic, and harmonic decline relations where the decline behavior is described by the decline exponent, *b*. Arps' rate-time and cumulative rate-time relations are summarized by **Table 2.2**. Arps' method is the most popular approach to rate-time data analysis because of its simplicity, but the method has several shortcomings including the assumption that the operating conditions remain constant during the life of the well and its inability to accurately analyze transient flow data.

Since Arps' introduction of the rate-time relations, production analysis methods have been developed for more specific applications. Maley (1985) expanded the use of Arps' rate-time relations to analyze tight gas well data. He proposed using the hyperbolic rate-time relation with a *b* value that exceeds one in order to obtain a match with observed production data. Robertson (1988) presented an alternative rate-time relation that couples the hyperbolic relation to match early production times and the exponential relation to match late production times. Camacho-V and Raghavan (1989) proposed a method to analyze boundary-

dominated flow data for wells in solution-gas-drive reservoirs. Ansah et al. (1996) and Ansah (1996) presented a semi-analytic rate-time relation that provides a direct solution for gas flow by coupling the boundary-dominated flow and gas material balance equations. Knowles (1999) and Buba (2003) offered the development and verification of semi-analytical methods used to evaluate gas well performance. El-Banbi and Wattenbarger (1998) offered an analytical approach to analyzing linear flow pressure and production data. The models were created for gas wells producing from reservoirs with high permeability streaks and for fractured wells. Rodriguez-Roman and Camacho-Velazquez (2005) proposed an analytical solution to describe production rate. Their work focused on analyzing decline curves considering the non-Darcy flow effect in dual-porosity reservoir systems. Li and Horne (2005) presented an analytical model to analyze production data for wells producing from naturally fractured reservoirs. Cox et al. (2002), Rushing et al. (2007), and Kupchenko et al.. (2008) realized the limitations of Arps decline relations when assessing production from tight gas wells. Ilk et al. (2008a) proposed the empirically derived "power law loss-ratio" rate relation to analyze production data from tight and shale gas wells. Cox et al.. (2003) and Cheng et al. (2007) presented a new procedure for analyzing production data from multilayer tight gas wells in order to minimize production forecasting errors. Blasingame and Rushing (2005) proposed a method using only production data to directly estimate gas-in-place and reserves. Clarkson et al. (2007), Clarkson et al. (2008), and Rushing et al. (2008) extended production analysis methods to analyze coalbed-methane production data. Lewis and Hughes (2008) modified material balance time to more accurately analyze production data from shale gas wells. Mattar et al. (2008) presented analytical and empirical analysis methods to evaluate shale gas production data. Johnson et al. (2009) proposed a method to evaluate unconventional gas production data with the use of semi-analytical and empirical formulations. Boulis (2009) proposed several alternative function forms to describe the *b* parameter in order to better evaluate production data for tight and shale gas wells.

2.2 Decline Type Curve Analysis

Fetkovich (1980 and 1987) presented the use of type curves to analyze transient and boundary-dominated flow data. He presented the analytical constant-pressure infinite and finite solutions in addition to the Arps rate-time relations as dimensionless log-log type curves. Carter (1985) offered finite radial and linear flow type curves to analyze gas production. Fraim et al. (1986) presented a new type curve to analyze vertically fractured wells. Fraim and Wattenbarger (1987) proposed type curves using real gas pseudopressure and normalized time. Palacio and Blasingame (1993) proposed a new method of analyzing gas production using decline type curves. Doublet et al. (1994) presented a procedure to analyze long-term oil production using decline type curves. Cox et al. (1996) offered a new set of type curves to analyze linear flow data from hydraulically fractured, low permeability gas wells. Wattenbarger et al. (1996) presented a decline curve method for analyzing fractured tight gas wells. Agarwal et al. (1999) presented new decline curves for radial and vertically fractured oil and gas wells. Chen and Teufel

(2000) extended the Fetkovich type curves to include linear and flow to better analyze production from tight gas wells. Marhaendrajana and Blasingame (2001) proposed a new method to analyze single well performance in a multi-well system. Camacho-Velazquez et al.. (2002) analyzed decline behavior for well producing from naturally fracture, vuggy carbonate reservoirs. Araya and Ozkan (2002) presented a compilation of the decline type curve methods used to analyze vertical, fractured, and horizontal wells. Pratikno et al.. (2003) proposed a new type curve for wells centered in a bounded, circular reservoir with a finite conductivity vertical fracture. Amini et al. (2007) offered a new set of type curves to analyze a system with a hydraulic fracture located at the center of an elliptical reservoir.

Table 2.2 — Arps' rate-time and cumulative-time relations for production data analysis.

Case	**Rate-Time Relation**
Exponential, $b = 0$	$q_g(t) = q_{gi} \exp[-D_i t]$
Hyperbolic, $0<b<1$	$q_g(t) = \frac{q_{gi}}{\left[1 + bD_i t\right]^{1/b}}$
Harmonic, $b = 1$	$q_g(t) = \frac{q_{gi}}{\left[1 + bD_i t\right]}$

Case	**Cumulative Rate-Time Relation**
Exponential, $b = 0$	$G_p(t) = \frac{q_{gi}}{D_i}[1 - \exp(-D_i t)]$
Hyperbolic, $0<b<1$	$G_p(t) = \frac{q_{gi}}{(1-b)D_i}\left[1 - (1 + bD_i t)^{1-1/b}\right]$
Harmonic, $b = 1$	$G_p(t) = \frac{q_{gi}}{D_i}\ln(1 + D_i t)$

2.3 Diagnostic Methods

Recently, more attention has been given to developing diagnostic tools for production data analysis. Mattar and Anderson (2003) presented an overview of the available production analysis methods and reviewed the strength and limitations of each method. They concluded that the most accurate analysis is obtained when all of the methods presented are used in conjunction. Anderson and Mattar (2004) offered

practical diagnostic procedures for production data analysis. Their procedures focused on assessing the quality of pressure and flowing pressure data. Anderson et al. (2006) reviewed the available production data analysis techniques and provided guidelines for analyzing production data. Kabir and Izgec (2006) proposed a diagnostic tool used to identify reservoir behavior. The tool uses pressure and rate data to improve the understanding of compartmentalization in the reservoir. Ilk et al. (2007) discussed the analysis of continuously measured, regularly measured, and legacy production data and recommended best practices for production data analysis. Ilk et al. (2008b) presented an integration of production analysis techniques to better assess tight gas reserves.

CHAPTER III
DEVELOPMENT OF THE CONTINUOUS *EUR* METHOD

We developed the "Continuous *EUR* Method" to identify the error associated with reserves estimation for unconventional gas reservoirs exhibiting long transient flow periods. From this approach we are able to quantify the change in *EUR* as a function of time and establish "upper" and "lower" limits for *EUR*. In this section we provide details related to the "Continuous *EUR* Method" workflow.

3.1 Data Editing and Interval Selection

Fig. 3.1 shows the first step of the workflow for the continuous *EUR* procedure. We start by obtaining rate-time data for an individual well. Prior to performing analysis, the rate-time dataset is edited and any points off trend from the dominant production profile are removed. The data editing process is critical since the noise in the production data is *significantly* amplified in the *D*-parameter and the *b*-parameter calculations. Recall that the *D*-parameter and *b*-parameter calculations require numerical differentiation of the dataset — the Bourdet algorithm (1989) is used for numerical differentiation purposes in this work.

The next step in the workflow is to create subsets of the production data (*i.e.* flow rate versus time). Each subset starts from the beginning of the production history (*i.e.* $t = 0$ days) and is analyzed individually with rate-time relations (*i.e.*, "hyperbolic" and power law exponential rate decline relations) and the straight line extrapolation technique.

3.2 Rate-Time Analysis

Fig. 3.2 presents the next step, which is the rate-time analysis procedure in our workflow. Each subset of the data is matched with the "hyperbolic" and power law exponential relations and an *EUR* value is obtained by extrapolating the rate-time model to a specified time limit or abandonment rate. For all the cases in this work, we specified a time limit of 30 years when calculating *EUR*. We analyzed the flow rate data with the "hyperbolic" and power law exponential rate decline relations, but this concept can be implemented with other rate-time relations.

3.3 Straight Line Extrapolation Technique

In addition to the "hyperbolic" and power law exponential relations, we use the straight line extrapolation technique to estimate a "lower" limit for *EUR* also shown by **Fig. 3.2**. We plot gas flow rate versus cumulative gas production for an individual well on a Cartesian scale. For each previously specified interval, we fit a straight line through the part of the data exhibiting linear trend. The *x*-axis intercept of the line yields an estimate for $G_{p,max}$. This method can be used to estimate the maximum oil production for oil wells under the boundary-dominated flow regime. By applying this technique to gas flow a conservative estimate for $G_{p,max}$ can be obtained which yields a "lower" limit for *EUR*.

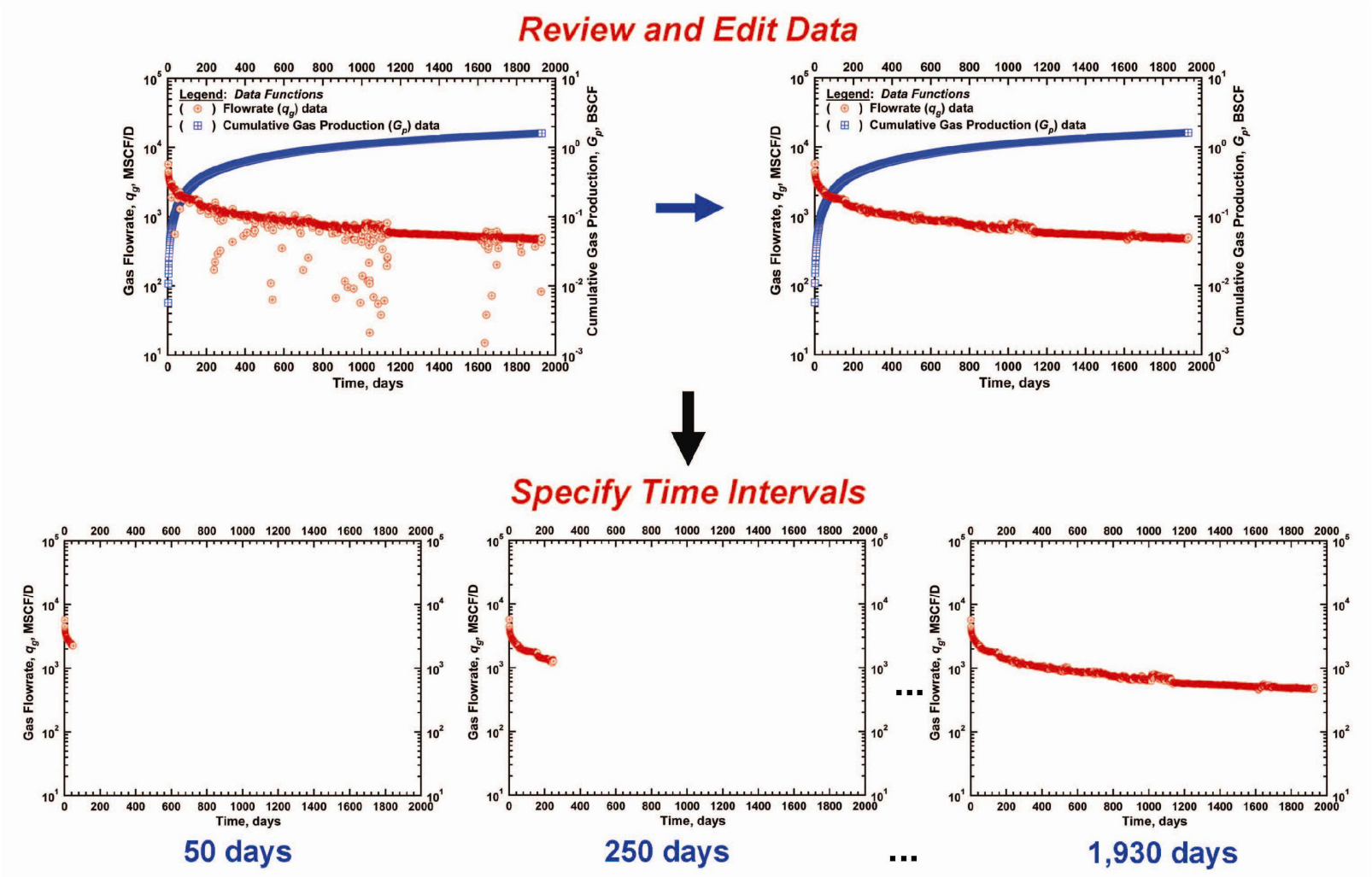

Figure 3.1 — First step of the continuous *EUR* method: Data is reviewed and edited, and intervals are selected for individual analysis.

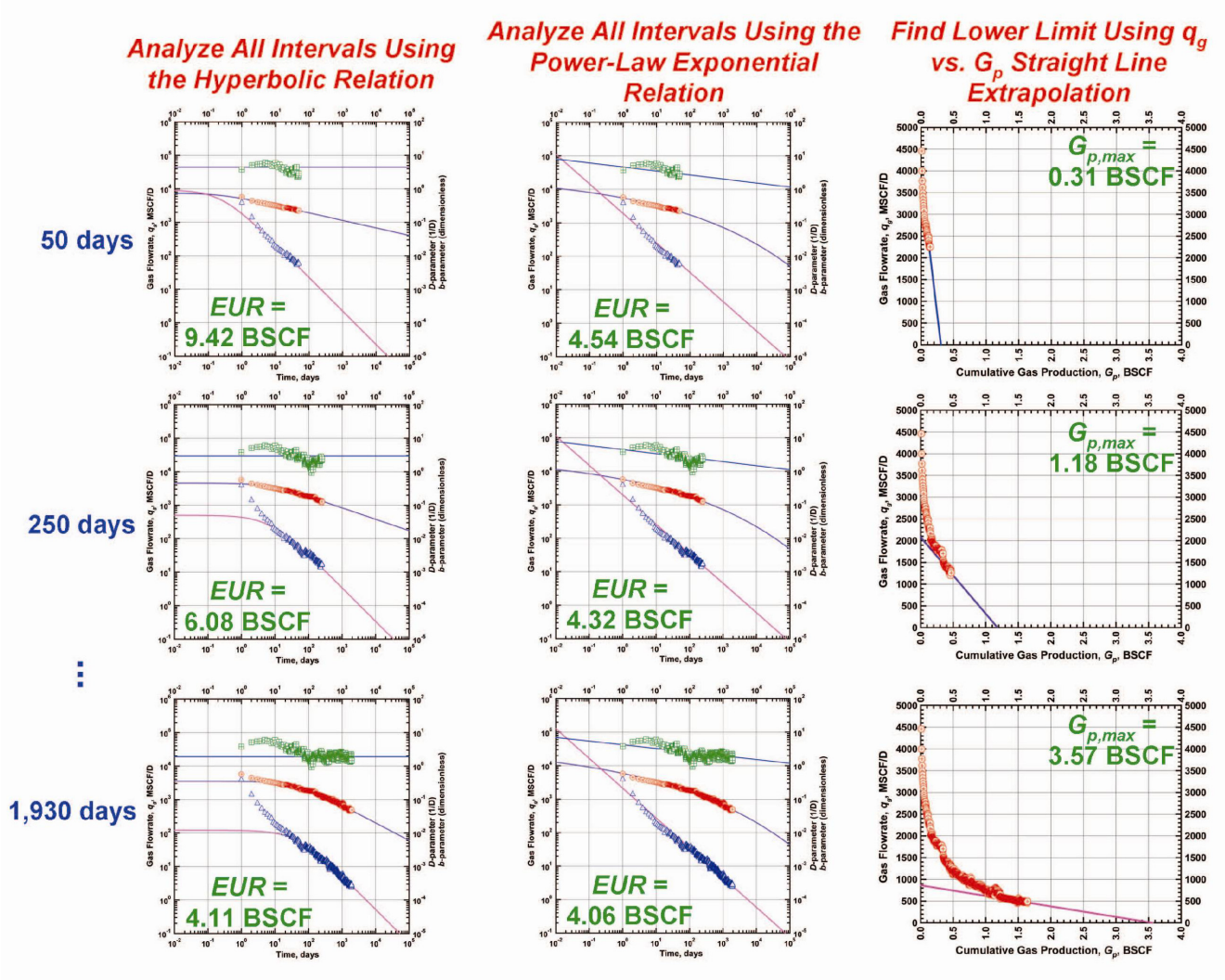

Figure 3.2 — Second step of the continuous *EUR* method: All previously specified intervals are evaluated and *EUR* values are obtained using the rate-time decline relations and a $G_{p,max}$ estimate is obtained using the straight line extrapolation technique.

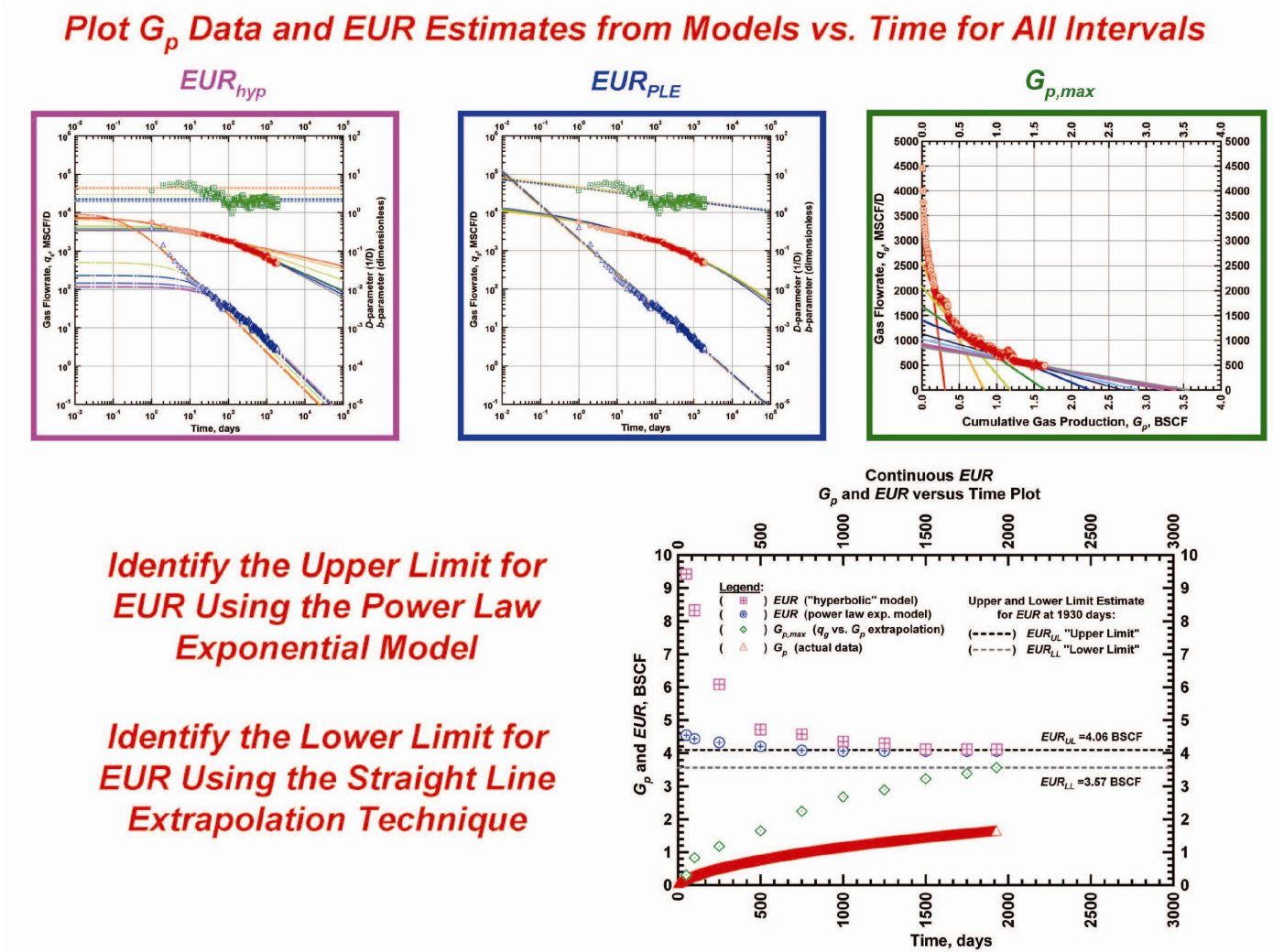

Figure 3.3 — Final step of the continuous *EUR* method: All *EUR* and $G_{p,max}$ values are plotted versus time, and "upper" and "lower" limits for *EUR* are established.

3.4 Continuous *EUR* Plots

The final step in the procedure is shown by **Fig. 3.3**. The *EUR* and the $G_{p,max}$ values obtained from the extrapolation of the rate-time relations and the straight line extrapolation technique are plotted together as a function of time. This *EUR* versus time plot provides a range that should encompass the true *EUR* value. We suggest that the *EUR* obtained from the power law exponential model be used as an "upper" limit and the $G_{p,max}$ estimate from the straight line extrapolation be used as a "lower" limit for reserves. We also note that with increasing time the difference between the "upper" and "lower" *EUR* limits is expected to decrease.

CHAPTER IV

APPLICATION OF THE METHOD TO FIELD EXAMPLES

In this section we demonstrate our proposed "Continuous *EUR* Method" by applying the approach to six field examples. Each example represents a well producing from a different tight sandstone or shale gas reservoir.

4.1 Field Example 1: East Tx Tight Gas Well (SPE 84287)

We apply our proposed methodology to a field dataset acquired from a hydraulically fractured vertical well completed in a tight gas reservoir. We present the flow rate and the cumulative production data that span nearly 9 years in **Fig. 4.1**. Prior to performing analysis, the data is edited and any points off trend from the dominant production profile are removed. The off trend rate data may be caused by liquid-loading effects and/or operational changes.

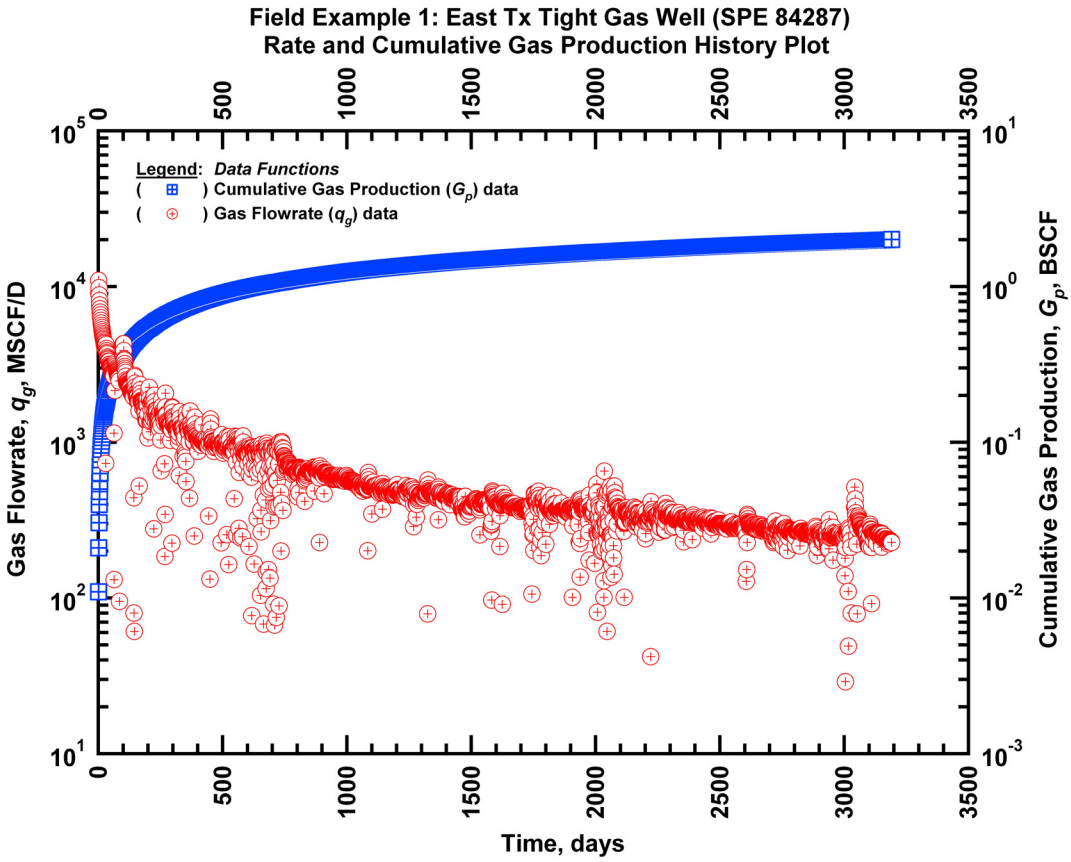

Figure 4.1 — (Semi-log Plot): Production history plot for field example 1 — flow rate (q_g) and cumulative production (G_p) versus production time.

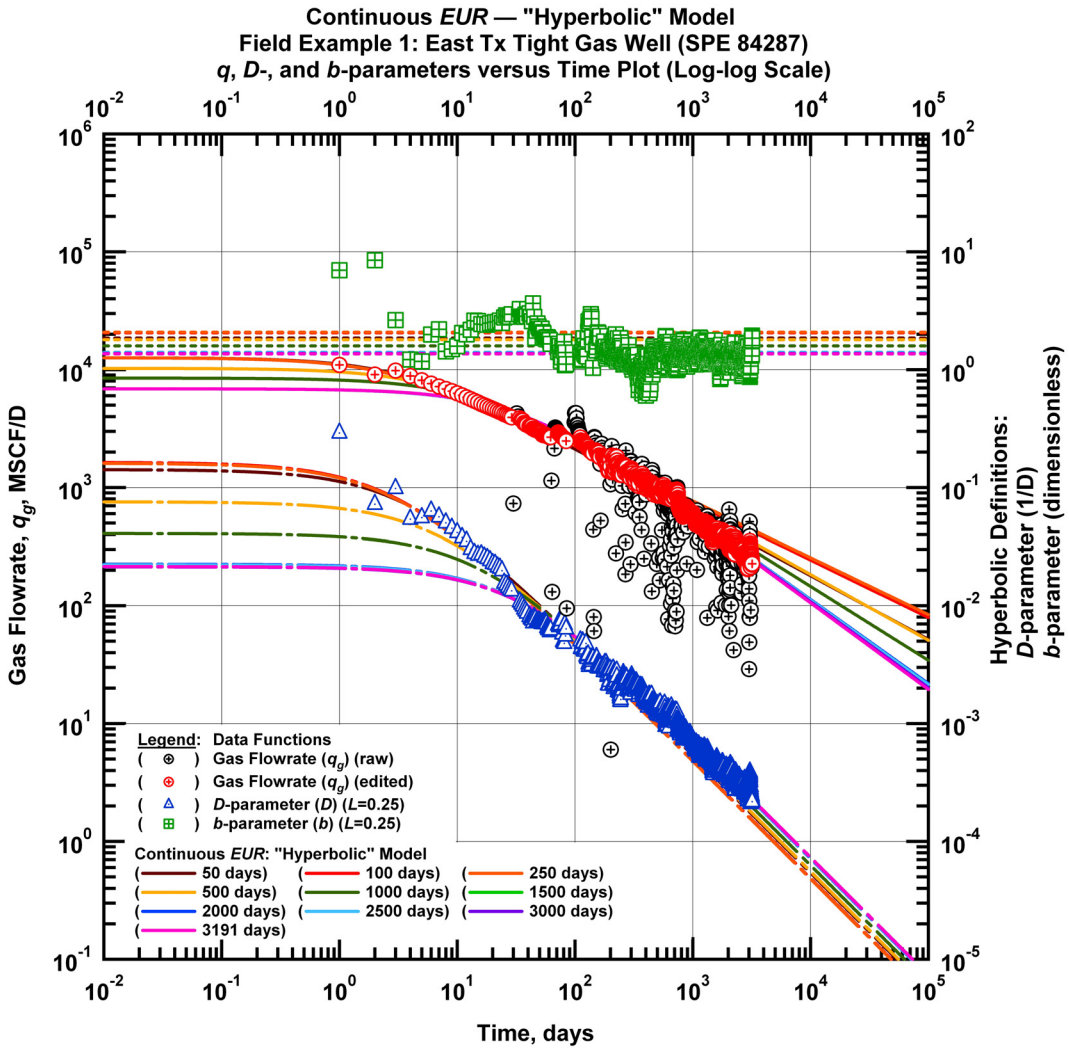

Figure 4.2 — (Log-log Plot): *qDb* plot — flow rate (q_g), *D*- and *b*-parameters versus production time and "hyperbolic" model matches for field example 1.

Our first task is to match the subsets of the flow rate data with the "hyperbolic" rate decline relation. **Fig. 4.2** presents the "hyperbolic" model matches imposed on the flow rate data along with the *D*- and *b*-parameter trends. We use the same matching technique as previously described in the simulated example. Since we do not observe any boundary-dominated flow effects, we attempt to find a best match with all of the data included in each interval.

In **Fig. 4.3** we observe that the value of the *b*-parameter stabilizes after around 1,500 days of production. Every subset (or interval) is matched with a "hyperbolic" *b*-parameter greater than 1 indicating that boundary-dominated flow has not been established. Specifically the *b*-parameter value decreases from

2.08 to 1.36 during the production history — this result may indicate that transient flow effects are still dominant in the production behavior. We do not observe any effects of the boundary-dominated flow regime.

Our next task is to match the subsets of the flow rate data with the power law exponential rate decline relation. In **Fig. 4.4** the power law exponential model matches are imposed on the flow rate data and *D*- and *b*-parameter trends are shown. For all matches a D_∞ value is not used indicating that boundary-dominated flow character is not observed (the behavior of the calculated *D*-parameter data trend may serve as a validation for not using the D_∞ parameter in the power law exponential relation as it exhibits only power law behavior). We observe that the model matched with the subsets of the data becomes constant after 100 days of production. This is expected since the *D*-parameter trend exhibits straight line behavior.

We use the straight line extrapolation technique to estimate $G_{p,max}$. In **Fig. 4.5** we show the lines fit through the end portion of the data for each interval. The *x*-axis intercept of the lines increase with time resulting in an increasing estimate of $G_{p,max}$ or "lower" limit estimate of *EUR*.

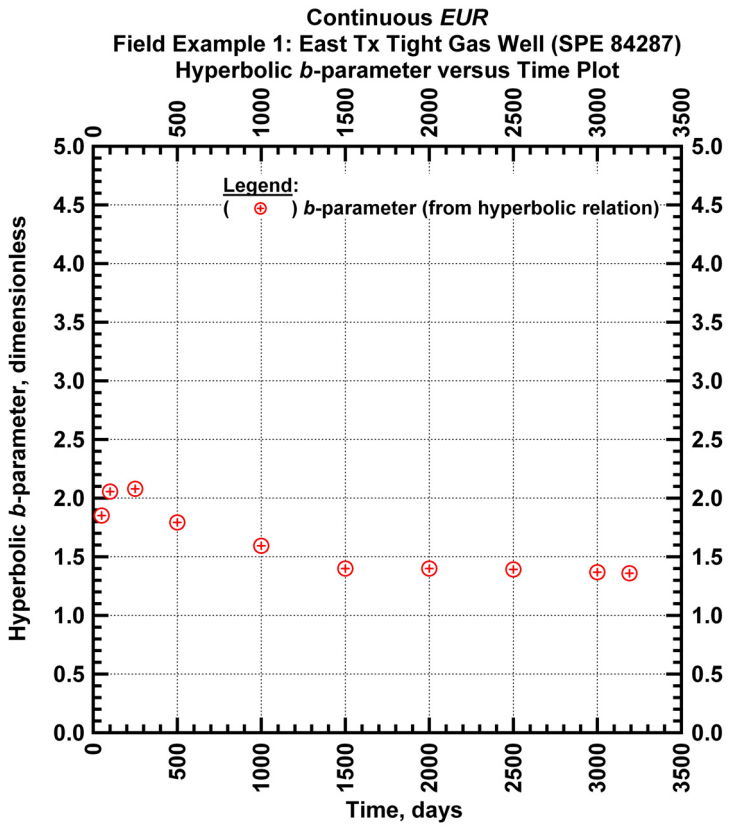

Figure 4.3 — (Cartesian Plot): Hyperbolic *b*-parameter values obtained from model matches with production data for field example 1.

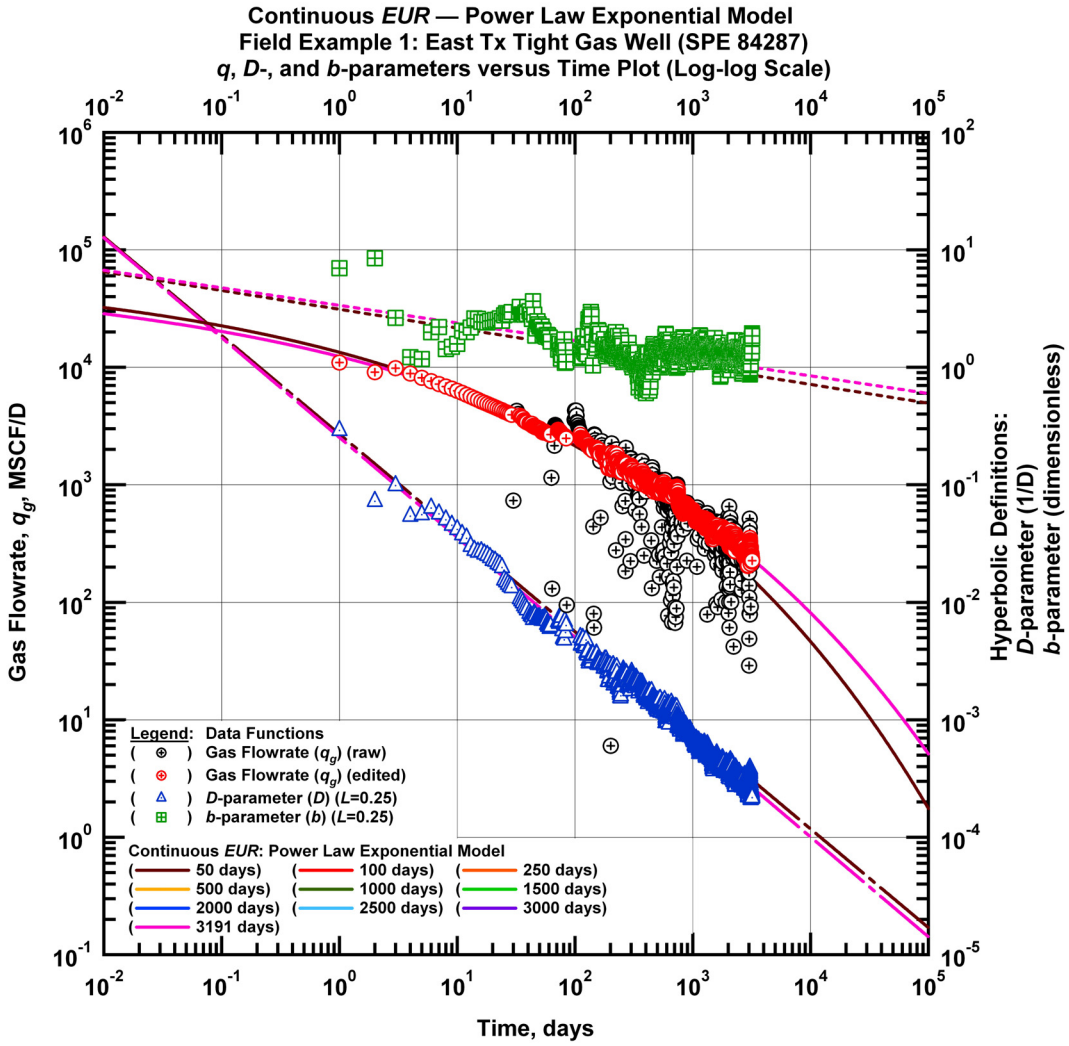

Figure 4.4 — (Log-log Plot): *qDb* plot — flow rate (q_g), *D*- and *b*-parameters versus production time and power law exponential model matches for field example 1.

The last step in our workflow is to plot the *EUR* values based on the matches obtained with the "hyperbolic" and the power law exponential rate decline relations and the $G_{p,max}$ estimates obtained from the straight line technique versus time. In **Fig. 4.6** we present the calculated *EUR* and the $G_{p,max}$ values versus production time. Early estimates of ultimate recovery from the "hyperbolic" and power law exponential relations are shown to increase. This is a common signature for wells that have been stimulated with a hydraulic fracture treatment and as a result experience flowback or clean-up effects in the early days of production while the frac fluids are being recovered. The *EUR* values obtained from the "hyperbolic" relation significantly overestimate reserves at early times and converge at late times to a value

of 3.21 BSCF. The estimates provided by the power law exponential model are constant at 3.05 BSCF after 100 days of production.

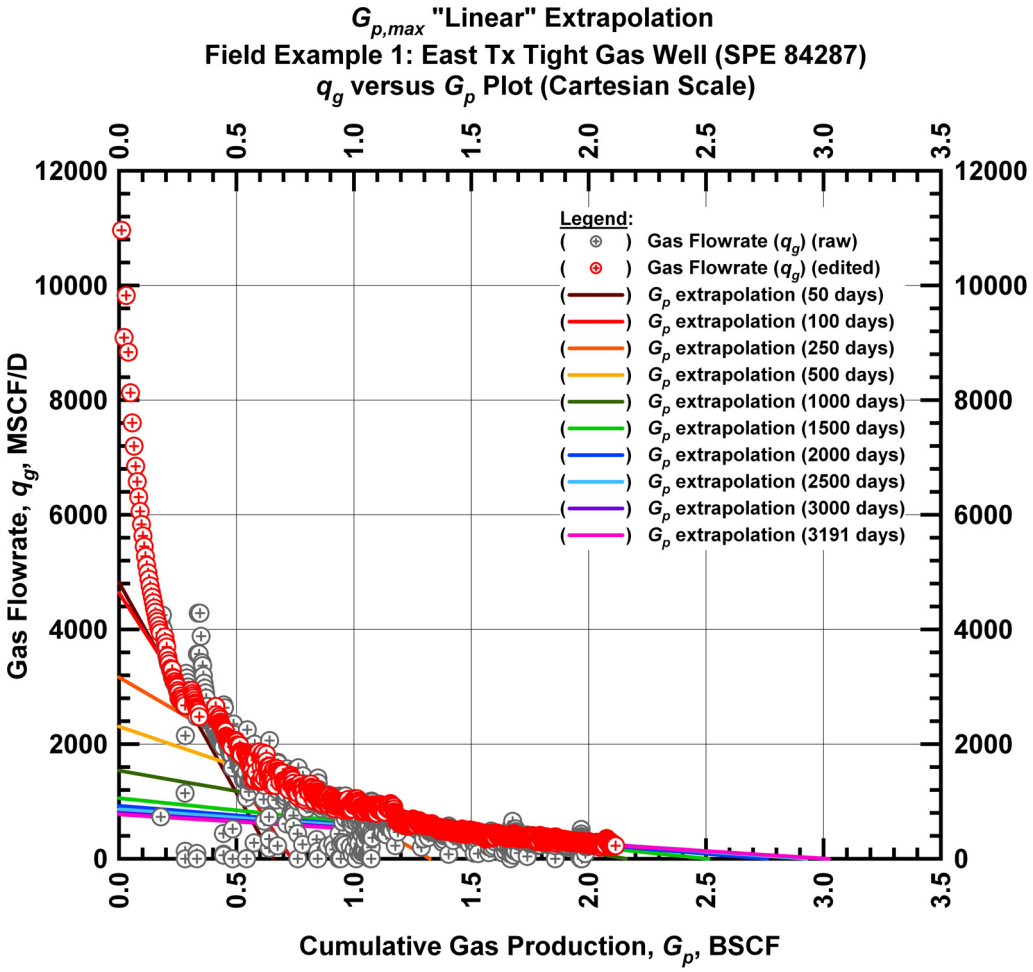

Figure 4.5 — (Cartesian Plot): Rate Cumulative Plot — flow rate (q_g) versus cumulative production (G_p) and the linear trends fit through the data for field example 1.

The $G_{p,max}$ values obtained from the straight line extrapolation increase with time and are always less than the estimates provided by the rate-time relations. The *EUR* of this well should be in between 3.02 BSCF (the "lower" limit given by the straight line extrapolation technique at 3,191 days) and 3.05 BSCF (the "upper" limit given by the power law exponential estimate at 3,191 days). All of the model parameters for this example are presented in **Tables 4.1, 4.2, and 4.3**.

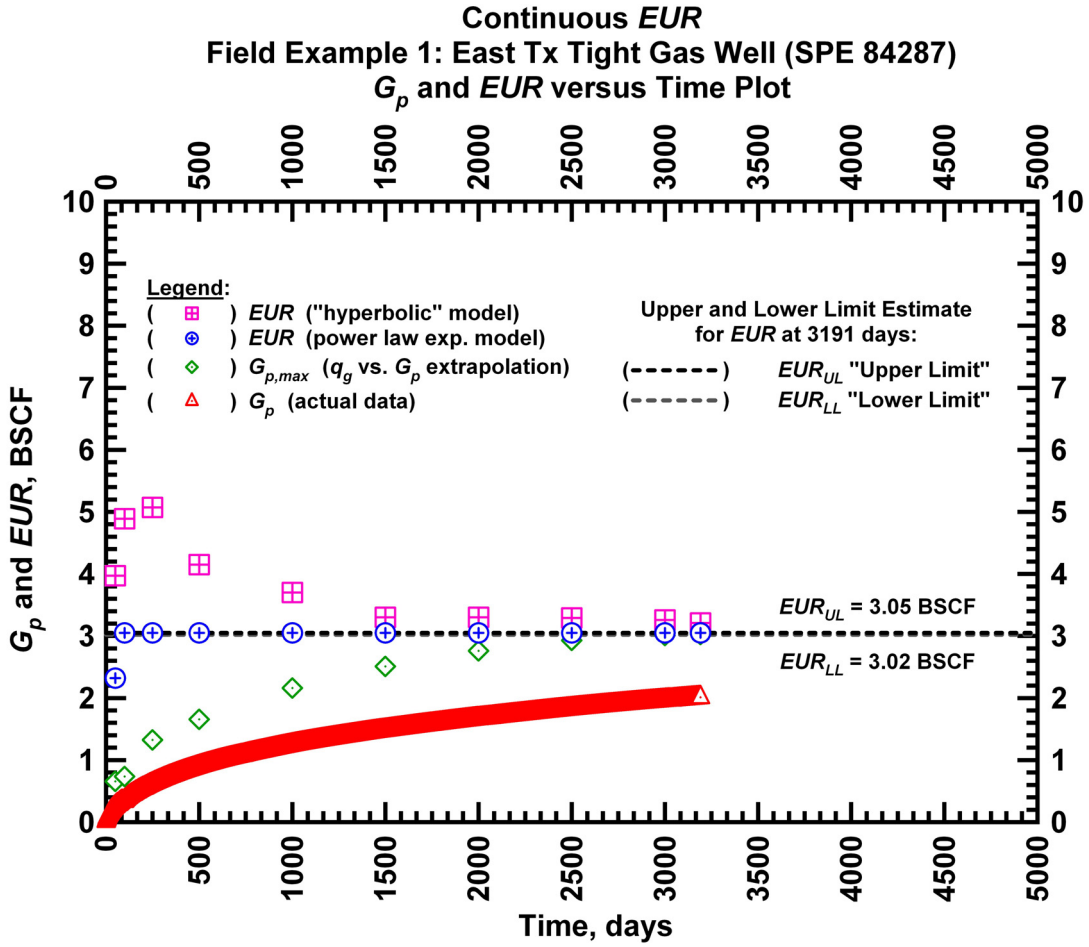

Figure 4.6 — (Cartesian Plot): *EUR* estimates from model matches and $G_{p,max}$ estimates from extrapolation technique for field example 1.

Table 4.1 — Analysis results for field example 1 — "hyperbolic" model parameters.

Time Interval, days	q_{gi} (MSCFD)	D_i (D^{-1})	b (dimensionless)	EUR_{hyp} (BSCF)
50	12,618	0.1420	1.85	3.97
100	12,618	0.1635	2.06	4.89
250	12,618	0.1607	2.08	5.07
500	10,264	0.0756	1.79	4.15
1,000	8,483	0.0408	1.59	3.70
1,500	6,879	0.0225	1.40	3.30
2,000	6,879	0.0225	1.40	3.30
2,500	6,879	0.0222	1.39	3.29
3,000	6,879	0.0213	1.37	3.26
3,191	6,879	0.0215	1.36	3.21

Table 4.2 — Analysis results for field example 1 — power law exponential model parameters.

Time Interval, days	$\hat{q}_{gi}$ (MSCFD)	$\hat{D}_i$ (D^{-1})	n (dimensionless)	D_∞ (D^{-1})	EUR_{PLE} (BSCF)
50	72,253	1.684	0.16	0	2.32
100	66,500	1.684	0.15	0	3.05
250	66,500	1.684	0.15	0	3.05
500	66,500	1.684	0.15	0	3.05
1,000	66,500	1.684	0.15	0	3.05
1,500	66,500	1.684	0.15	0	3.05
2,000	66,500	1.684	0.15	0	3.05
2,500	66,500	1.684	0.15	0	3.05
3,000	66,500	1.684	0.15	0	3.05
3,191	66,500	1.684	0.15	0	3.05

Table 4.3 — Analysis results for field example 1 — straight line extrapolation.

Time Interval, days	Slope, 10^{-6} D^{-1}	Intercept, MSCF/D	$G_{p,max}$ (BSCF)
50	7,341	4,819	0.66
100	6,315	4,638	0.73
250	2,390	3,165	1.32
500	1,392	2,307	1.66
1,000	711	1,536	2.16
1,500	421	1,057	2.51
2,000	335	925	2.76
2,500	295	864	2.93
3,000	267	803	3.01
3,191	256	774	3.02

4.2 Field Example 2: Tight Gas Well (Holly Branch Field)

We apply the "Continuous *EUR* Method" to a second field dataset acquired from a hydraulically fractured vertical well completed in a tight gas reservoir. The flow rate and the cumulative production data that span almost 5.5 years are shown in **Fig. 4.7**. We observe the effects of liquid loading and operational changes (specifically at 1,000 days of production) on the flow rate profile.

The subsets of the flow rate data are matched with the "hyperbolic" rate decline relation initially. In **Fig. 4.8** we present the "hyperbolic" model matches imposed on the flow rate data, and *D*- and *b*-parameter trends. We use calibration by hand and regression to find a best match with the observed production profile for each interval. Every subset of the data is matched with a "hyperbolic" *b*-parameter greater than 1 indicating that complete boundary-dominated flow regime effects are not established. In **Fig. 4.9** we observe that the *b*-parameter is relatively stable after about 500 days of production. The *b*-parameter values decrease from 4.46 to 1.91 during the production history.

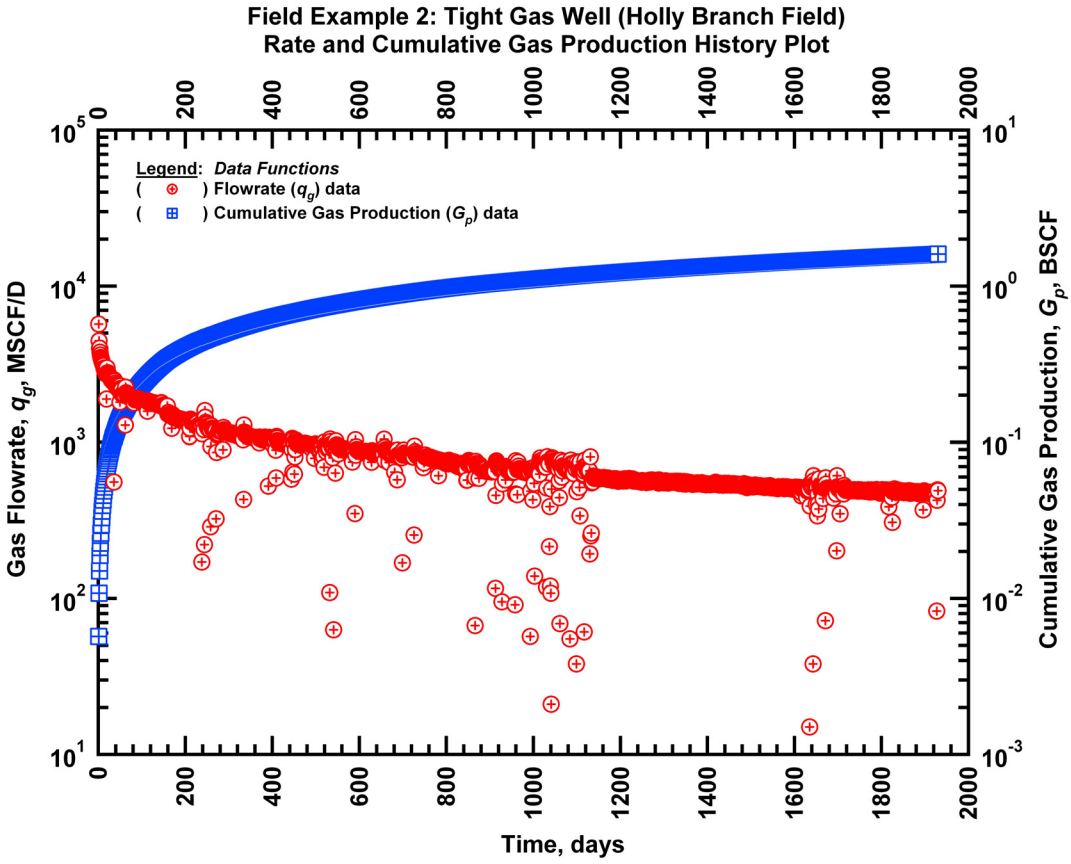

Figure 4.7 — (Semi-log Plot): Production history plot for field example 2 — flow rate (q_g) and cumulative production (G_p) versus production time.

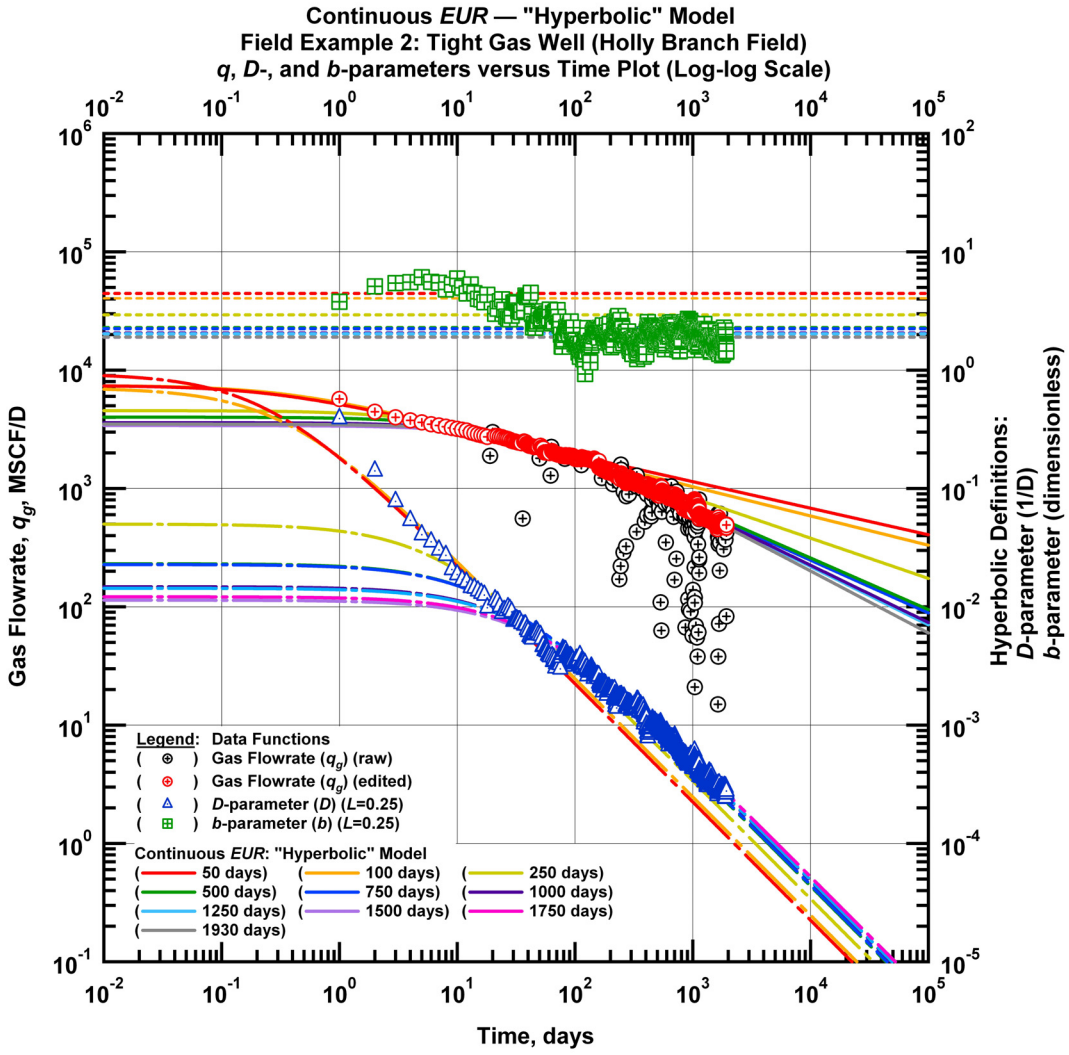

Figure 4.8 — (Log-log Plot): *qDb* plot — flow rate (q_g), *D*- and *b*-parameters versus production time and "hyperbolic" model matches for field example 2.

The selected subsets of the flow rate data are matched with the power law exponential rate decline relation. In **Fig. 4.10** we present the power law exponential model matches imposed on the flow rate data, and the *D*- and *b*-parameter trends. For all matches a D_∞ value is not used in the model — as dictated by the data character (*i.e.*, power law *D*-parameter trend). The model matches are for the most part identical during the entire production history. In particular, we note that the character of the data — specifically the computed *D*-parameter trend — for the smallest interval (50 days) is almost identical to the character of the data for the largest interval (1,930 days) resulting in almost identical power law exponential model

matches. Therefore, the *EUR* values from the power law exponential model will be relatively constant for this case.

In **Fig. 4.11** we show the results of the straight line extrapolation technique for this case. The *x*-axis intercept of the extrapolated lines increase with time resulting in an increasing estimate of $G_{p,max}$.

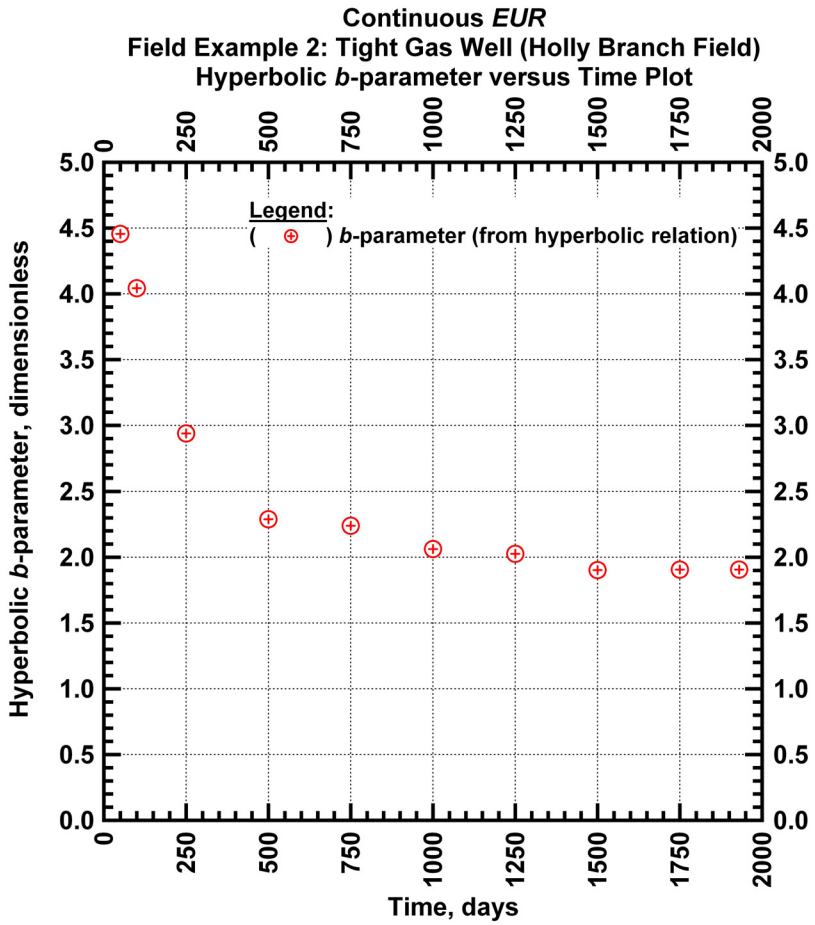

Figure 4.9 — (Cartesian Plot): Hyperbolic *b*-parameter values obtained from model matches with production data for field example 2.

The last step in our workflow is to calculate the *EUR* based on the matches obtained with the "hyperbolic" and the power law exponential rate decline relations. In **Fig. 4.12** we present the calculated *EUR* values versus production time. The *EUR* obtained from the "hyperbolic" relation converge at late times to a value of 4.11 BSCF. The estimates provided by the power law exponential relation are constant at 4.06 BSCF after 1,000 days (and close before 1,000 days).

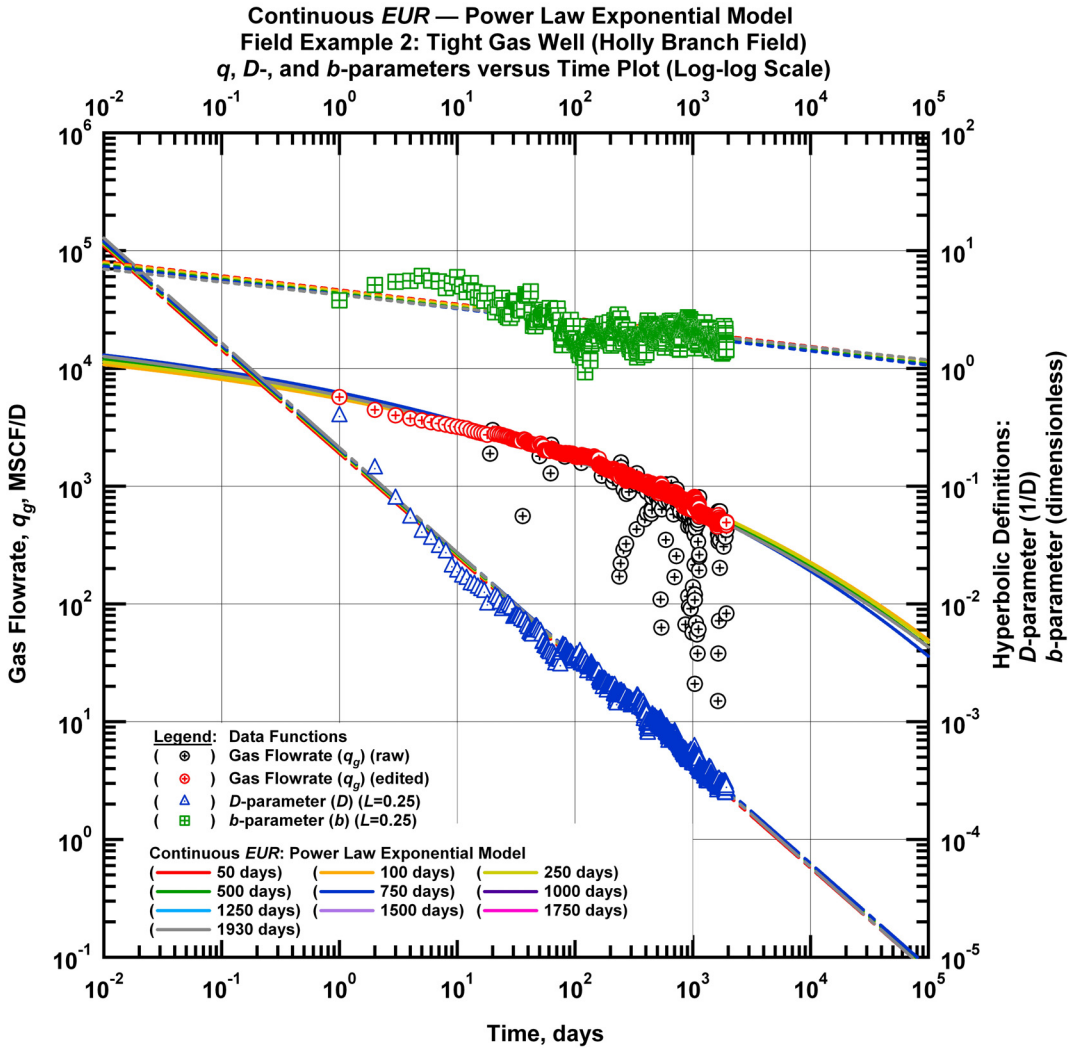

Figure 4.10 — (Log-log Plot): *qDb* plot — flow rate (q_g), *D*- and *b*-parameters versus production time and power law exponential model matches for field example 2.

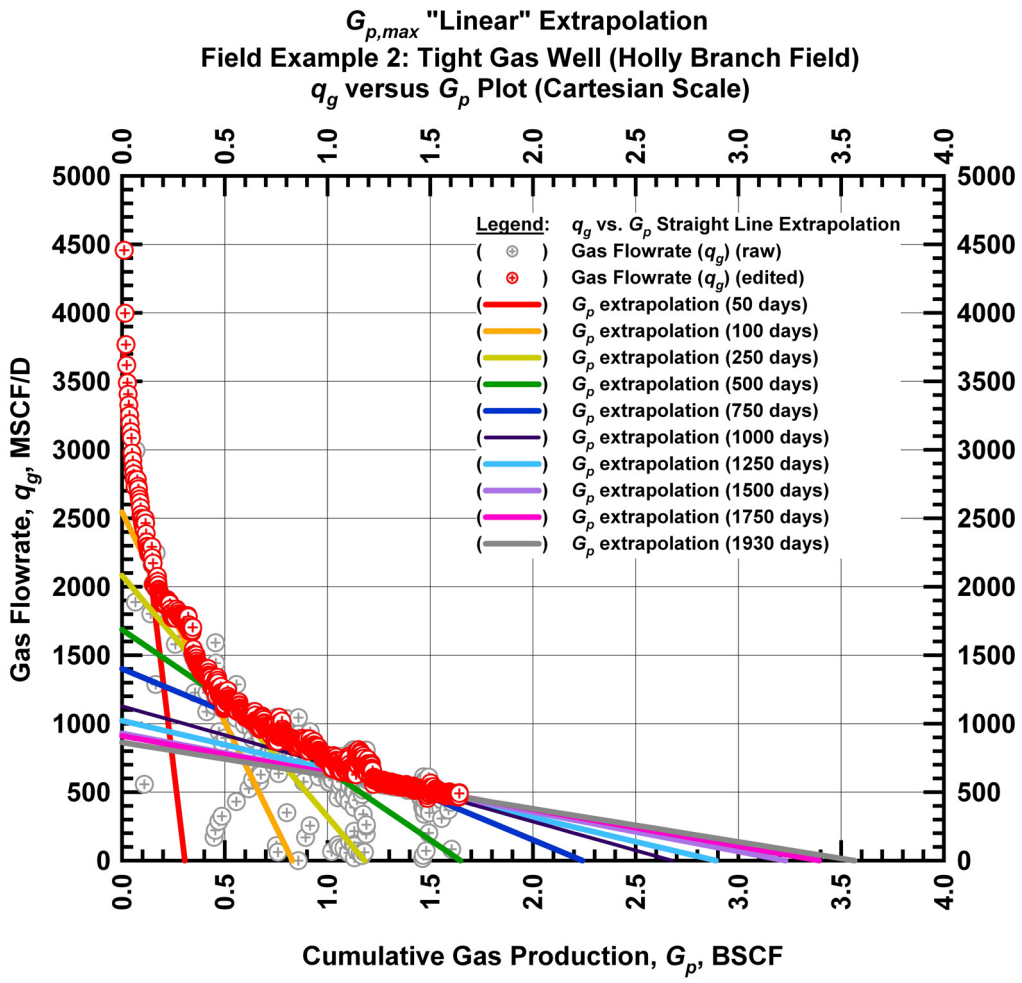

Figure 4.11 — (Cartesian Plot): Rate Cumulative Plot — flow rate (q_g) versus cumulative production (G_p) and the linear trends fit through the data for field example 2.

The $G_{p,max}$ values obtained from straight line extrapolation are also shown in **Fig. 12** and appear to increase with time. The $G_{p,max}$ values are always less than the estimates provided by the rate-time relations. Also the $G_{p,max}$ values obtained from straight line extrapolation still appear to increase at late times — the values do not appear to stabilize. Consequently, the *EUR* of this well should be in between 3.57 BSCF (the "lower" limit given by the straight line extrapolation technique at 1,930 days) and 4.06 BSCF (the "upper" limit given by the power law exponential estimate at 1,930 days). All the model parameters for this well are summarized in **Tables 4.4, 4.5, and 4.6**.

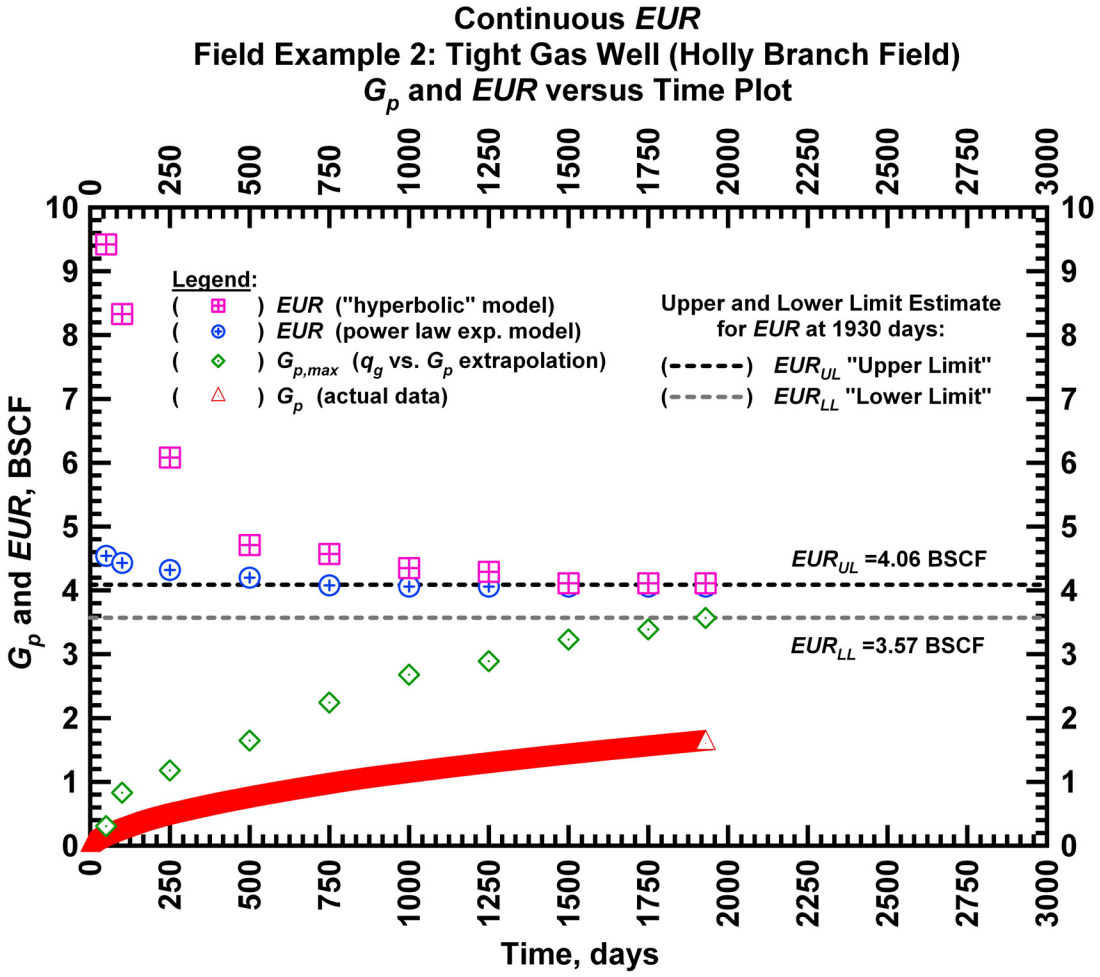

Figure 4.12 — (Cartesian Plot): *EUR* estimates from model matches and $G_{p,max}$ estimates from extrapolation technique for field example 2.

Table 4.4 — Analysis results for field example 2 — "hyperbolic" model parameters.

Time Interval, days	q_{gi} (MSCFD)	D_i (D^{-1})	b (dimensionless)	EUR_{hyp} (BSCF)
50	7,419	0.9360	4.46	9.42
100	7,419	0.7096	4.04	8.33
250	4,550	0.0500	2.94	6.08
500	4,008	0.0231	2.29	4.71
750	4,008	0.0228	2.24	4.57
1,000	3,602	0.0148	2.06	4.35
1,250	3,602	0.0143	2.03	4.29
1,500	3,405	0.0114	1.90	4.11
1,750	3,500	0.0122	1.91	4.11
1,930	3,500	0.0122	1.91	4.11

Table 4.5 — Analysis results for field example 2 — power law exponential model parameters.

Time Interval, days	$\hat{q}_{gi}$ (MSCFD)	$\hat{D}_i$ (D^{-1})	n (dimensionless)	D_∞ (D^{-1})	EUR_{PLE} (BSCF)
50	26,695	1.58	0.12	0	4.54
100	28,606	1.61	0.12	0	4.43
250	30,654	1.65	0.12	0	4.32
500	32,849	1.69	0.12	0	4.20
750	35,200	1.73	0.12	0	4.08
1,000	40,421	1.93	0.11	0	4.06
1,250	40,421	1.93	0.11	0	4.06
1,500	40,421	1.93	0.11	0	4.06
1,750	40,421	1.93	0.11	0	4.06
1,930	40,421	1.93	0.11	0	4.06

Table 4.6 — Analysis results for field example 2 — straight line extrapolation.

Time Interval, days	Slope, 10^{-6} D^{-1}	Intercept, MSCF/D	$G_{p,max}$ (BSCF)
50	12,459	3,805	0.31
100	3,068	2,544	0.83
250	1,762	2,082	1.18
500	1,023	1,686	1.65
750	625	1,401	2.24
1,000	421	1,127	2.68
1,250	354	1,023	2.89
1,500	288	930	2.23
1,750	268	910	3.39
1,930	242	863	3.57

Table 4.7 — Analysis results for field examples from the Holly Branch field.

Field Example	Producing Time (D)	b (dimensionless)	EUR_{hyp} (BSCF)	EUR_{PLE} (BSCF)	$G_{p,max}$ (BSCF)
2	1,930	1.91	4.11	4.06	3.57
7	1,995	1.62	2.47	2.28	2.04
8	2,384	1.70	3.78	3.78	3.39
9	512	2.30	2.17	1.82	0.86
10	331	2.31	1.86	1.30	0.53
11	981	2.46	2.05	1.91	1.20
12	671	1.41	2.40	2.19	1.45
13	337	2.85	3.68	2.95	1.03
14	269	2.35	3.14	2.50	0.88
15	336	2.24	2.13	1.80	0.68
16	764	1.98	4.67	3.87	2.46

Additional continuous *EUR* examples for the tight gas wells producing from the Holly Branch field are included in **Appendix C**. **Table 4.7** includes analysis results for the 11 vertical hydraulically fractured tight gas wells producing from the Holly Branch field. The *EUR* values and $G_{p,max}$ estimates shown for each well were obtained from the analysis of the entire production history. The *EUR* values obtained using the "hyperbolic" model are up to 43% or 0.56 BSCF greater than the estimates obtained using the power law exponential model. The *EUR* values given by the power law exponential model range between 1.30 and 4.06 BSCF. **Fig. 4.13** shows a comparison of the *EUR* values versus time obtained using the "hyperbolic" relation, and **Fig. 4.14** shows a comparison of the *EUR* values versus time obtained using the power law exponential relation for all of the wells analyzed from the Holly Branch field. For examples 2, 7, and 8, the *EUR* values given by the power law exponential model stabilize around 750 to 1,000 days. The *EUR* values given by the power law exponential model stabilize earlier (after 50 to 300 days) for examples 9 through 16. **Fig. 4.15** shows a comparison of the "hyperbolic" *b*-parameter versus time for all of the wells analyzed from the Holly Branch field. The *b*-parameter appears to remain relatively constant with time for field examples 9, 10, 12, 13, 14, 15, and 16 and ranges between 1.41 and 2.85 obtained from the model fit with the entire dataset. The *b*-parameter exhibits a similar trend for field examples 2, 7, 8, and 11 and decreases significantly especially at early times and then become relatively constant at late times. For all cases, the *b*-parameter is greater than 1 indicating that transient flow effects are still dominant.

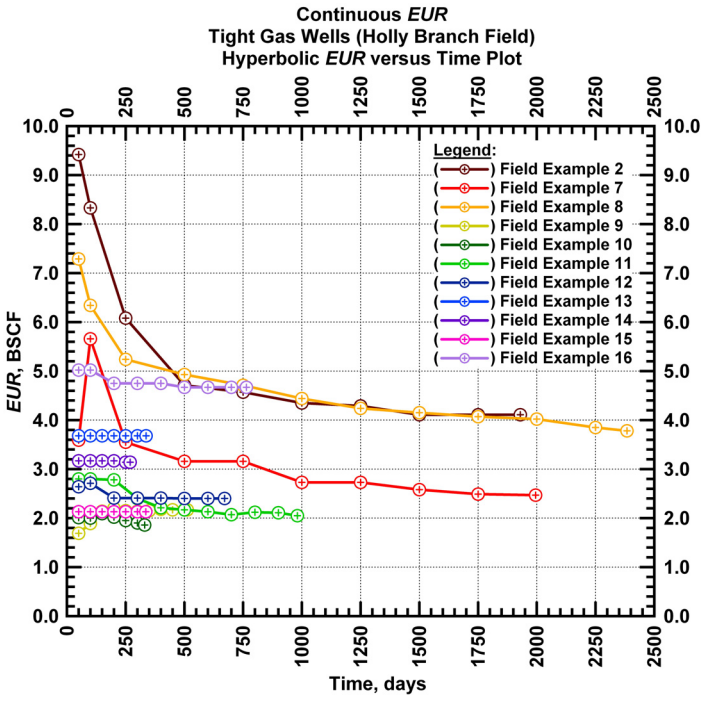

Figure 4.13 — (Cartesian Plot): Comparison of the hyperbolic *EUR* estimates for the tight gas wells producing from the Holly Branch field.

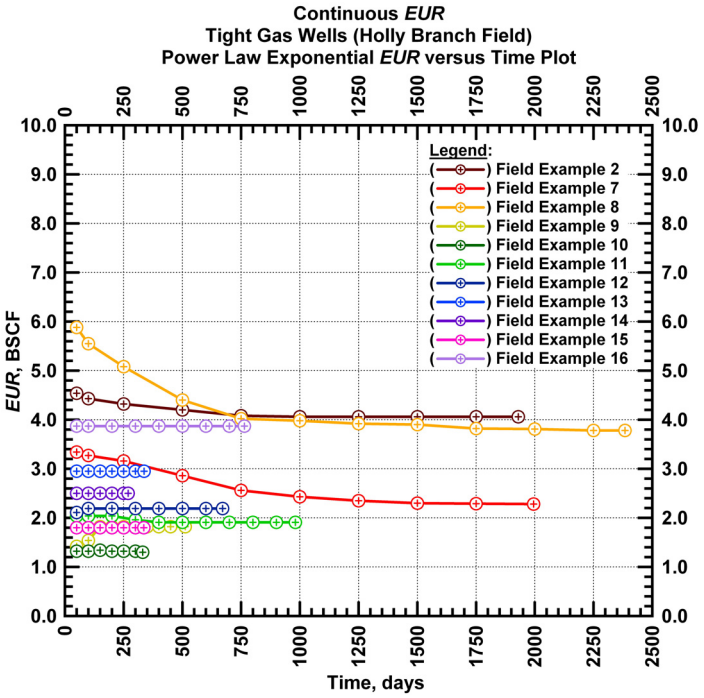

Figure 4.14 — (Cartesian Plot): Comparison of the power law exponential *EUR* estimates for the tight gas wells producing from the Holly Branch field.

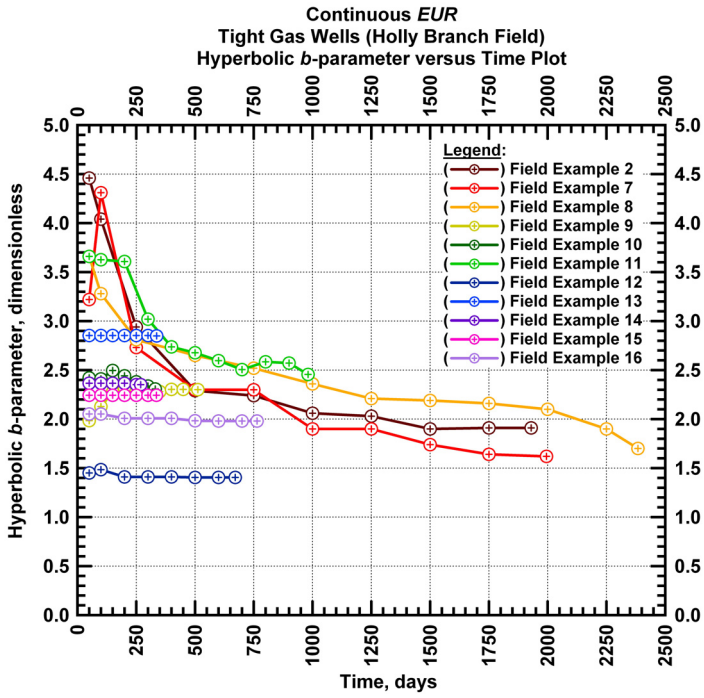

Figure 4.15 — (Cartesian Plot): Comparison of the hyperbolic *b*-parameter for the tight gas wells producing from the Holly Branch field.

4.3 Field Example 3: Shale Gas Well (Field A)

The third field dataset includes the daily rate-time data for a hydraulically fractured vertical well completed in a shale gas reservoir. We present the flow rate data and the cumulative production data which spans almost 7.8 years in **Fig. 4.16**.

Our first task is to match the subsets of the flow rate data with the "hyperbolic" rate decline relation. In **Fig. 4.17** we present the "hyperbolic" model matches imposed on the flow rate data, the and *D*- and *b*-parameter trends. Every subset of the data is matched with a "hyperbolic" *b*-parameter greater than 1 indicating that complete boundary-dominated flow has not been established. In **Fig. 4.18** the *b*-parameter value changes over time and is relatively stable after about 1,000 days of production — in particular, the *b*-parameter value decreases from 2.84 to 1.95 during the production history. This change corresponds to the change in *EUR* with time. The *EUR* predicted by the "hyperbolic" relation decrease from 3.23 BSCF to 2.00 BSCF during the 2,844 days of production for this well.

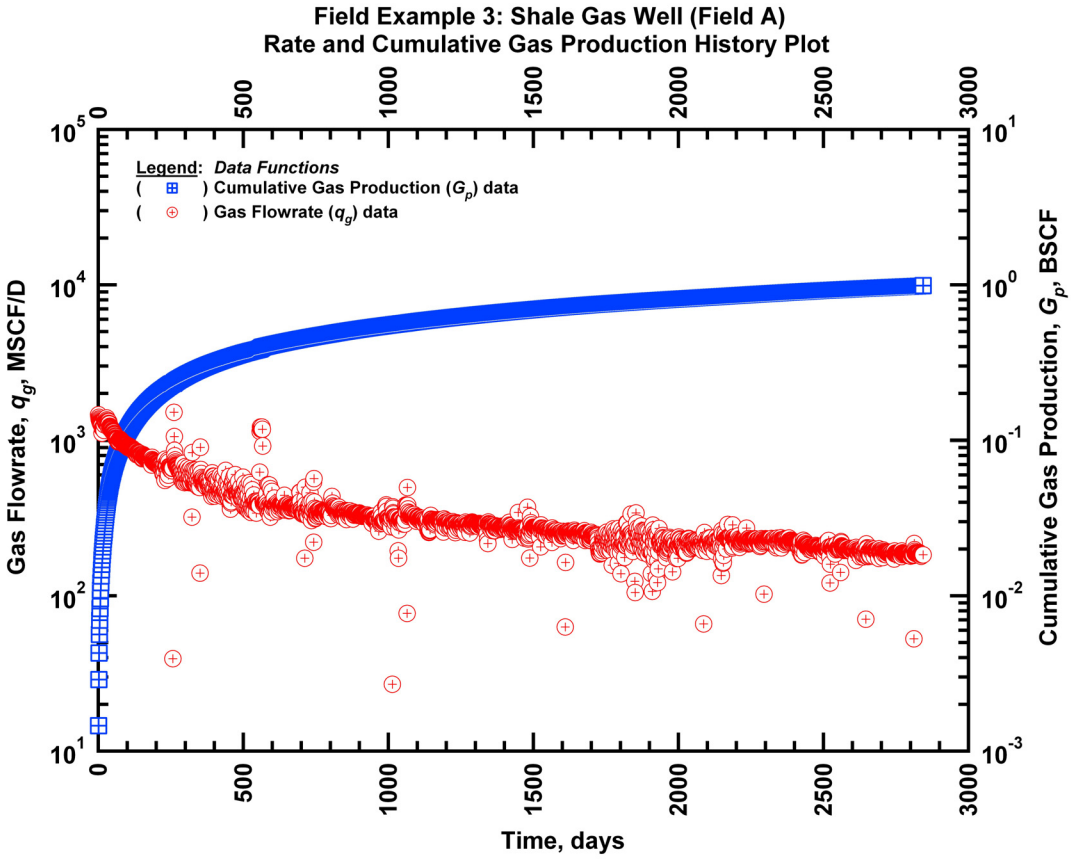

Figure 4.16 — (Semi-log Plot): Production history plot for field example 3 — flow rate (q_g) and cumulative production (G_p) versus production time.

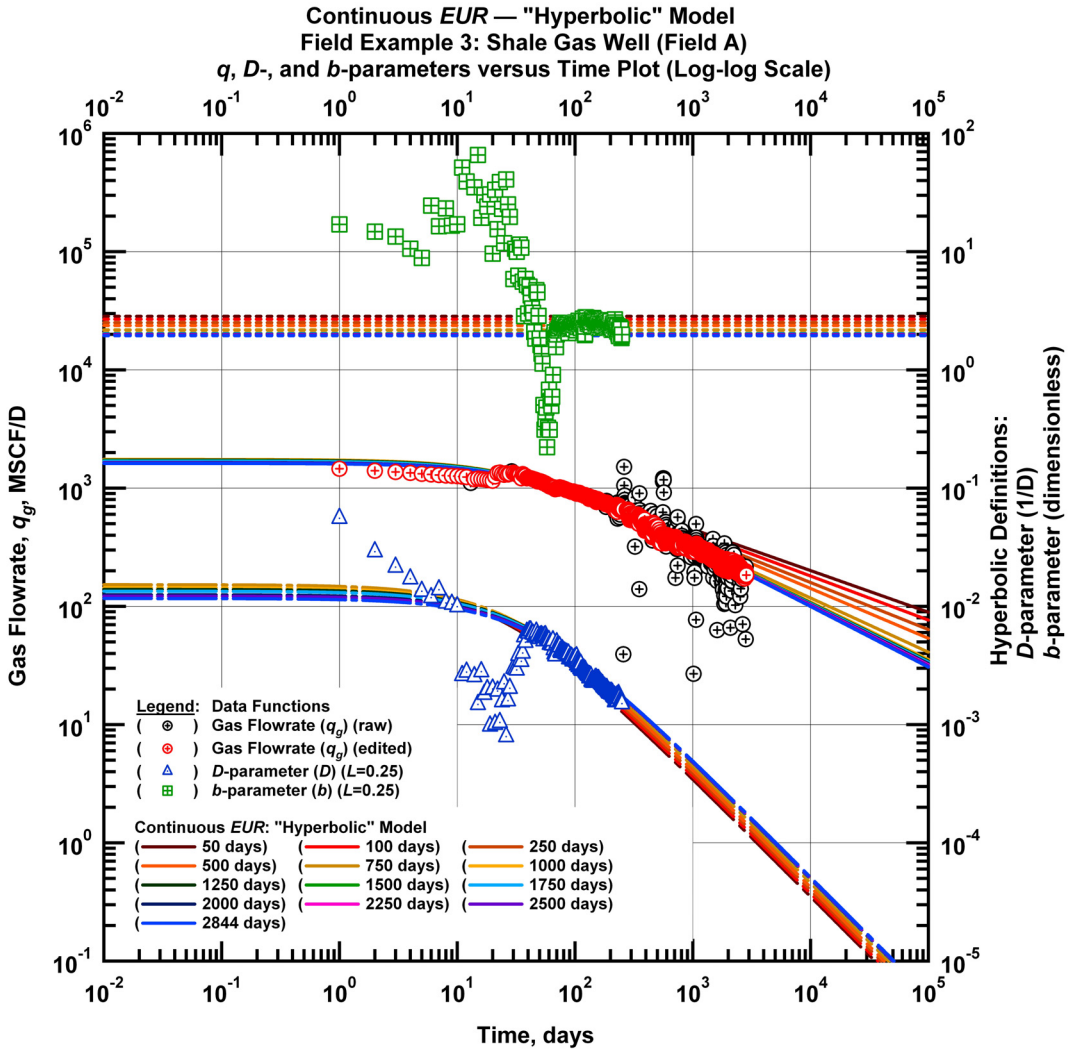

Figure 4.17 — (Log-log Plot): *qDb* plot — flow rate (q_g), *D*- and *b*-parameters versus production time and "hyperbolic" model matches for field example 3.

Next we employ the power law exponential rate decline relation to obtain an estimate of *EUR* for each interval (or subset) of the data. In **Fig. 4.19** we present the power law exponential model matches imposed on the flow rate data and the *D*- and *b*-parameter trends. Again for this case a D_∞ value is not used for all of the model matches indicating that boundary-dominated flow character is not observed. The model matches stabilize and become relatively constant after about 750 days of production for each additional interval.

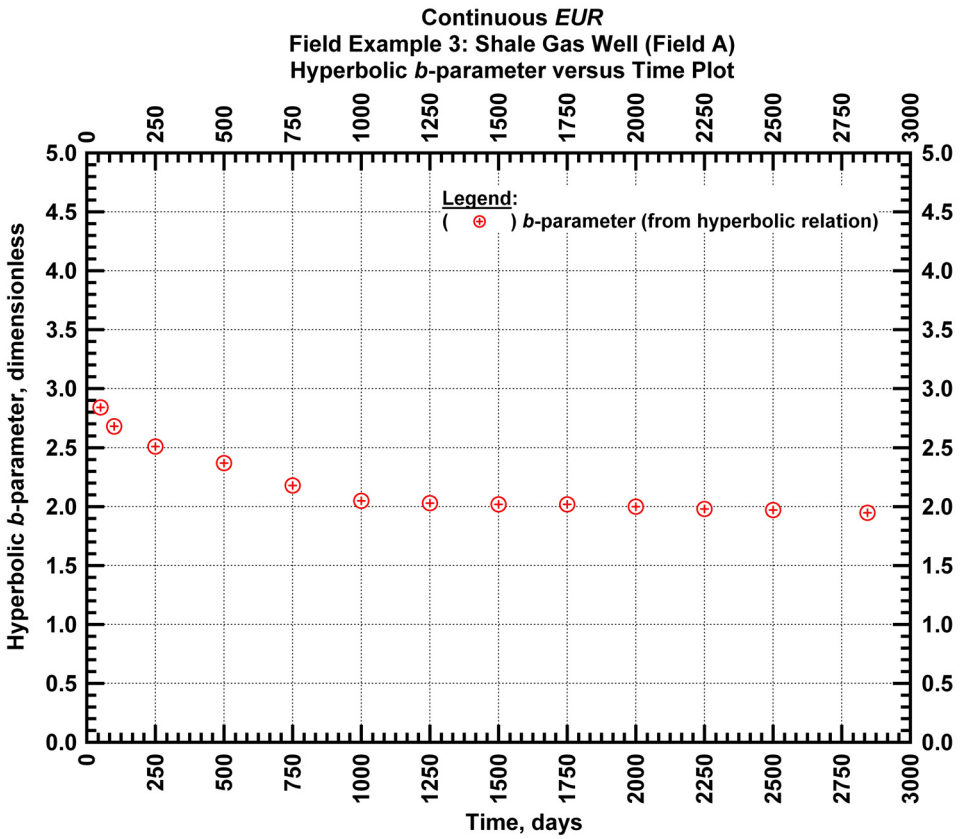

Figure 4.18 — (Cartesian Plot): Hyperbolic *b*-parameter values obtained from model matches with production data for field example 3.

In **Fig. 4.20** we show the results of the straight line extrapolation technique for this case. The *x*-axis intercepts of the extrapolated lines increase with time resulting in an increasing estimate of $G_{p,max}$ over time.

The last step in our workflow is to calculate the *EUR* values based on the matches obtained with the "hyperbolic" and the power law exponential rate decline relations and the $G_{p,max}$ values obtained from the straight line extrapolation technique. In **Fig. 4.21** we present the calculated *EUR* and $G_{p,max}$ values versus production time. The *EUR* values obtained from the "hyperbolic" and power law exponential model matches decrease at early times but appear to stabilize after about 750 days of production. The *EUR* values estimated from the "hyperbolic" model matches converge at late times to a value of 2.00 BSCF. The *EUR* from the power law exponential model is constant at 1.88 BSCF after 1,250 days of production. The *EUR* of this well should be between 1.85 BSCF (the "lower" limit given by the straight line extrapolation technique at 2,844 days) and 1.88 BSCF (the "upper" limit given by the power law exponential estimate at 2,844 days).

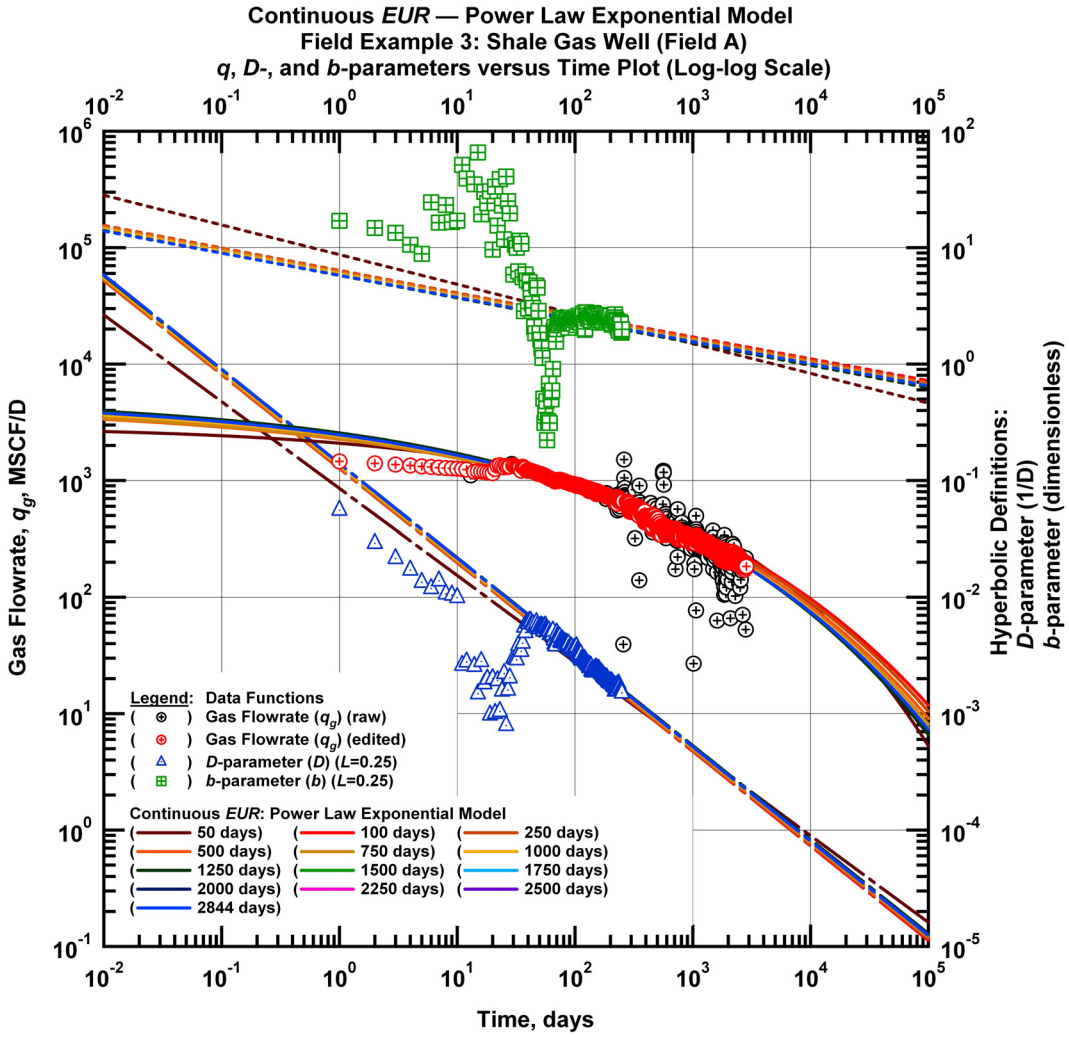

Figure 4.19 — (Log-log Plot): *qDb* plot — flow rate (q_g), *D*- and *b*-parameters versus production time and power law exponential model matches for field example 3.

Tables 4.8, 4.9, and 4.10 present the model parameters along with the *EUR* values for each interval using the rate-time models and the straight line extrapolation technique.

Additional continuous *EUR* examples for the shale gas wells producing from the field A are included in **Appendix D**. **Table 4.11** includes analysis results for the 11 shale gas wells producing from field A. The *EUR* values and $G_{p,max}$ estimates shown for each well were obtained from the analysis of the entire production history. The *EUR* values obtained using the "hyperbolic" model are up to 60% or 1.5 BSCF greater than the estimates given by the power law exponential model. **Fig. 4.24** shows a comparison of the *EUR* values obtained using the "hyperbolic" relation, and **Fig. 4.25** shows a comparison of the *EUR*

obtained using the power law exponential relation for all of the wells analyzed from field A. Field examples 3 and 17 through 20 are hydraulically fractured vertical wells. The final *EUR* values given by the power law exponential model for these wells range between 0.98 and 2.18 BSCF. The *EUR* values given by the power law exponential model stabilize after 250 to 750 days of production. Field examples 21 through 26 are horizontal wells that were stimulated with hydraulic fracture treatments. The final *EUR* values given by the power law exponential model for these wells range between 2.50 and 3.54 BSCF. These estimates appear to stabilize after 100 to 400 days of production. **Fig. 4.26** shows a comparison of the "hyperbolic" *b*-parameter for all of the wells analyzed from field A. The *b*-parameter trends exhibit similar behavior and decrease at early times then stabilize at late times. The *b*-parameter for the wells with the longest producing times (field examples 3, 17, 18, and 19) stabilize between 1.95 and 2.14.

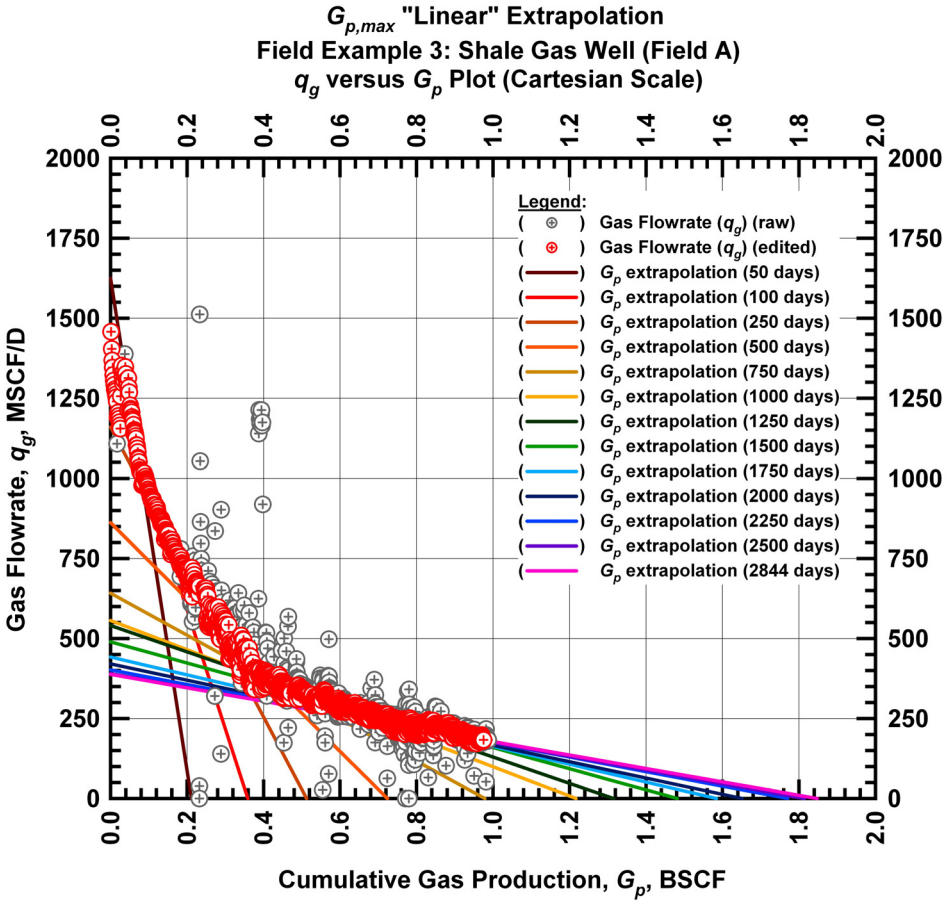

Figure 4.20 — (Cartesian Plot): Rate Cumulative Plot — flow rate (q_g) versus cumulative production (G_p) and the linear trends fit through the data for field example 3.

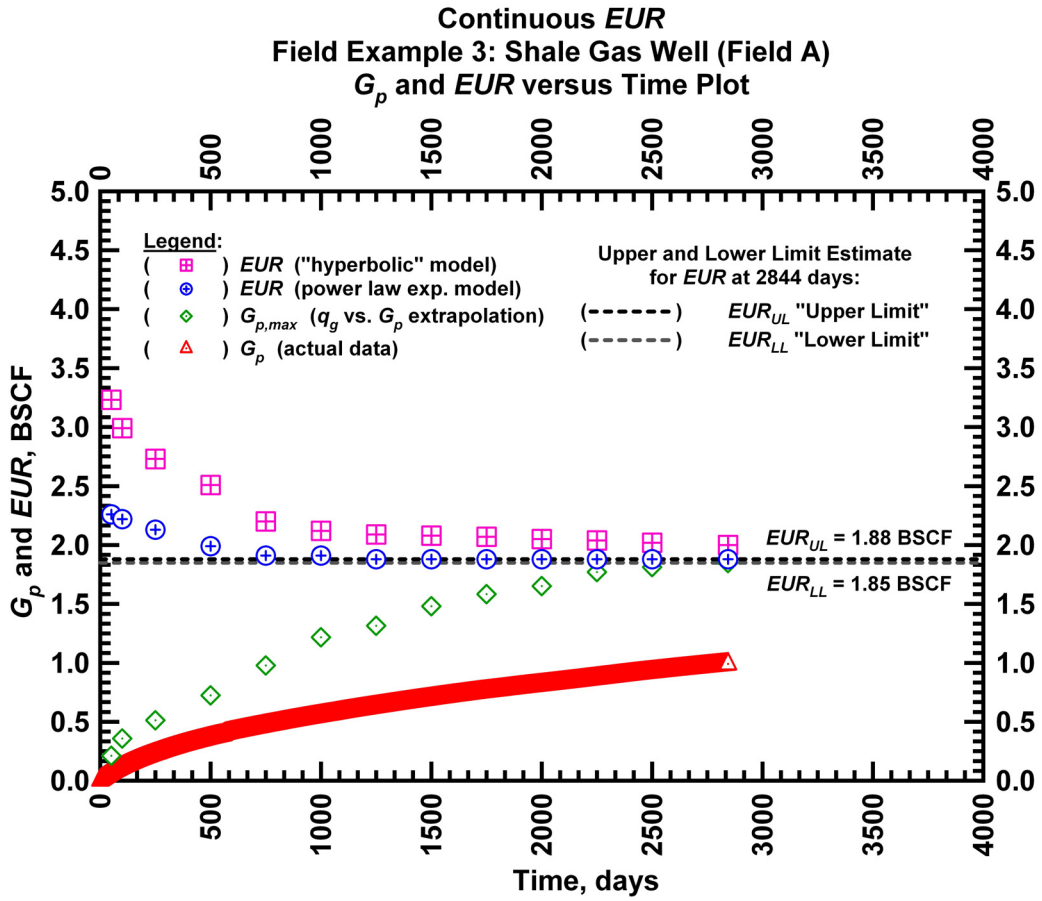

Figure 4.21 — (Cartesian Plot): *EUR* estimates from model matches and $G_{p,max}$ estimates from extrapolation technique for field example 3.

Table 4.8 — Analysis results for field example 3 — "hyperbolic" model parameters.

Time Interval, days	q_{gi} (MSCFD)	D_i (D^{-1})	b (dimensionless)	EUR_{hyp} (BSCF)
50	1,703	0.0152	2.84	3.23
100	1,703	0.0152	2.68	2.99
250	1,703	0.0152	2.51	2.73
500	1,703	0.0152	2.37	2.51
750	1,691	0.0152	2.18	2.20
1,000	1,751	0.0144	2.05	2.12
1,250	1,727	0.0139	2.03	2.09
1,500	1,703	0.0134	2.02	2.08
1,750	1,691	0.0134	2.02	2.07
2,000	1,645	0.0125	2.00	2.05
2,250	1,634	0.0121	1.98	2.04
2,500	1,634	0.0122	1.97	2.02
2,844	1,618	0.0116	1.95	2.00

Table 4.9 — Analysis results for field example 3 — power law exponential model parameters.

Time Interval, days	$\hat{q}_{gi}$ (MSCFD)	$\hat{D}_i$ (D^{-1})	n (dimensionless)	D_∞ (D^{-1})	EUR_{PLE} (BSCF)
50	2,921	0.335	0.255	0	2.26
100	4,739	0.689	0.188	0	2.22
250	4,422	0.656	0.193	0	2.13
500	4,422	0.671	0.193	0	1.99
750	4,546	0.686	0.193	0	1.91
1,000	4,872	0.702	0.193	0	1.91
1,250	5,293	0.725	0.193	0	1.88
1,500	5,149	0.736	0.190	0	1.88
1,750	5,149	0.736	0.190	0	1.88
2,000	5,149	0.736	0.190	0	1.88
2,250	5,149	0.736	0.190	0	1.88
2,500	5,149	0.736	0.190	0	1.88
2,844	5,149	0.736	0.190	0	1.88

Table 4.10 — Analysis results for field example 3 — straight line extrapolation.

Time Interval, days	Slope, 10^{-6} D^{-1}	Intercept, MSCF/D	$G_{p,max}$ (BSCF)
50	7,690	1,625	0.21
100	3,712	1,332	0.36
250	2,263	1,160	0.51
500	1,190	862	0.72
750	656	642	0.98
1,000	457	556	1.22
1,250	411	541	1.32
1,500	330	490	1.48
1,750	279	442	1.58
2,000	255	421	1.65
2,250	227	402	1.77
2,500	215	390	1.81
2,844	210	388	1.85

Table 4.11 — Analysis results for field examples from field A.

Field Example	Producing Time (D)	b (dimensionless)	EUR_{hyp} (BSCF)	EUR_{PLE} (BSCF)	$G_{p,max}$ (BSCF)
3	2,844	1.95	2.00	1.88	1.85
17	2,692	2.09	1.61	1.53	1.44
18	2,558	2.01	1.07	0.98	0.89
19	3,159	2.14	1.87	1.78	1.68
20	2,485	1.41	2.18	2.18	1.96
21	1,071	2.68	3.72	3.54	2.25
22	350	2.06	4.00	2.50	1.52
23	899	2.18	2.92	2.77	1.91
24	919	1.85	3.03	2.94	1.87
25	504	2.57	3.30	2.73	1.10
26	502	2.01	2.75	2.60	1.06

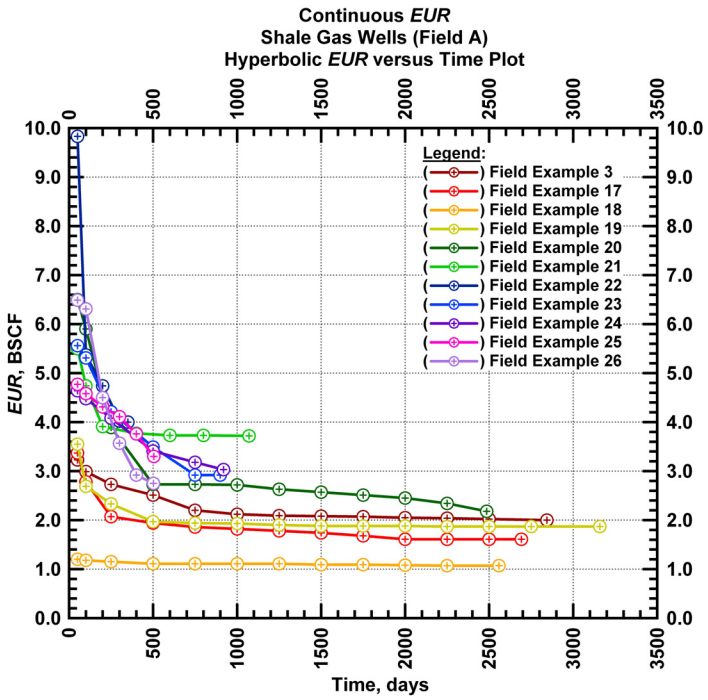

Figure 4.22 — (Cartesian Plot): Comparison of the hyperbolic *EUR* estimates for the shale gas wells producing from field A.

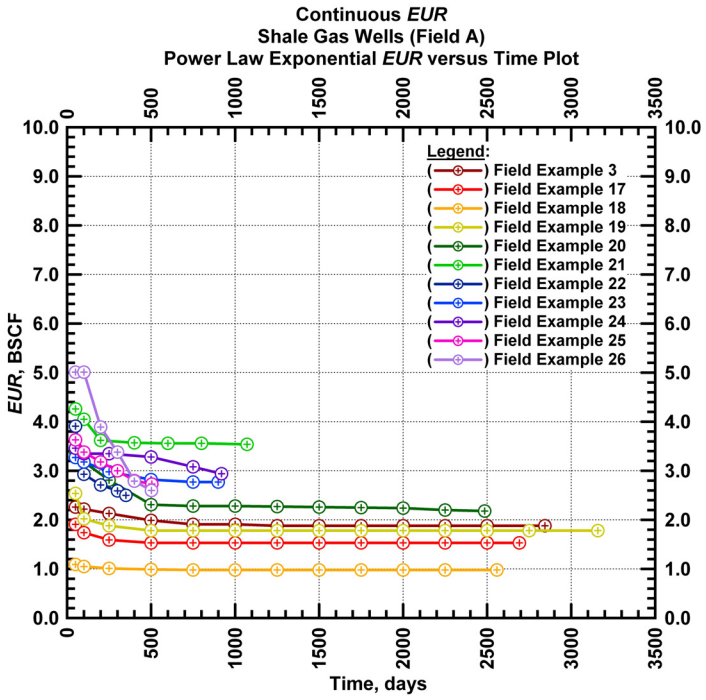

Figure 4.23 — (Cartesian Plot): Comparison of the power law exponential *EUR* estimates for the shale gas wells producing from field A.

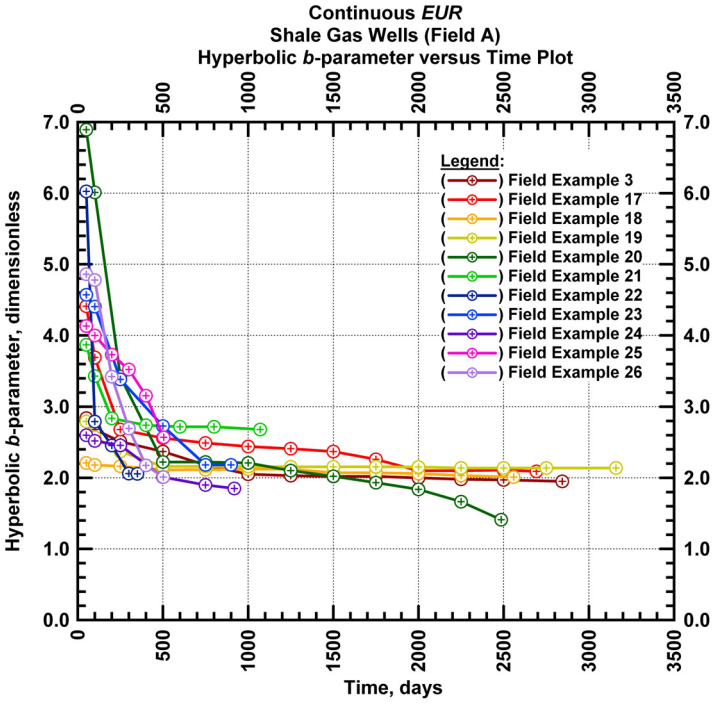

Figure 4.24 — (Cartesian Plot): Comparison of the hyperbolic *b*-parameter for the shale gas wells producing from field A.

4.4 Field Example 4: Shale Gas Well (Field B)

We apply our proposed methodology to the production data acquired from a hydraulically fractured horizontal well completed in a shale gas reservoir. We present the flow rate data and the cumulative production data which spans over 1 year in **Fig. 4.25**.

Our first task is to match the subsets of the flow rate data with the "hyperbolic" rate decline relation. In **Fig. 4.26** we present the "hyperbolic" model matches imposed on the flow rate data, and *D*- and *b*-parameter trends. We use calibration by hand and regression to find a best match with each previously specified interval. For all of the model matches using the "hyperbolic" relation, we obtain *b*-parameter values greater than 1 again indicating that transient flow regime effects are still dominant. In **Fig. 4.27** we observe that the *b*-parameter value decreases at early times and begins to stabilize at late times (for longer intervals). Specifically, the *b*-parameter value decreases from 2.59 to 1.49 during the production history (from the shortest subset of 50 days to the entire production history).

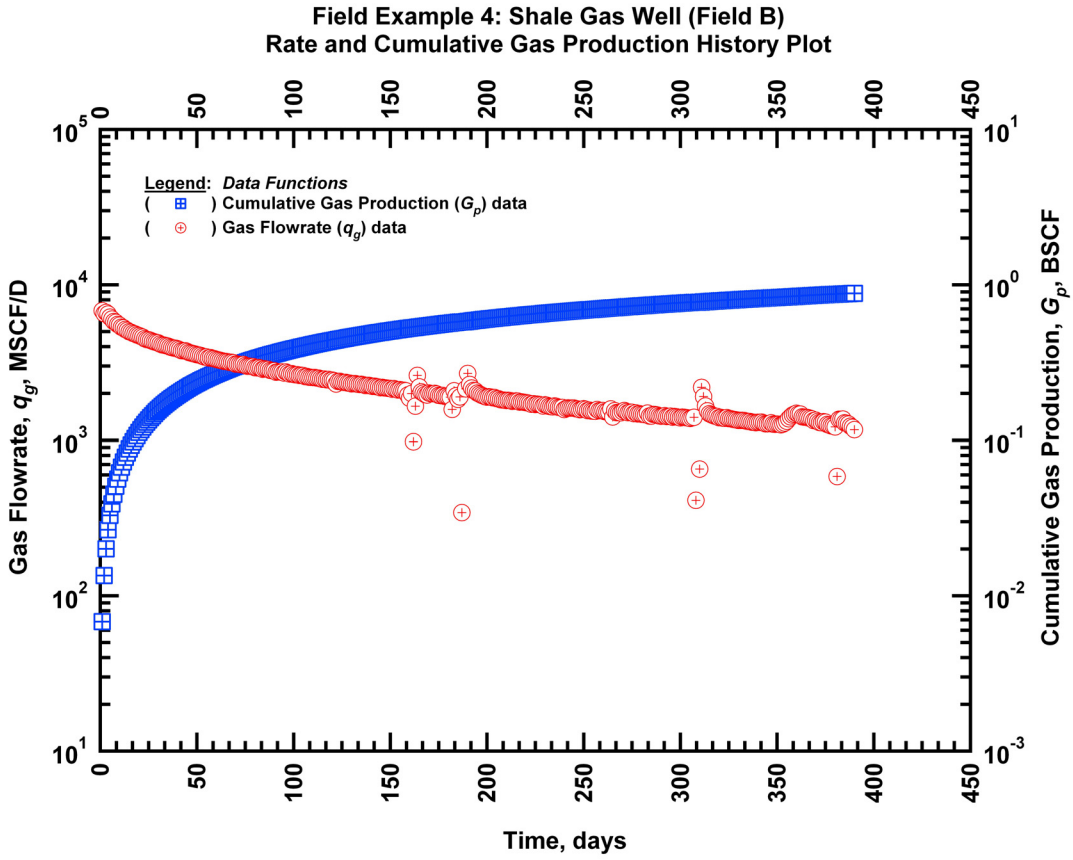

Figure 4.25 — (Semi-log Plot): Production history plot for field example 4 — flow rate (q_g) and cumulative production (G_p) versus production time.

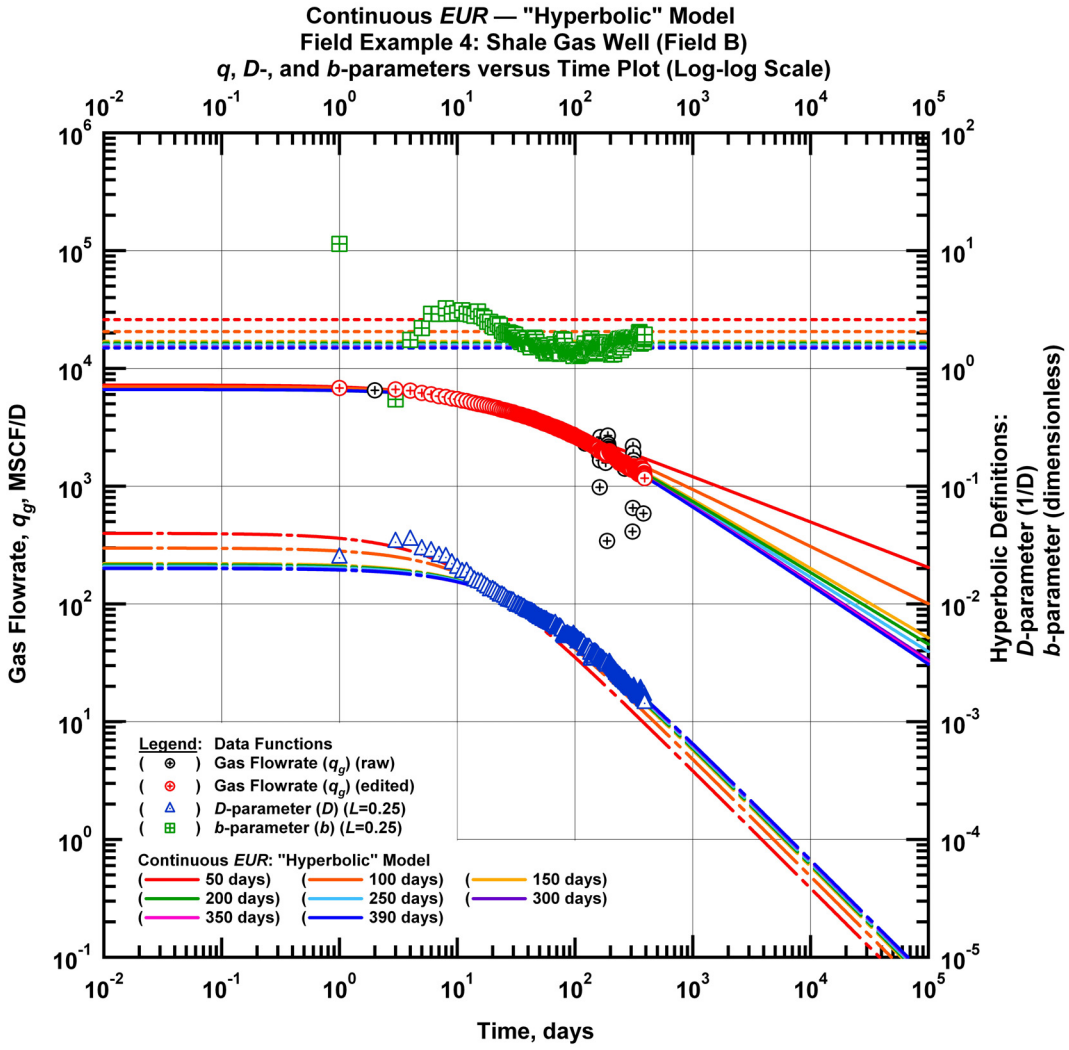

Figure 4.26 — (Log-log Plot): *qDb* plot — flow rate (q_g), *D*- and *b*-parameters versus production time and "hyperbolic" model matches for field example 4.

Following our procedure, we next use the power law exponential model to match the subsets of the flow rate data and estimate the *EUR* values. In **Fig. 4.28** we present the power law exponential model matches imposed on the flow rate data, and *D*- and *b*-parameter trends. Once again the D_∞ term is not used in the power law exponential model which suggests that boundary-dominated flow regime effects have not started to evolve. The model stabilizes and becomes relatively constant after 100 days of production.

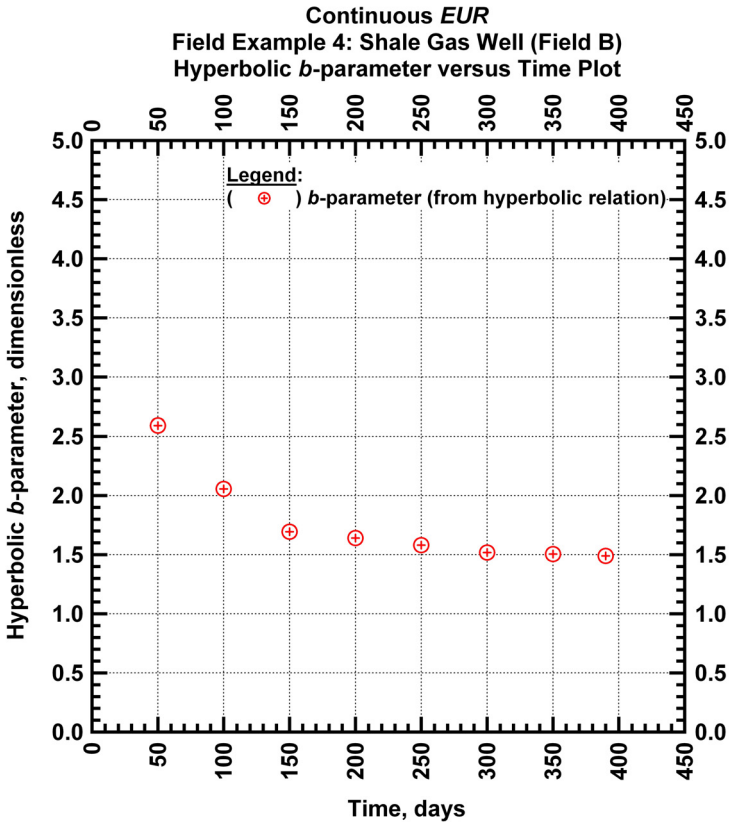

Figure 4.27 — (Cartesian Plot): Hyperbolic *b*-parameter values obtained from model matches with production data for field example 4.

In **Fig. 4.29** we show the results of the straight line extrapolation technique for this case. The *x*-axis intercept of the extrapolated lines increases with time resulting in an increasing estimate of $G_{p,max}$.

Finally we plot the *EUR* based on the matches obtained with the "hyperbolic" and the power law exponential rate decline relations. In **Fig. 4.30** we present the calculated *EUR* and $G_{p,max}$ values versus production time.

The *EUR* values obtained from the "hyperbolic" relation continue to decrease with time as the estimates obtained from the power law exponential model are almost constant after 100 days of production. As mentioned earlier the *EUR* values estimated from the power law exponential model matches are more conservative the than value estimated from the hyperbolic model matches especially at early times. The *EUR* of this well should be between 1.60 BSCF (the "lower" limit given by the straight line extrapolation technique at 2,000 days) and 3.03 BSCF (the "upper" limit given by the power law exponential estimate at 2,000 days). For reference the model parameter values and the *EUR* values for each interval analyzed are presented in **Tables 4.12, 4.13, and 4.14**.

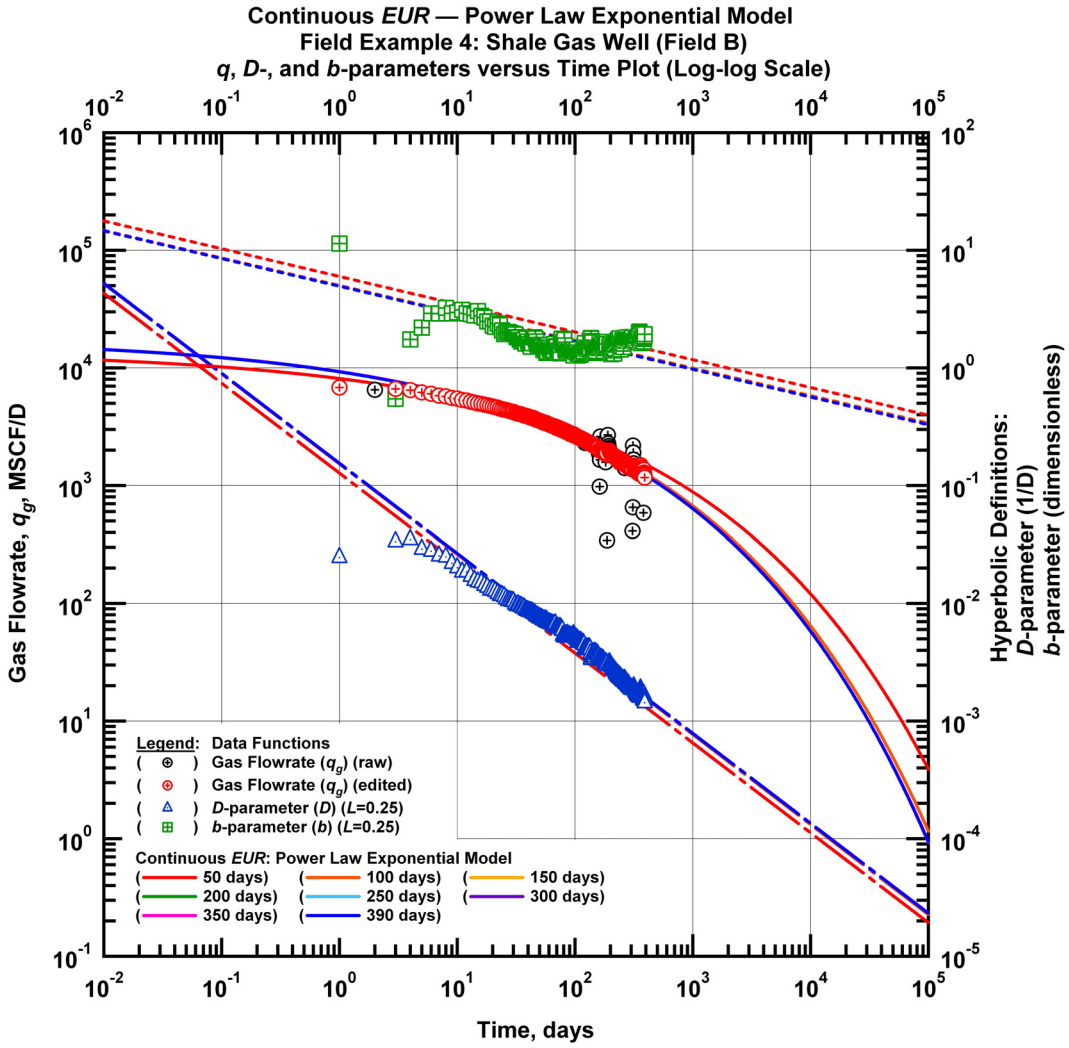

Figure 4.28 — (Log-log Plot): *qDb* plot — flow rate (q_g), *D*- and *b*-parameters versus production time and power law exponential model matches for field example 4.

Additional continuous *EUR* examples for the shale gas wells producing from the field B are included in **Appendix E**. **Table 4.15** includes analysis results for the 9 hydraulically fractured horizontal shale gas wells producing from field B. The *EUR* values and $G_{p,max}$ estimates shown for each well were obtained from the analysis of the entire production history. The *EUR* values obtained using the "hyperbolic" model are 6.5 to 75% or 0.13 to 1.92 BSCF greater than the estimates given by the power law exponential model. **Fig. 4.31** shows a comparison of the *EUR* values obtained using the "hyperbolic" relation, and **Fig. 4.32** shows a comparison of the *EUR* values obtained using the power law exponential relation for all of the wells analyzed from field B. The final *EUR* values given by the power law exponential model for

examples 4 and 27 through 32 range between 1.54 and 3.03 BSCF, and the estimates stabilize after 100 to 250 days of production. The final *EUR* values given by the power law exponential model for examples 33 and 34 range between 5.85 and 9.44 BSCF. The *EUR* for field example 33 become constant after 350 days of production, and the estimates for field example 34 continue to decrease after 200 days of production. Field examples 33 and 34 are producing from a different area of the field explaining the difference in the *EUR* compared to values obtained for the other examples. **Fig. 4.33** shows a comparison of the "hyperbolic" *b*-parameter for all of the wells analyzed from field B. The *b*-parameter appears to stabilize between 1.19 and 1.49 for most of the wells indicating that boundary-dominated flow has not been established.

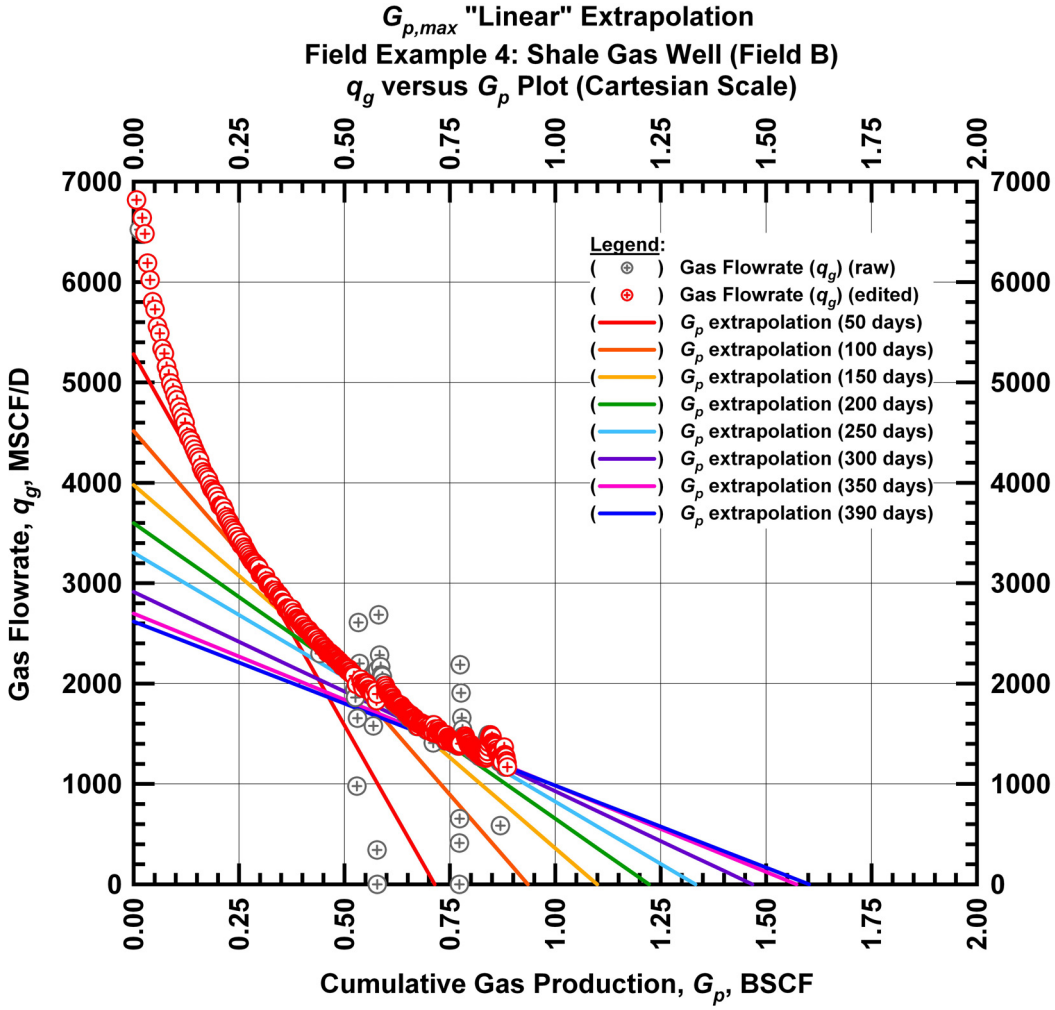

Figure 4.29 — (Cartesian Plot): Rate Cumulative Plot — flow rate (q_g) versus cumulative production (G_p) and the linear trends fit through the data for field example 4.

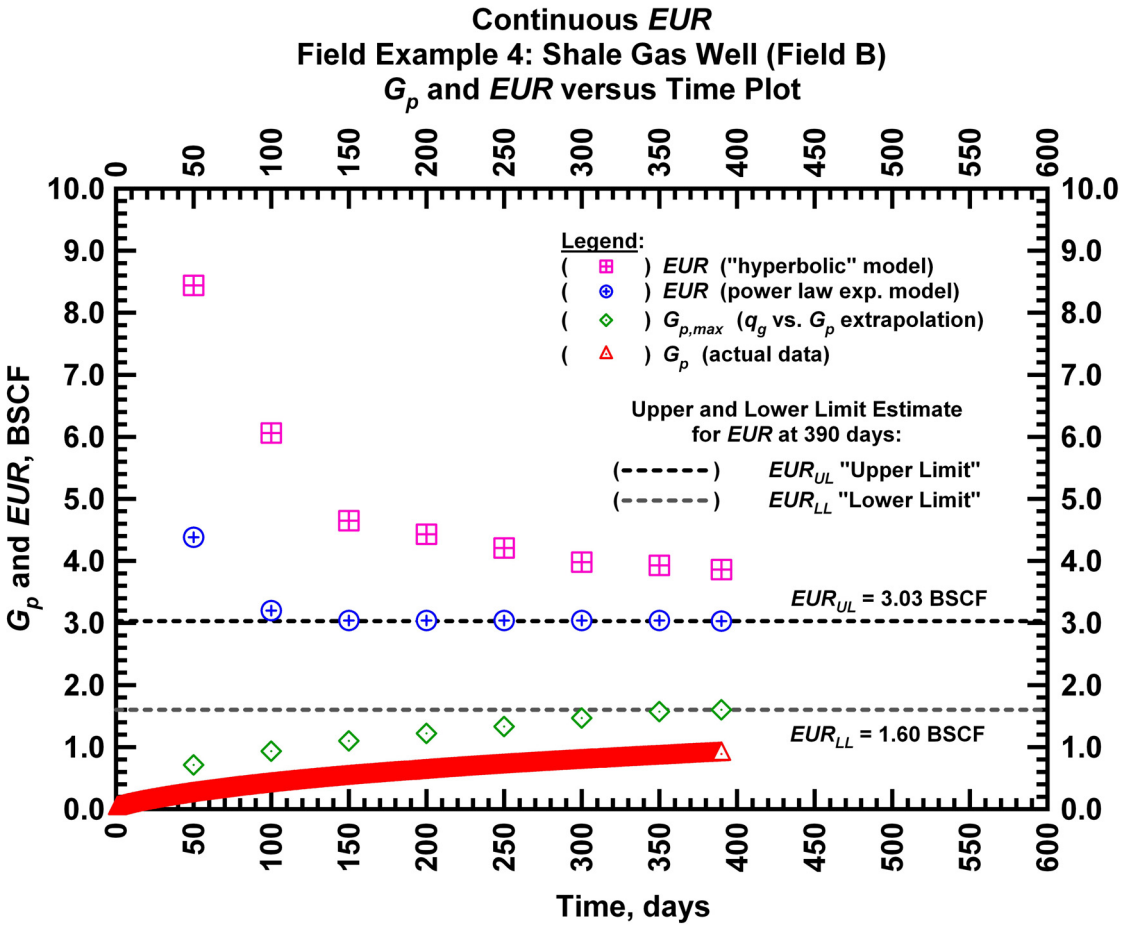

Figure 4.30 — (Cartesian Plot): *EUR* estimates from model matches and $G_{p,max}$ estimates from extrapolation technique for field example 4.

Table 4.12 — Analysis results for field example 4 — "hyperbolic" model parameters.

Time Interval, days	q_{gi} (MSCFD)	D_i (D^{-1})	b (dimensionless)	EUR_{hyp} (BSCF)
50	7,226	0.03981	2.59	8.44
100	6,984	0.02983	2.06	6.06
150	6,612	0.02204	1.69	4.65
200	6,612	0.02153	1.64	4.43
250	6,612	0.02087	1.58	4.21
300	6,612	0.02014	1.52	3.98
350	6,612	0.01997	1.50	3.93
390	6,612	0.01997	1.49	3.86

Table 4.13 — Analysis results for field example 4 — power law exponential model parameters.

Time Interval, days	$\hat{q}_{gi}$ (MSCFD)	$\hat{D}_i$ (D^{-1})	n (dimensionless)	D_∞ (D^{-1})	EUR_{PLE} (BSCF)
50	13,936	0.541	0.236	0	4.38
100	17,875	0.652	0.234	0	3.20
150	17,875	0.652	0.236	0	3.04
200	17,875	0.652	0.236	0	3.04
250	17,875	0.652	0.236	0	3.04
300	17,875	0.652	0.236	0	3.04
350	17,875	0.652	0.236	0	3.04
390	17,875	0.657	0.235	0	3.03

Table 4.14 — Analysis results for field example 4 — straight line extrapolation.

Time Interval, days	Slope, 10^{-6} D^{-1}	Intercept, MSCF/D	$G_{p,max}$ (BSCF)
50	7,395	5,281	0.71
100	4,829	4,515	0.93
150	3,618	3,978	1.10
200	2,944	3,598	1.22
250	2,479	3,303	1.33
300	1,985	2,913	1.47
350	1,716	2,698	1.57
390	1,634	2,618	1.60

Table 4.15 — Analysis results for field examples from field B.

Field Example	Producing Time (D)	b (dimensionless)	EUR_{hyp} (BSCF)	EUR_{PLE} (BSCF)	$G_{p,max}$ (BSCF)
4	390	1.49	3.86	3.03	1.60
27	301	1.53	2.68	1.80	0.94
28	313	1.19	2.74	2.02	1.24
29	272	1.35	4.48	2.56	1.86
30	207	1.40	2.83	1.71	1.05
31	171	1.24	2.14	2.01	0.77
32	222	2.41	1.79	1.54	0.36
33	373	1.29	7.20	5.85	3.20
34	206	1.15	11.32	9.44	4.56

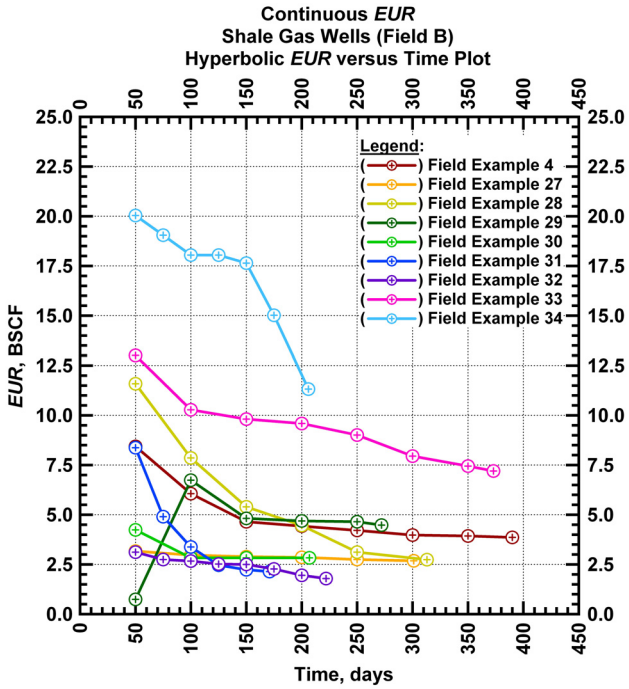

Figure 4.31 — (Cartesian Plot): Comparison of the hyperbolic *EUR* estimates for the shale gas wells producing from field B.

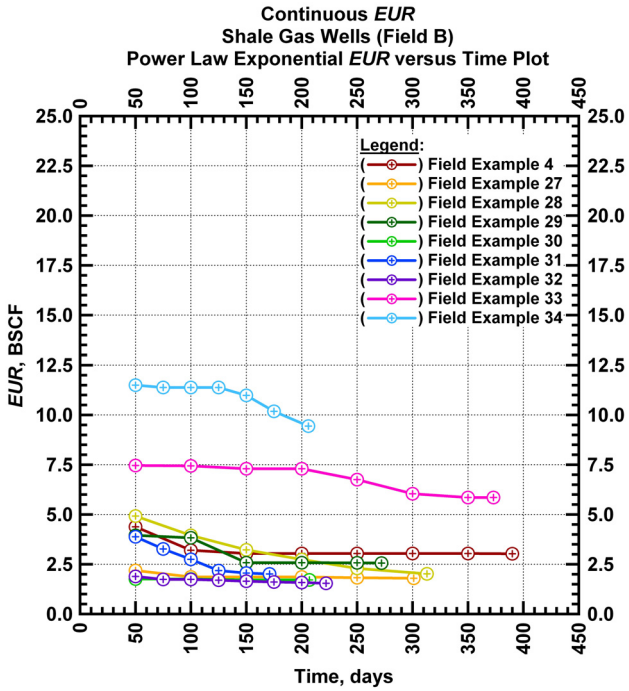

Figure 4.32 — (Cartesian Plot): Comparison of the power law exponential *EUR* estimates for the shale gas wells producing from field B.

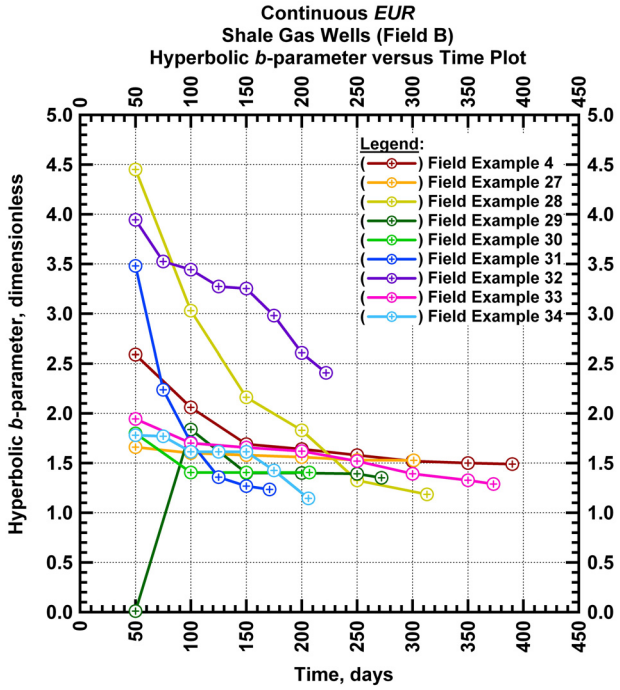

Figure 4.33 — (Cartesian Plot): Comparison of the hyperbolic *b*-parameter for the shale gas wells producing from field B.

4.5 Field Example 5: Shale Gas Well (Field C)

We apply our proposed methodology to the production data acquired from a hydraulically fractured horizontal well completed in a shale gas reservoir. We present the flow rate data and the cumulative production data which spans 0.8 years in **Fig. 4.34**.

The subsets of the flow rate data are matched with the "hyperbolic" rate decline relation initially. In **Fig. 4.35** we present the "hyperbolic" model matches imposed on the flow rate data, and *D*- and *b*-parameter trends. Every subset of the data is matched with a "hyperbolic" *b*-parameter greater than 1 indicating that complete boundary-dominated flow regime effects are not established. In **Fig. 4.36** we observe the behavior of the *b*-parameter as a function of time. The *b*-parameter value increases at early times and then stabilizes after around 2.8 after about 100 days of production. We attribute the early time behavior to well clean-up or flowback from the stimulation treatment performed on this well.

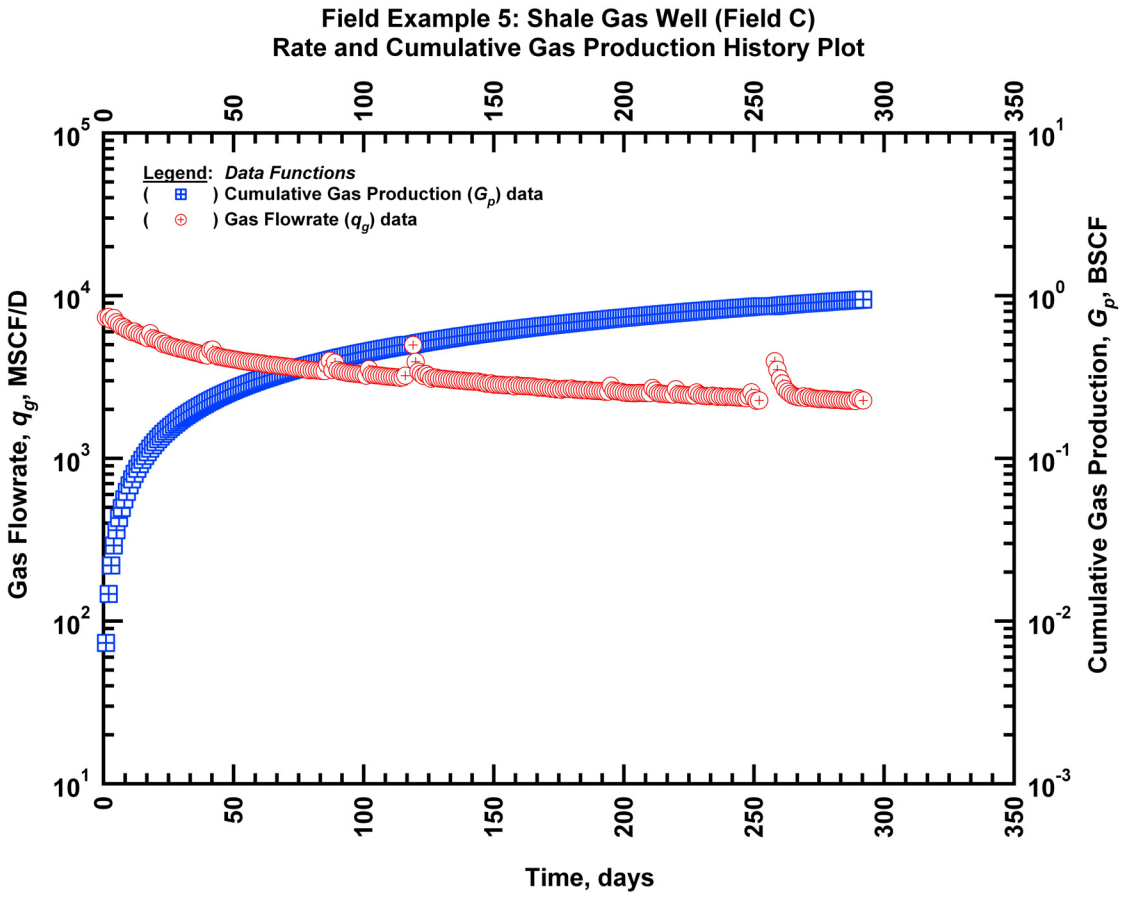

Figure 4.34 — (Semi-log Plot): Production history plot for field example 5 — flow rate (q_g) and cumulative production (G_p) versus production time.

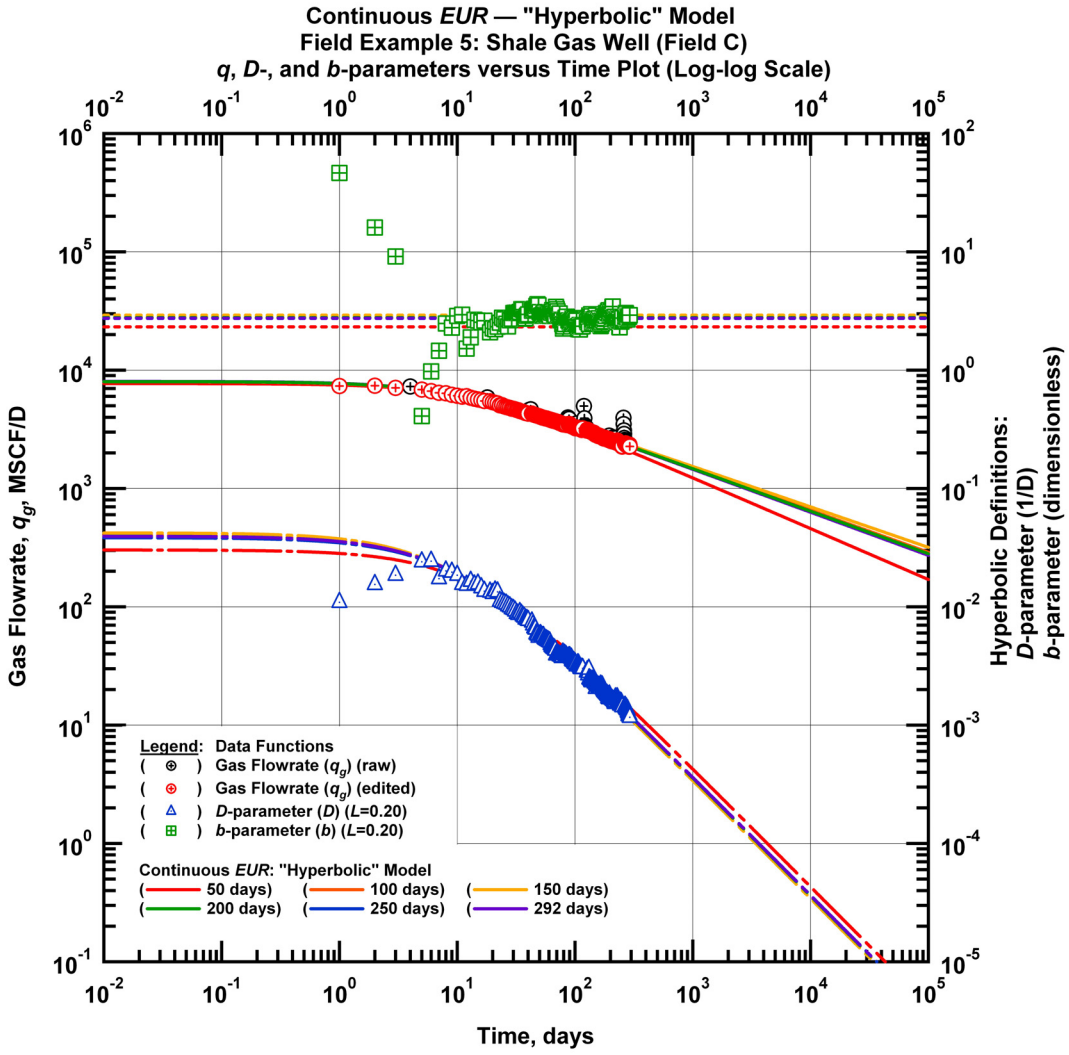

Figure 4.35 — (Log-log Plot): *qDb* plot — flow rate (q_g), *D*- and *b*-parameters versus production time and "hyperbolic" model matches for field example 5.

Next the selected subsets of the flow rate data are matched with the power law exponential rate decline relation. In **Fig. 4.37** we present the power law exponential model matches imposed on the flow rate data, and *D*- and *b*-parameter trends. For all matches the D_∞ term is not used in the model — as dictated by the data character (*i.e.*, power law *D*-parameter trend). The model matches are identical during the entire production history. In particular, the character of the data — specifically the computed *D*-parameter trend — for the smallest interval (50 days) is identical to the character of the data for the largest interval (292 days) resulting in almost identical power law exponential rate model matches. Therefore, the *EUR* from the power law exponential model is constant for this case.

In **Fig. 38** we show the results of the straight line extrapolation technique for this case. The *x*-axis intercept of the extrapolated lines increase with time resulting in an increasing estimate of $G_{p,max}$.

The last step in our workflow is to calculate the *EUR* based on the matches obtained with the "hyperbolic" and the power law exponential rate decline relations. In **Fig. 4.39** we present the calculated *EUR* values versus production time. The *EUR* obtained from the "hyperbolic" relation stabilize around 10.4 BSCF after 250 days of production. The estimates provided by the power law exponential relation are constant at 6.82 BSCF during the entire producing life of this well.

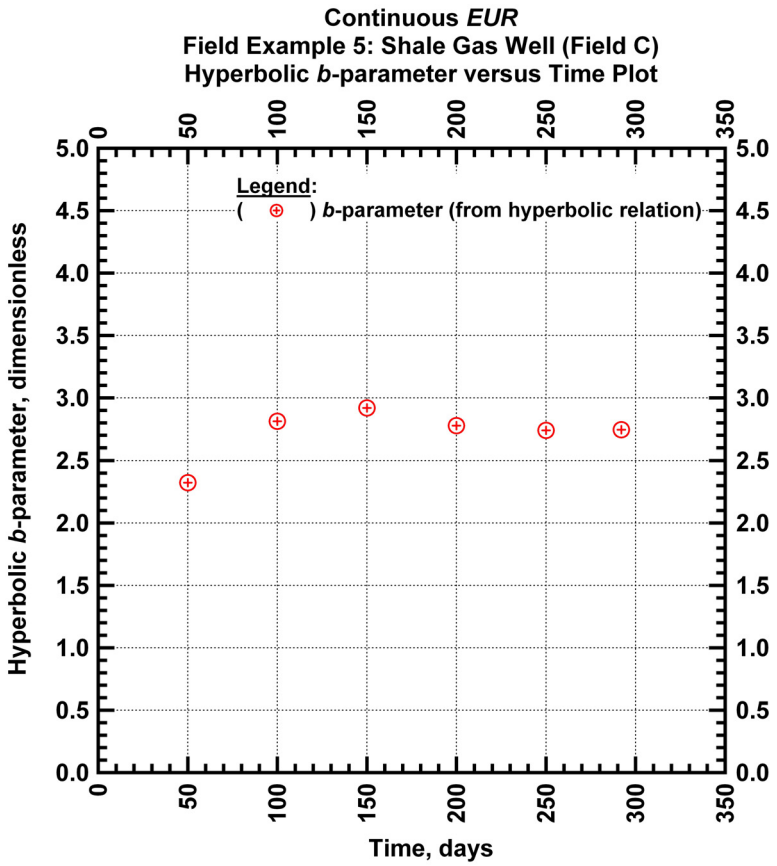

Figure 4.36 — (Cartesian Plot): Hyperbolic *b*-parameter values obtained from model matches with production data for field example 5.

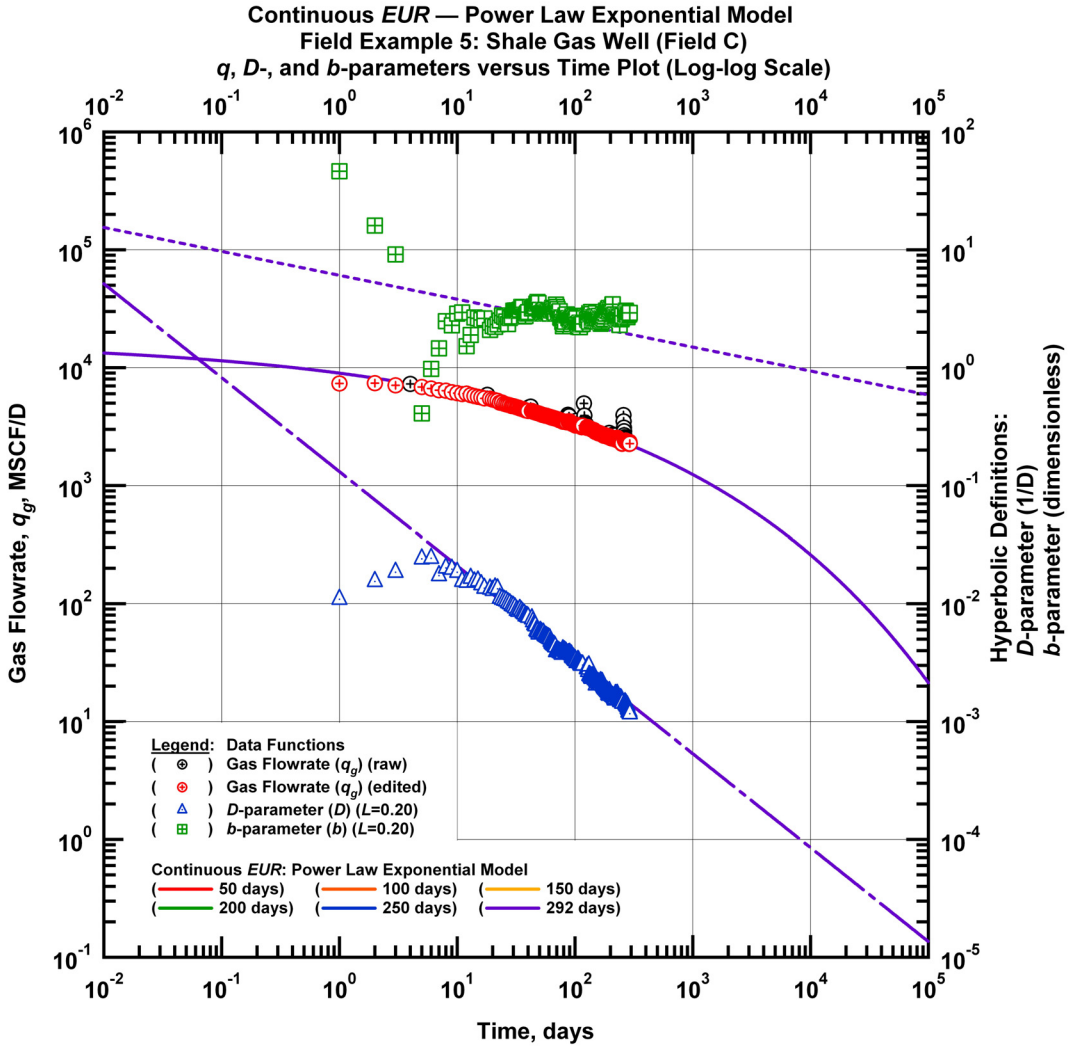

Figure 4.37 — (Log-log Plot): *qDb* plot — flow rate (q_g), *D*- and *b*-parameters versus production time and power law exponential model matches for field example 5.

The $G_{p,max}$ values obtained from straight line extrapolation also shown by **Fig. 4.39** increase with time, and they are always less than the estimates provided by the rate-time relations. Also we observe that $G_{p,max}$ values obtained from straight line extrapolation still appear to increase at late times — $G_{p,max}$ values appear not to stabilize. Consequently, the *EUR* of this well should be in between 2.97 BSCF (the "lower" limit given by the straight line extrapolation technique at 292 days) and 6.82 BSCF (the "upper" limit given by the power law exponential estimate at 292 days). The model parameters for this well are summarized in **Tables 4.16, 4.17, and 4.18**.

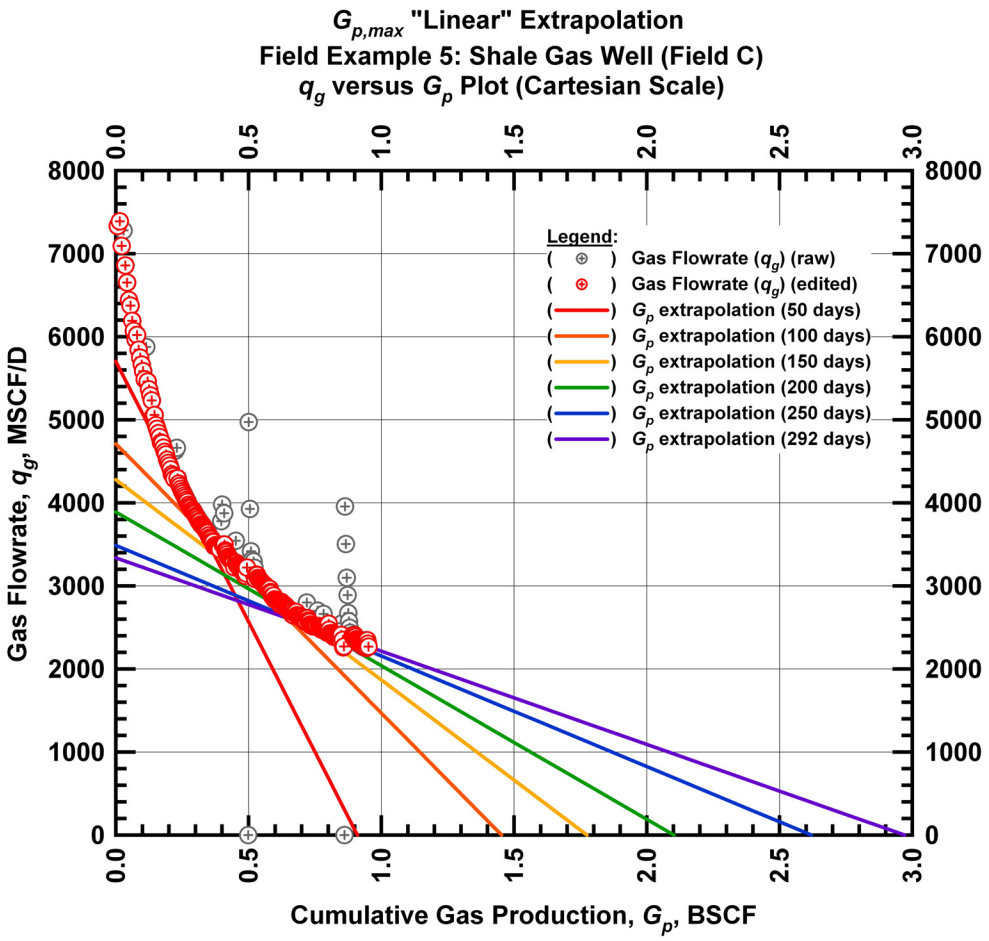

Figure 4.38 — (Cartesian Plot): Rate Cumulative Plot — flow rate (q_g) versus cumulative production (G_p) and the linear trends fit through the data for field example 5.

Additional continuous *EUR* examples for shale gas wells producing from the field C are included in **Appendix F**. **Table 4.19** includes analysis results for the 7 horizontal shale gas wells producing from field C. The *EUR* values obtained using the "hyperbolic" model are 15% to 107% or 0.8 to 6.1 BSCF greater than the estimates given by the power law exponential model. **Fig. 4.40** shows a comparison of the *EUR* values obtained using the "hyperbolic" relation, and **Fig. 4.41** shows a comparison of the *EUR* values obtained using the power law exponential relation for all of the wells analyzed from field C. The final *EUR* values given by the power law exponential model range between 2.47 and 6.82 BSCF, and the estimates are relatively stable or constant for the entire production history for each well. **Fig. 4.42** shows a comparison of the "hyperbolic" *b*-parameter for all of the wells analyzed from field C. The *b*-parameter stabilizes between 2.15 and 2.82 for the examples shown.

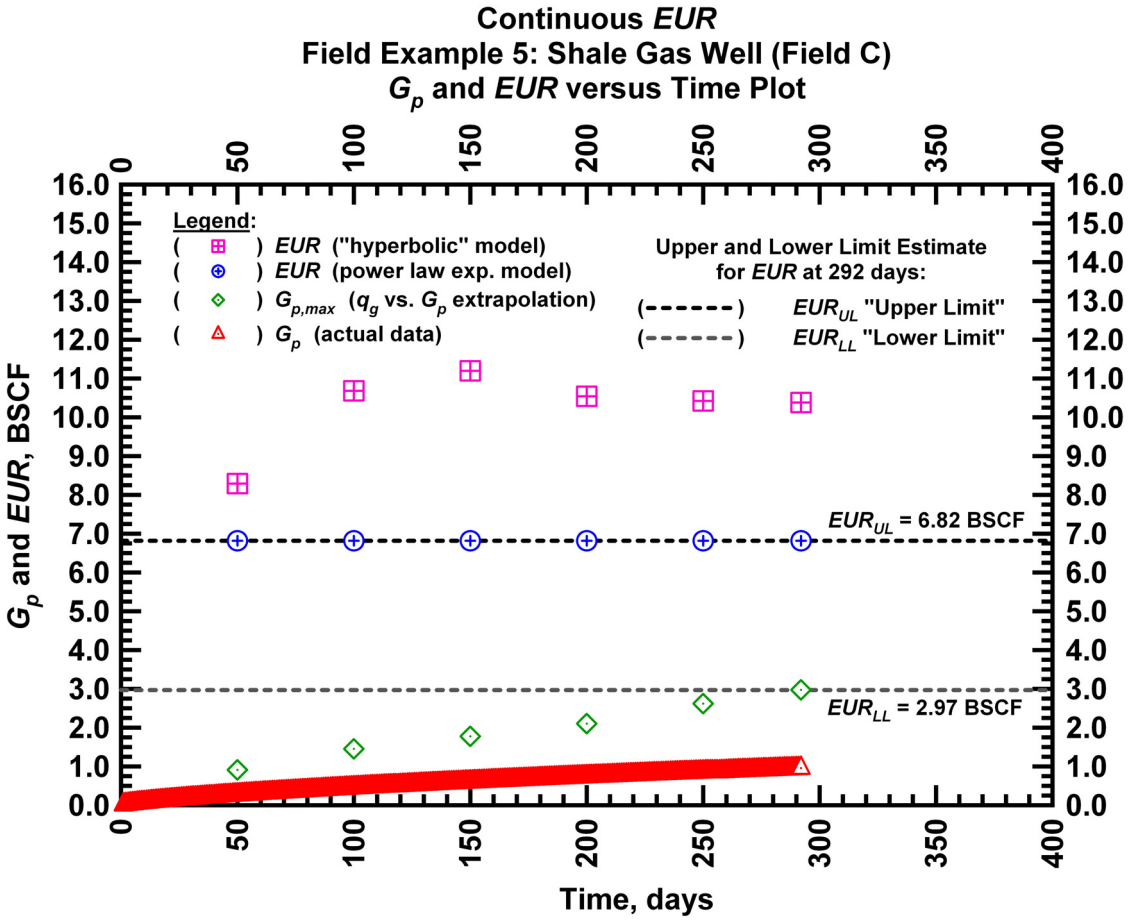

Figure 4.39 — (Cartesian Plot): *EUR* estimates from model matches and $G_{p,max}$ estimates from extrapolation technique for field example 5.

Table 4.16 — Analysis results for field example 5 — "hyperbolic" model parameters.

Time Interval, days	q_{gi} (MSCFD)	D_i (D^{-1})	b (dimensionless)	EUR_{hyp} (BSCF)
50	7,707	0.0302	2.32	8.29
100	8,000	0.0404	2.81	10.68
150	8,000	0.0422	2.92	11.20
200	8,000	0.0395	2.78	10.54
250	8,000	0.0384	2.74	10.42
292	8,032	0.0395	2.74	10.38

Table 4.17 — Analysis results for field example 5 — power law exponential model parameters.

Time Interval, days	$\hat{q}_{gi}$ (MSCFD)	$\hat{D}_i$ (D^{-1})	n (dimensionless)	D_∞ (D^{-1})	EUR_{PLE} (BSCF)
50	17,149	0.6462	0.203	0	6.82
100	17,149	0.6462	0.203	0	6.82
150	17,149	0.6462	0.203	0	6.82
200	17,149	0.6462	0.203	0	6.82
250	17,149	0.6462	0.203	0	6.82
292	17,149	0.6462	0.203	0	6.82

Table 4.18 — Analysis results for field example 5 — straight line extrapolation.

Time Interval, days	Slope, 10^{-6} D^{-1}	Intercept, MSCF/D	$G_{p,max}$ (BSCF)
50	6,268	5,703	0.91
100	3,242	4,711	1.45
150	2,411	4,279	1.77
200	1,850	3,890	2.10
250	1,331	3,487	2.62
292	1,123	3,337	2.97

Table 4.19 — Analysis results for field examples from field C.

Field Example	Producing Time (D)	b (dimensionless)	EUR_{hyp} (BSCF)	EUR_{PLE} (BSCF)	$G_{p,max}$ (BSCF)
5	292	2.74	10.38	6.82	2.97
35	255	2.82	6.84	5.93	1.77
36	286	2.71	12.87	6.81	3.51
37	553	2.43	9.00	6.24	3.87
38	320	2.27	6.12	5.32	1.98
39	305	2.15	3.98	2.47	1.20
40	218	2.46	5.53	2.67	1.35

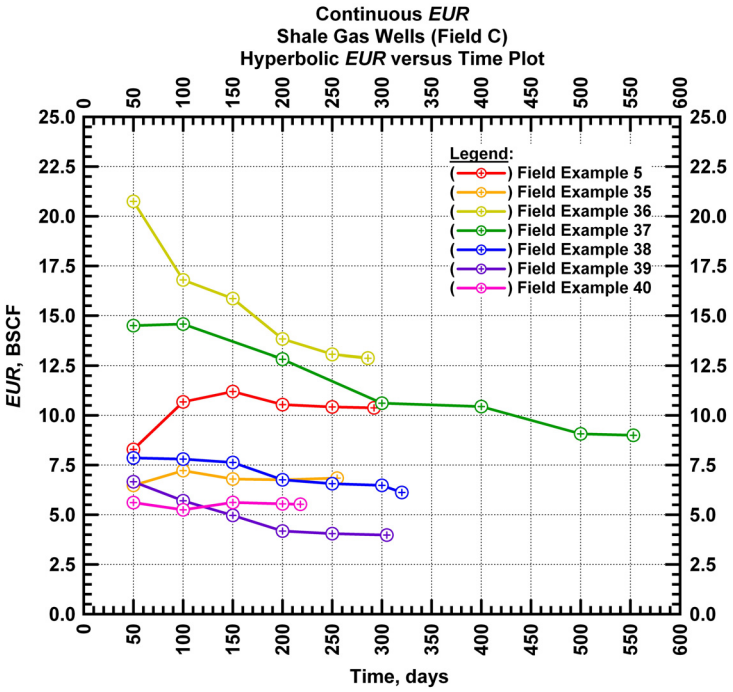

Figure 4.40 — (Cartesian Plot): Comparison of the hyperbolic *EUR* estimates for the shale gas wells producing from field C.

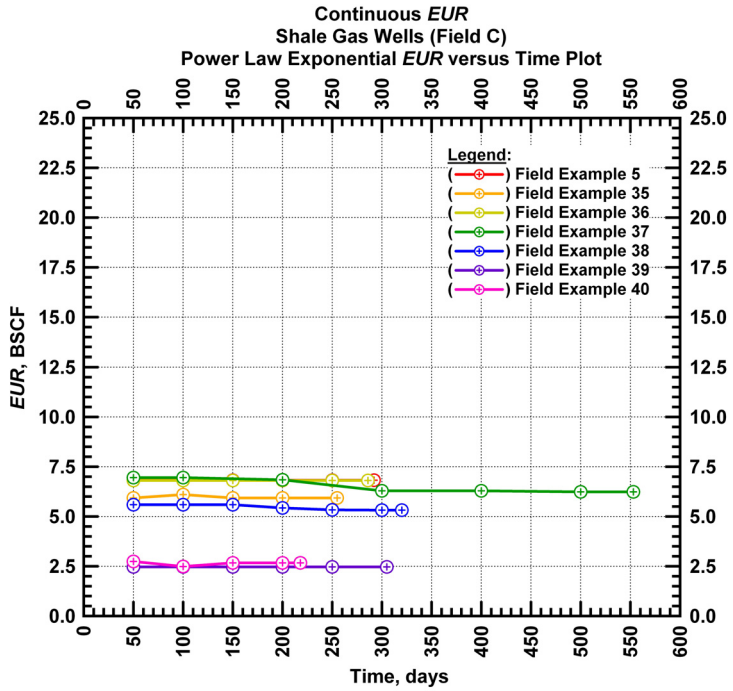

Figure 4.41 — (Cartesian Plot): Comparison of the power law exponential *EUR* estimates for the shale gas wells producing from field C.

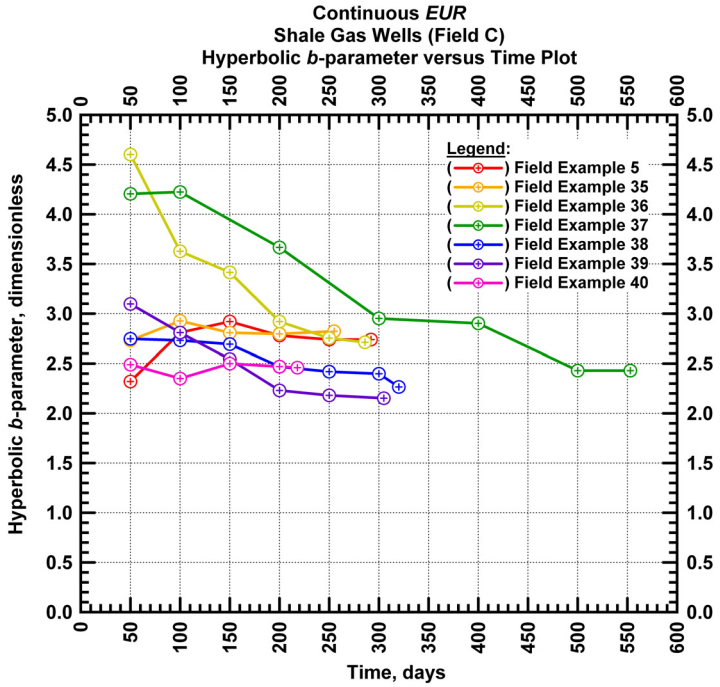

Figure 4.42 — (Cartesian Plot): Comparison of the hyperbolic *b*-parameter for the shale gas wells producing from field C.

4.6 Field Example 6: Shale Gas Well (Field D)

We apply our proposed methodology to a field dataset acquired from a hydraulically fractured vertical well completed in a shale gas reservoir. We present the flow rate data and the cumulative production data which spans almost 2 years in **Fig. 4.43**.

Our first task is to match the subsets of the flow rate data with the "hyperbolic" rate decline relation. **Fig. 4.44** presents the "hyperbolic" model matches imposed on the flow rate data along with the *D*- and *b*-parameter trends. We use the same matching technique as previously described in the simulated example and match the entire portion of the data for each selected interval using calibration and regression.

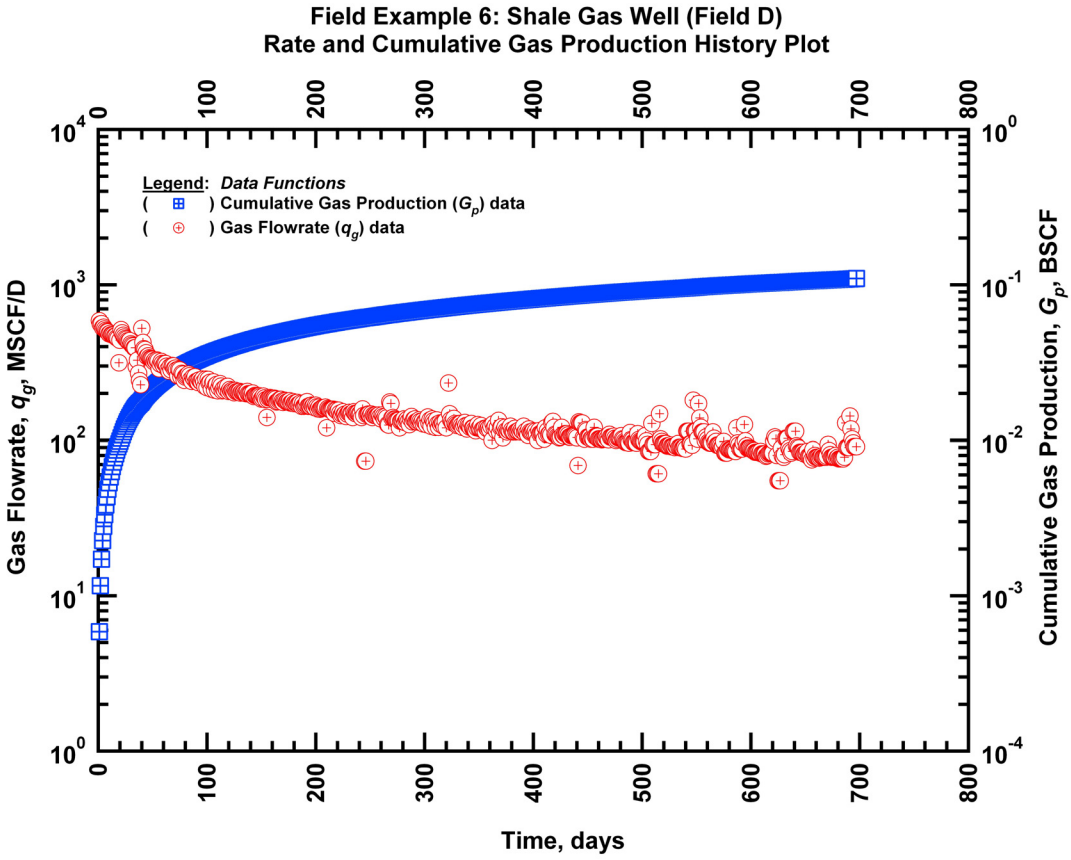

Figure 4.43 — (Semi-log Plot): Production history plot for field example 6 — flow rate (q_g) and cumulative production (G_p) versus production time.

In **Fig. 4.45** we observe the value of the *b*-parameter as a function of time. Every subset (or interval) is matched with a "hyperbolic" *b*-parameter greater than 1 indicating that the boundary-dominated flow

regime has not been established. Specifically the *b*-parameter values decrease at early times and then become stable around 1.6 after 100 days of production— this result may indicate that transient flow effects are still dominant in the production behavior.

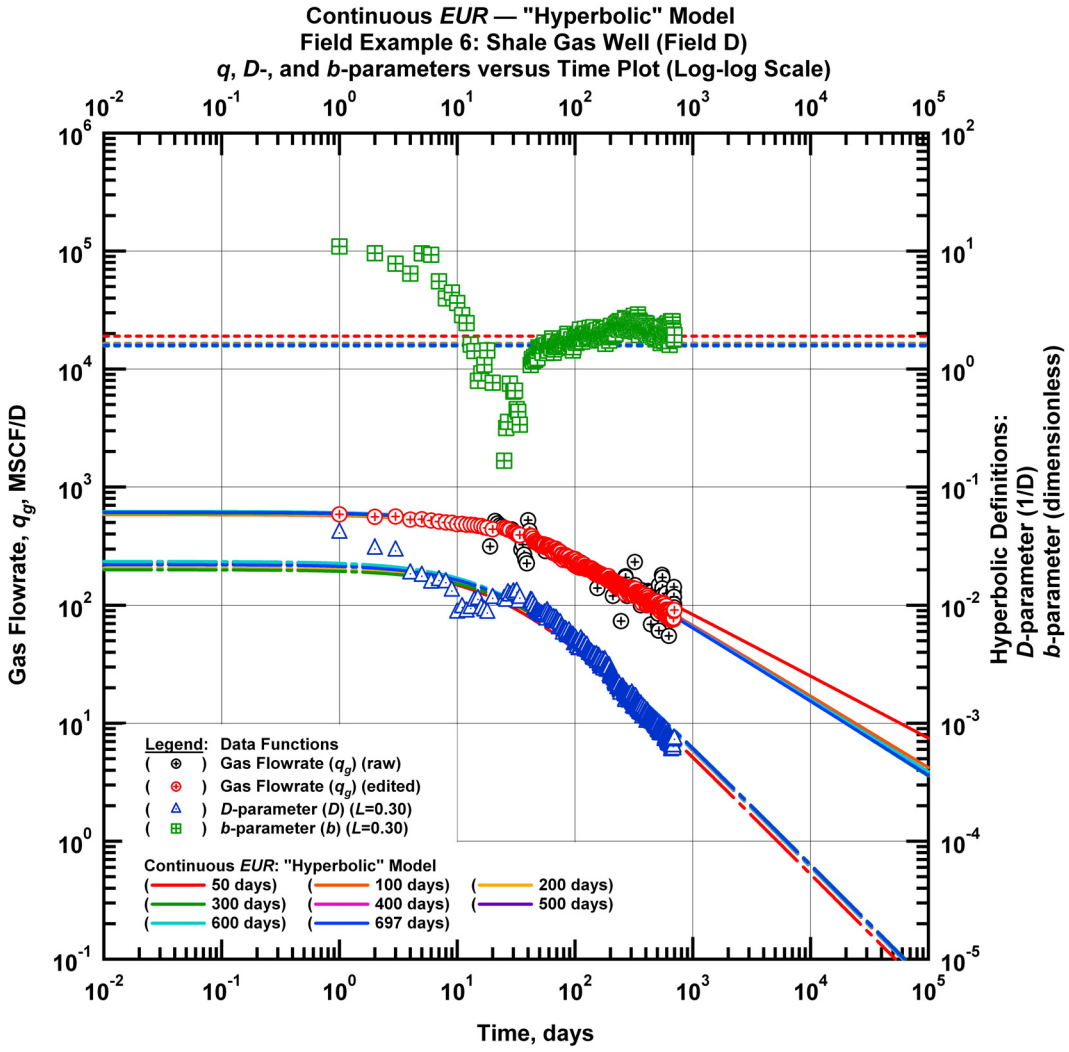

Figure 4.44 — (Log-log Plot): *qDb* plot — flow rate (q_g), *D*- and *b*-parameters versus production time and "hyperbolic" model matches for field example 6.

Our next task is to match the subsets of the flow rate data with the power law exponential rate decline relation. In **Fig. 4.46** the power law exponential model matches imposed on the flow rate data and *D*- and *b*-parameter trends are shown. For all matches a D_∞ value is not used indicating that boundary-dominated flow character is not observed (the behavior of the calculated *D*-parameter data trend may serve as a

validation for not using the D_∞ parameter in the power law exponential relation as it exhibits only power law behavior for this case). The model matches stabilize and become relatively stable after about 100 days of production for each additional interval.

We use the straight line extrapolation technique to estimate $G_{p,max}$. In **Fig. 4.47** we show the lines fit through the end portion of the data for each interval. The x-axis intercept of the lines increase with time resulting in an increasing estimate of $G_{p,max}$ or "lower" limit estimate of *EUR*.

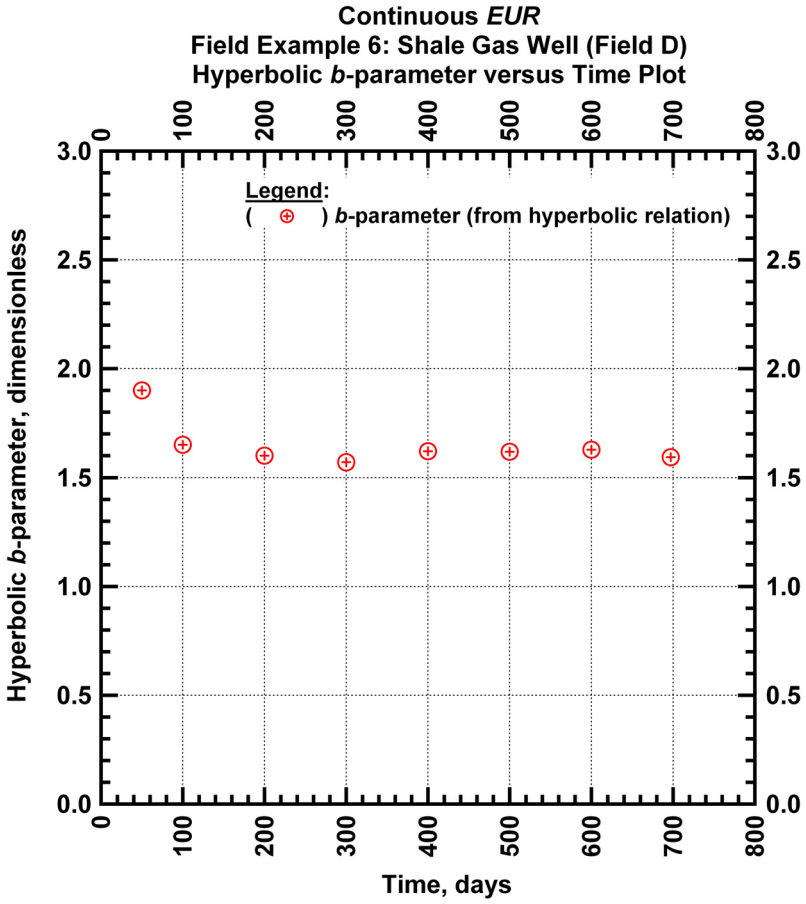

Figure 4.45 — (Cartesian Plot): Hyperbolic *b*-parameter values obtained from model matches with production data for field example 6.

The last step in our workflow is to plot the *EUR* based on the matches obtained with the "hyperbolic" and the power law exponential rate decline relations and the $G_{p,max}$ estimates obtained using the straight line extrapolation technique versus time. In **Fig. 4.48** we present the calculated *EUR* values versus production time. The *EUR* values obtained from the "hyperbolic" relation are stable after 100 days of production and

converge at late times to a value of 0.38 BSCF. The estimates provided by the power law exponential model are constant at 0.34 BSCF after 200 days. The *EUR* of this well should be in between 0.27 BSCF (the "lower" limit given by the straight line extrapolation technique at 697 days) and 0.34 BSCF (the "upper" limit given by the power law exponential estimate at 697 days). All of the model parameters for this example are presented in **Tables 4.20, 4.21, and 4.22**. Additional continuous *EUR* examples for the shale gas wells producing from the field D are included in **Appendix G**.

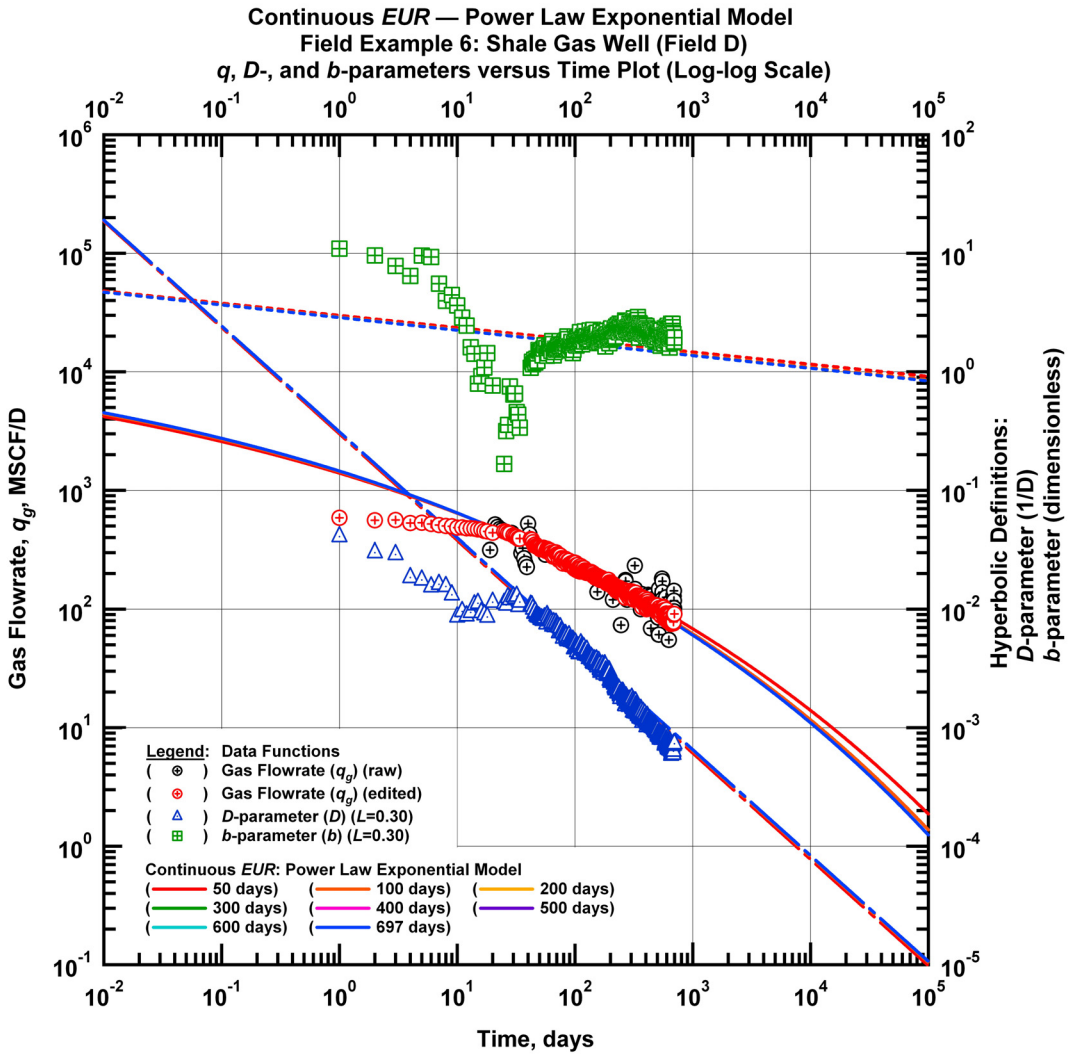

Figure 4.46 — (Log-log Plot): *qDb* plot — flow rate (q_g), *D*- and *b*-parameters versus production time and power law exponential model matches for field example 6.

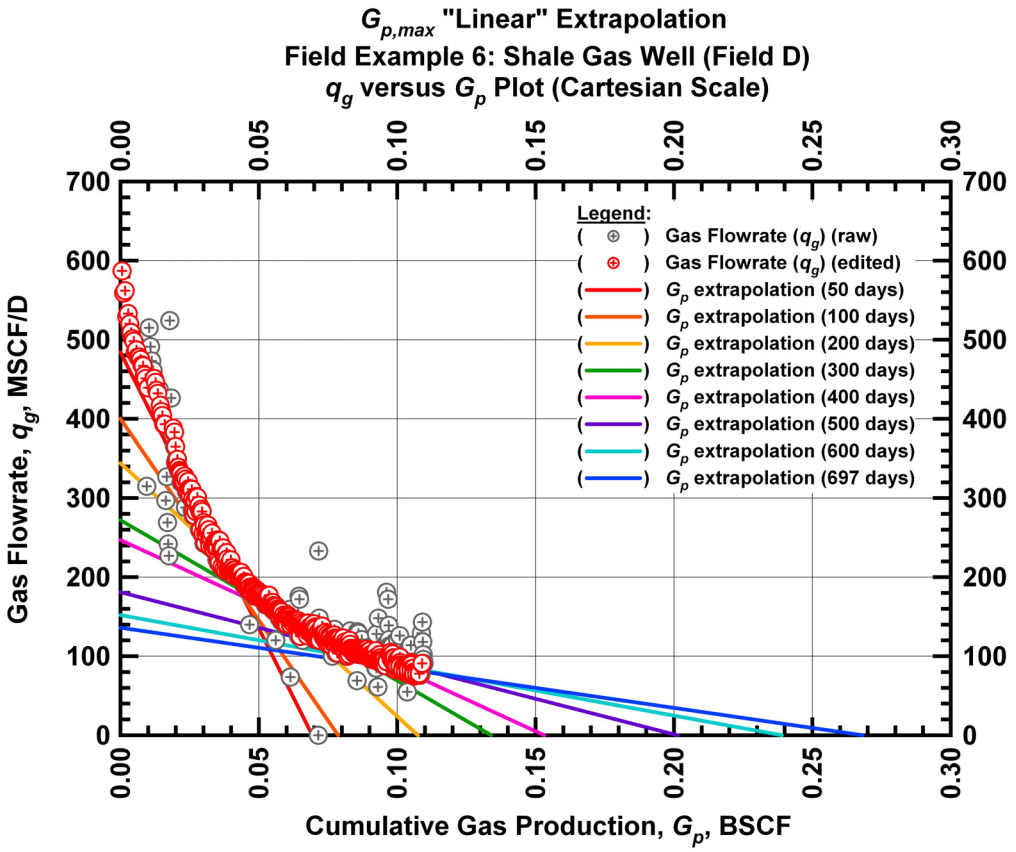

Figure 4.47 — (Cartesian Plot): Rate Cumulative Plot — flow rate (q_g) versus cumulative production (G_p) and the linear trends fit through the data for field example 6.

Table 4.23 includes analysis results for the 3 hydraulically fractured shale gas wells producing from field D. The *EUR* values and $G_{p,max}$ estimates shown for each well were obtained from the analysis of the entire production history. The *EUR* values obtained using the "hyperbolic" model are 11.8 to 61.2% or 0.04 to 1.75 BSCF greater than the estimates given by the power law exponential model. **Fig. 4.49** shows a comparison of *EUR* versus time obtained using the "hyperbolic" relation, and **Fig. 4.50** shows a comparison of *EUR* versus time obtained using the power law exponential relation for all of the wells analyzed from field D. Field examples 6 and 41 are vertical wells, and the final *EUR* values given by the power law exponential model for these wells range between 0.20 BSCF and 0.34 BSCF. The *EUR* values given by the power law exponential model stabilize after 50 to 100 days of production. Field example 42 is a horizontal well, and the final *EUR* obtained from the power law exponential model for this well is 2.86 BSCF. **Fig. 4.51** shows a comparison of the "hyperbolic" *b*-parameter for all of the wells analyzed from field D. The *b*-parameter lies between 1.59 and 2.51 based on the model match with the entire production history for the examples shown.

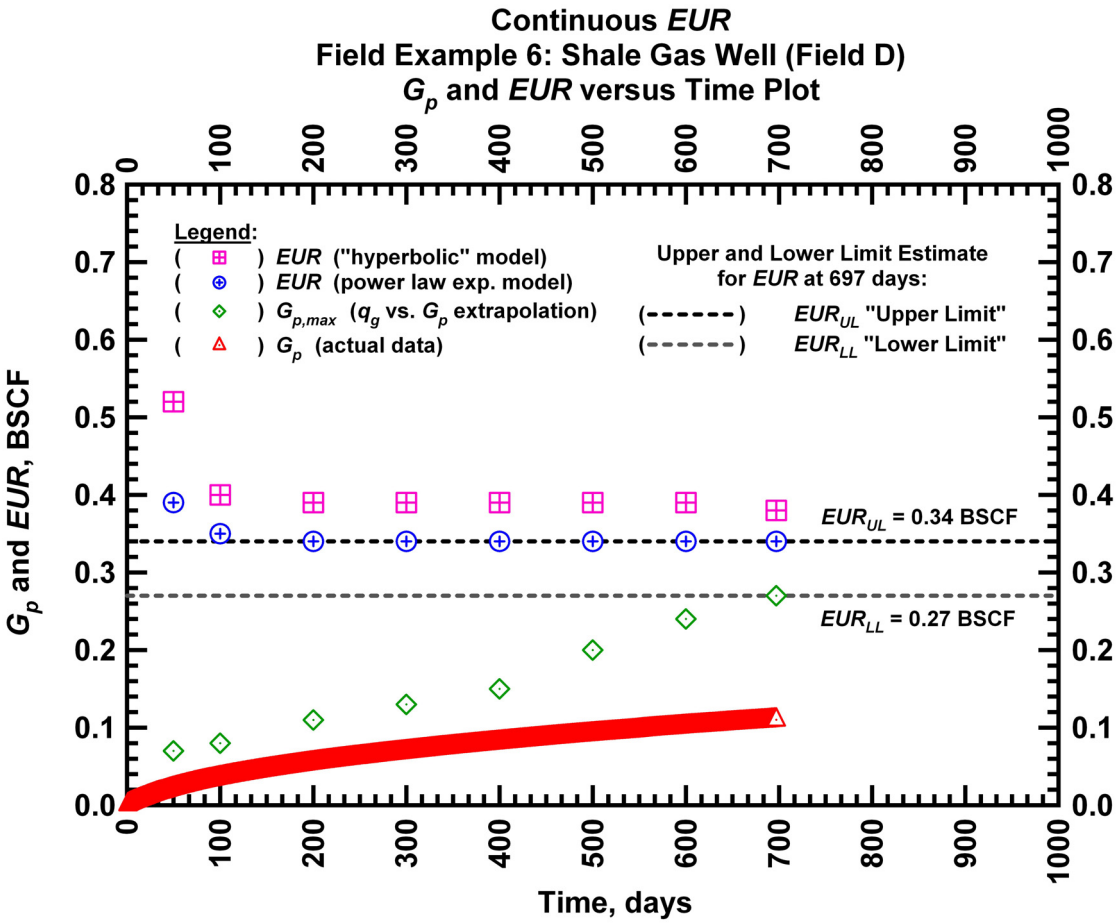

Figure 4.48 — (Cartesian Plot): *EUR* estimates from model matches and $G_{p,max}$ estimates from extrapolation technique for field example 6.

Table 4.20 — Analysis results for field example 6 — "hyperbolic" model parameters.

Time Interval, days	q_{gi} (MSCFD)	D_i (D^{-1})	b (dimensionless)	EUR_{hyp} (BSCF)
50	583	0.0207	1.90	0.52
100	583	0.0207	1.65	0.4
200	594	0.0207	1.60	0.39
300	602	0.0200	1.57	0.39
400	614	0.0225	1.62	0.39
500	618	0.0232	1.62	0.39
600	620	0.0235	1.63	0.39
697	610	0.0221	1.59	0.38

Table 4.21 — Analysis results for field example 6 — power law exponential model parameters.

Time Interval, days	$\hat{q}_{gi}$ (MSCFD)	$\hat{D}_i$ (D^{-1})	n (dimensionless)	D_∞ (D^{-1})	EUR_{PLE} (BSCF)
50	25,610	2.91	0.103	0	0.39
100	26,328	2.91	0.106	0	0.35
200	26,695	2.91	0.107	0	0.34
300	26,695	2.91	0.107	0	0.34
400	26,695	2.91	0.107	0	0.34
500	26,695	2.91	0.107	0	0.34
600	26,695	2.91	0.107	0	0.34
697	26,695	2.91	0.107	0	0.34

Table 4.22 — Analysis results for field example 6 — straight line extrapolation.

Time Interval, days	Slope, 10^{-6} D^{-1}	Intercept, MSCF/D	$G_{p,max}$ (BSCF)
50	6,981	484	0.07
100	5,087	400	0.08
200	3,200	344	0.11
300	2,030	272	0.13
400	1,613	247	0.15
500	899	181	0.20
600	636	152	0.24
697	507	136	0.27

Table 4.23 — Analysis results for field examples from field D.

Field Example	Producing Time (D)	b (dimensionless)	EUR_{hyp} (BSCF)	EUR_{PLE} (BSCF)	$G_{p,max}$ (BSCF)
6	697	1.59	0.38	0.34	0.27
41	728	2.31	0.25	0.20	0.13
42	331	2.51	4.61	2.86	1.35

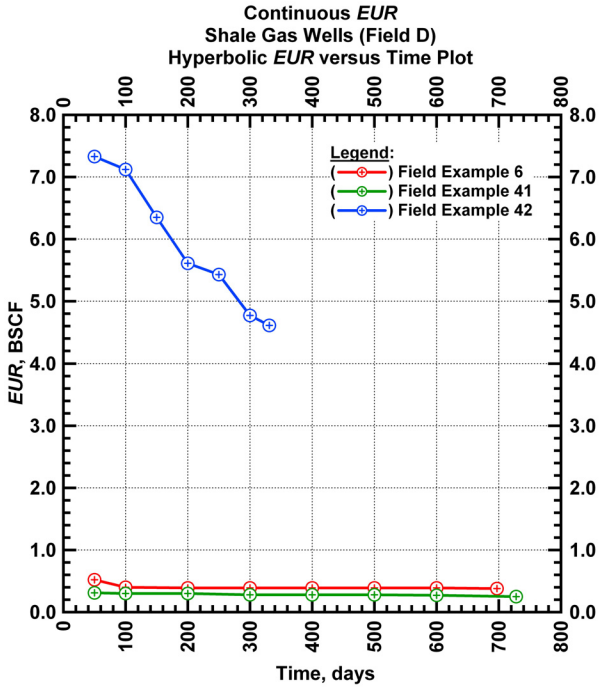

Figure 4.49 — (Cartesian Plot): Comparison of the hyperbolic *EUR* estimates for the shale gas wells producing from field D.

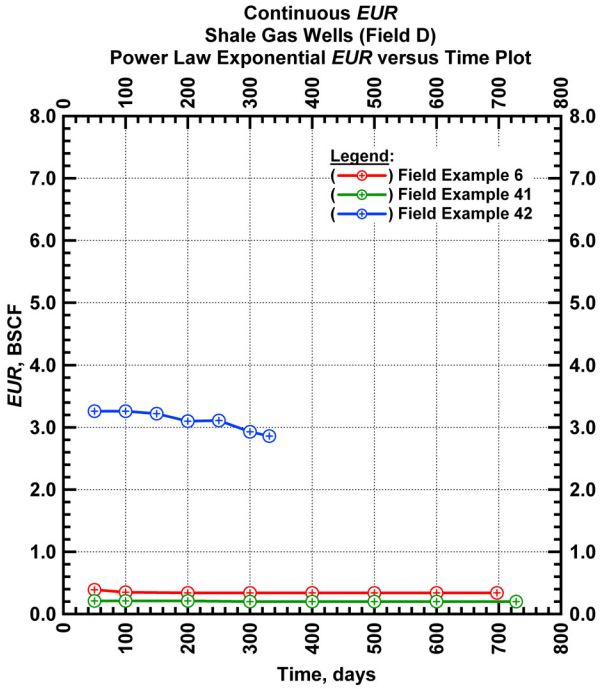

Figure 4.50 — (Cartesian Plot): Comparison of the power law exponential *EUR* estimates for the shale gas wells producing from field D.

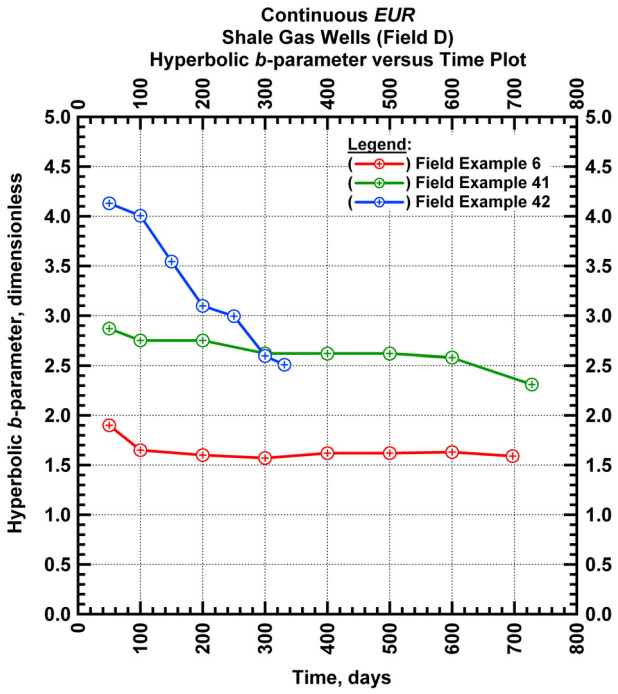

Figure 4.51 — (Cartesian Plot): Comparison of the hyperbolic *b*-parameter for the shale gas wells producing from field D.

An additional continuous *EUR* example applied to a shale gas well is included in **Appendix H**.

CHAPTER V
SUMMARY, CONCLUSIONS, AND RECOMMENDATIONS FOR FUTURE WORK

5.1 Summary

In this work we propose the "Continuous *EUR* Method" to reduce the uncertainty in reserves estimation particularly for unconventional gas reservoirs. We utilize rate-time functions and a simple extrapolation technique in a continuous manner as a means of generating a time-dependent profile of *EUR*. We have demonstrated the "Continuous *EUR* Method" by applying the procedure to 43 field examples producing from 7 tight sandstone and shale gas reservoirs. The proposed methodology is especially useful because it provides "upper" and "lower" limits for *EUR* prior to the onset of boundary-dominated flow.

5.2 Conclusions

We state the following conclusions based on this work.

1. The proposed "Continuous *EUR* Method" shows that *EUR* values obtained using rate-time relations provide an "upper" limit of ultimate recovery at early time for unconventional gas reservoirs. *EUR* values may stabilize (or become constant) during the producing life of a well — this observation should not be confused with the boundary-dominated flow regime. *EUR* values obtained using the power law exponential model appear to stabilize earlier in the life of a well and provide more conservative *EUR* estimates than those obtained using the "hyperbolic" relation.
2. The proposed "Continuous *EUR* Method" uses the "hyperbolic" and the power law exponential rate decline relations. Other rate decline relations (such as the modified hyperbolic relation) can be implemented using this approach.
3. The straight line extrapolation technique offers the most conservative estimate of maximum cumulative production, and hence provides a "lower" limit for *EUR*. Based on this observation, we use the straight line extrapolation technique to prevent the overestimation of reserves.
4. The tight gas and shale gas field examples shown do not exhibit signs of boundary-dominated flow behavior. As a result, all model matches made with the "hyperbolic" rate decline relation use a *b*-parameter value greater than 1, and the model matches made with the power law exponential rate decline relation are made without using the boundary-dominated flow parameter, D_∞.

5.3 Recommendations for Future Work

This work should be continued as follows.

- The time-dependent behavior of *EUR* and the model parameters of rate-time relations should be investigated in terms of identifying a characteristic behavior for the wells producing from the same field. For example, future efforts should focus on the behavior of the *b*-parameter in the "hyperbolic" relation changing over time so that the future production forecast of a particular well can be performed with more confidence.
- The concept of the "Continuous *EUR* Method" is general and applicable to model-based analyses as well (*i.e.*, production data analysis with the inclusion of pressure data). The use of model-based analyses to estimate cumulative production at a specified time limit can be performed continuously and the results can be compared with the continuous *EUR* values obtained using rate-time relations. This procedure should further reduce the uncertainty in reserves estimation.
- Additional rate-time methods for reserves estimation (*e.g.*, the modified hyperbolic relation, *etc*.) should be implemented with the "Continuous *EUR* Method" for unconventional gas reservoirs. The time-dependent *EUR* profile obtained by additional rate-time methods should be compared with the rate-time relations used in this work (*i.e.*, power law exponential model or hyperbolic rate decline relation) to determine which relation is more suitable for estimating reserves.

NOMENCLATURE

b	Arps' decline exponent, dimensionless
D	Loss ratio, D^{-1}
D_i	Initial decline constant for hyperbolic rate relation, D^{-1}
D_∞	Decline constant at "infinite time" for power law exponential relation [*i.e.*, $D(t=\infty)$], D^{-1}
$\hat{D}_i$	Decline constant for power law exponential relation, D^{-1}
EUR	Estimate of ultimate recovery, BSCF
EUR_{LL}	Lower limit for estimate of ultimate recovery, BSCF
EUR_{UL}	Upper limit for estimate of ultimate recovery, BSCF
G	Original (contacted) gas-in-place, MSCF
G_p	Cumulative gas production, MSCF
$G_{p,max}$	Maximum gas production ($t\rightarrow\infty$), MSCF
n	Time exponent for power law exponential relation, dimensionless
q_g	Gas production rate, MSCF/D
q_{gi}	Gas initial production rate for hyperbolic rate relation, MSCF/D
$\hat{q}_{gi}$	Rate "intercept" for power law exponential relation [*i.e.*, $q_g(t=0)$], MSCF/D
t	Production time, days
t_{lim}	Time limit for reserves extrapolation, days

REFERENCES

Agarwal, R.G., Gardner, D.C., Kleinsteiber, S.W., and Fussell, D.D. 1999. Analyzing Well Production Data Using Combined-Type-Curve and Decline-Curve Analysis Concepts. *SPE Reservoir Evaluation & Engineering* (October): 478-486. SPE-57916-PA.

Amini, S., Ilk, D., and Blasingame, T.A. 2007. Evaluation of the Elliptical Flow Period for Hydraulically-Fractured Wells in Tight Gas Sands — Theoretical Aspects and Practical Considerations. Paper SPE 106308 presented at the SPE Hydraulic Fracturing Technology Conference, College Station, Texas, 29-31 January.

Anderson, D., and Mattar, L. 2004. Practical Diagnostics Using Production Data and Flowing Pressures. Paper SPE 89939 presented at the SPE Annual Technical Conference and Exhibition, Houston, Texas, 26-29 September.

Anderson, D.M., Stotts, G.W.J., Mattar, L., Ilk, D., and Blasingame, T.A. 2006. Production Data Analysis — Challenges, Pitfalls, Diagnostics. Paper SPE 102048 presented at the SPE Annual Technical Conference and Exhibition, San Antonio, Texas, 24-27 September.

Ansah, J. 1996. Production Rate and Cumulative Production Models for Advanced Decline Curve Analysis of Gas Reservoirs. PhD dissertation, Texas A&M University, College Station, Texas.

Ansah, J., Knowles, R.S., and Blasingame, T.A. 1996. A Semi-Analytic (p/z) Rate-Time Relation for the Analysis and Prediction of Gas Well Performance. Paper SPE 35268 presented at the SPE Mid-Continent Gas Symposium, Amarillo, Texas, 28-30 April.

Araya, A. and Ozkan, E. 2002. An Account of Decline-Type Curve Analysis of Vertical, Fractured, and Horizontal Wells Production Data. Paper SPE 77690 presented at the SPE Annual Technical Conference and Exhibition, San Antonio, Texas, 29 September-2 October.

Arps, J.J. 1945. Analysis of Decline Curves. *Trans*. AIME **160**: 228-247.

Blasingame, T.A., and Rushing, J.A. 2005. A Production-Based Method for Direct Estimation of Gas-in-Place and Reserves. Paper SPE 98042 presented at the SPE Eastern Regional Meeting, Morgantown, West Virginia, 14-16 September.

Boulis, A.S., Ilk, D., and Blasingame, T.A. 2009. A New Series of Rate Decline Relations Based on the Diagnosis of Rate-Time Data. Paper CIPC 2009-202 presented at the Canadian International Petroleum Conference, Calgary, Alberta, 16-18 June.

Bourdet, D., Ayoub, J.A., and Pirard, Y.M. 1989. Use of Pressure Derivative in Well-Test Interpretation. *SPEFE* **4** (2): 228-293-302.

Buba, I. 2003. Direct Estimation of Gas Reserves Using Production Data. MS thesis, Texas A&M University, College Station, Texas.

Camacho-V., R.G. and Raghavan, R. 1989. Boundary-Dominated Flow in Solution Gas-Drive Reservoirs. *SPE Res Eng* **4** (4): 503-512. SPE-18562-PA.

Camacho-V., R.G., Vasquez-Cruz, M., Castrejon-Aivar, R., and Arana-Ortiz, V. 2005. Pressure-Transient and Decline-Curve Behaviors in Naturally Fractured Vuggy Carbonate Reservoirs. *SPE Res Eval & Eng* **8** (2): 95-110. SPE-77689-PA.

Carter, R.D. 1985. Type Curves for Finite Radial and Linear Gas-Flow Systems: Constant-Terminal-Pressure Case. *SPE Journal* (October 1985): 719-728. SPE-12917-PA.

Chen, H.Y. and Teufel, L.W. 2000. A New Rate-Time Type Curve for Analysis of Tight-Gas Linear and Radial Flows. Paper SPE 63094 presented at the SPE Annual Technical Conference and Exhibition, Dallas, Texas, 1-4 October.

Cheng, Y., Lee, W.J., and McVay, D.A. 2007. Improving Reserves Estimates from Decline Curve Analysis of Tight and Multilayer Gas Wells. *SPE Reservoir Eval & Eng* (October 2008): 912-920. SPE-10817-PA.

Clarkson, C.R., Bustin, R.M., and Seidle, J.P. 2007. Production Data Analysis of Single-Phase Coalbed-Methane Wells. *SPE Res Eval & Eng* **10** (3): 312-331. SPE-100313-PA.

Clarkson, C.R., Jordan, C.L., Gierhart, R.R., and Seidle, J.P. 2008. Production Data Analysis of Coalbed-Methane Wells. *SPE Res Eval & Eng* **11** (3): 311-325. SPE-107705-PA.

Cox, D.O., Kuuskraa, V.A., and Hansen, J.T. 1996. Advanced Type Curve Analysis for Low Permeability Gas Reservoirs. Paper SPE 35595 presented at the SPE Gas Technology Conference, Calgary, Alberta, 28 April – 1 May.

Cox, S.A., Gilbert, J.V., Sutton, R.P., and Stoltz, R.P. 2002. Reserve Analysis for Tight Gas. Paper SPE 78695 presented at the SPE Eastern Regional Meeting, Lexington, Kentucky, 23-25 October.

Cox, S.A., Stoltz, R.P., Wilson, A.S., and Sutton, R.P. 2003. Reserve Analysis for Multilayered Tight Gas Reservoirs. Paper SPE 84814 presented at the SPE Eastern Regional/AAPG Eastern Section Joint Meeting, Pittsburgh, Pennsylvania, 6-10 September.

Cutler, W.W. 1924. Estimation of Underground Oil Reserves by Oil-Well Production Curves. *Bull*. USBM **228** (1).

Doublet, L.E., Pande, P.K., McCollum, T.J., and Blasingame, T.A. 1994. Decline Curve Analysis Using Type Curves — Analysis of Oil Well Production Data Using Material Balance Time: Application to Field Cases. Paper SPE 28688 presented at the Petroleum Conference and Exhibition of Mexico, Veracruz, Mexico, 10-13 October.

El-Banbi, A.H. and Wattenbarger, R.A. 1998. Analysis of Linear Flow in Gas Flow Production. Paper SPE 39972 presented at the SPE Gas Technology Symposium, Calgary, Alberta, 15-18 March.

Fetkovich, M.J. 1980. Decline Curve Analysis Using Type Curves. *JPT*. 32 (6): 1065-1077. SPE-4629-PA.

Fetkovich, M.J., Vienot, M.E., Bradley, M.D., and Kiesow, U.G. 1987. Decline Curve Analysis Using Type Curves — Case Histories. *SPE Formation Evaluation* (December 1987): 637-656. SPE-13169-PA.

Fraim, M.L., Lee, W.J., and Gatens, J.M. 1986. Advanced Decline Curve Analysis Using Normalized-Time and Type Curves for Vertically Fractured Wells. Paper SPE 15524 presented at the SPE Annual Technical Conference and Exhibition, New Orleans, Louisiana, 5-8 October.

Fraim, M.L. and Wattenbarger, R.A. 1987. Gas Reservoir Decline-Curve Analysis Using Type Curves with Real Gas Pseudopressure and Normalized Time. *SPE Res Eval & Eng* **2** (4): 671-682. SPE-14238-PA.

Ilk, D., Mattar, L., and Blasingame, T.A. 2007. Production Data Analysis — Future Practices for Analysis and Interpretation. Paper CIPC 2007-174 presented at the Canadian International Petroleum Conference, 12-14 June.

Ilk, D., Perego, A.D., Rushing, J.A., and Blasingame, T.A. 2008a. Exponential vs. Hyperbolic Decline in Tight Gas Sands – Understanding the Origin and Implications for Reserve Estimates Using Arps' Decline Curves. Paper SPE 116731 presented at the SPE Annual Technical Conference and Exhibition, Denver, Colorado, 21-24 September.

Ilk, D., Perego, A.D., Rushing, J.A., and Blasingame, T.A. 2008b. Integrating Multiple Production Analysis Techniques To Assess Tight Gas Sand Reserves: Defining a New Paradigm for Industry Best Practices. Paper SPE 114947 presented at the SPE Gas Technology Symposium, Calgary, Alberta, 17-19 June.

Johnson, N.L., Currie, S.M., Ilk, D., and Blasingame, T.A. 2009. A Simple Methodology for Direct Estimation of Gas-in-Place and Reserves Using Rate-Time Data. Paper SPE 123298 presented at the SPE Rocky Mountain Petroleum Technology Conference, Denver, Colorado, 14-16 April.

Johnson, R.H. and Bollens, A.L. 1927. The Loss Ratio Method of Extrapolating Oil Well Decline Curves. *Trans*. AIME 77: 771. SPE-927771-G.

Kabir, C.S. and Izgec, B. 2006. Diagnosis of Reservoir Behavior from Measured Pressure/Rate Data. Paper SPE 100384 presented at the SPE Gas Technology Symposium, Calgary, Alberta, 15-17 May.

Knowles, S. 1999. Development and Verification of New Semi-Analytical Methods for the Analysis and Prediction of Gas Well Performance. MS thesis, Texas A&M University, College Station, Texas.

Kupchenko, C.L., Gault, B.W., and Mattar, L. 2008. Tight Gas Production Performance Using Decline Curves. Paper SPE 114991 presented at the CIPC/SPE Gas Technology Symposium, Calgary, Alberta, 16-19 June.

Lewis, A.M. and Hughes, R.G. 2008. Production Data Analysis of Shale Gas Reservoirs. Paper SPE 116688 presented at the SPE Annual Technical Conference and Exhibition, Denver, Colorado, 21-24 September.

Li, K. and Horne, R.N. 2005. An Analytical Model for Production Decline-Curve Analysis in Naturally Fractured Reservoirs. *SPE Reservoir Eval & Eng* (June 2005): 197-204. SPE-83470-PA.

Maley, S. 1985. The Use of Conventional Decline Curve Analysis in Tight Gas Well Applications. Paper SPE/DOE 13898 presented at the SPE/DOE Low Permeability Gas Reservoirs, Denver, Colorado, 19-22 May.

Marhaendrajana, T., and Blasingame, T.A. 2001. Decline Curve Analysis Using Type Curves — Evaluation of Well Performance Behavior in a Multiwell Reservoir System. Paper SPE 71514 presented at the SPE Annual Technical Conference and Exhibition, New Orleans, Louisiana, 20 September-3 October.

Mattar, L. and Anderson, D.M. 2003. A Systematic and Comprehensive Methodology for Advanced Analysis of Production Data. Paper SPE 84472 presented at the SPE Annual Technical Conference and Exhibition, Denver, Colorado, 5-8 October.

Mattar, L., Gault, B., Morad, K., Clarkson, C.R., Freeman, C.M., Ilk, D., and Blasingame, T.A. 2008. Production Analysis and Forecasting of Shale Gas Reservoirs: Case History-Based Approach. Paper SPE 119897 presented at the SPE Shale Gas Production Conference, Fort Worth, Texas, 16-18 November.

Palacio, J.C. and Blasingame, T.A. 1993. Decline-Curve Analysis Using Type Curves: Analysis of Gas Well Production Data. Paper SPE 25909 presented at the SPE Rocky Mountain Regional Meeting/Low Permeability Reservoirs Symposium and Exhibition, Denver, Colorado, 26-28 April.

Pratikno, H., Rushing, J.A., and Blasingame, T.A. 2003. Decline Curve Analysis Using Type Curves: Fractured Wells. Paper SPE 84287 presented at the SPE Annual Technical Conference and Exhibition, Denver, Colorado, 5-8 October.

Robertson, S. 1988. Generalized Hyperbolic Equation. Paper SPE 18731 available from SPE, Richardson, Texas.

Rodriguez-Roman, J. and Camacho-Velazquez, R. 2005. Decline Curve Analysis Considering Nonlaminar Flow in Dual-Porosity Systems. *SPE Res Eval & Eng* **8** (6): 478-490. SPE-74388-PA.

Rushing, J.A., Perego, A.D., Sullivan, R.B., and Blasingame, T.A. 2007. Estimating Reserves in Tight Gas Sands at HP/HT Reservoir Conditions: Use and Misuse of an Arps Decline Curve Methodology. Paper SPE 109625 presented at the SPE Annual Technical Conference and Exhibition, Anaheim, California, 11-14 November.

Rushing, J.A., Perego, A.D., and Blasingame, T.A. 2008. Applicability of the Arps Rate-Time Relationships for Evaluating Decline Behavior and Ultimate Gas Recovery of Coalbed Methane Wells. Paper SPE 114514 presented at the CIPC/SPE Gas Technology Symposium, Calgary, Alberta, 16-19 June.

Wattenbarger, R.A., El-Banbi, A.H., Villegas, M.E, and Maggard, J.B. 1998. Production Analysis of Linear Flow Into Fractured Tight Gas Wells. Paper SPE 39931 presented at the SPE Rocky Mountain Regional/Low-Permeability Reservoirs Symposium and Exhibition, Denver, Colorado, 5-8 April.

APPENDIX A
ARPS' HYPERBOLIC RATE DECLINE RELATION

The Arps' exponential and hyperbolic rate decline relations (Johnson and Bollens 1937, Arps 1945) are empirical relations used to analyze rate-time data. The decline behavior is described by the loss ratio, $1/D$, and the derivative of the loss ratio, b, given by:

$$\frac{1}{D} = -\frac{q_g}{dq_g/dt} \quad \text{(A-1)}$$

$$b = \frac{d}{dt}\left[\frac{1}{D}\right] = -\frac{d}{dt}\left[\frac{q_g}{dq_g/dt}\right] \quad \text{(A-2)}$$

When the derivative of the loss ratio, b is constant then the hyperbolic rate decline relation is obtained and this relation is given as:

$$q_g(t) = \frac{q_{gi}}{[1+bD_it]^{1/b}} \quad \text{(A-3)}$$

Using Eq. A-1, the D-function for the hyperbolic rate decline relation can be formulated as:

$$D(t) = \frac{D_i}{[1+bD_it]} \quad \text{(A-4)}$$

We integrate Eq. A-3 for cumulative production relation and the result is given as:

$$G_p(t) = \frac{q_{gi}}{(1-b)D_i}[1-(1+bD_it)^{1-(1/b)}] \quad \text{(A-5)}$$

For the calculation of maximum production ($G_{p,max}$), we take the limit of Eq. A-5 to infinite time.

$$G_{p,\max} = \lim_{t\to\infty}\left[\frac{q_{gi}}{(1-b)D_i}[1-(1+bD_it)^{1-(1/b)}]\right] \quad \text{(A-6)}$$

When the b-function is bounded between 0 and 1 (*i.e.*, $0<b<1$), the maximum production is ($G_{p,max}$) equal to:

$$G_{p,\max} = \frac{q_{gi}}{(1-b)D_i} \qquad (\text{for } 0<b<1) \quad \text{(A-7)}$$

It is worth mentioning that if the b-function is greater than one (*i.e.*, $b>1$), Eq. A-6 converges to infinity. As a result estimation of reserves is not theoretically possible unless a time limit or abandonment rate is specified.

APPENDIX B
POWER LAW EXPONENTIAL RATE DECLINE RELATION

The power law exponential rate decline relation (Ilk et al. 2008a) is based on the continuous evaluation of the loss ratio, $1/D$, and the loss ratio derivative, b, as functions of time and is flexible enough to model transient, transition, and boundary-dominated flow. The power law exponential rate decline relation models the inverse of the loss ratio as:

$$D(t) = D_\infty + \hat{D}_i n t^{n-1} \quad \text{(B-1)}$$

The loss ratio derivative is given as:

$$b(t) = \frac{-\hat{D}_i (n-1) n t^n}{(D_\infty t + \hat{D}_i n t^n)^2} \quad \text{(B-2)}$$

The D-parameter exhibits power law behavior at early times and becomes constant at large times (for representing the boundary-dominated flow regime). Eq. B-1 is substituted into Eq. A-1 (*i.e.*, the definition of loss-ratio) and solved for the flow rate function to yield the power law exponential relation as:

$$q_g(t) = \hat{q}_i \exp[-D_\infty t - \hat{D}_i t^n] \quad \text{(B-3)}$$

Since direct integration of Eq. B-3 is not possible, cumulative production must be calculated using numerical methods.

Ilk et al. verified that the power law exponential model is flexible enough to model transient, transition, and boundary-dominated flow by applying the model to numerically simulated and field datasets. The D_∞ term controls the late time behavior often exhibiting boundary-dominated flow behavior. For datasets that do not exhibit boundary-dominated flow, the D_∞ term will be equal to 0. Johnson et al. (2009) presented further application of the model using type curve solutions for the power law exponential rate-time relation.

APPENDIX C
EXAMPLES FROM HOLLY BRANCH FIELD

Field Example 7

We present the flow rate data and the cumulative production data which spans almost 5.5 years for a vertical well producing from a tight gas reservoir in **Fig. C1**. **Fig. C2** presents the "hyperbolic" model matches imposed on the flow rate data along with the *D*- and *b*-parameter trends. In **Fig. C3** we observe that the value of the *b*-parameter as a function of time. The *b*-parameter value decreases from 4.31 to 1.62 during the production history. Every interval is matched with a "hyperbolic" *b*-parameter greater than 1 indicating that boundary-dominated flow has not been established. **Fig. C4** shows the power law exponential model matches imposed on the flow rate data and *D*- and *b*-parameter trends. In **Fig. C5** we show the results of the straight line extrapolation technique, and in **Fig. C6** we present the calculated *EUR* values versus production time. All of the model parameters for this example are presented in **Tables C1, C2, and C3**. The *EUR* of this well should be in between 2.04 BSCF (the "lower" limit given by the straight line extrapolation technique at 1,995 days) and 2.28 BSCF (the "upper" limit given by the power law exponential estimate at 1,995 days).

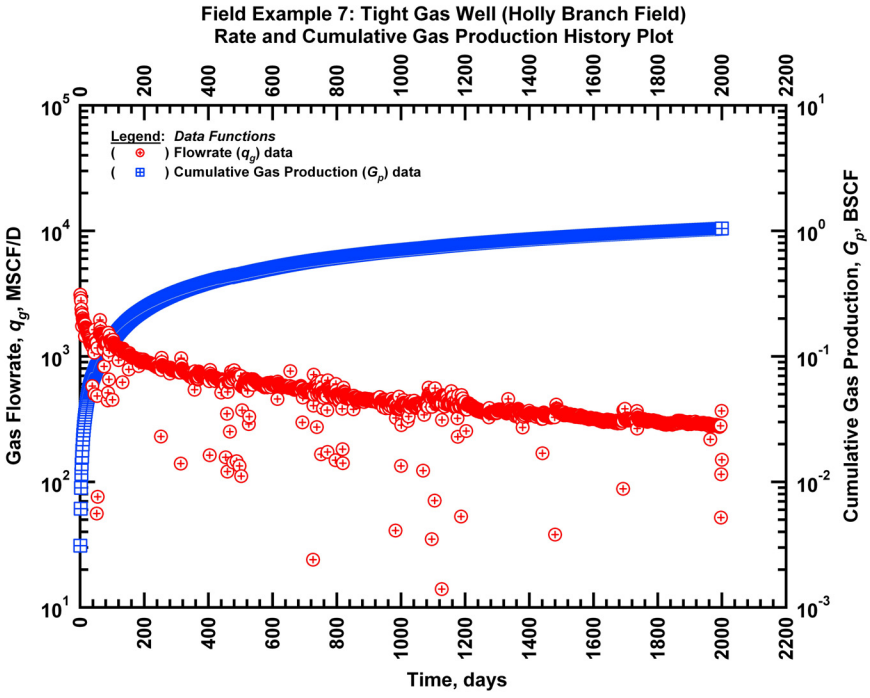

Figure C1 — (Semi-log Plot): Production history plot for field example 7 — flow rate (q_g) and cumulative production (G_p) versus production time.

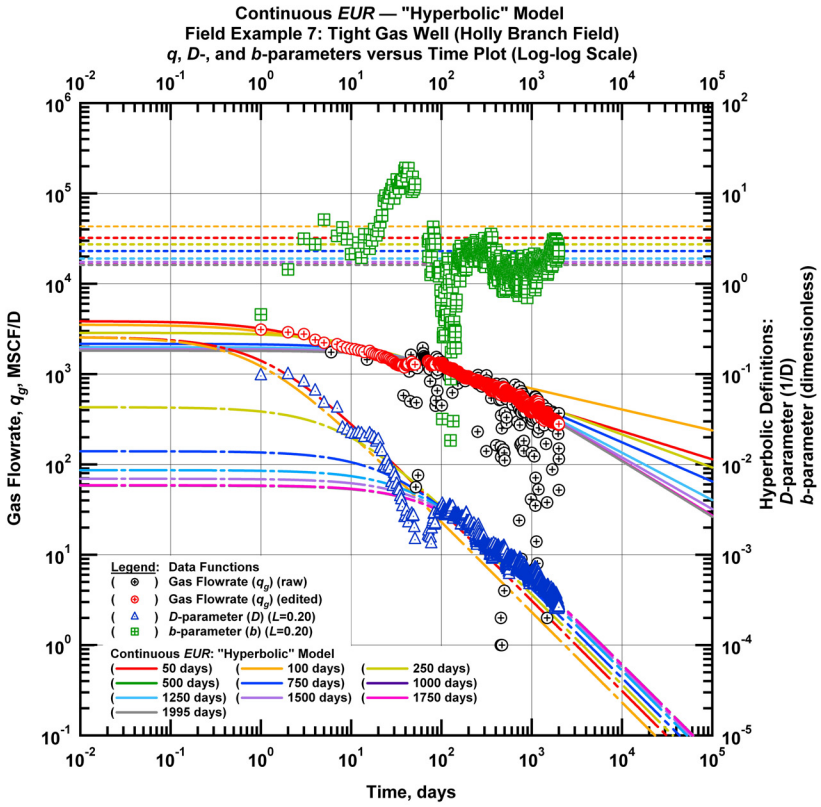

Figure C2 — (Log-log Plot): *qDb* plot — flow rate (q_g), *D*- and *b*-parameters versus production time and "hyperbolic" model matches for field example 7.

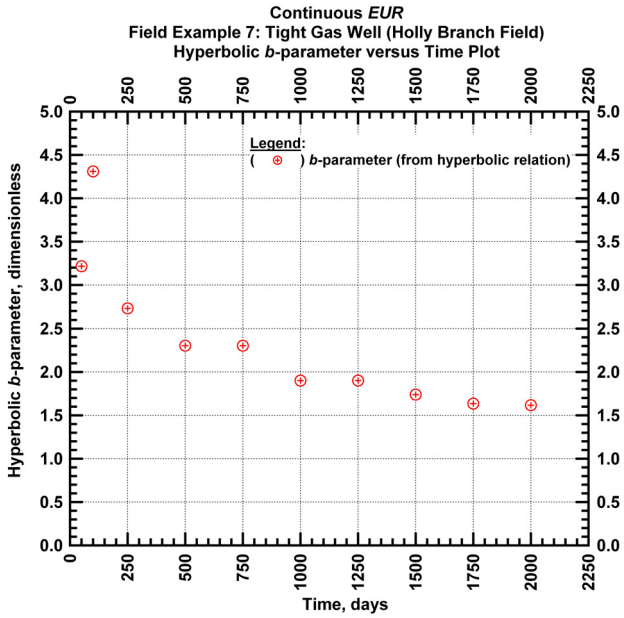

Figure C3 — (Cartesian Plot): Hyperbolic *b*-parameter values obtained from model matches with production data for field example 7.

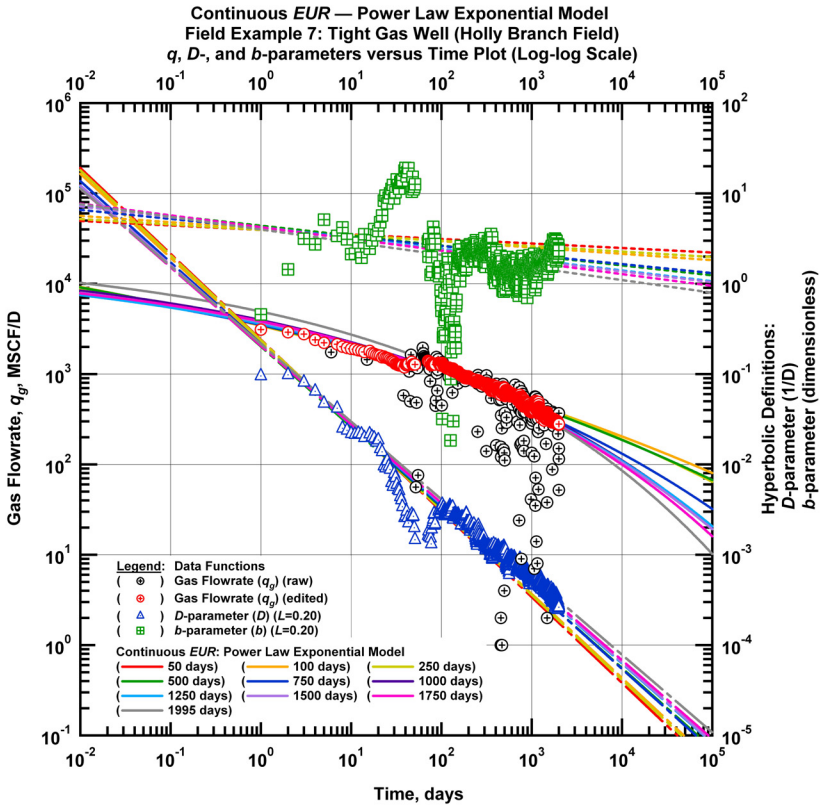

Figure C4 — (Log-log Plot): *qDb* plot — flow rate (q_g), *D*- and *b*-parameters versus production time and power law exponential model matches for field example 7.

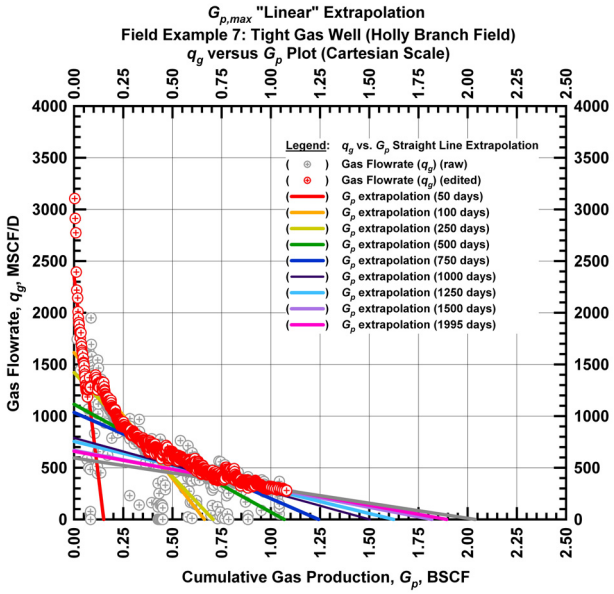

Figure C5 — (Cartesian Plot): Rate Cumulative Plot — flow rate (q_g) versus cumulative production (G_p) and the linear trends fit through the data for field example 7.

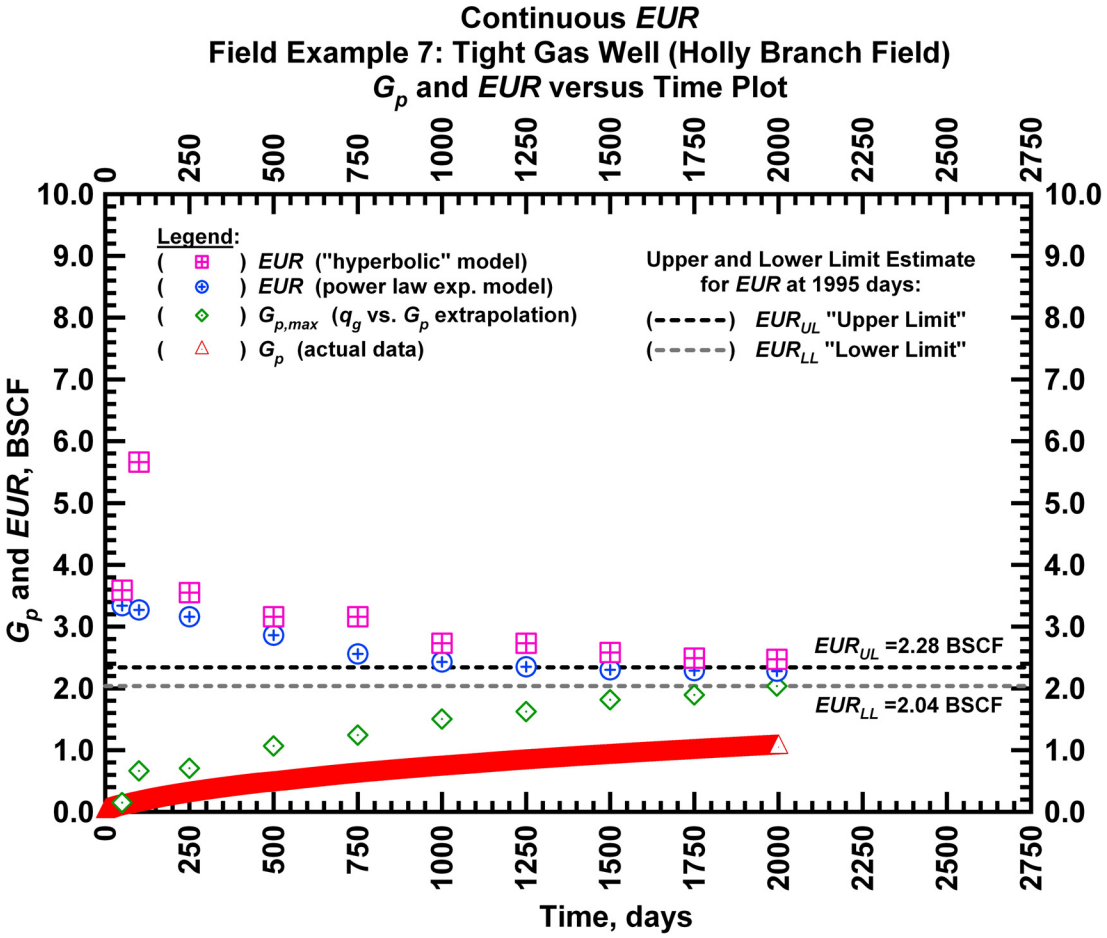

Figure C6 — (Cartesian Plot): *EUR* estimates from model matches and $G_{p,max}$ estimates from extrapolation technique for field example 7.

Table C1 — Analysis results for field example 7 — "hyperbolic" model parameters.

Time Interval, days	q_{gi} (MSCFD)	D_i (D^{-1})	b (dimensionless)	EUR_{hyp} (BSCF)
50	3,848	0.25677	3.22	3.59
100	3,520	0.25677	4.31	5.66
250	2,861	0.04302	2.73	3.55
500	2,160	0.01398	2.30	3.16
750	2,160	0.01398	2.30	3.16
1,000	1,979	0.00864	1.90	2.73
1,250	1,979	0.00864	1.90	2.73
1,500	1,891	0.00694	1.74	2.58
1,750	1,815	0.00588	1.64	2.49
1,995	1,815	0.00580	1.62	2.47

Table C2 — Analysis results for field example 7 — power law exponential model parameters.

Time Interval, days	$\hat{q}_{gi}$ (MSCFD)	$\hat{D}_i$ (D^{-1})	n (dimensionless)	D_∞ (D^{-1})	EUR_{PLE} (BSCF)
50	424,256	4.82	0.05	0	3.34
100	92,676	3.25	0.07	0	3.27
250	185,041	3.97	0.06	0	3.16
500	23,247	1.84	0.11	0	2.86
750	30,654	2.17	0.10	0	2.56
1,000	23,247	1.77	0.12	0	2.43
1,250	20,244	1.73	0.12	0	2.35
1,500	21,966	1.77	0.12	0	2.30
1,750	18,632	1.58	0.13	0	2.29
1,995	22,928	1.54	0.14	0	2.28

Table C3 — Analysis results for field example 7 — straight line extrapolation.

Time Interval, days	Slope, 10^{-6} D^{-1}	Intercept, MSCF/D	$G_{p,max}$ (BSCF)
50	15,589	2,351	0.15
100	2,436	1,614	0.66
250	2,010	1,421	0.71
500	1,043	1,114	1.07
750	833	1,036	1.24
1,000	525	789	1.50
1,250	465	755	1.62
1,500	368	669	1.82
1,750	348	659	1.89
1,995	292	595	2.04

Field Example 8

We present the flow rate data and the cumulative production data which spans over 6.5 years for a vertical well producing from a tight gas reservoir in **Fig. C7**. **Fig. C8** presents the "hyperbolic" model matches imposed on the flow rate data along with the *D*- and *b*-parameter trends. In **Fig. C9** we observe that the value of the *b*-parameter as a function of time. The *b*-parameter value decreases from 3.66 to 1.70 during the production history. Every interval is matched with a "hyperbolic" *b*-parameter greater than 1 indicating that boundary-dominated flow has not been established. **Fig. C10** shows the power law exponential model matches imposed on the flow rate data and *D*- and *b*-parameter trends. In **Fig. C11** we show the results of the straight line extrapolation technique, and in **Fig. C12** we present the calculated *EUR* values versus production time. All of the model parameters for this example are presented in **Tables C4, C5, and C6**. The *EUR* of this well should be in between 3.39 BSCF (the "lower" limit given by the straight line extrapolation technique at 2,384 days) and 3.78 BSCF (the "upper" limit given by the power law exponential estimate at 2,384 days).

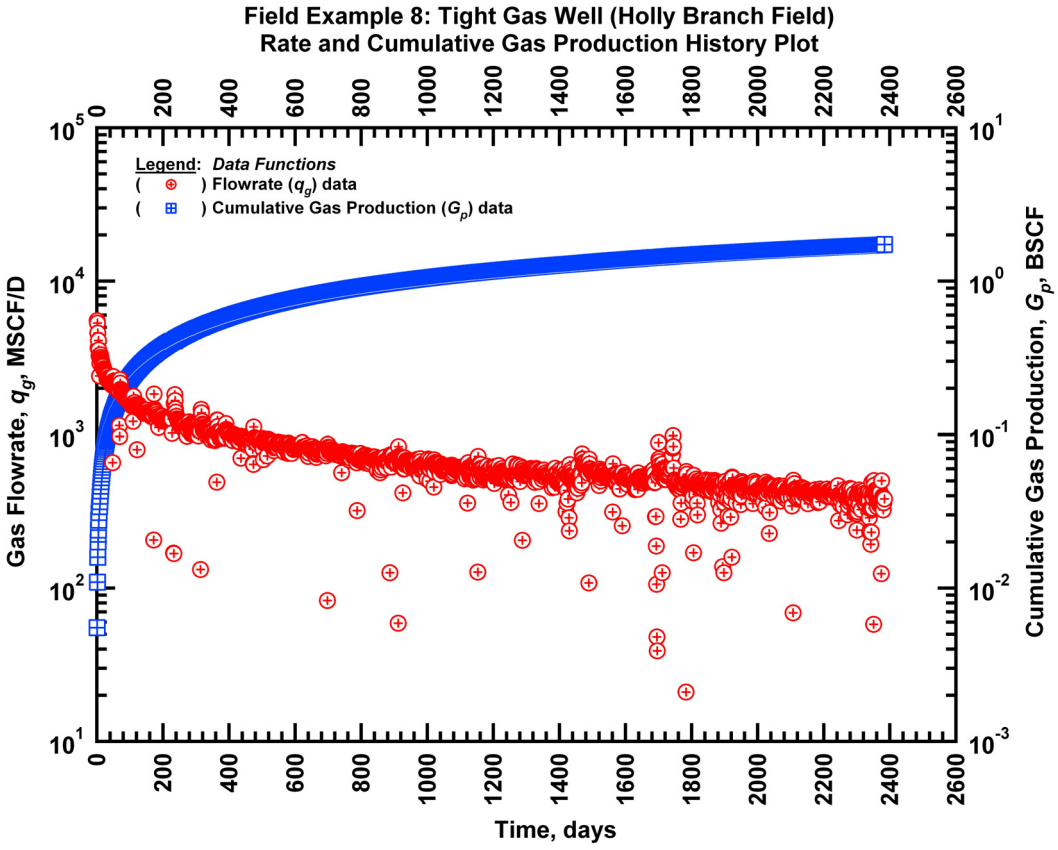

Figure C7 — (Semi-log Plot): Production history plot for field example 8 — flow rate (q_g) and cumulative production (G_p) versus production time.

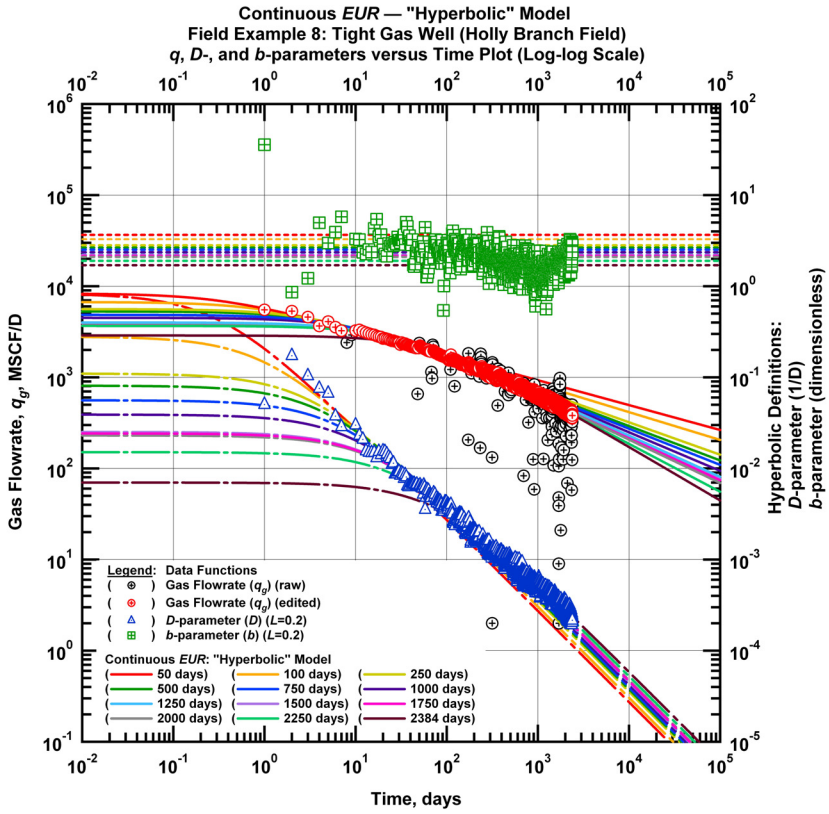

Figure C8 — (Log-log Plot): *qDb* plot — flow rate (q_g), *D*- and *b*-parameters versus production time and "hyperbolic" model matches for field example 8.

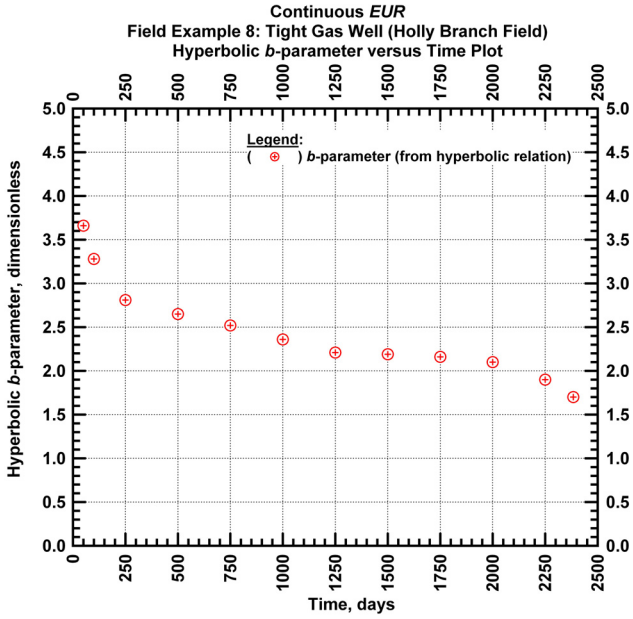

Figure C9 — (Cartesian Plot): Hyperbolic *b*-parameter values obtained from model matches with production data for field example 8.

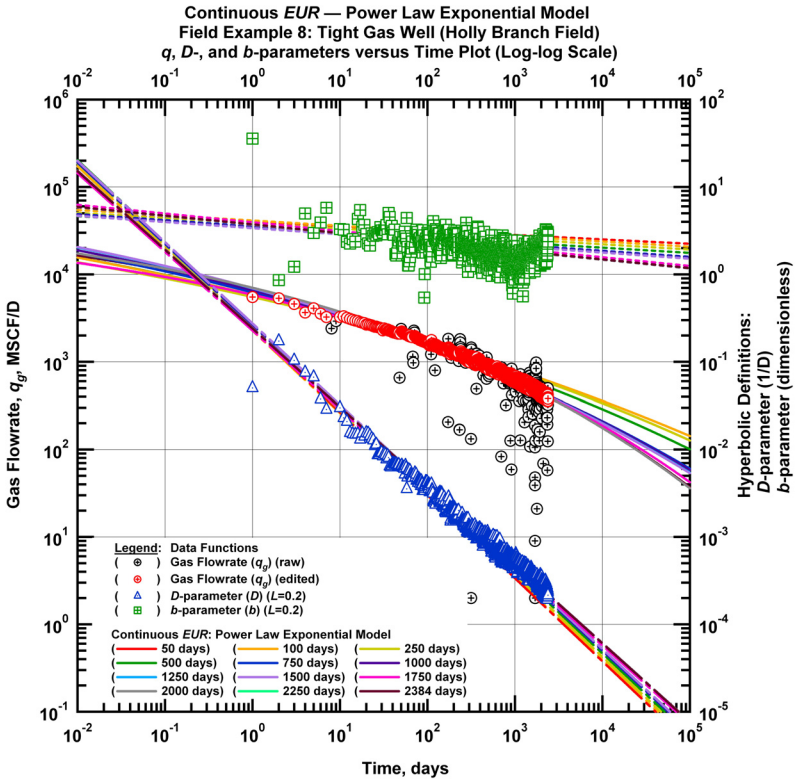

Figure C10 — (Log-log Plot): *qDb* plot — flow rate (q_g), *D*- and *b*-parameters versus production time and power law exponential model matches for field example 8.

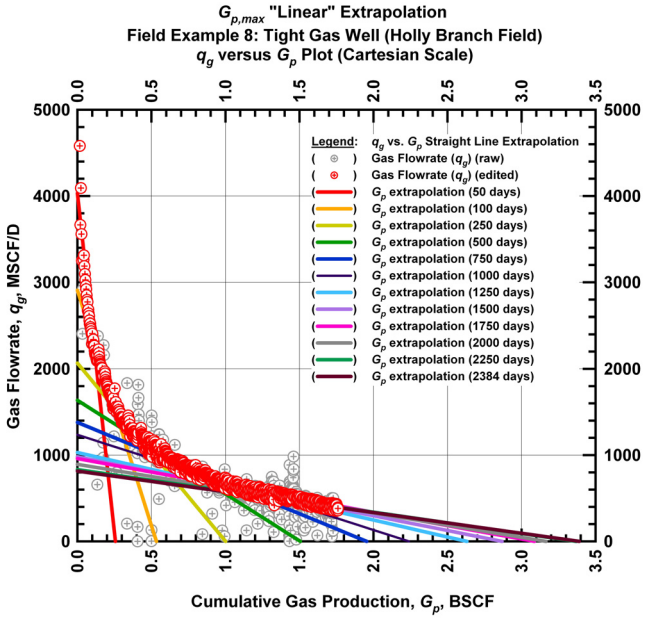

Figure C11 — (Cartesian Plot): Rate Cumulative Plot — flow rate (q_g) versus cumulative production (G_p) and the linear trends fit through the data for field example 8.

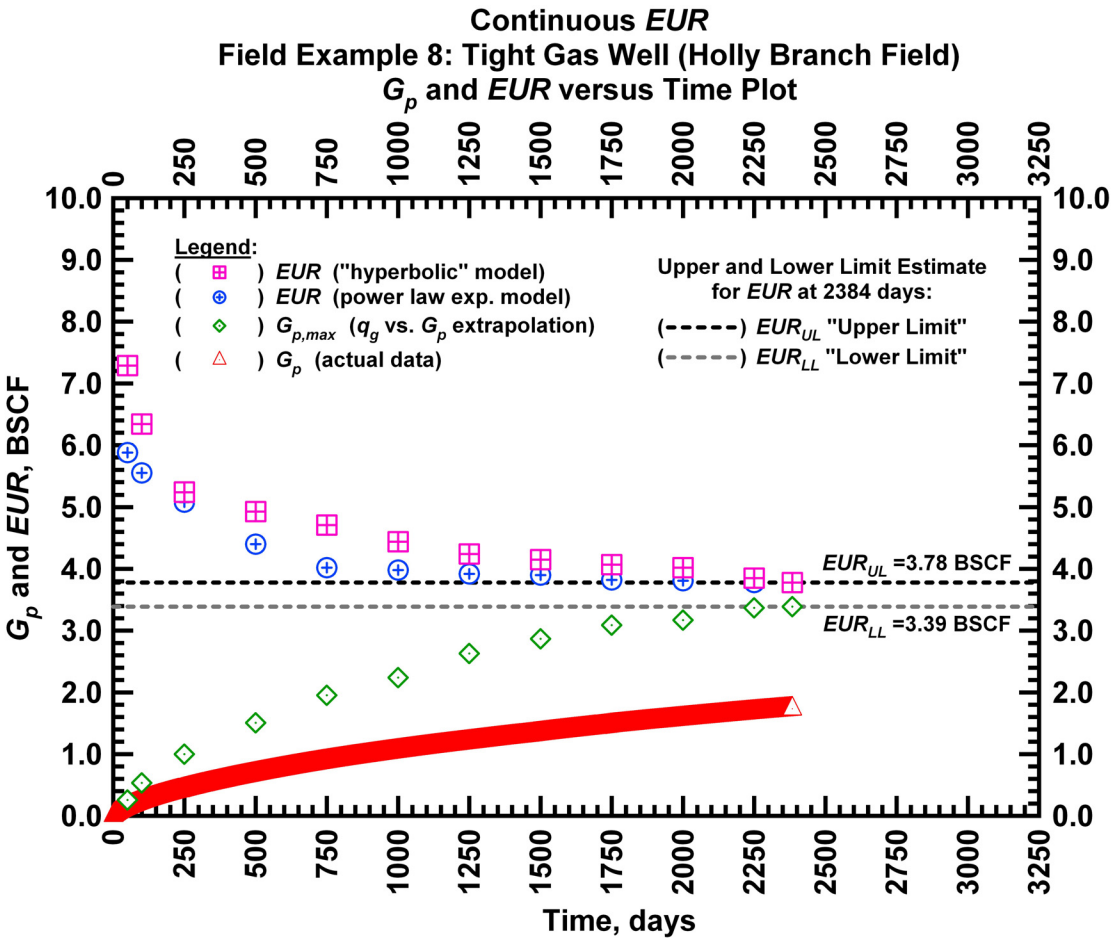

Figure C12 — (Cartesian Plot): *EUR* estimates from model matches and $G_{p,max}$ estimates from extrapolation technique for field example 8.

Table C4 — Analysis results for field example 8 — "hyperbolic" model parameters.

Time Interval, days	q_{gi} (MSCFD)	D_i (D^{-1})	b (dimensionless)	EUR_{hyp} (BSCF)
50	8,315	0.8310	3.66	7.29
100	6,704	0.2800	3.28	6.34
250	5,606	0.1100	2.81	5.24
500	5,280	0.0810	2.65	4.93
750	4,852	0.0560	2.52	4.71
1,000	4,500	0.0390	2.36	4.44
1,250	4,000	0.0250	2.21	4.24
1,500	3,932	0.0251	2.19	4.15
1,750	3,905	0.0242	2.16	4.07
2,000	3,932	0.0230	2.10	4.02
2,250	3,669	0.0151	1.90	3.85
2,384	2,880	0.0070	1.70	3.78

Table C5 — Analysis results for field example 8 — power law exponential model parameters.

Time Interval, days	$\hat{q}_{gi}$ (MSCFD)	$\hat{D}_i$ (D^{-1})	n (dimensionless)	D_∞ (D^{-1})	EUR_{PLE} (BSCF)
50	688,395	4.77	0.05	0	5.88
100	243,999	3.79	0.06	0	5.55
250	344,776	4.08	0.06	0	5.08
500	522,057	4.46	0.06	0	4.40
750	261,467	3.74	0.07	0	4.02
1,000	300,246	3.82	0.07	0	3.98
1,250	344,776	3.91	0.07	0	3.92
1,500	354,446	3.93	0.07	0	3.90
1,750	57,116	2.28	0.10	0	3.82
2,000	80,706	2.44	0.10	0	3.81
2,250	75,314	2.41	0.10	0	3.78
2,384	75,314	2.41	0.10	0	3.78

Table C6 — Analysis results for field example 8 — straight line extrapolation.

Time Interval, days	Slope, 10^{-6} D^{-1}	Intercept, MSCF/D	$G_{p,max}$ (BSCF)
50	15,697	4,033	0.26
100	5,449	2,908	0.53
250	2,064	2,066	1.00
500	1,086	1,635	1.51
750	705	1,379	1.95
1,000	552	1,236	2.24
1,250	392	1,030	2.63
1,500	342	980	2.87
1,750	311	959	3.09
2,000	282	893	3.17
2,250	247	832	3.37
2,384	240	815	3.39

Field Example 9

We present the flow rate data and the cumulative production data which spans over 1.4 years for a vertical well producing from a tight gas reservoir in **Fig. C13**. **Fig. C14** presents the "hyperbolic" model matches imposed on the flow rate data along with the *D*- and *b*-parameter trends. In **Fig. C15** we observe that the value of the *b*-parameter as a function of time. The *b*-parameter value is stable around 2.3 after 150 days of production. Every interval is matched with a "hyperbolic" *b*-parameter greater than 1 indicating that boundary-dominated flow has not been established. **Fig. C16** shows the power law exponential model matches imposed on the flow rate data and *D*- and *b*-parameter trends. In **Fig. C17** we show the results of the straight line extrapolation technique, and in **Fig. C18** we present the calculated *EUR* values versus production time. All of the model parameters for this example are presented in **Tables C7, C8, and C9**. The *EUR* of this well should be in between 0.86 BSCF (the "lower" limit given by the straight line extrapolation technique at 512 days) and 1.82 BSCF (the "upper" limit given by the power law exponential estimate at 512 days).

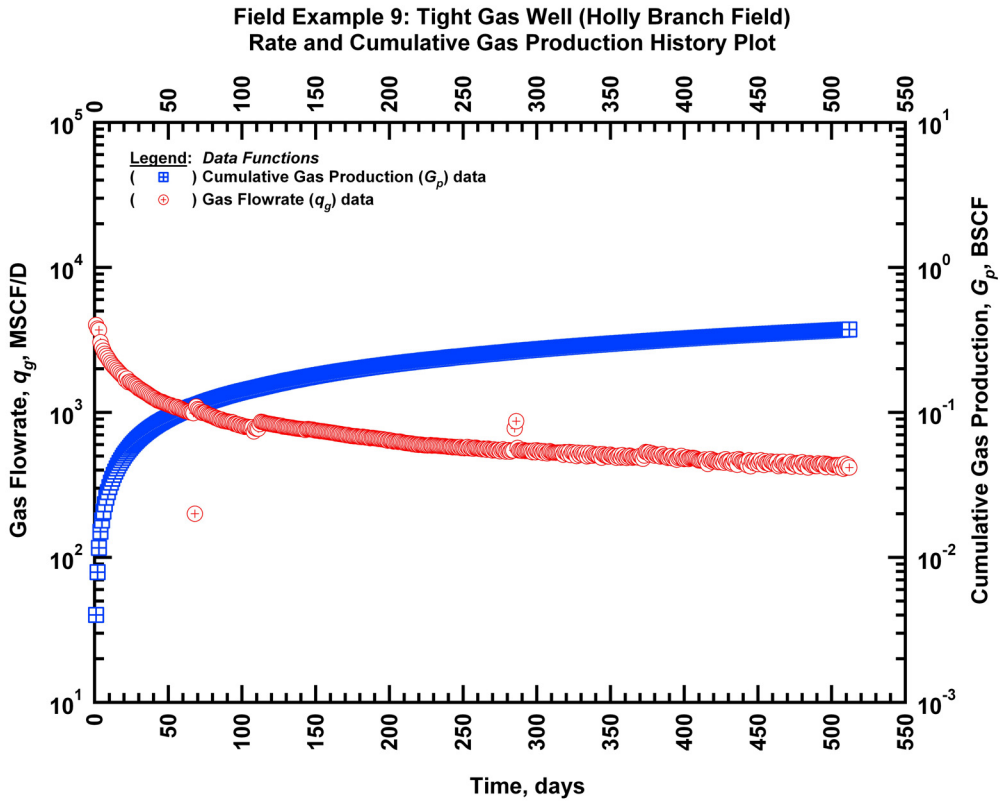

Figure C13 — (Semi-log Plot): Production history plot for field example 9 — flow rate (q_g) and cumulative production (G_p) versus production time.

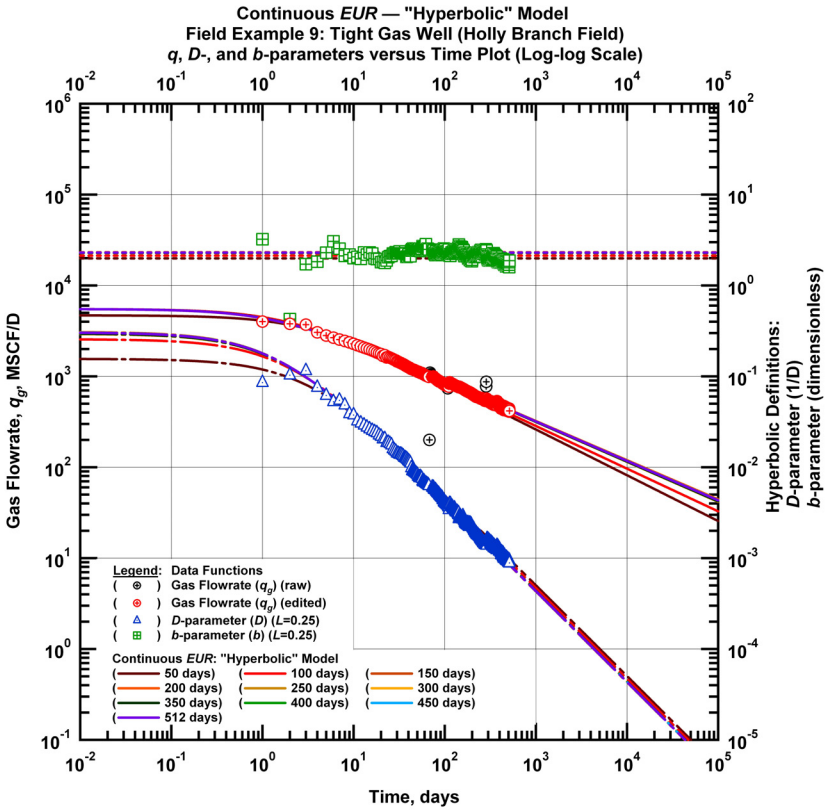

Figure C14 — (Log-log Plot): *qDb* plot — flow rate (q_g), *D*- and *b*-parameters versus production time and "hyperbolic" model matches for field example 9.

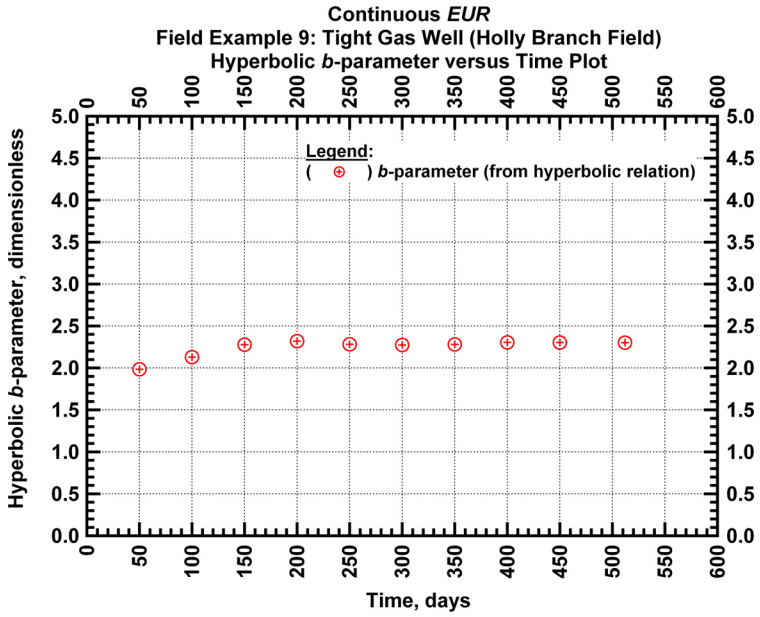

Figure C15 — (Cartesian Plot): Hyperbolic *b*-parameter values obtained from model matches with production data for field example 9.

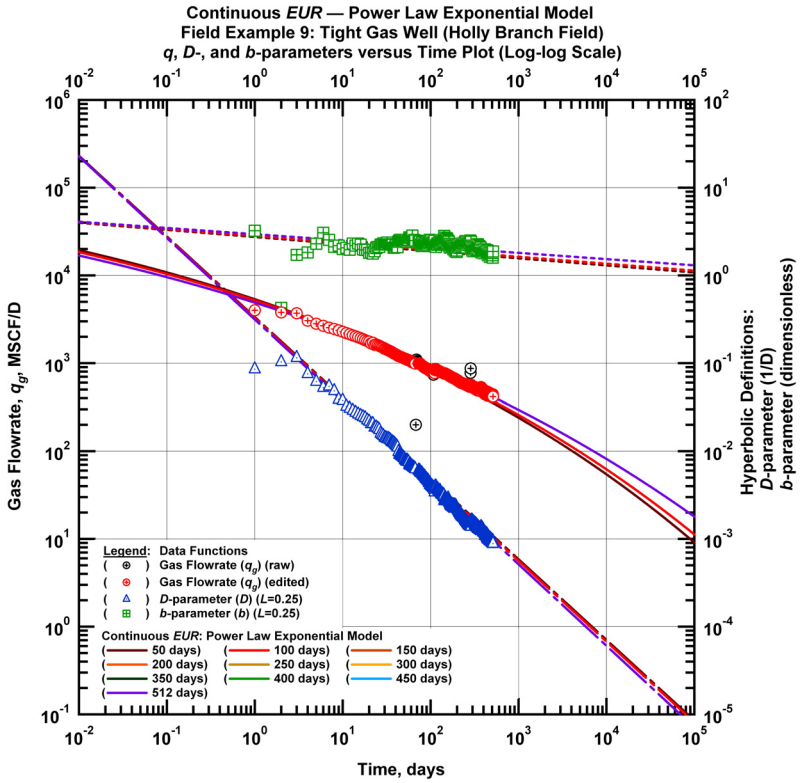

Figure C16 — (Log-log Plot): *qDb* plot — flow rate (q_g), *D*- and *b*-parameters versus production time and power law exponential model matches for field example 9.

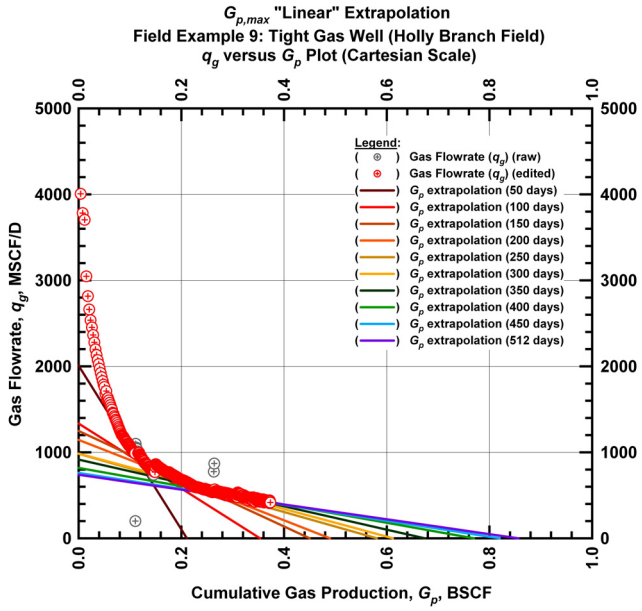

Figure C17 — (Cartesian Plot): Rate Cumulative Plot — flow rate (q_g) versus cumulative production (G_p) and the linear trends fit through the data for field example 9.

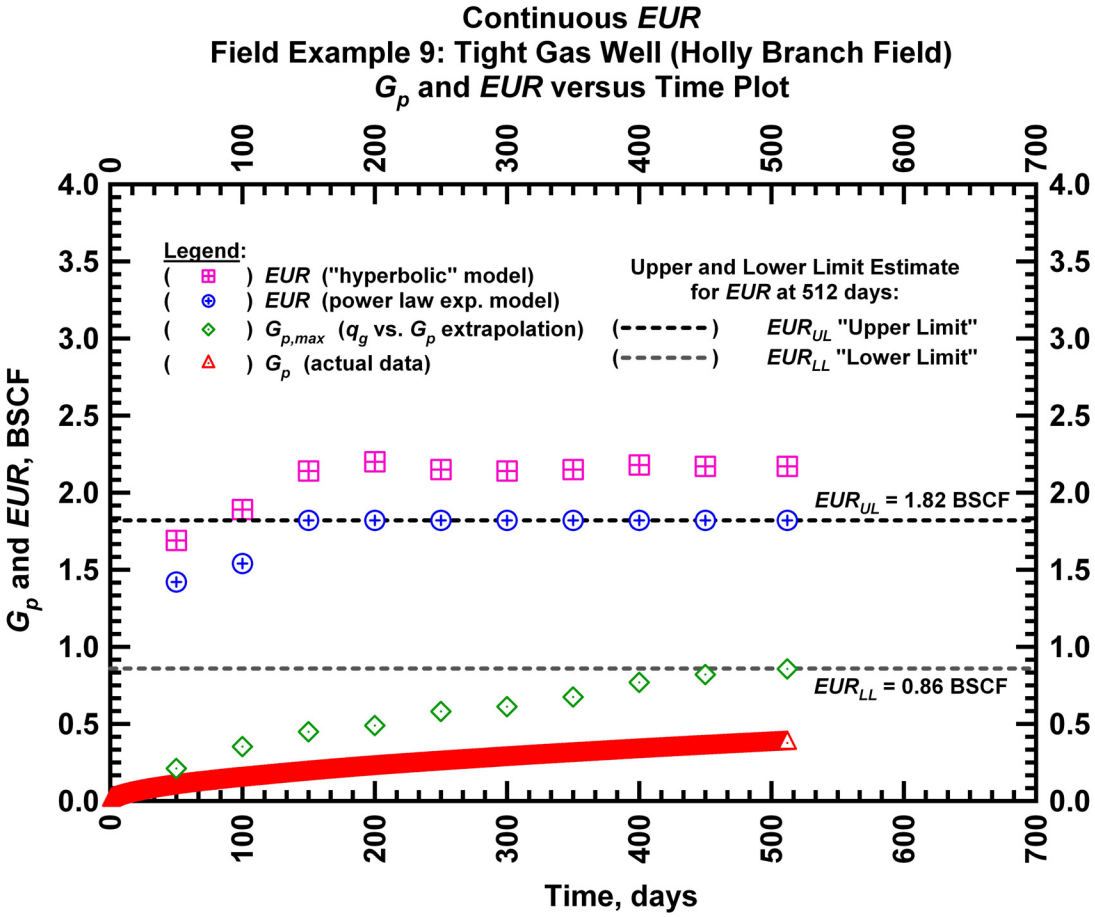

Figure C18 — (Cartesian Plot): *EUR* estimates from model matches and $G_{p,max}$ estimates from extrapolation technique for field example 9.

Table C7 — Analysis results for field example 9 — "hyperbolic" model parameters.

Time Interval, days	q_{gi} (MSCFD)	D_i (D^{-1})	b (dimensionless)	EUR_{hyp} (BSCF)
50	4,689	0.15571	1.984	1.69
100	5,502	0.25638	2.128	1.89
150	5,502	0.29572	2.277	2.14
200	5,502	0.30868	2.319	2.20
250	5,502	0.29580	2.281	2.15
300	5,502	0.29322	2.274	2.14
350	5,502	0.29584	2.281	2.15
400	5,502	0.30508	2.304	2.18
450	5,502	0.30448	2.303	2.17
512	5,502	0.30367	2.301	2.17

Table C8 — Analysis results for field example 9 — power law exponential model parameters.

Time Interval, days	$\hat{q}_{gi}$ (MSCFD)	$\hat{D}_i$ (D^{-1})	n (dimensionless)	D_∞ (D^{-1})	EUR_{PLE} (BSCF)
50	335,371	4.138	0.081	0	1.42
100	326,222	4.138	0.079	0	1.54
150	412,682	4.435	0.071	0	1.82
200	412,682	4.435	0.071	0	1.82
250	412,682	4.435	0.071	0	1.82
300	412,682	4.435	0.071	0	1.82
350	412,682	4.435	0.071	0	1.82
400	412,682	4.435	0.071	0	1.82
450	412,682	4.435	0.071	0	1.82
512	412,682	4.435	0.071	0	1.82

Table C9 — Analysis results for field example 9 — straight line extrapolation.

Time Interval, days	Slope, 10^{-6} D^{-1}	Intercept, MSCF/D	$G_{p,max}$ (BSCF)
50	9,527	2,008	0.21
100	3,776	1,334	0.35
150	2,777	1,249	0.45
200	2,340	1,145	0.49
250	1,693	983	0.58
300	1,611	986	0.61
350	1,357	915	0.67
400	1,064	819	0.77
450	928	761	0.82
512	863	739	0.86

Field Example 10

We present the flow rate data and the cumulative production data which spans almost 1 year for a vertical well producing from a tight gas reservoir in **Fig. C19**. **Fig. C20** presents the "hyperbolic" model matches imposed on the flow rate data along with the *D*- and *b*-parameter trends. In **Fig. C21** we observe that the value of the *b*-parameter as a function of time. The *b*-parameter value stabilizes around 2.31 after 331 days of production. Every interval is matched with a "hyperbolic" *b*-parameter greater than 1 indicating that boundary-dominated flow has not been established. **Fig. C22** shows the power law exponential model matches imposed on the flow rate data and *D*- and *b*-parameter trends. In **Fig. C23** we show the results of the straight line extrapolation technique, and in **Fig. C24** we present the calculated *EUR* values versus production time. All of the model parameters for this example are presented in **Tables C10, C11, and C12**. The *EUR* of this well should be in between 0.53 BSCF (the "lower" limit given by the straight line extrapolation technique at 331 days) and 1.30 BSCF (the "upper" limit given by the power law exponential estimate at 331 days).

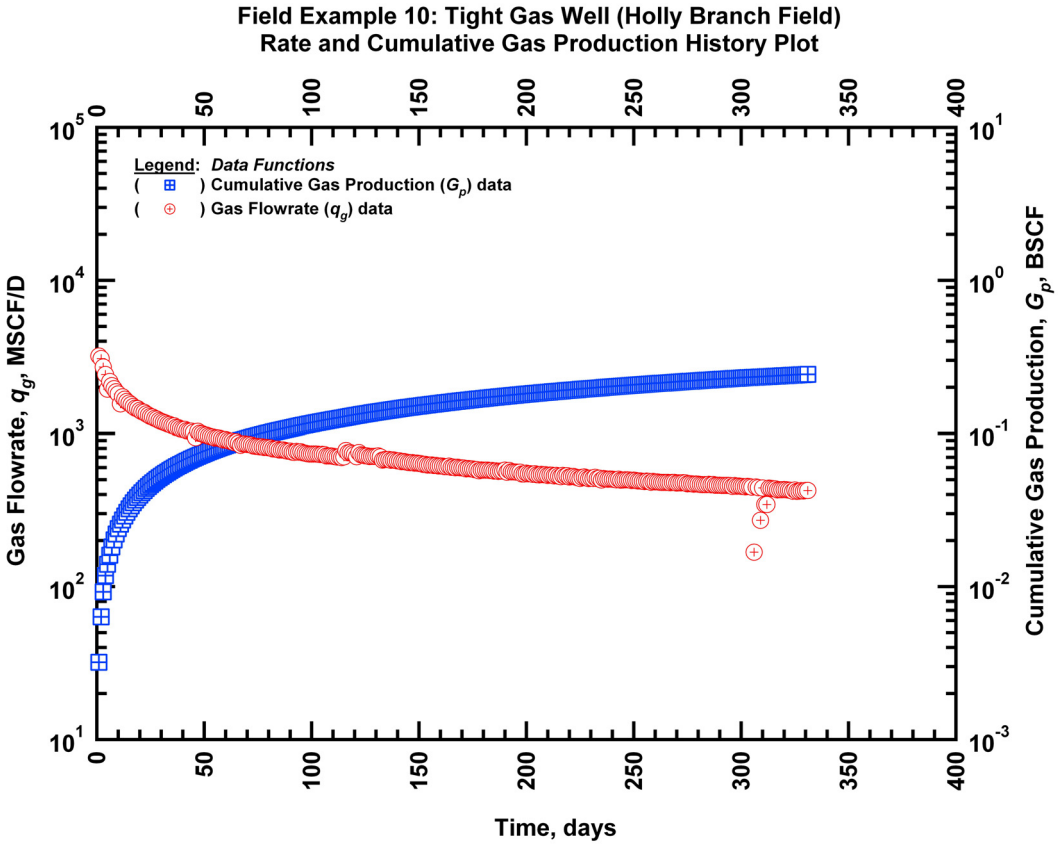

Figure C19 — (Semi-log Plot): Production history plot for field example 10 — flow rate (q_g) and cumulative production (G_p) versus production time.

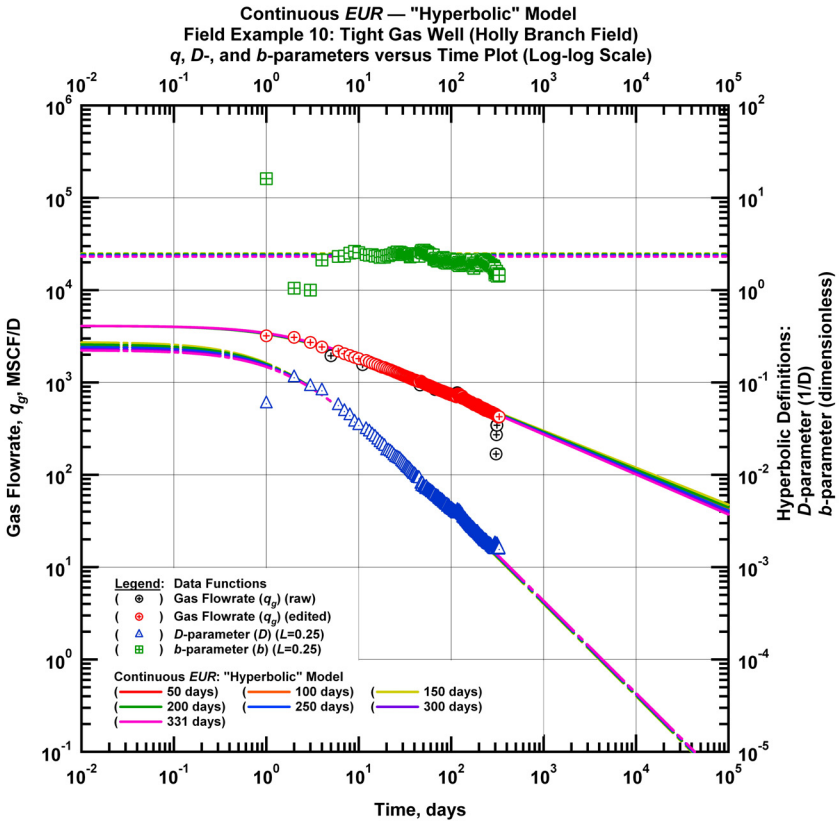

Figure C20 — (Log-log Plot): *qDb* plot — flow rate (q_g), *D*- and *b*-parameters versus production time and "hyperbolic" model matches for field example 10.

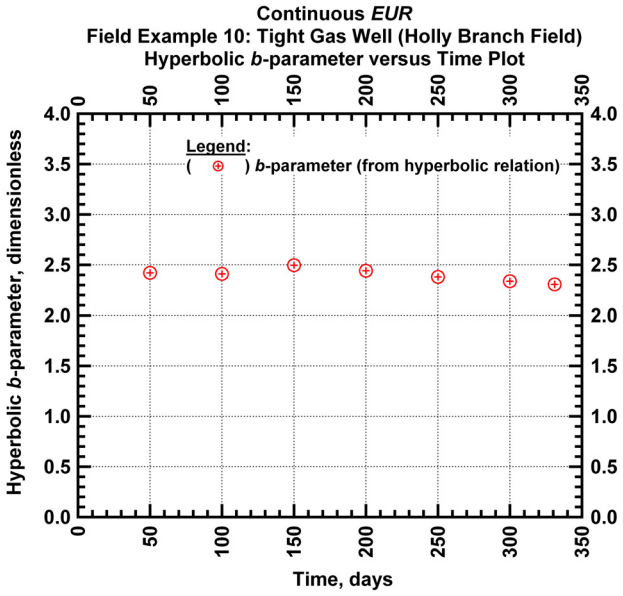

Figure C21 — (Cartesian Plot): Hyperbolic *b*-parameter values obtained from model matches with production data for field example 10.

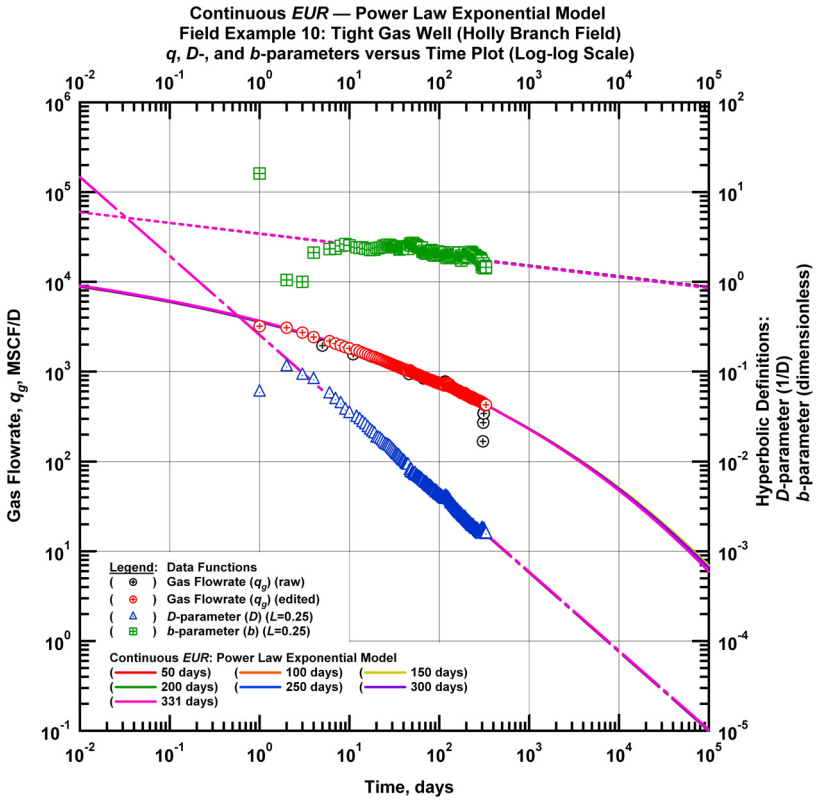

Figure C22 — (Log-log Plot): *qDb* plot — flow rate (q_g), *D*- and *b*-parameters versus production time and power law exponential model matches for field example 10.

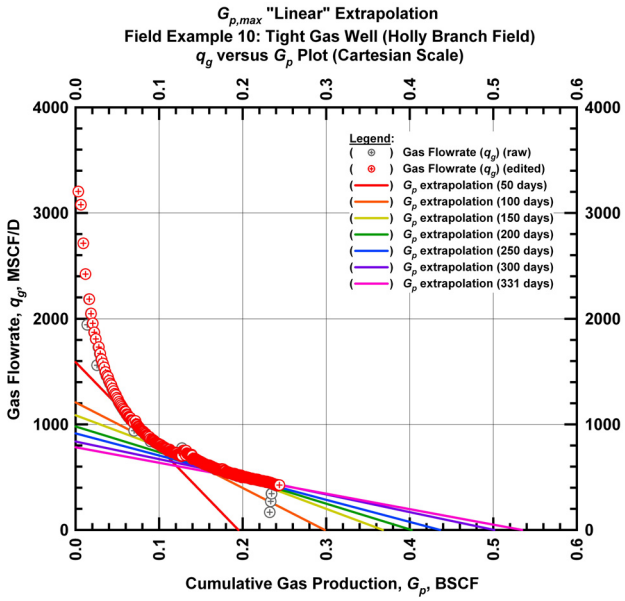

Figure C23 — (Cartesian Plot): Rate Cumulative Plot — flow rate (q_g) versus cumulative production (G_p) and the linear trends fit through the data for field example 10.

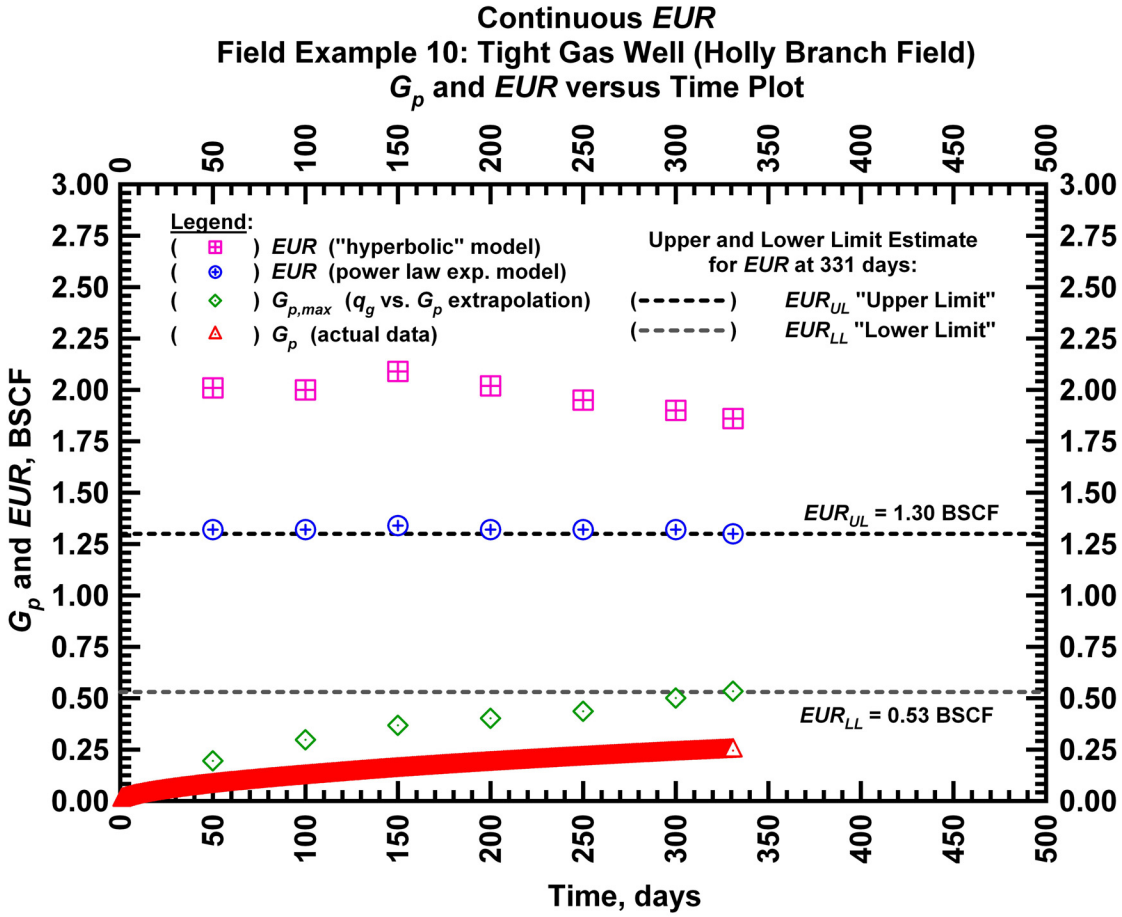

Figure C24 — (Cartesian Plot): *EUR* estimates from model matches and $G_{p,max}$ estimates from extrapolation technique for field example 10.

Table C10 — Analysis results for field example 10 — "hyperbolic" model parameters.

Time Interval, days	q_{gi} (MSCFD)	D_i (D^{-1})	b (dimensionless)	EUR_{hyp} (BSCF)
50	4,099	0.24889	2.420	2.01
100	4,099	0.24520	2.410	2.00
150	4,099	0.27308	2.496	2.09
200	4,099	0.25891	2.442	2.02
250	4,099	0.24260	2.380	1.95
300	4,099	0.23129	2.337	1.90
331	4,099	0.22314	2.307	1.86

Table C11 — Analysis results for field example 10 — power law exponential model parameters.

Time Interval, days	$\hat{q}_{gi}$ (MSCFD)	$\hat{D}_i$ (D^{-1})	n (dimensionless)	D_∞ (D^{-1})	EUR_{PLE} (BSCF)
50	30,654	2.147	0.119	0	1.32
100	30,654	2.147	0.119	0	1.32
150	30,654	2.157	0.118	0	1.34
200	30,654	2.147	0.119	0	1.32
250	30,654	2.147	0.119	0	1.32
300	30,654	2.147	0.119	0	1.32
331	30,654	2.123	0.121	0	1.30

Table C12 — Analysis results for field example 10 — straight line extrapolation.

Time Interval, days	Slope, 10^{-6} D^{-1}	Intercept, MSCF/D	$G_{p,max}$ (BSCF)
50	8,155	1,590	0.19
100	4,051	1,208	0.30
150	2,952	1,086	0.37
200	2,436	980	0.40
250	2,097	915	0.44
300	1,672	838	0.50
331	1,465	783	0.53

Field Example 11

We present the flow rate data and the cumulative production data which spans almost 2.7 years for a vertical well producing from a tight gas reservoir in **Fig. C25**. **Fig. C26** presents the "hyperbolic" model matches imposed on the flow rate data along with the *D*- and *b*-parameter trends. In **Fig. C27** we observe that the value of the *b*-parameter as a function of time. The *b*-parameter value decreases from 3.66 to 2.46 during the production history. Every interval is matched with a "hyperbolic" *b*-parameter greater than 1 indicating that boundary-dominated flow has not been established. **Fig. C28** shows the power law exponential model matches imposed on the flow rate data and *D*- and *b*-parameter trends. In **Fig. C29** we show the results of the straight line extrapolation technique, and in **Fig. C30** we present the calculated *EUR* values versus production time. All of the model parameters for this example are presented in **Tables C13, C14, and C15**. The *EUR* of this well should be in between 1.20 BSCF (the "lower" limit given by the straight line extrapolation technique at 981 days) and 1.91 BSCF (the "upper" limit given by the power law exponential estimate at 981 days).

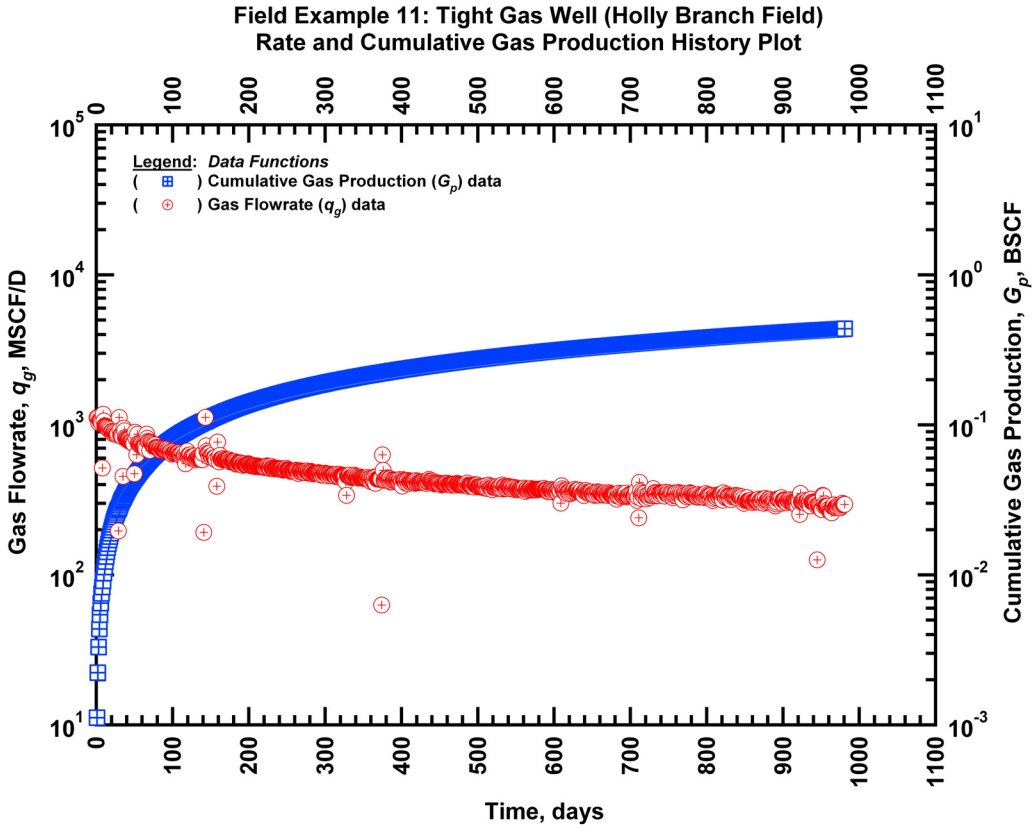

Figure C25 — (Semi-log Plot): Production history plot for field example 11 — flow rate (q_g) and cumulative production (G_p) versus production time.

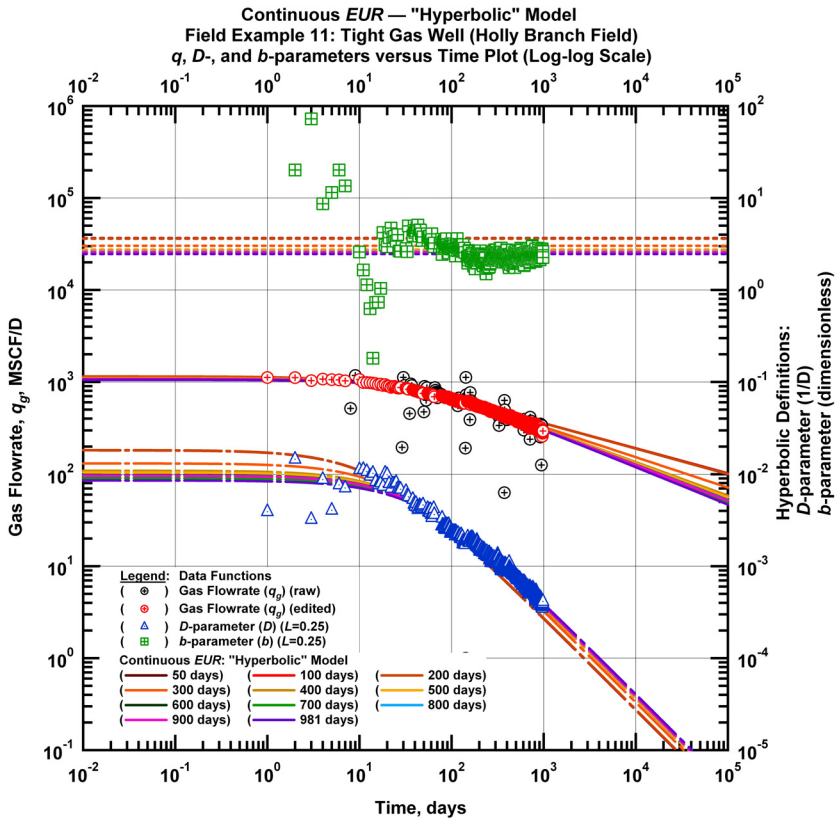

Figure C26 — (Log-log Plot): *qDb* plot — flow rate (q_g), *D*- and *b*-parameters versus production time and "hyperbolic" model matches for field example 11.

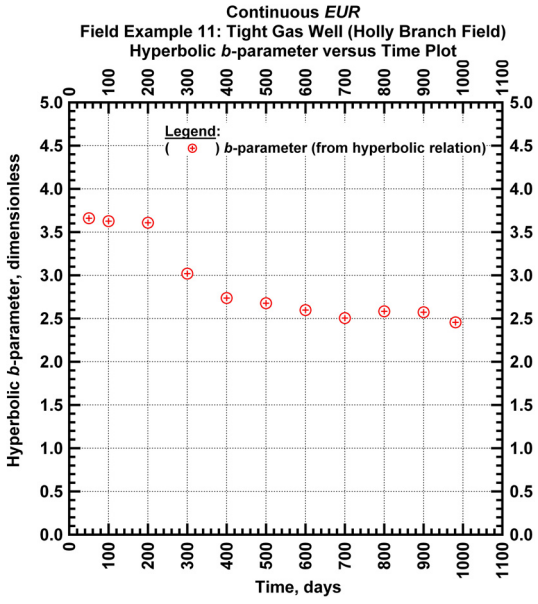

Figure C27 — (Cartesian Plot): Hyperbolic *b*-parameter values obtained from model matches with production data for field example 11.

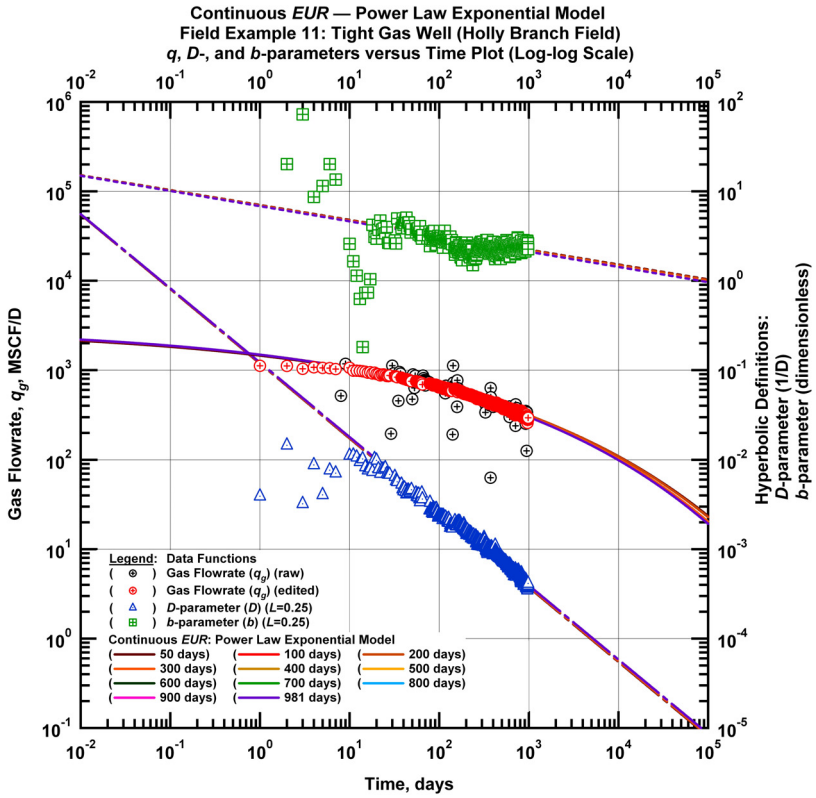

Figure C28 — (Log-log Plot): *qDb* plot — flow rate (q_g), *D*- and *b*-parameters versus production time and power law exponential model matches for field example 11.

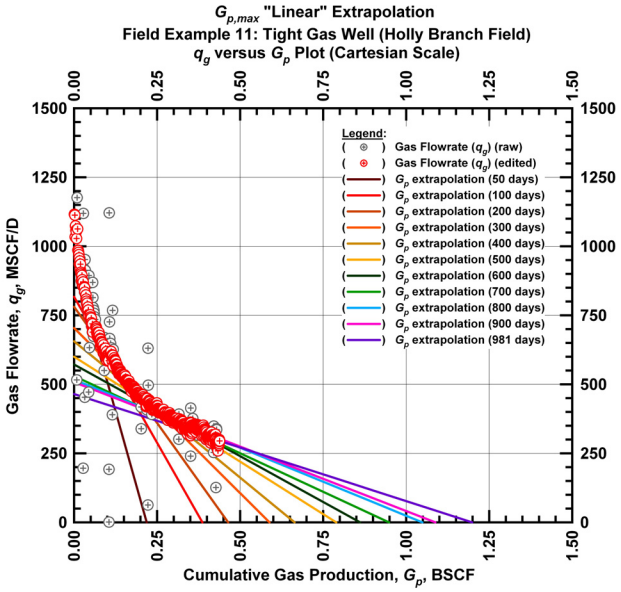

Figure C29 — (Cartesian Plot): Rate Cumulative Plot — flow rate (q_g) versus cumulative production (G_p) and the linear trends fit through the data for field example 11.

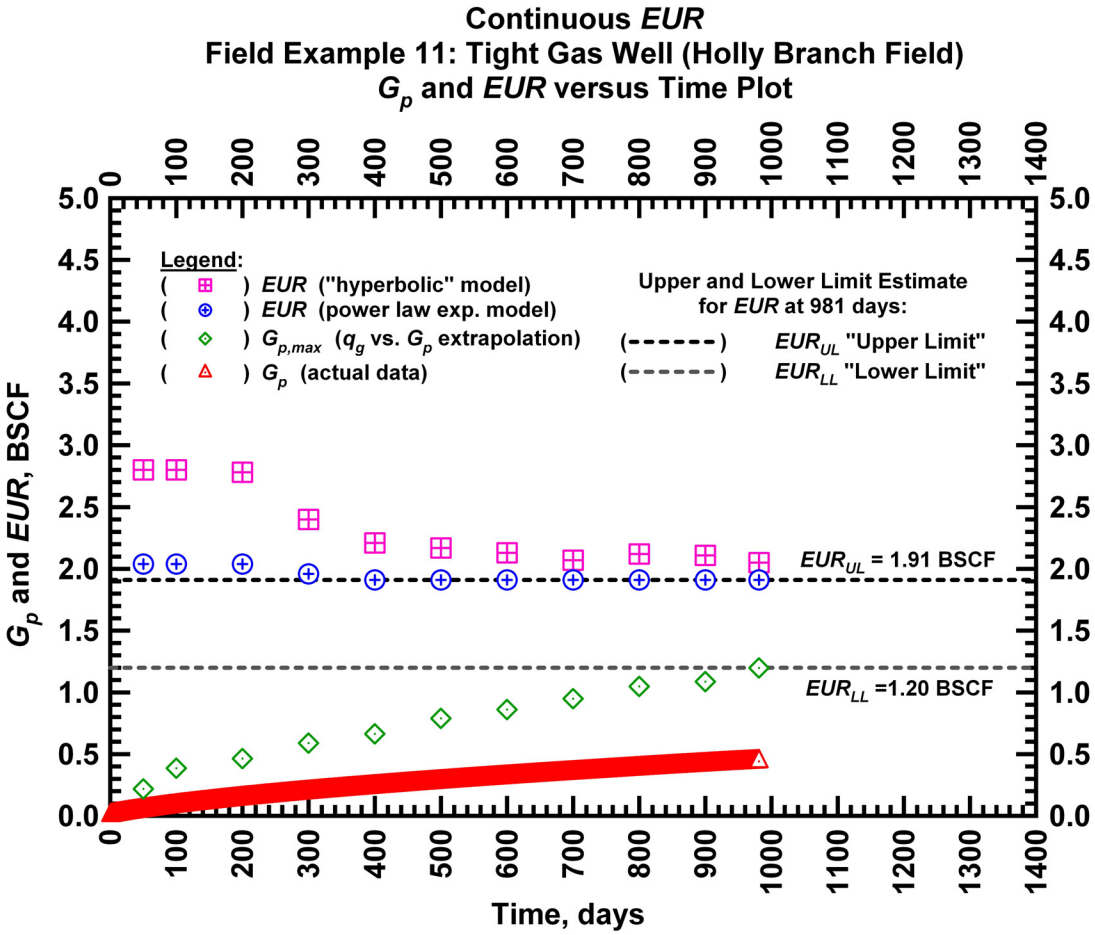

Figure C30 — (Cartesian Plot): *EUR* estimates from model matches and $G_{p,max}$ estimates from extrapolation technique for field example 11.

Table C13 — Analysis results for field example 11 — "hyperbolic" model parameters.

Time Interval, days	q_{gi} (MSCFD)	D_i (D^{-1})	b (dimensionless)	EUR_{hyp} (BSCF)
50	1,133	0.018205	3.660	2.80
100	1,146	0.018205	3.626	2.80
200	1,147	0.018309	3.608	2.78
300	1,112	0.013117	3.019	2.40
400	1,089	0.010913	2.737	2.21
500	1,084	0.010449	2.677	2.17
600	1,075	0.009811	2.597	2.13
700	1,063	0.009067	2.505	2.07
800	1,072	0.009687	2.584	2.12
900	1,072	0.009625	2.572	2.11
981	1,053	0.008548	2.456	2.05

Table C14 — Analysis results for field example 11 — power law exponential model parameters.

Time Interval, days	$\hat{q}_{gi}$ (MSCFD)	$\hat{D}_i$ (D^{-1})	n (dimensionless)	D_∞ (D^{-1})	EUR_{PLE} (BSCF)
50	2,961	0.7110	0.167	0	2.04
100	3,044	0.7155	0.167	0	2.04
200	3,044	0.7155	0.167	0	2.04
300	3,044	0.7155	0.169	0	1.96
400	3,044	0.7155	0.170	0	1.91
500	3,044	0.7155	0.170	0	1.91
600	3,044	0.7155	0.170	0	1.91
700	3,044	0.7155	0.170	0	1.91
800	3,044	0.7155	0.170	0	1.91
900	3,044	0.7155	0.170	0	1.91
981	3,044	0.7155	0.170	0	1.91

Table C15 — Analysis results for field example 11 — straight line extrapolation.

Time Interval, days	Slope, 10^{-6} D^{-1}	Intercept, MSCF/D	$G_{p,max}$ (BSCF)
50	4,292	939	0.22
100	2,115	817	0.39
200	1,684	781	0.46
300	1,196	704	0.59
400	988	656	0.66
500	760	600	0.79
600	664	572	0.86
700	559	530	0.95
800	493	517	1.05
900	467	508	1.09
981	388	465	1.20

Field Example 12

We present the flow rate data and the cumulative production data which spans almost 2 years for a vertical well producing from a tight gas reservoir in **Fig. C31**. **Fig. C32** presents the "hyperbolic" model matches imposed on the flow rate data along with the *D*- and *b*-parameter trends. In **Fig. C33** we observe that the value of the *b*-parameter as a function of time. The *b*-parameter value stabilizes around 1.41 after 200 days of production. Every interval is matched with a "hyperbolic" *b*-parameter greater than 1 indicating that boundary-dominated flow has not been established. **Fig. C34** shows the power law exponential model matches imposed on the flow rate data and *D*- and *b*-parameter trends. In **Fig. C35** we show the results of the straight line extrapolation technique, and in **Fig. C36** we present the calculated *EUR* values versus production time. All of the model parameters for this example are presented in **Tables C16, C17, and C18**. The *EUR* of this well should be in between 1.45 BSCF (the "lower" limit given by the straight line extrapolation technique at 671 days) and 2.19 BSCF (the "upper" limit given by the power law exponential estimate at 671 days).

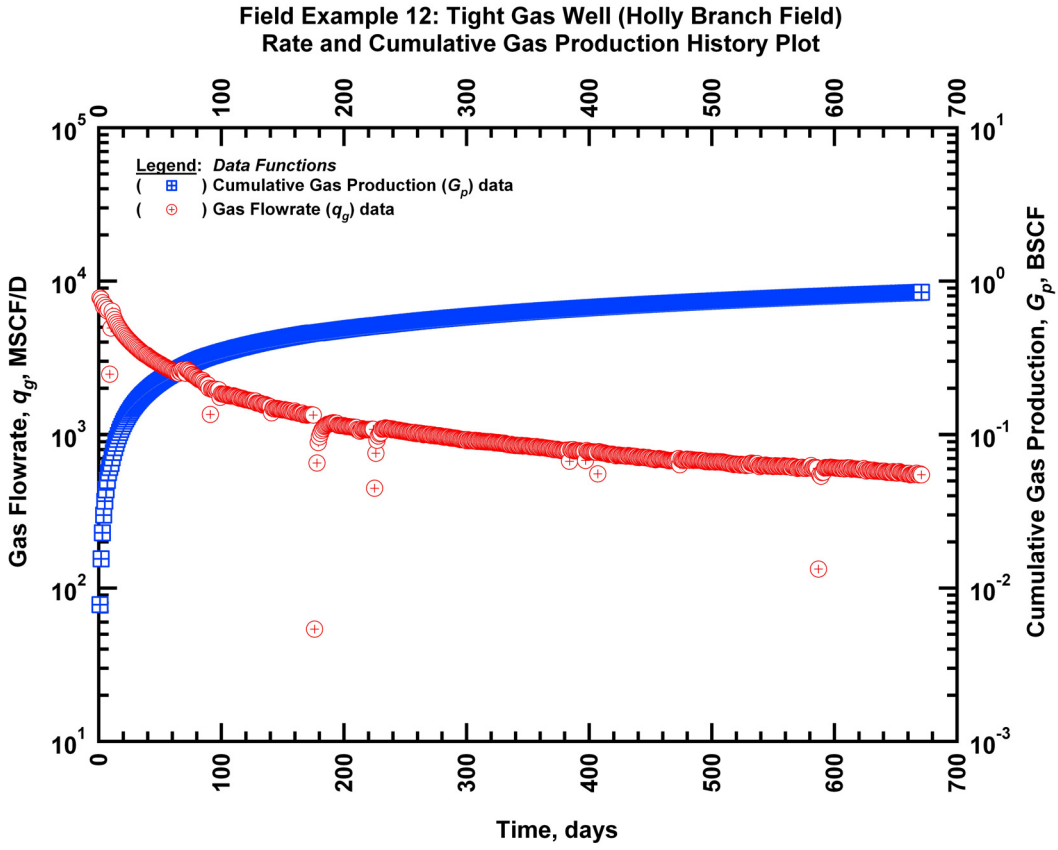

Figure C31 — (Semi-log Plot): Production history plot for field example 12 — flow rate (q_g) and cumulative production (G_p) versus production time.

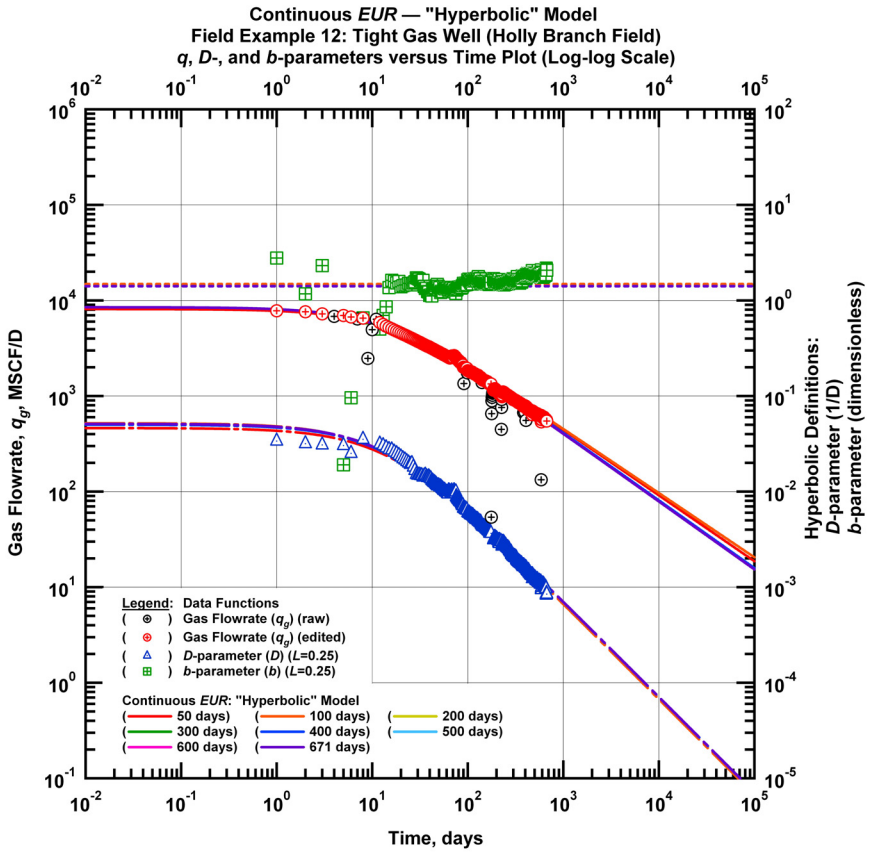

Figure C32 — (Log-log Plot): *qDb* plot — flow rate (q_g), *D*- and *b*-parameters versus production time and "hyperbolic" model matches for field example 12.

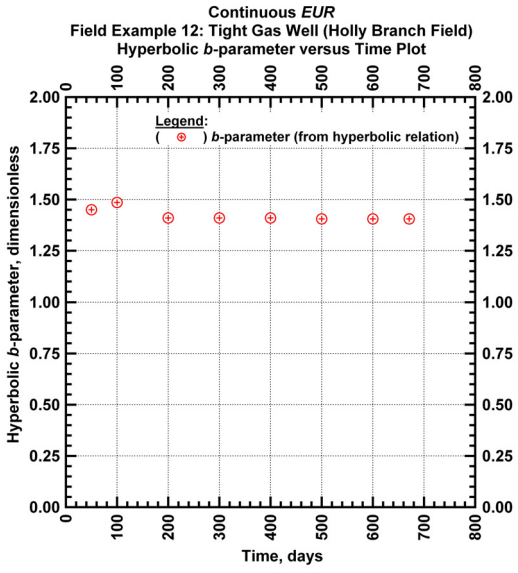

Figure C33 — (Cartesian Plot): Hyperbolic *b*-parameter values obtained from model matches with production data for field example 12.

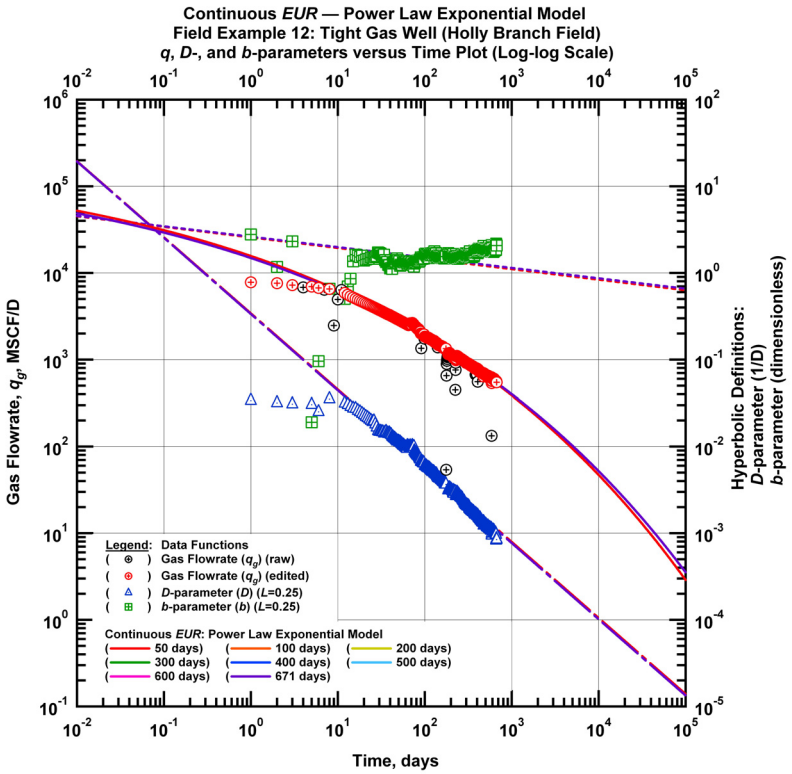

Figure C34 — (Log-log Plot): *qDb* plot — flow rate (q_g), *D*- and *b*-parameters versus production time and power law exponential model matches for field example 12.

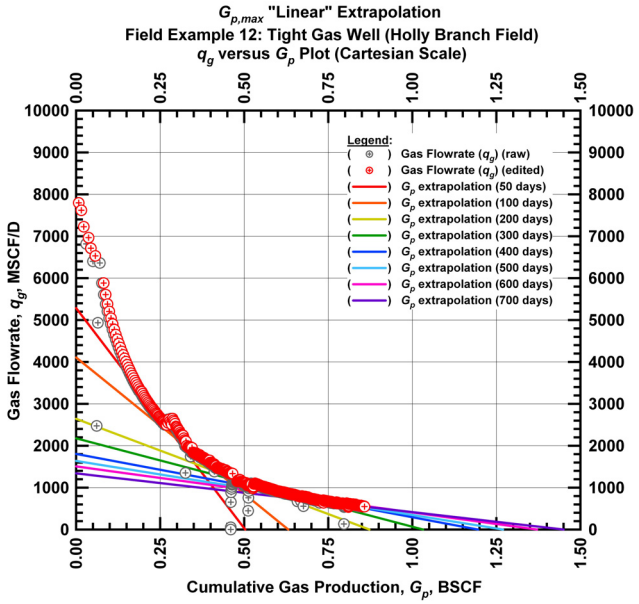

Figure C35 — (Cartesian Plot): Rate Cumulative Plot — flow rate (q_g) versus cumulative production (G_p) and the linear trends fit through the data for field example 12.

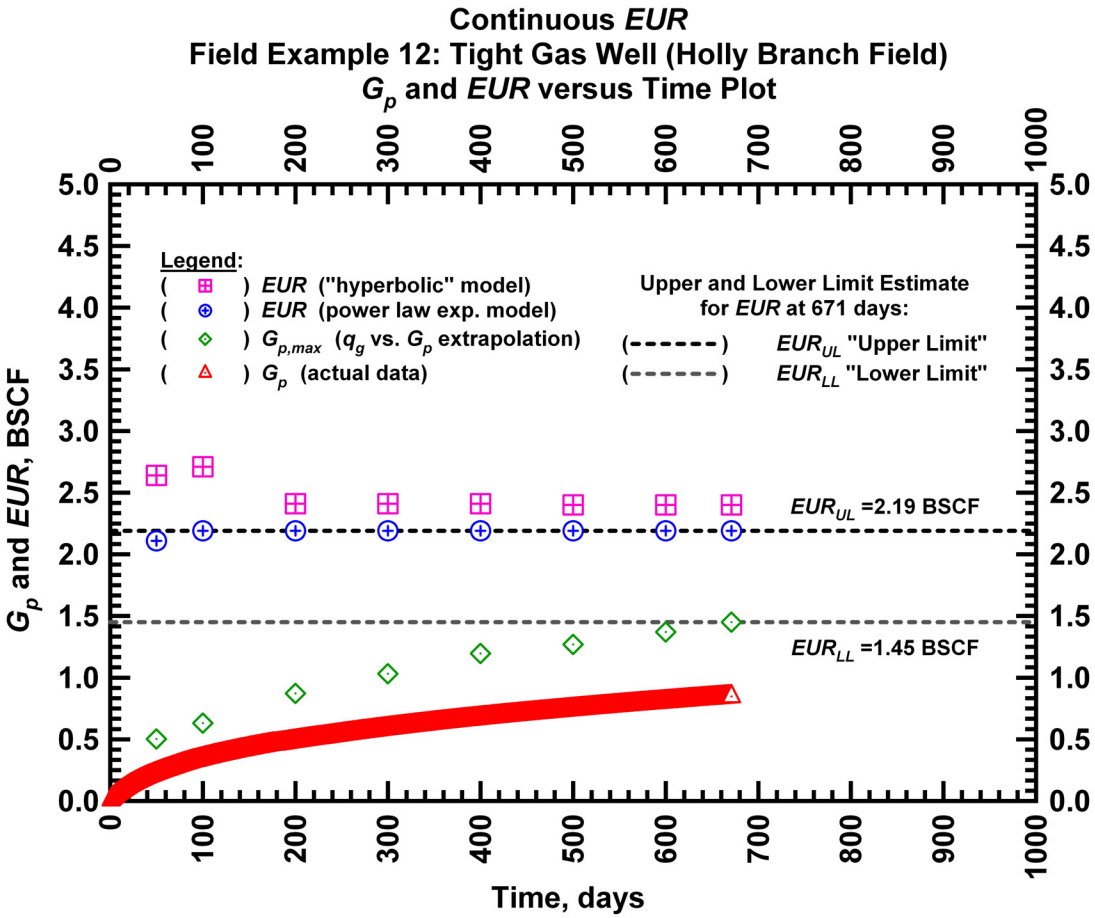

Figure C36 — (Cartesian Plot): *EUR* estimates from model matches and $G_{p,max}$ estimates from extrapolation technique for field example 12.

Table C16 — Analysis results for field example 12 — "hyperbolic" model parameters.

Time Interval, days	q_{gi} (MSCFD)	D_i (D^{-1})	b (dimensionless)	EUR_{hyp} (BSCF)
50	8,127	0.046197	1.450	2.64
100	8,500	0.051903	1.485	2.71
200	8,500	0.050069	1.410	2.41
300	8,500	0.050069	1.410	2.41
400	8,500	0.050069	1.410	2.41
500	8,500	0.051146	1.405	2.40
600	8,500	0.051146	1.405	2.40
671	8,500	0.051146	1.405	2.40

Table C17 — Analysis results for field example 12 — power law exponential model parameters.

Time Interval, days	$\hat{q}_{gi}$ (MSCFD)	$\hat{D}_i$ (D^{-1})	n (dimensionless)	D_∞ (D^{-1})	EUR_{PLE} (BSCF)
50	257,876	2.799	0.122	0	2.11
100	243,999	2.799	0.120	0	2.19
200	243,999	2.799	0.120	0	2.19
300	243,999	2.799	0.120	0	2.19
400	243,999	2.799	0.120	0	2.19
500	243,999	2.799	0.120	0	2.19
600	243,999	2.799	0.120	0	2.19
671	243,999	2.799	0.120	0	2.19

Table C18 — Analysis results for field example 12 — straight line extrapolation.

Time Interval, days	Slope, 10^{-6} D^{-1}	Intercept, MSCF/D	$G_{p,max}$ (BSCF)
50	10,507	5,286	0.50
100	6,509	4,108	0.63
200	3,029	2,642	0.87
300	2,109	2,177	1.03
400	1,509	1,804	1.20
500	1,289	1,637	1.27
600	1,099	1,507	1.37
671	924	1,340	1.45

Field Example 13

We present the flow rate data and the cumulative production data which spans almost 1 year for a vertical well producing from a tight gas reservoir in **Fig. C37**. **Fig. C38** presents the "hyperbolic" model matches imposed on the flow rate data along with the *D*- and *b*-parameter trends. In **Fig. C39** we observe that the value of the *b*-parameter as a function of time. The *b*-parameter value is stable around 2.85 during the production history. Every interval is matched with a "hyperbolic" *b*-parameter greater than 1 indicating that boundary-dominated flow has not been established. **Fig. C40** shows the power law exponential model matches imposed on the flow rate data and *D*- and *b*-parameter trends. In **Fig. C41** we show the results of the straight line extrapolation technique, and in **Fig. C42** we present the calculated *EUR* values versus production time. All of the model parameters for this example are presented in **Tables C19, C20, and C21**. The *EUR* of this well should be in between 1.03 BSCF (the "lower" limit given by the straight line extrapolation technique at 337 days) and 2.95 BSCF (the "upper" limit given by the power law exponential estimate at 337 days).

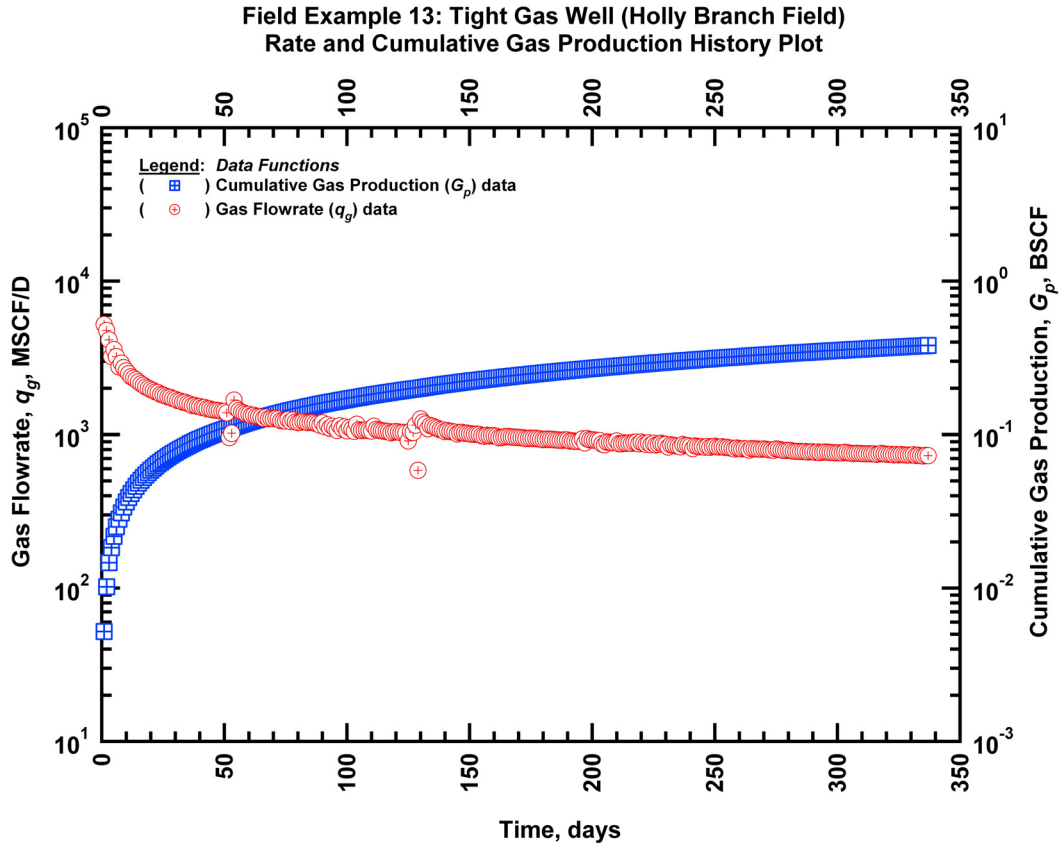

Figure C37 — (Semi-log Plot): Production history plot for field example 13 — flow rate (q_g) and cumulative production (G_p) versus production time.

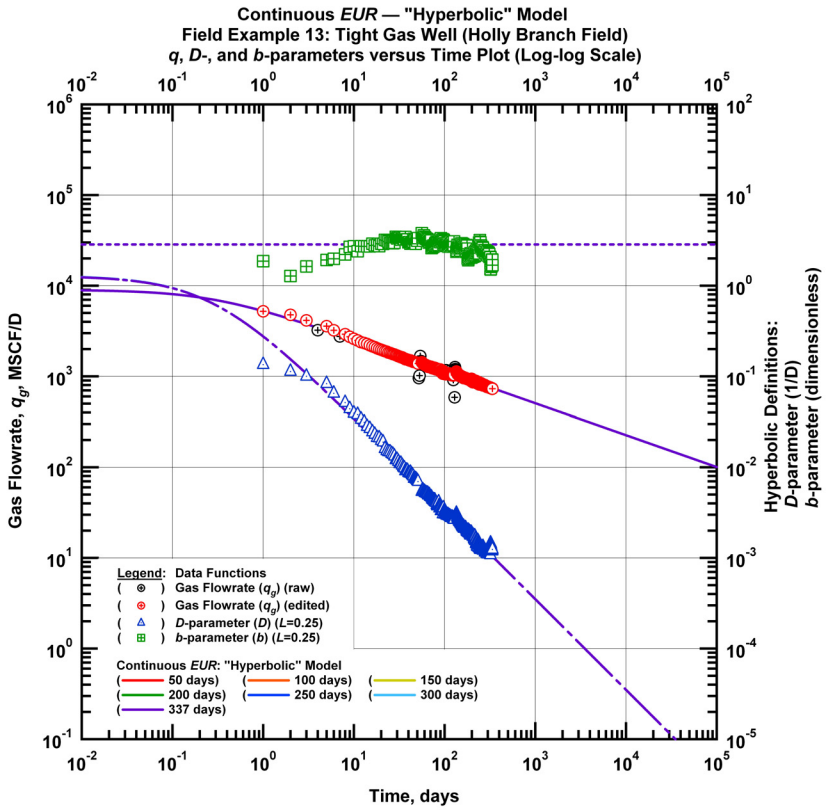

Figure C38 — (Log-log Plot): *qDb* plot — flow rate (q_g), *D*- and *b*-parameters versus production time and "hyperbolic" model matches for field example 13.

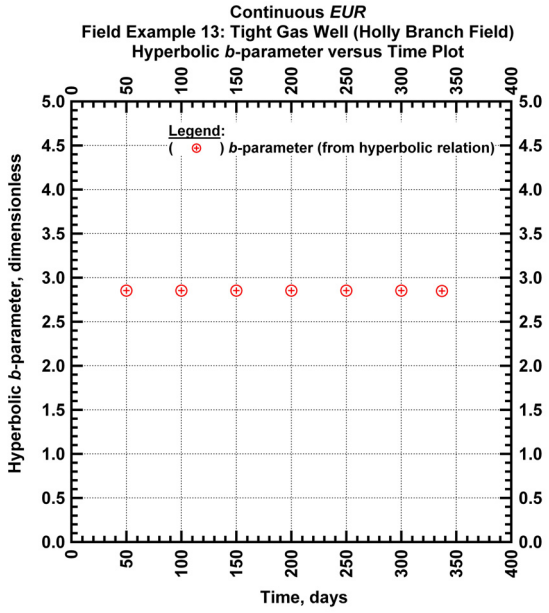

Figure C39 — (Cartesian Plot): Hyperbolic *b*-parameter values obtained from model matches with production data for field example 13.

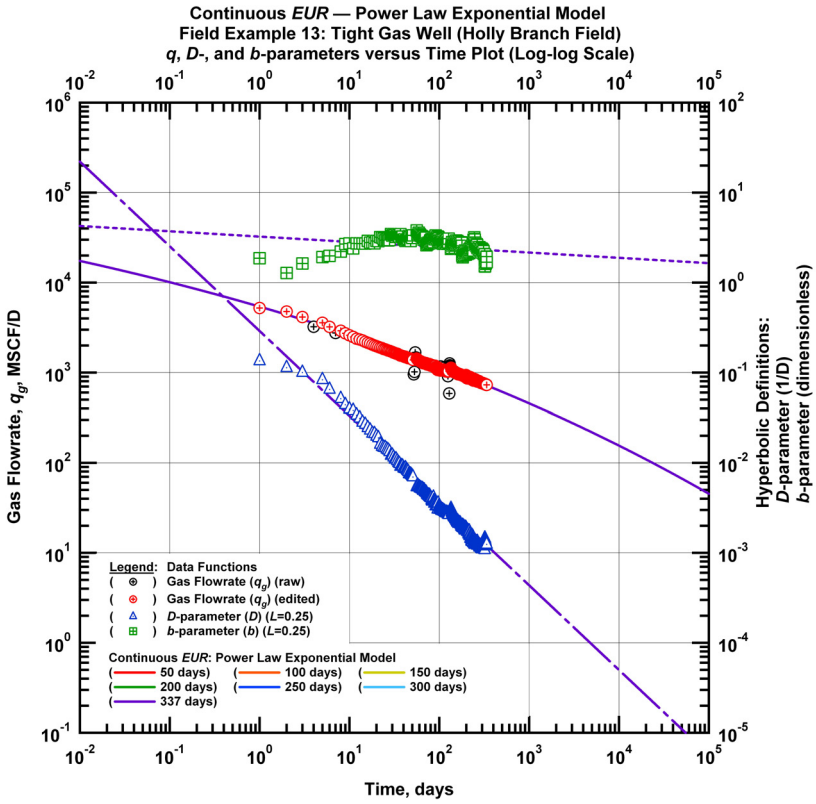

Figure C40 — (Log-log Plot): *qDb* plot — flow rate (q_g), *D*- and *b*-parameters versus production time and power law exponential model matches for field example 13.

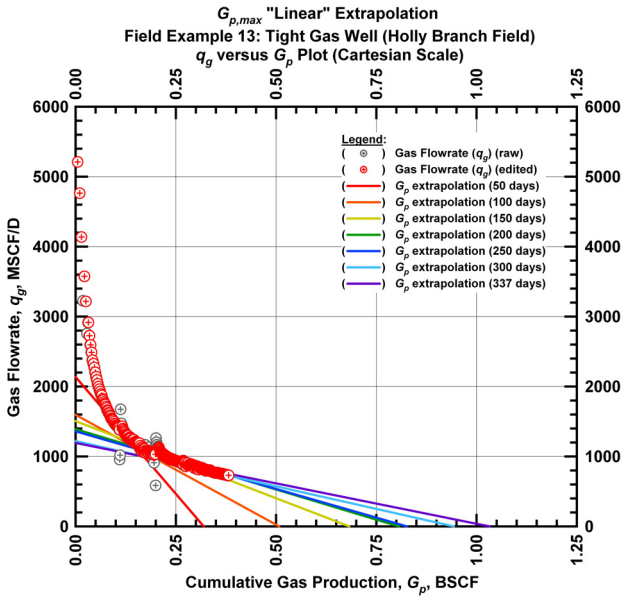

Figure C41 — (Cartesian Plot): Rate Cumulative Plot — flow rate (q_g) versus cumulative production (G_p) and the linear trends fit through the data for field example 13.

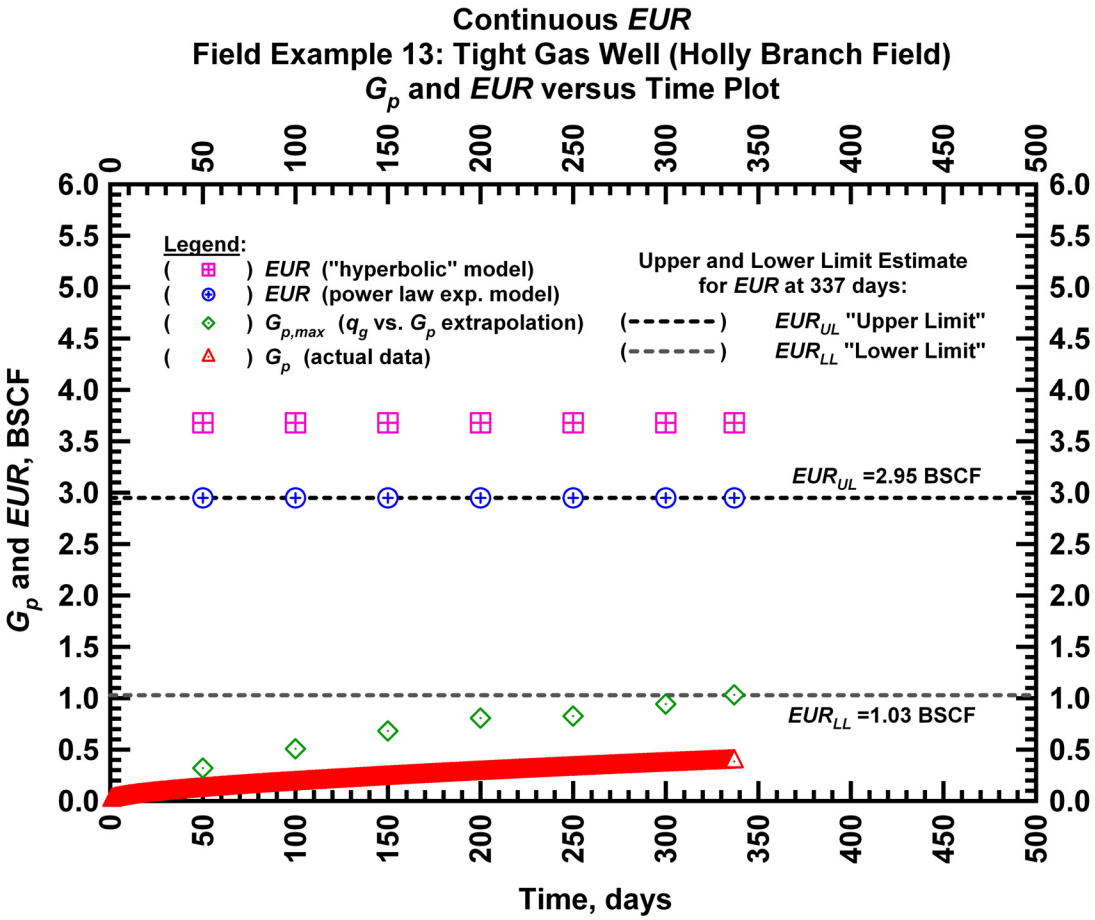

Figure C42 — (Cartesian Plot): *EUR* estimates from model matches and $G_{p,max}$ estimates from extrapolation technique for field example 13.

Table C19 — Analysis results for field example 13 — "hyperbolic" model parameters.

Time Interval, days	q_{gi} (MSCFD)	D_i (D^{-1})	b (dimensionless)	EUR_{hyp} (BSCF)
50	9,000	1.289606	2.8523	3.68
100	9,000	1.289606	2.8523	3.68
150	9,000	1.289606	2.8523	3.68
200	9,000	1.289606	2.8523	3.68
250	9,000	1.289606	2.8523	3.68
300	9,000	1.289606	2.8523	3.68
337	9,000	1.280480	2.8493	3.68

Table C20 — Analysis results for field example 13 — power law exponential model parameters.

Time Interval, days	$\hat{q}_{gi}$ (MSCFD)	$\hat{D}_i$ (D^{-1})	n (dimensionless)	D_∞ (D^{-1})	EUR_{PLE} (BSCF)
50	737,680	4.916	0.059	0	2.95
100	737,680	4.916	0.059	0	2.95
150	737,680	4.916	0.059	0	2.95
200	737,680	4.916	0.059	0	2.95
250	737,680	4.916	0.059	0	2.95
300	737,680	4.916	0.059	0	2.95
337	737,680	4.916	0.059	0	2.95

Table C21 — Analysis results for field example 13 — straight line extrapolation.

Time Interval, days	Slope, 10^{-6} D^{-1}	Intercept, MSCF/D	$G_{p,max}$ (BSCF)
50	6,683	2,136	0.32
100	3,143	1,596	0.51
150	2,208	1,507	0.68
200	1,725	1,391	0.81
250	1,645	1,359	0.83
300	1,293	1,220	0.94
337	1,155	1,193	1.03

Field Example 14

We present the flow rate data and the cumulative production data which spans almost 0.75 years for a vertical well producing from a tight gas reservoir in **Fig. C43**. **Fig. C44** presents the "hyperbolic" model matches imposed on the flow rate data along with the *D*- and *b*-parameter trends. In **Fig. C45** we observe that the value of the *b*-parameter as a function of time. The *b*-parameter value decreases from 2.37 to 2.35 during the production history. Every interval is matched with a "hyperbolic" *b*-parameter greater than 1 indicating that boundary-dominated flow has not been established. **Fig. C46** shows the power law exponential model matches imposed on the flow rate data and *D*- and *b*-parameter trends. In **Fig. C47** we show the results of the straight line extrapolation technique, and in **Fig. C48** we present the calculated *EUR* values versus production time. All of the model parameters for this example are presented in **Tables C22, C23, and C24**. The *EUR* of this well should be in between 0.88 BSCF (the "lower" limit given by the straight line extrapolation technique at 269 days) and 2.50 BSCF (the "upper" limit given by the power law exponential estimate at 269 days).

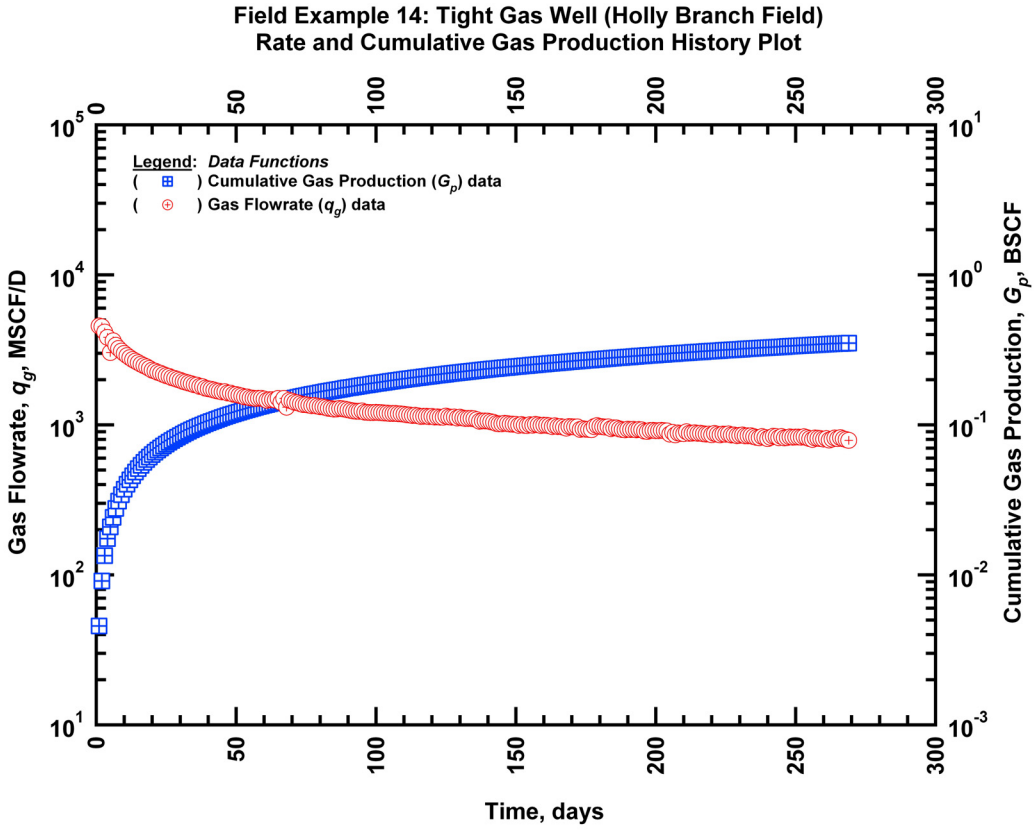

Figure C43 — (Semi-log Plot): Production history plot for field example 14 — flow rate (q_g) and cumulative production (G_p) versus production time.

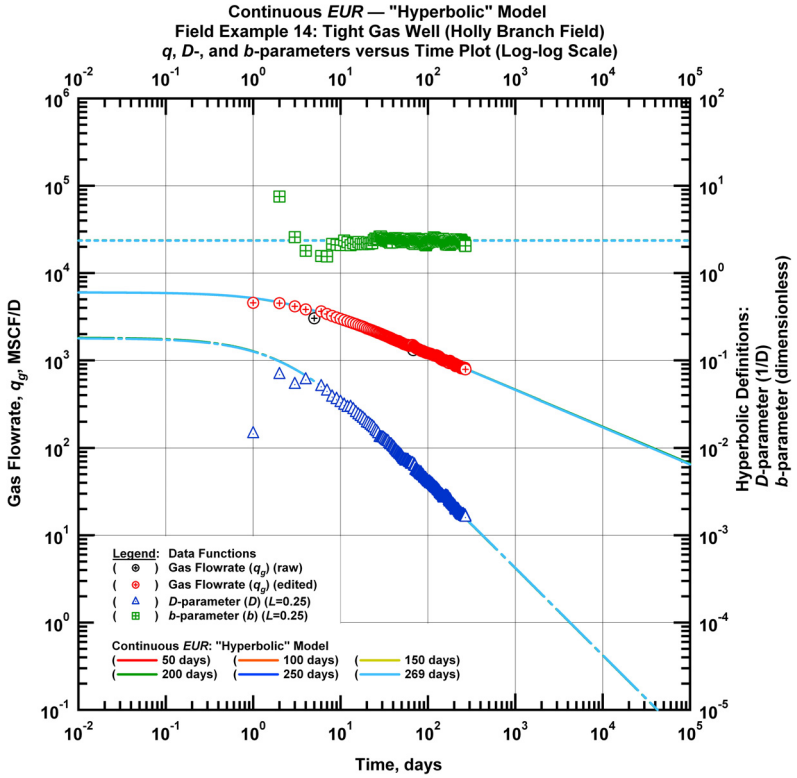

Figure C44 — (Log-log Plot): *qDb* plot — flow rate (q_g), *D*- and *b*-parameters versus production time and "hyperbolic" model matches for field example 14.

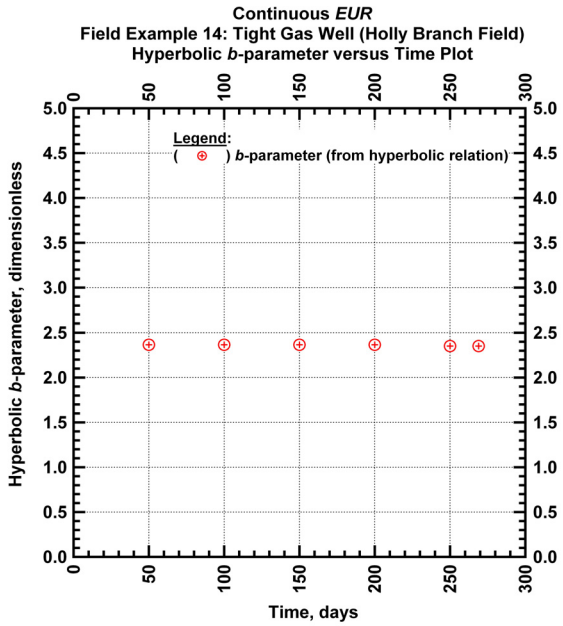

Figure C45 — (Cartesian Plot): Hyperbolic *b*-parameter values obtained from model matches with production data for field example 14.

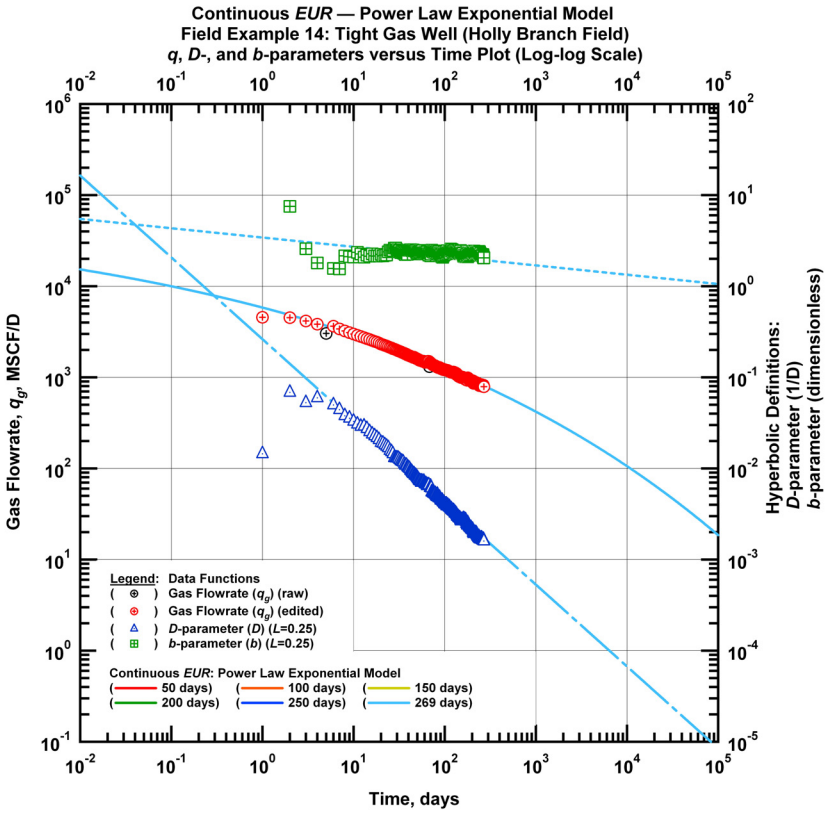

Figure C46 — (Log-log Plot): qDb plot — flow rate (q_g), D- and b-parameters versus production time and power law exponential model matches for field example 14.

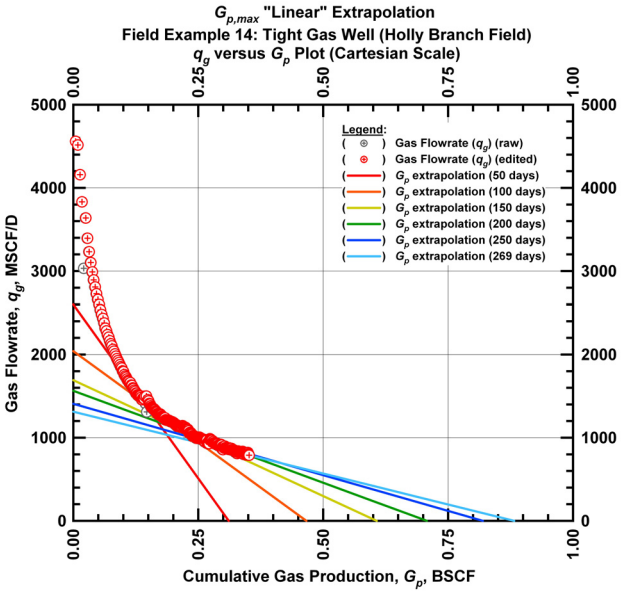

Figure C47 — (Cartesian Plot): Rate Cumulative Plot — flow rate (q_g) versus cumulative production (G_p) and the linear trends fit through the data for field example 14.

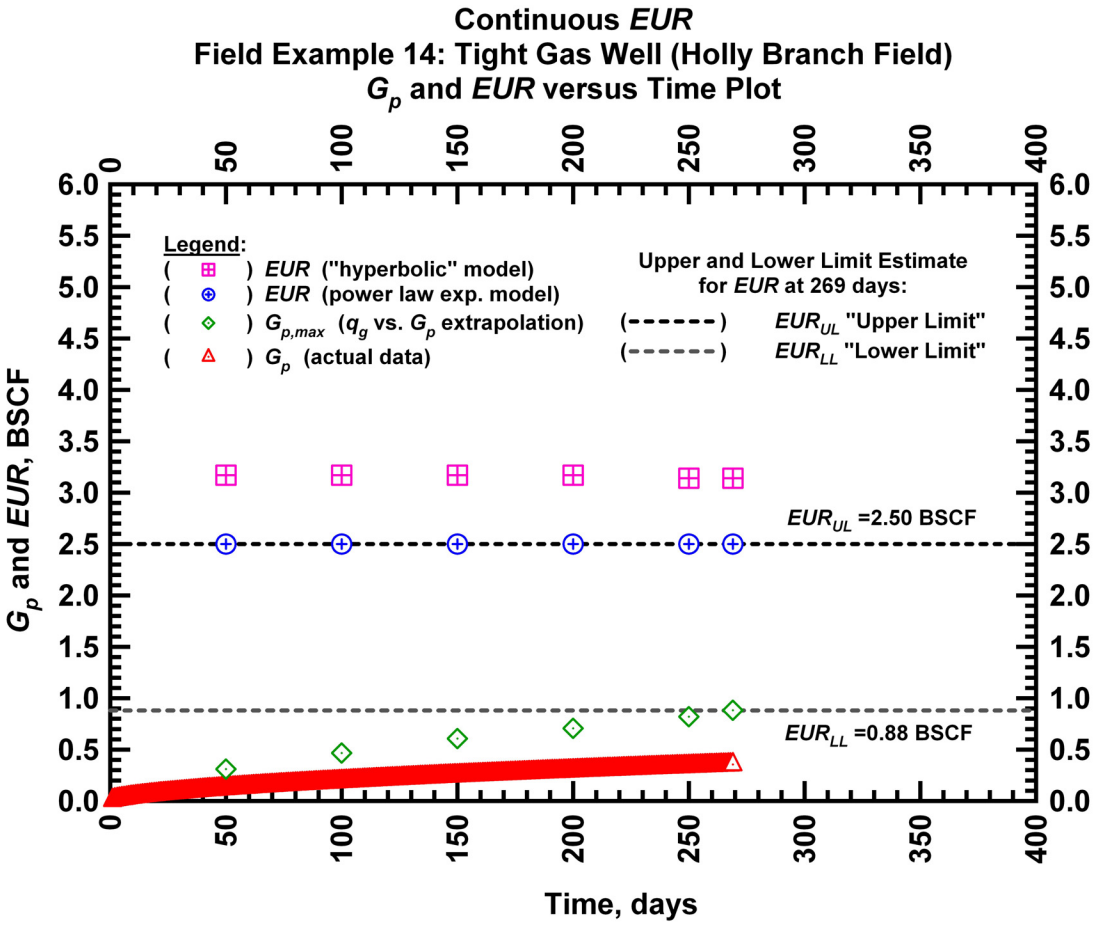

Figure C48 — (Cartesian Plot): *EUR* estimates from model matches and $G_{p,max}$ estimates from extrapolation technique for field example 14.

Table C22 — Analysis results for field example 14 — "hyperbolic" model parameters.

Time Interval, days	q_{gi} (MSCFD)	D_i (D^{-1})	b (dimensionless)	EUR_{hyp} (BSCF)
50	6,000	0.181666	2.3664	3.17
100	6,000	0.181666	2.3664	3.17
150	6,000	0.181666	2.3664	3.17
200	6,000	0.181666	2.3664	3.17
250	6,000	0.178982	2.3510	3.14
269	6,000	0.178982	2.3510	3.14

Table C23 — Analysis results for field example 14 — power law exponential model parameters.

Time Interval, days	$\hat{q}_{gi}$ (MSCFD)	$\hat{D}_i$ (D^{-1})	n (dimensionless)	D_∞ (D^{-1})	EUR_{PLE} (BSCF)
50	76,363	2.572	0.102	0	2.50
100	76,363	2.572	0.102	0	2.50
150	76,363	2.572	0.102	0	2.50
200	76,363	2.572	0.102	0	2.50
250	76,363	2.572	0.102	0	2.50
269	76,363	2.572	0.102	0	2.50

Table C24 — Analysis results for field example 14 — straight line extrapolation.

Time Interval, days	Slope, 10^{-6} D^{-1}	Intercept, MSCF/D	$G_{p,max}$ (BSCF)
50	8,360	2,600	0.31
100	4,376	2,041	0.47
150	2,787	1,692	0.61
200	2,211	1,564	0.71
250	1,718	1,408	0.82
269	1,488	1,313	0.88

Field Example 15

We present the flow rate data and the cumulative production data which spans almost 1 year for a vertical well producing from a tight gas reservoir in **Fig. C49**. **Fig. C50** presents the "hyperbolic" model matches imposed on the flow rate data along with the *D*- and *b*-parameter trends. In **Fig. C51** we observe that the value of the *b*-parameter as a function of time. The *b*-parameter value remains constant at 2.24 during the production history. Every interval is matched with a "hyperbolic" *b*-parameter greater than 1 indicating that boundary-dominated flow has not been established. **Fig. C52** shows the power law exponential model matches imposed on the flow rate data and *D*- and *b*-parameter trends. In **Fig. C53** we show the results of the straight line extrapolation technique, and in **Fig. C54** we present the calculated *EUR* values versus production time. All of the model parameters for this example are presented in **Tables C25, C26, and C27**. The *EUR* of this well should be in between 0.68 BSCF (the "lower" limit given by the straight line extrapolation technique at 336 days) and 1.80 BSCF (the "upper" limit given by the power law exponential estimate at 336 days).

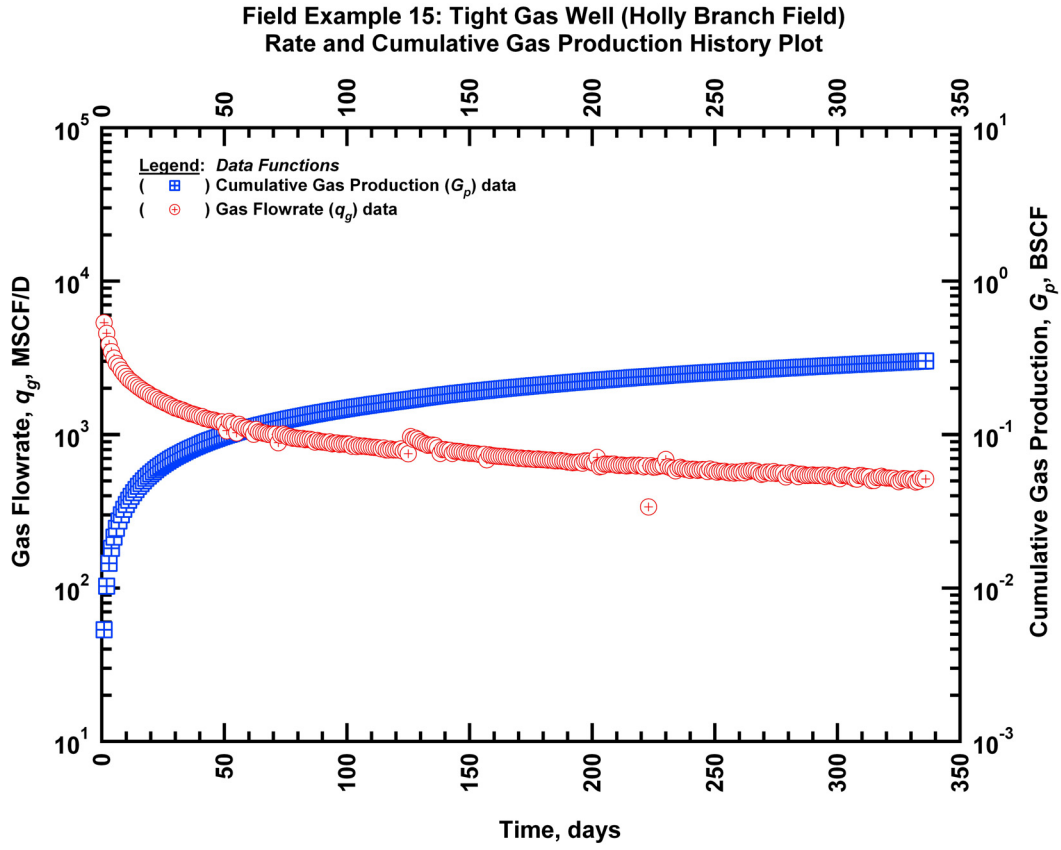

Figure C49 — (Semi-log Plot): Production history plot for field example 15 — flow rate (q_g) and cumulative production (G_p) versus production time.

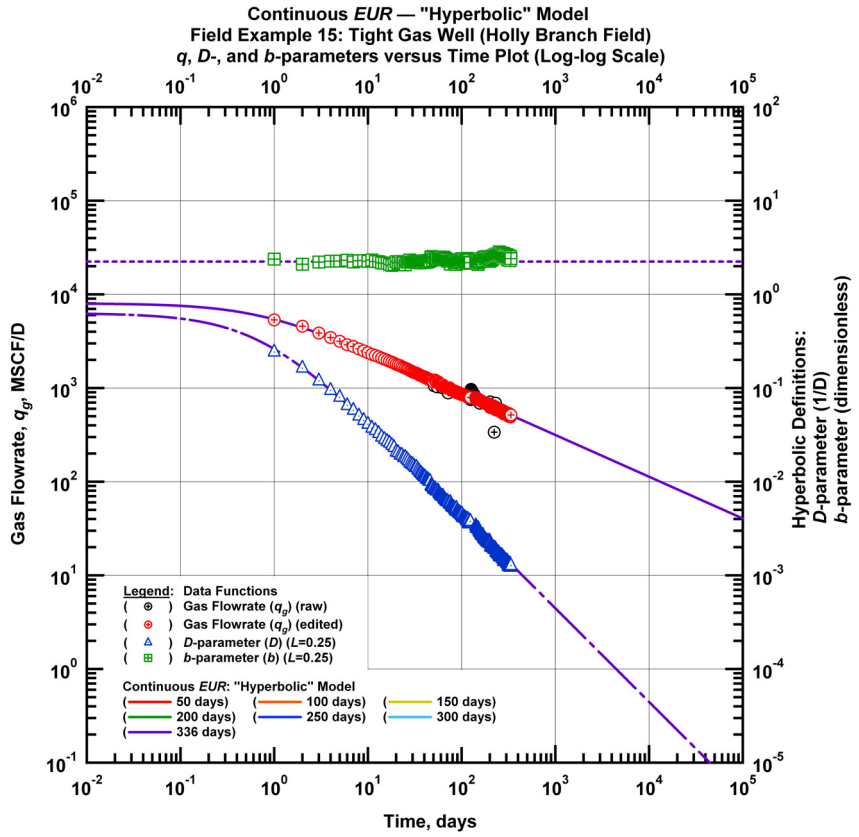

Figure C50 — (Log-log Plot): *qDb* plot — flow rate (q_g), *D*- and *b*-parameters versus production time and "hyperbolic" model matches for field example 15.

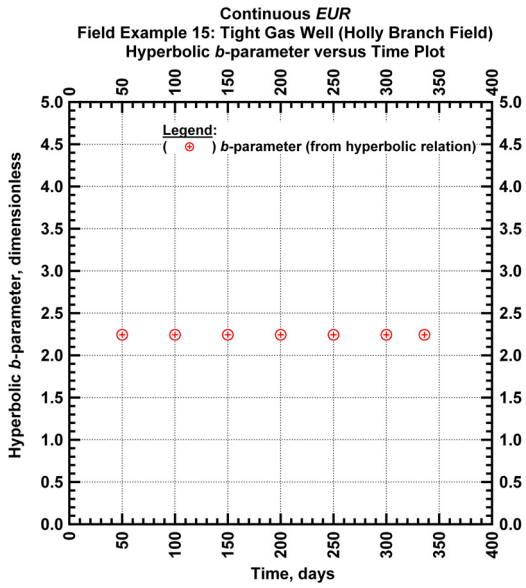

Figure C51 — (Cartesian Plot): Hyperbolic *b*-parameter values obtained from model matches with production data for field example 15.

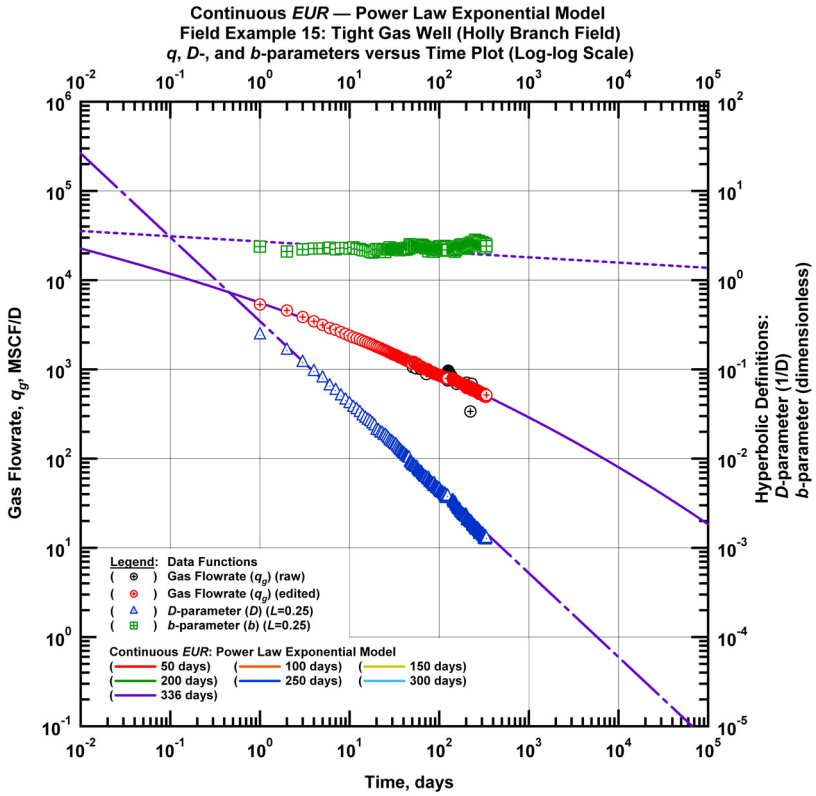

Figure C52 — (Log-log Plot): *qDb* plot — flow rate (q_g), *D*- and *b*-parameters versus production time and power law exponential model matches for field example 15.

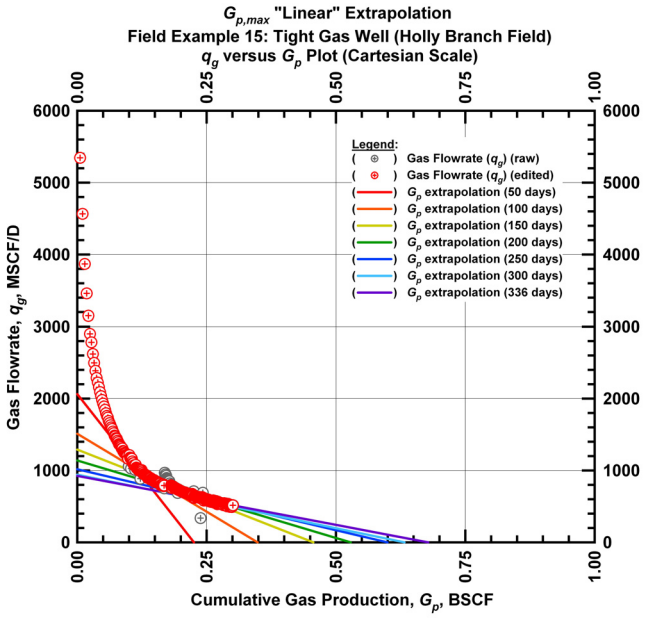

Figure C53 — (Cartesian Plot): Rate Cumulative Plot — flow rate (q_g) versus cumulative production (G_p) and the linear trends fit through the data for field example 15.

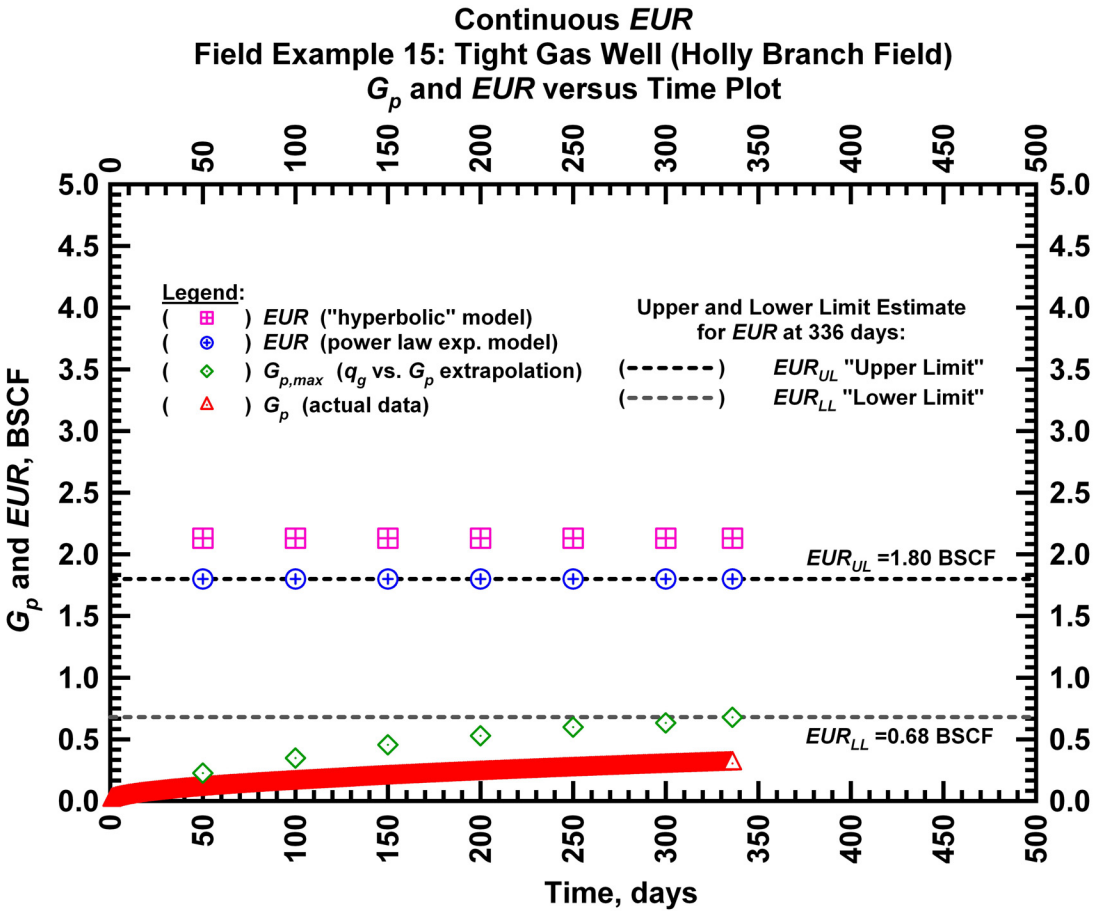

Figure C54 — (Cartesian Plot): *EUR* estimates from model matches and $G_{p,max}$ estimates from extrapolation technique for field example 15.

Table C25 — Analysis results for field example 15 — "hyperbolic" model parameters.

Time Interval, days	q_{gi} (MSCFD)	D_i (D^{-1})	b (dimensionless)	EUR_{hyp} (BSCF)
50	8,000	0.629024	2.243	2.13
100	8,000	0.629024	2.243	2.13
150	8,000	0.629024	2.243	2.13
200	8,000	0.629024	2.243	2.13
250	8,000	0.629024	2.243	2.13
300	8,000	0.629024	2.243	2.13
336	8,000	0.629024	2.243	2.13

Table C26 — Analysis results for field example 15 — power law exponential model parameters.

Time Interval, days	$\hat{q}_{gi}$ (MSCFD)	$\hat{D}_i$ (D^{-1})	n (dimensionless)	D_∞ (D^{-1})	EUR_{PLE} (BSCF)
50	1,996,642	5.8794	0.059	0	1.80
100	1,996,642	5.8794	0.059	0	1.80
150	1,996,642	5.8794	0.059	0	1.80
200	1,996,642	5.8794	0.059	0	1.80
250	1,996,642	5.8794	0.059	0	1.80
300	1,996,642	5.8794	0.059	0	1.80
336	1,996,642	5.8794	0.059	0	1.80

Table C27 — Analysis results for field example 15 — straight line extrapolation.

Time Interval, days	Slope, 10^{-6} D^{-1}	Intercept, MSCF/D	$G_{p,max}$ (BSCF)
50	9,141	2,062	0.23
100	4,336	1,511	0.35
150	2,826	1,290	0.46
200	2,155	1,139	0.53
250	1,696	1,017	0.60
300	1,489	942	0.63
336	1,364	925	0.68

Field Example 16

We present the flow rate data and the cumulative production data which spans over 2 years for a vertical well producing from a tight gas reservoir in **Fig. C55**. **Fig. C56** presents the "hyperbolic" model matches imposed on the flow rate data along with the *D*- and *b*-parameter trends. In **Fig. C57** we observe that the value of the *b*-parameter as a function of time. The *b*-parameter value decreases from 2.05 to 1.98 during the production history. Every interval is matched with a "hyperbolic" *b*-parameter greater than 1 indicating that boundary-dominated flow has not been established. **Fig. C58** shows the power law exponential model matches imposed on the flow rate data and *D*- and *b*-parameter trends. In **Fig. C59** we show the results of the straight line extrapolation technique, and in **Fig. C60** we present the calculated *EUR* values versus production time. All of the model parameters for this example are presented in **Tables C28, C29, and C30**. The *EUR* of this well should be in between 2.46 BSCF (the "lower" limit given by the straight line extrapolation technique at 764 days) and 3.87 BSCF (the "upper" limit given by the power law exponential estimate at 764 days).

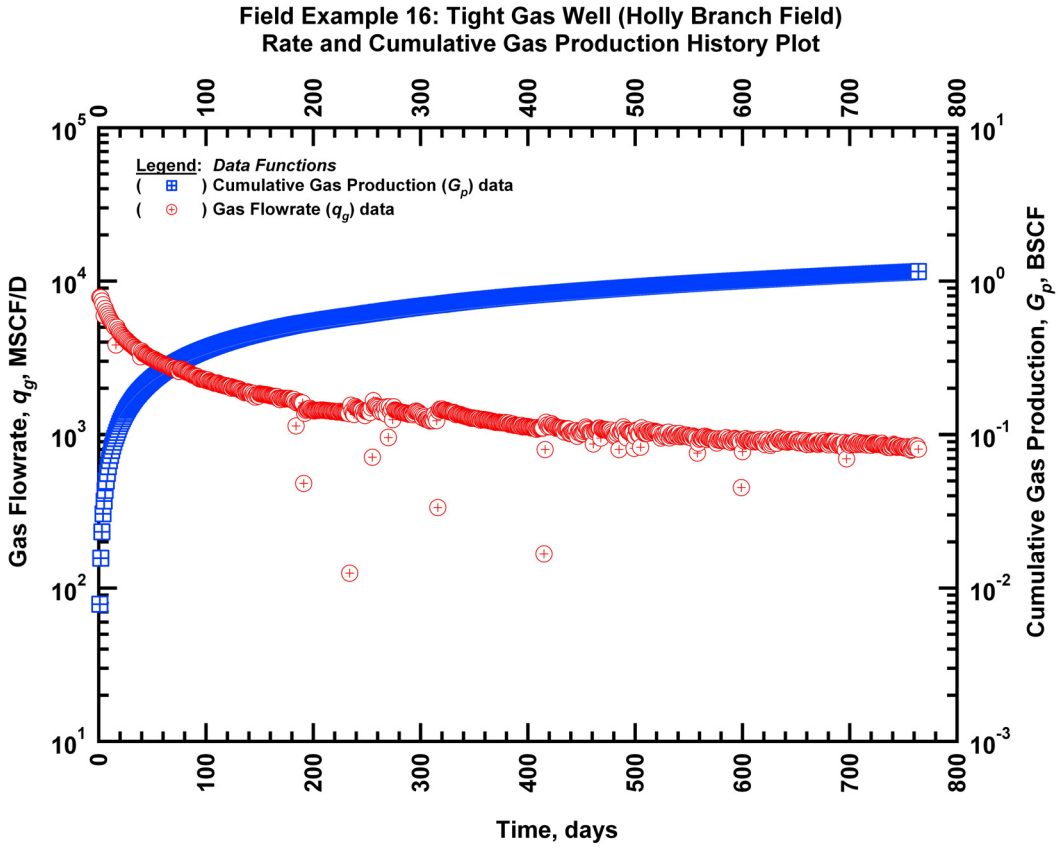

Figure C55 — (Semi-log Plot): Production history plot for field example 16 — flow rate (q_g) and cumulative production (G_p) versus production time.

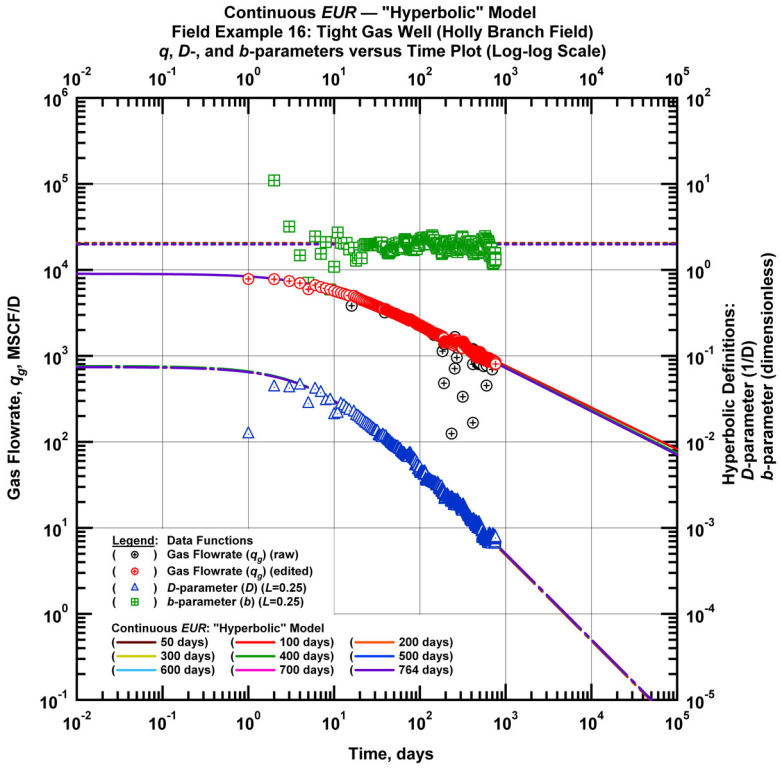

Figure C56 — (Log-log Plot): *qDb* plot — flow rate (q_g), *D*- and *b*-parameters versus production time and "hyperbolic" model matches for field example 16.

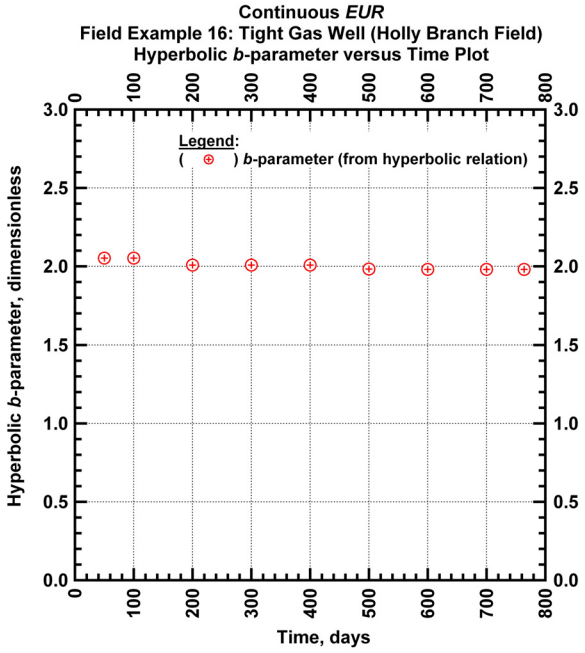

Figure C57 — (Cartesian Plot): Hyperbolic *b*-parameter values obtained from model matches with production data for field example 16.

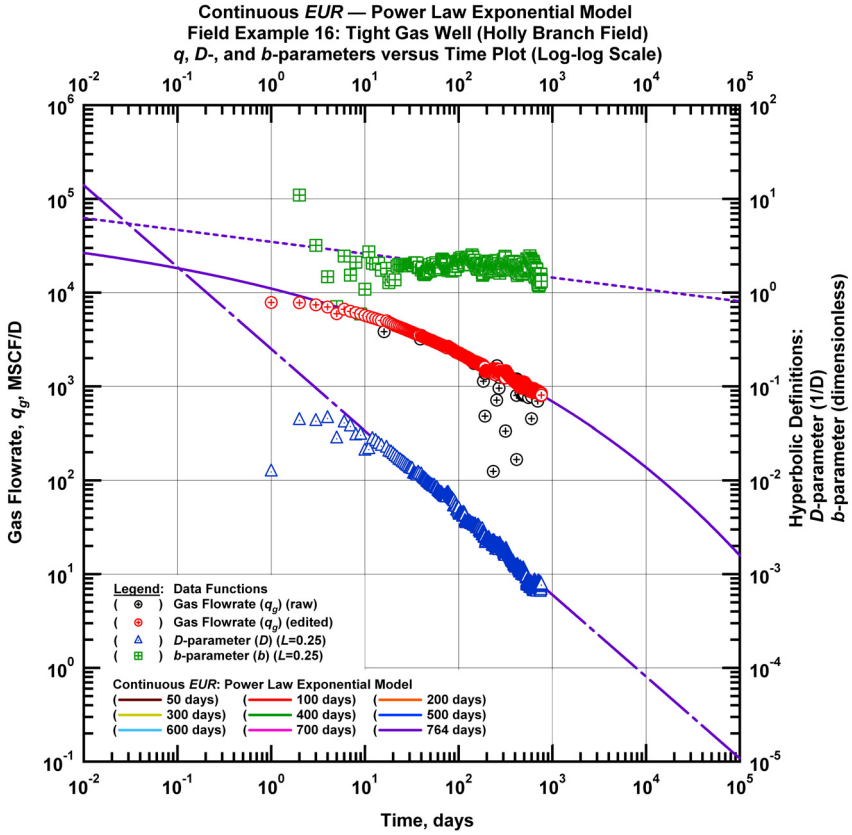

Figure C58 — (Log-log Plot): *qDb* plot — flow rate (q_g), *D*- and *b*-parameters versus production time and power law exponential model matches field example 16.

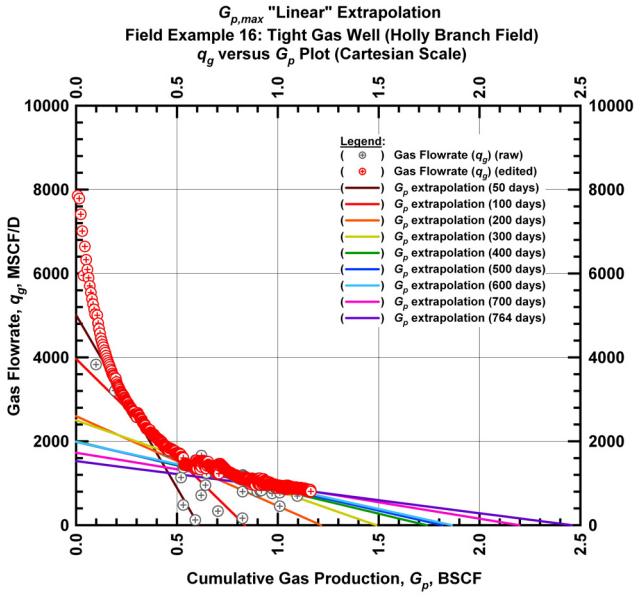

Figure C59 — (Cartesian Plot): Rate Cumulative Plot — flow rate (q_g) versus cumulative production (G_p) and the linear trends fit through the data field example 16.

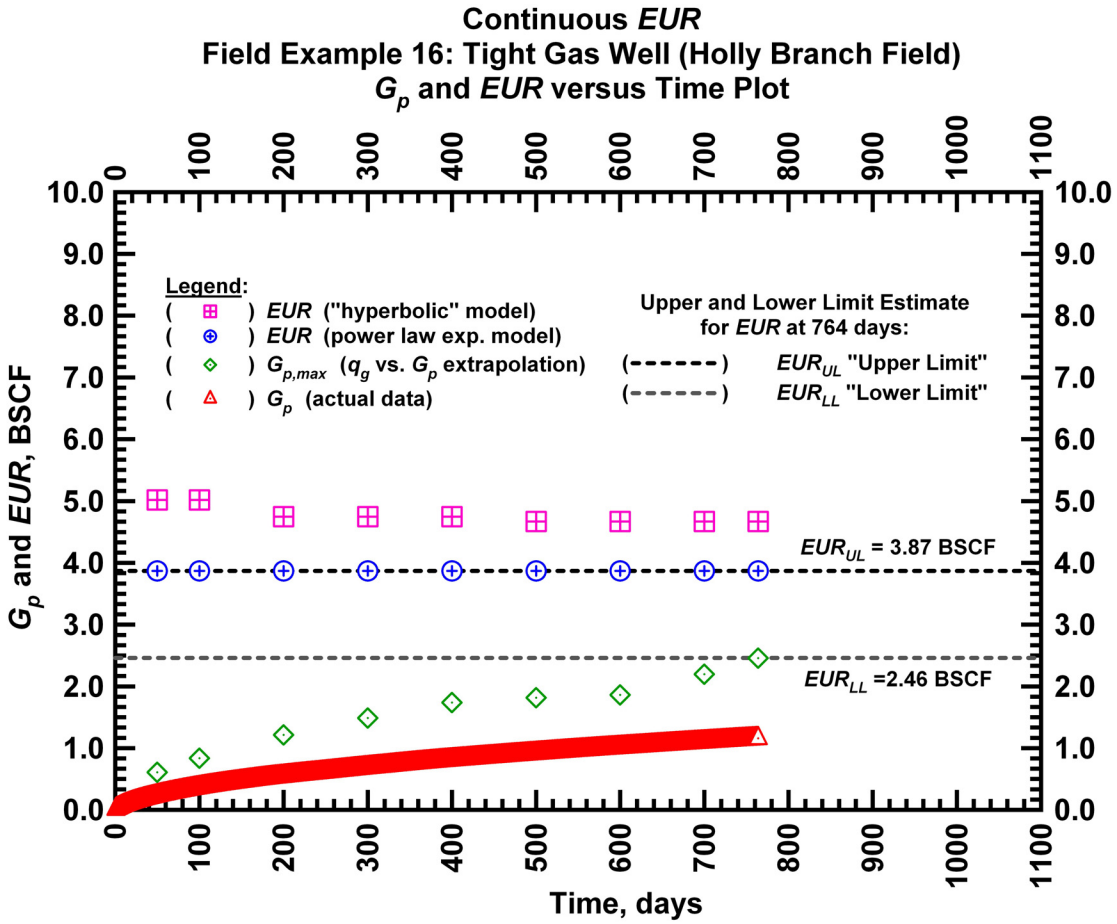

Figure C60 — (Cartesian Plot): *EUR* estimates from model matches and $G_{p,max}$ estimates from extrapolation technique field example 16.

Table C28 — Analysis results for field example 16 — "hyperbolic" model parameters.

Time Interval, days	q_{gi} (MSCFD)	D_i (D^{-1})	b (dimensionless)	EUR_{hyp} (BSCF)
50	9,000	0.075631	2.0525	5.02
100	9,000	0.075631	2.0525	5.02
200	9,000	0.076154	2.0082	4.75
300	9,000	0.076154	2.0082	4.75
400	9,000	0.076154	2.0082	4.75
500	9,000	0.074222	1.9825	4.67
600	9,000	0.074083	1.9807	4.67
700	9,000	0.074083	1.9807	4.67
764	9,000	0.074083	1.9807	4.67

Table C29 — Analysis results for field example 16 — power law exponential model parameters.

Time Interval, days	$\hat{q}_{gi}$ (MSCFD)	$\hat{D}_i$ (D^{-1})	n (dimensionless)	D_∞ (D^{-1})	EUR_{PLE} (BSCF)
50	79,598	1.975	0.127	0	3.87
100	79,598	1.975	0.127	0	3.87
200	79,598	1.975	0.127	0	3.87
300	79,598	1.975	0.127	0	3.87
400	79,598	1.975	0.127	0	3.87
500	79,598	1.975	0.127	0	3.87
600	79,598	1.975	0.127	0	3.87
700	79,598	1.975	0.127	0	3.87
764	79,598	1.975	0.127	0	3.87

Table C30 — Analysis results for field example 16 — straight line extrapolation.

Time Interval, days	Slope, 10^{-6} D^{-1}	Intercept, MSCF/D	$G_{p,max}$ (BSCF)
50	8,246	5,011	0.61
100	4,734	3,963	0.84
200	2,140	2,598	1.21
300	1,679	2,499	1.49
400	1,150	2,000	1.74
500	1,093	1,985	1.82
600	1,067	1,988	1.86
700	786	1,727	2.20
764	622	1,529	2.46

APPENDIX D
EXAMPLES FROM FIELD A

Field Example 17

We present the flow rate data and the cumulative production data which spans almost 7.5 years for a vertical well producing from a shale gas reservoir in **Fig. D1**. **Fig. D2** presents the "hyperbolic" model matches imposed on the flow rate data along with the *D*- and *b*-parameter trends. In **Fig. D3** we observe that the value of the *b*-parameter as a function of time. The *b*-parameter value decreases from 4.41 to 2.09 during the production history. Every interval is matched with a "hyperbolic" *b*-parameter greater than 1 indicating that boundary-dominated flow has not been established. **Fig. D4** shows the power law exponential model matches imposed on the flow rate data and *D*- and *b*-parameter trends. In **Fig. D5** we show the results of the straight line extrapolation technique, and in **Fig. D6** we present the calculated *EUR* values versus production time. All of the model parameters for this example are presented in **Tables D1, D2, and D3**. The *EUR* of this well should be in between 1.44 BSCF (the "lower" limit given by the straight line extrapolation technique at 2,692 days) and 1.53 BSCF (the "upper" limit given by the power law exponential estimate at 2,692 days).

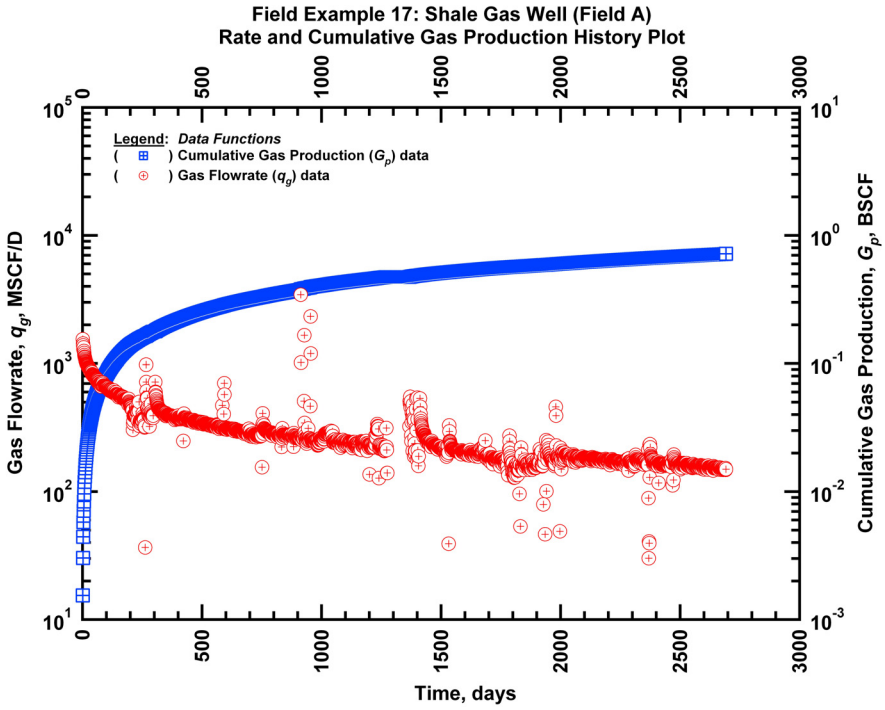

Figure D1 — (Semi-log Plot): Production history plot for field example 17 — flow rate (q_g) and cumulative production (G_p) versus production time.

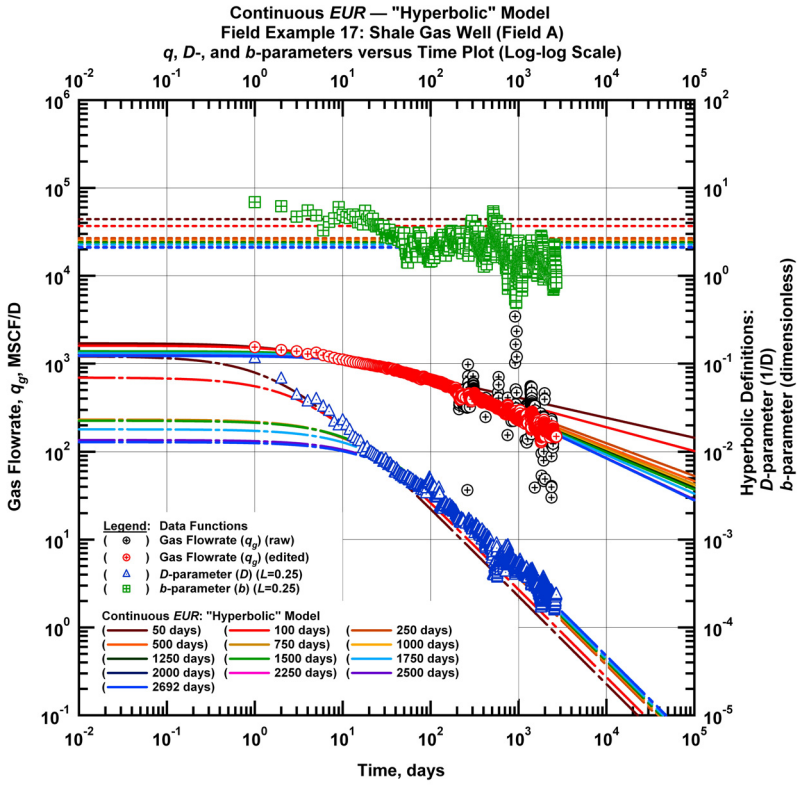

Figure D2 — (Log-log Plot): *qDb* plot — flow rate (q_g), *D*- and *b*-parameters versus production time and "hyperbolic" model matches for field example 17.

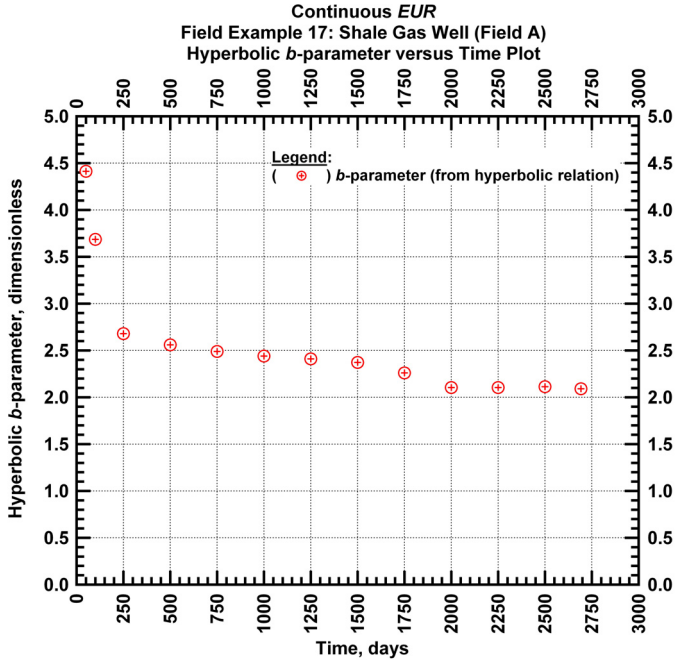

Figure D3 — (Cartesian Plot): Hyperbolic *b*-parameter values obtained from model matches with production data for field example 17.

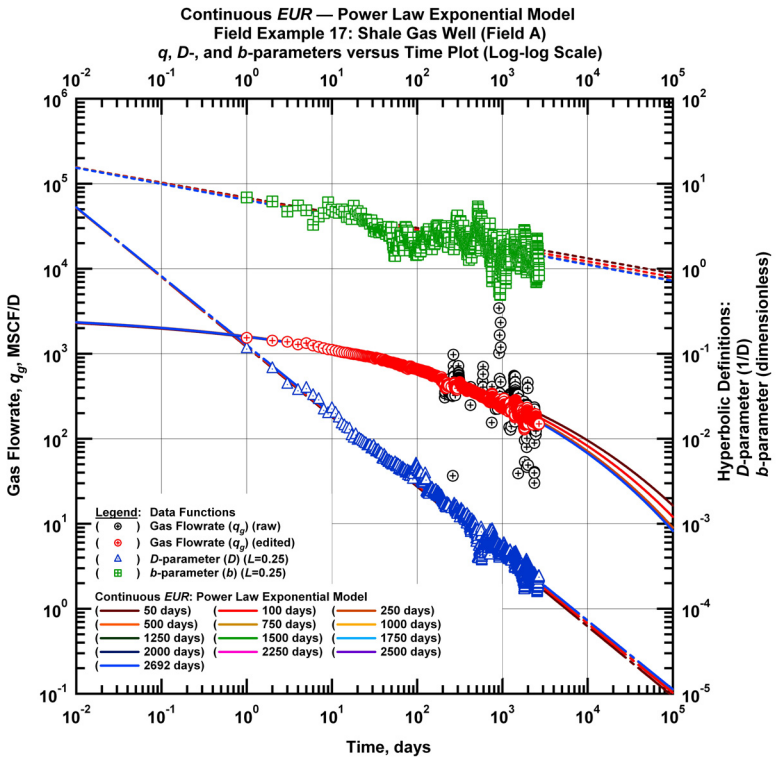

Figure D4 — (Log-log Plot): *qDb* plot — flow rate (q_g), *D*- and *b*-parameters versus production time and power law exponential model matches for field example 17.

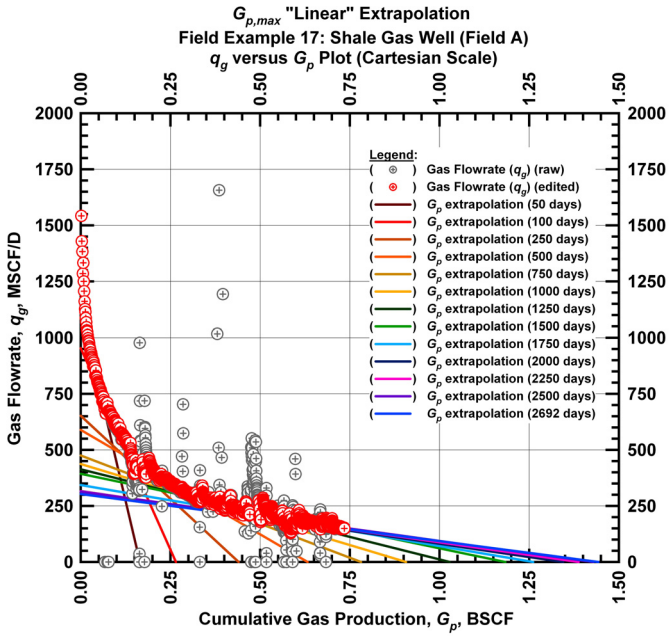

Figure D5 — (Cartesian Plot): Rate Cumulative Plot — flow rate (q_g) versus cumulative production (G_p) and the linear trends fit through the data for field example 17.

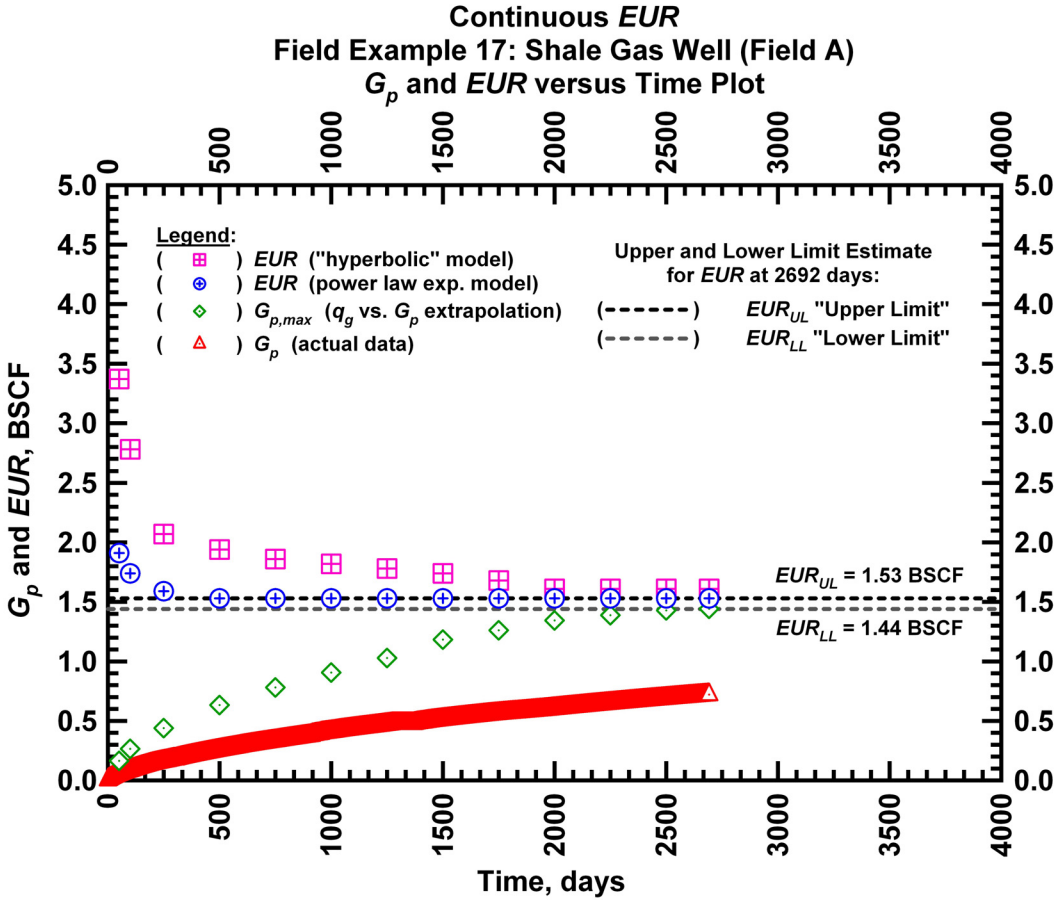

Figure D6 — (Cartesian Plot): *EUR* estimates from model matches and $G_{p,max}$ estimates from extrapolation technique for field example 17.

Table D1 — Analysis results for field example 17 — "hyperbolic" model parameters.

Time Interval, days	q_{gi} (MSCFD)	D_i (D^{-1})	b (dimensionless)	EUR_{hyp} (BSCF)
50	1,702	0.121285	4.41	3.37
100	1,599	0.069314	3.69	2.78
250	1,381	0.023233	2.68	2.07
500	1,381	0.023233	2.56	1.94
750	1,381	0.023087	2.49	1.86
1,000	1,381	0.022551	2.44	1.82
1,250	1,381	0.022551	2.41	1.78
1,500	1,381	0.022551	2.37	1.74
1,750	1,316	0.017997	2.26	1.68
2,000	1,237	0.013452	2.10	1.61
2,250	1,237	0.013452	2.10	1.61
2,500	1,237	0.013580	2.11	1.61
2,692	1,221	0.012866	2.09	1.61

Table D2 — Analysis results for field example 17 — power-law exponential model parameters.

Time Interval, days	$\hat{q}_{gi}$ (MSCFD)	$\hat{D}_i$ (D^{-1})	n (dimensionless)	D_∞ (D^{-1})	EUR_{PLE} (BSCF)
50	3,087	0.674	0.178	0	1.91
100	3,087	0.663	0.185	0	1.74
250	3,087	0.655	0.190	0	1.59
500	3,087	0.665	0.190	0	1.53
750	3,087	0.665	0.190	0	1.53
1,000	3,087	0.665	0.190	0	1.53
1,250	3,087	0.665	0.190	0	1.53
1,500	3,087	0.665	0.190	0	1.53
1,750	3,087	0.665	0.190	0	1.53
2,000	3,087	0.665	0.190	0	1.53
2,250	3,087	0.665	0.190	0	1.53
2,500	3,087	0.665	0.190	0	1.53
2,692	3,087	0.665	0.190	0	1.53

Table D3 — Analysis results for field example 17 — straight line extrapolation.

Time Interval, days	Slope, 10^{-6} D^{-1}	Intercept, MSCF/D	$G_{p,max}$ (BSCF)
50	6,837	1,128	0.16
100	3,598	954	0.27
250	1,481	652	0.44
500	932	589	0.63
750	608	475	0.78
1,000	482	437	0.91
1,250	402	414	1.03
1,500	332	393	1.18
1,750	272	343	1.26
2,000	235	316	1.34
2,250	227	315	1.39
2,500	219	313	1.43
2,692	210	303	1.44

Field Example 18

We present the flow rate data and the cumulative production data which spans over 7 years for a vertical well producing from a shale gas reservoir in **Fig. D7**. **Fig. D8** presents the "hyperbolic" model matches imposed on the flow rate data along with the *D*- and *b*-parameter trends. In **Fig. D9** we observe that the value of the *b*-parameter as a function of time. The *b*-parameter value decreases from 2.21 to 2.01 during the production history. Every interval is matched with a "hyperbolic" *b*-parameter greater than 1 indicating that boundary-dominated flow has not been established. **Fig. D10** shows the power law exponential model matches imposed on the flow rate data and *D*- and *b*-parameter trends. In **Fig. D11** we show the results of the straight line extrapolation technique, and in **Fig. D12** we present the calculated *EUR* values versus production time. All of the model parameters for this example are presented in **Tables D4, D5, and D6**. The *EUR* of this well should be in between 0.89 BSCF (the "lower" limit given by the straight line extrapolation technique at 2,558 days) and 0.98 BSCF (the "upper" limit given by the power law exponential estimate at 2,558 days).

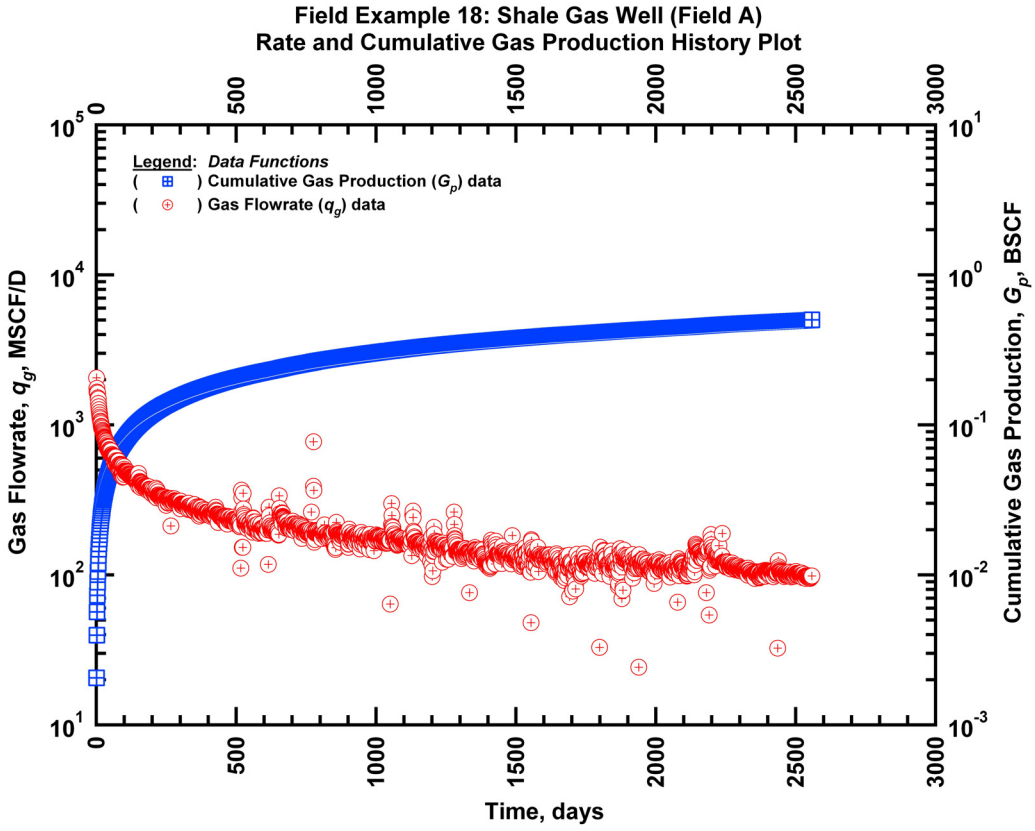

Figure D7 — (Semi-log Plot): Production history plot for field example 18 — flow rate (q_g) and cumulative production (G_p) versus production time.

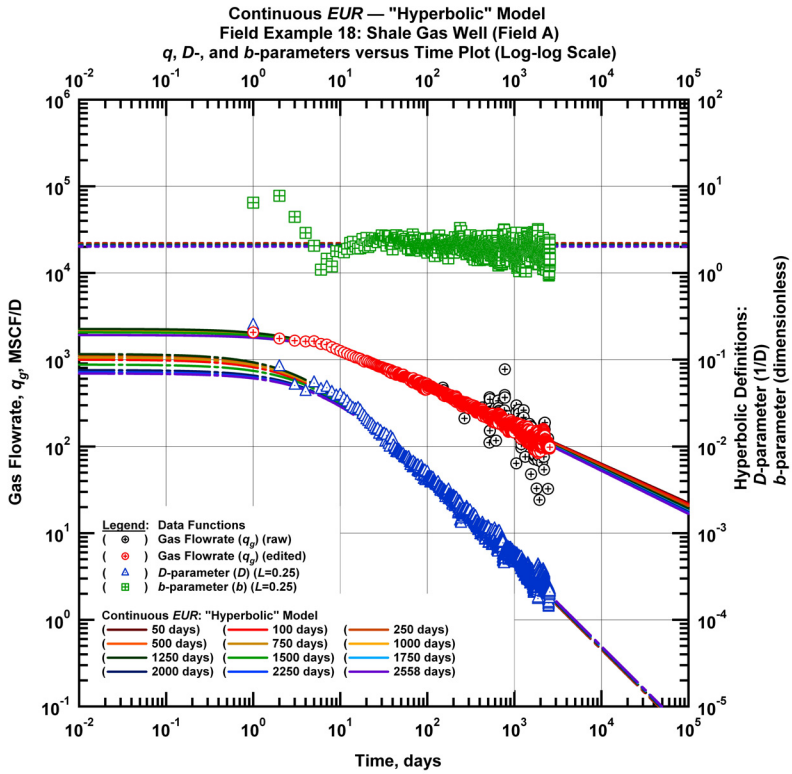

Figure D8 — (Log-log Plot): *qDb* plot — flow rate (q_g), *D*- and *b*-parameters versus production time and "hyperbolic" model matches for field example 18.

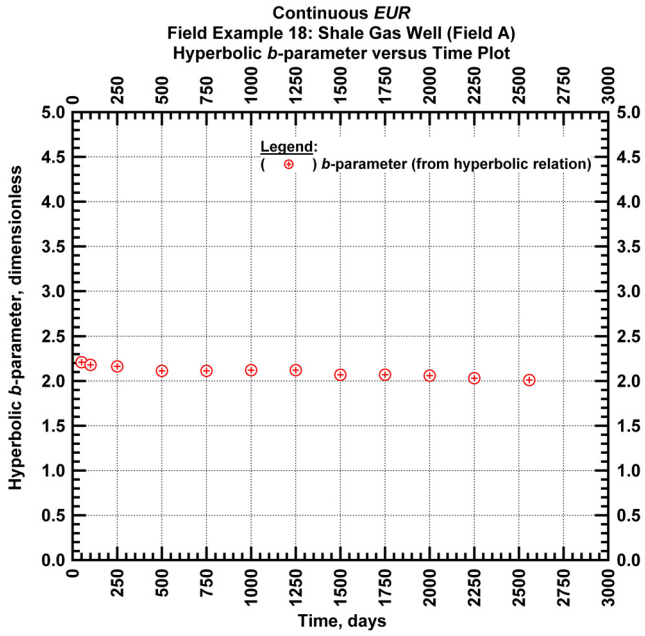

Figure D9 — (Cartesian Plot): Hyperbolic *b*-parameter values obtained from model matches with production data for field example 18.

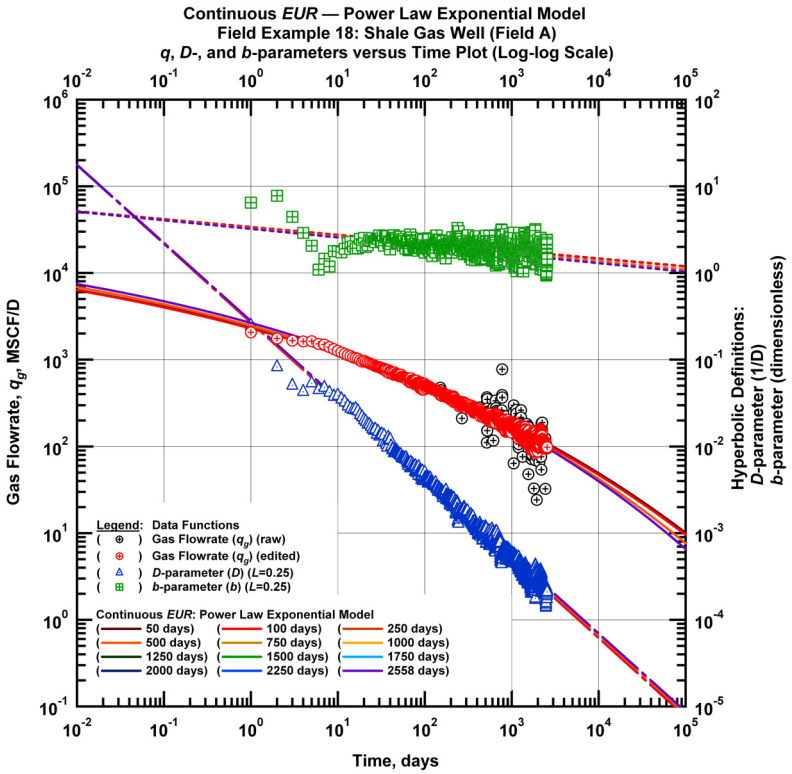

Figure D10 — (Log-log Plot): *qDb* plot — flow rate (q_g), *D*- and *b*-parameters versus production time and power law exponential model matches for field example 18.

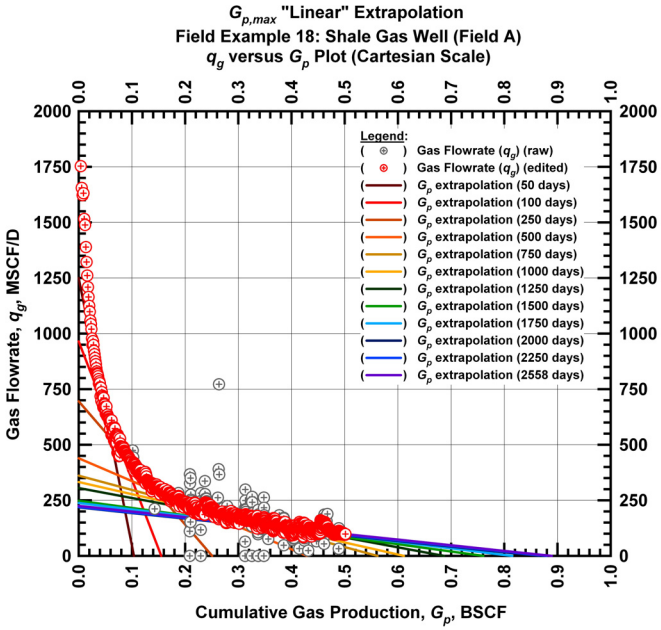

Figure D11 — (Cartesian Plot): Rate Cumulative Plot — flow rate (q_g) versus cumulative production (G_p) and the linear trends fit through the data for field example 18.

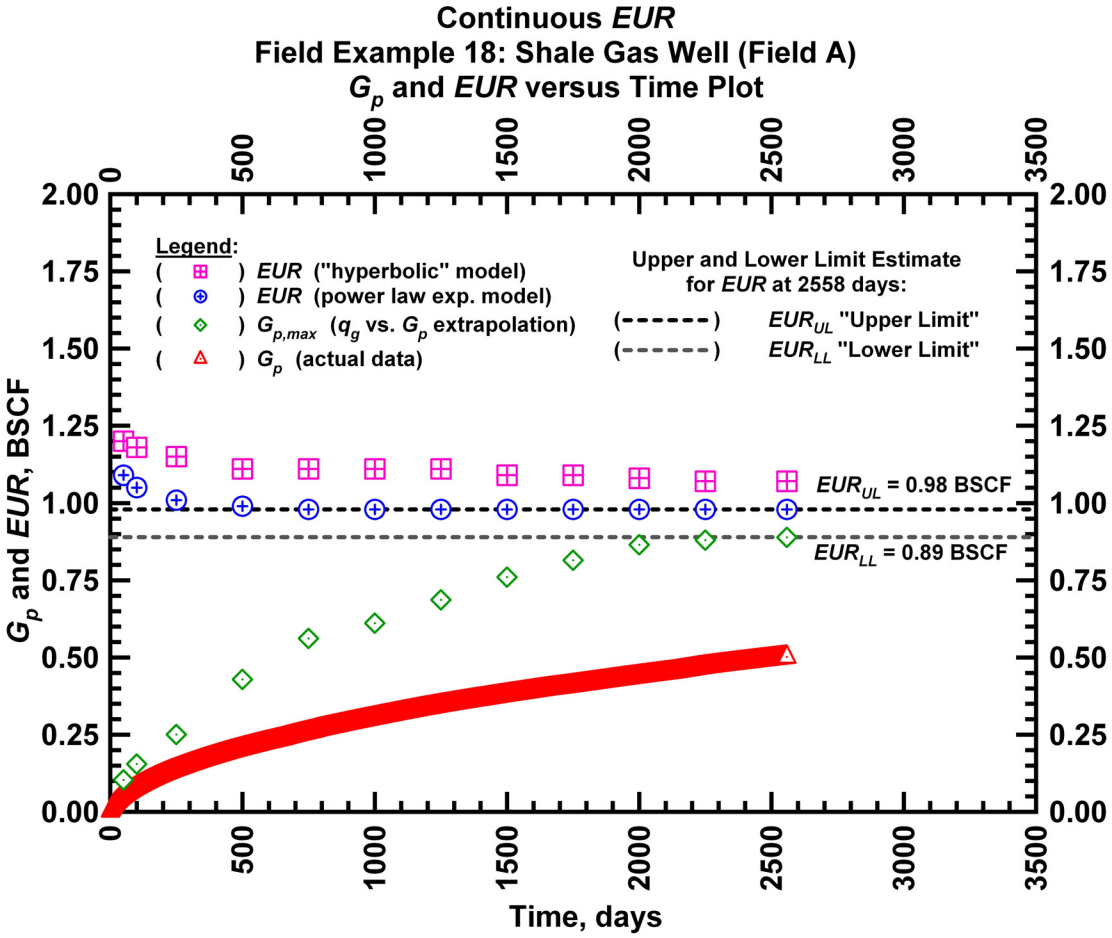

Figure D12 — (Cartesian Plot): *EUR* estimates from model matches and $G_{p,max}$ estimates from extrapolation technique for field example 18.

Table D4 — Analysis results for field example 18 — "hyperbolic" model parameters.

Time Interval, days	q_{gi} (MSCFD)	D_i (D^{-1})	b (dimensionless)	EUR_{hyp} (BSCF)
50	2,067	0.09977	2.210	1.20
100	2,100	0.10000	2.180	1.18
250	2,182	0.11130	2.163	1.15
500	2,182	0.10566	2.113	1.11
750	2,182	0.10615	2.114	1.11
1,000	2,258	0.11579	2.122	1.11
1,250	2,258	0.11579	2.122	1.11
1,500	2,060	0.08751	2.070	1.09
1,750	1,919	0.07566	2.070	1.09
2,000	1,919	0.07566	2.060	1.08
2,250	1,919	0.07148	2.032	1.07
2,558	1,919	0.06905	2.010	1.07

Table D5 — Analysis results for field example 18 — power-law exponential model parameters.

Time Interval, days	$\hat{q}_{gi}$ (MSCFD)	$\hat{D}_i$ (D^{-1})	n (dimensionless)	D_∞ (D^{-1})	EUR_{PLE} (BSCF)
50	44,530	2.950	0.0908	0	1.09
100	44,530	2.970	0.0908	0	1.05
250	44,530	2.823	0.0990	0	1.01
500	44,530	2.898	0.0952	0	0.99
750	44,530	2.823	0.0990	0	0.98
1,000	44,530	2.823	0.0990	0	0.98
1,250	44,530	2.823	0.0990	0	0.98
1,500	44,530	2.823	0.0990	0	0.98
1,750	44,530	2.823	0.0990	0	0.98
2,000	44,530	2.823	0.0990	0	0.98
2,250	44,530	2.823	0.0990	0	0.98
2,558	44,530	2.823	0.0990	0	0.98

Table D6 — Analysis results for field example 18 — straight line extrapolation.

Time Interval, days	Slope, 10^{-6} D^{-1}	Intercept, MSCF/D	$G_{p,max}$ (BSCF)
50	12,035	1,250	0.10
100	6,215	965	0.16
250	2,772	696	0.25
500	1,023	439	0.43
750	643	361	0.56
1,000	543	332	0.61
1,250	444	305	0.69
1,500	326	248	0.76
1,750	292	238	0.82
2,000	252	218	0.87
2,250	250	220	0.88
2,558	253	225	0.89

Field Example 19

We present the flow rate data and the cumulative production data which spans over 8.5 years for a vertical well producing from a shale gas reservoir in **Fig. D13**. **Fig. D14** presents the "hyperbolic" model matches imposed on the flow rate data along with the *D*- and *b*-parameter trends. In **Fig. D15** we observe that the value of the *b*-parameter as a function of time. The *b*-parameter value decreases from 2.79 to 2.14 during the production history. Every interval is matched with a "hyperbolic" *b*-parameter greater than 1 indicating that boundary-dominated flow has not been established. **Fig. D16** shows the power law exponential model matches imposed on the flow rate data and *D*- and *b*-parameter trends. In **Fig. D17** we show the results of the straight line extrapolation technique, and in **Fig. D18** we present the calculated *EUR* values versus production time. All of the model parameters for this example are presented in **Tables D7, D8, and D9**. The *EUR* of this well should be in between 1.68 BSCF (the "lower" limit given by the straight line extrapolation technique at 3,159 days) and 1.78 BSCF (the "upper" limit given by the power law exponential estimate at 3,159 days).

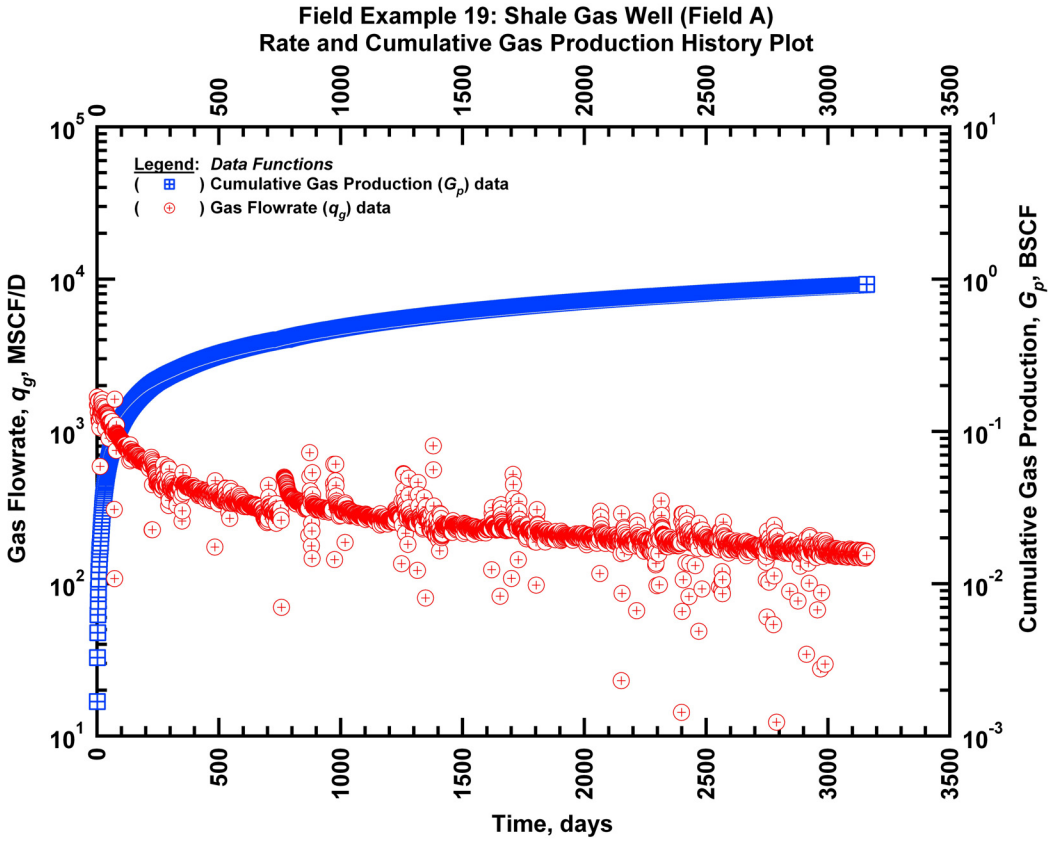

Figure D13 — (Semi-log Plot): Production history plot for field example 19 — flow rate (q_g) and cumulative production (G_p) versus production time.

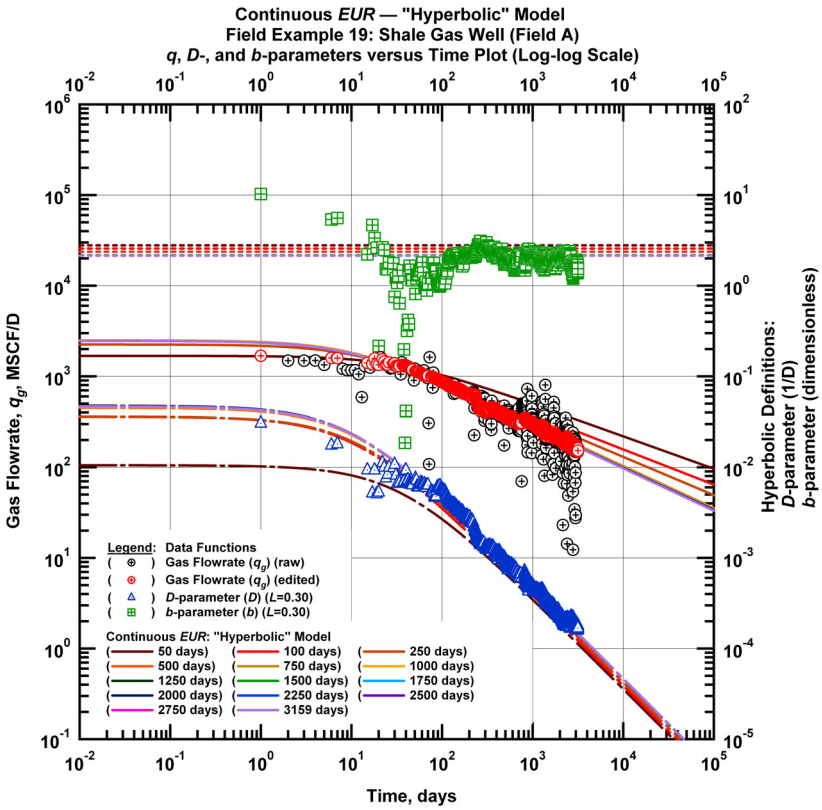

Figure D14 — (Log-log Plot): *qDb* plot — flow rate (q_g), *D*- and *b*-parameters versus production time and "hyperbolic" model matches for field example 19.

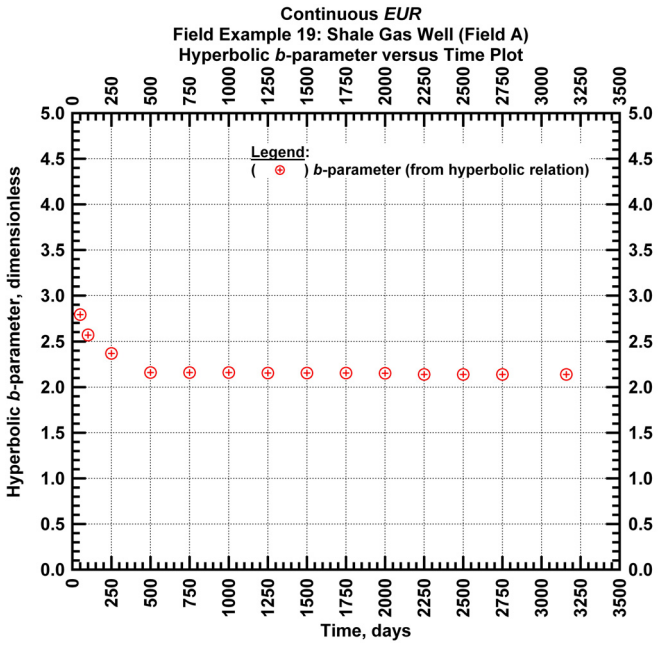

Figure D15 — (Cartesian Plot): Hyperbolic *b*-parameter values obtained from model matches with production data for field example 19.

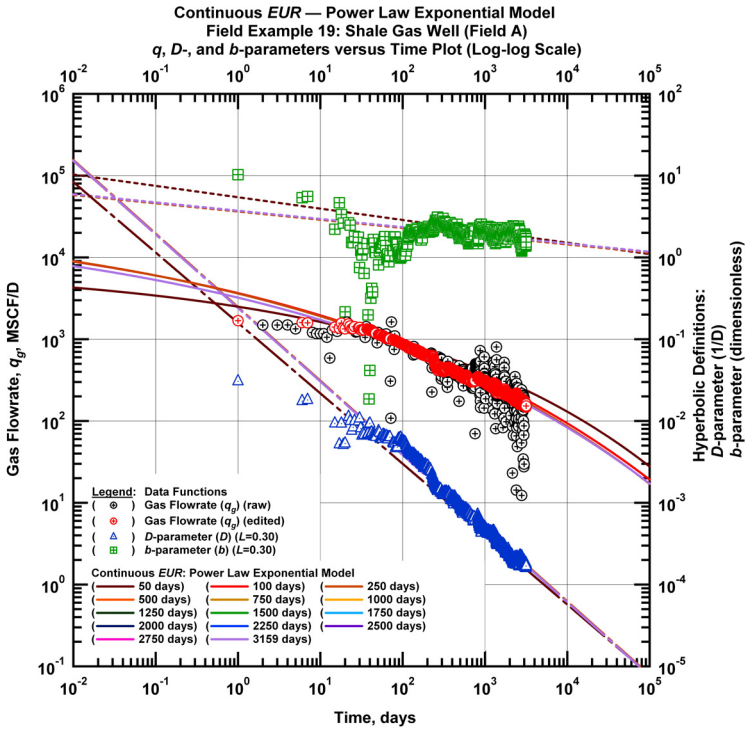

Figure D16 — (Log-log Plot): qDb plot — flow rate (q_g), D- and b-parameters versus production time and power law exponential model matches for field example 19.

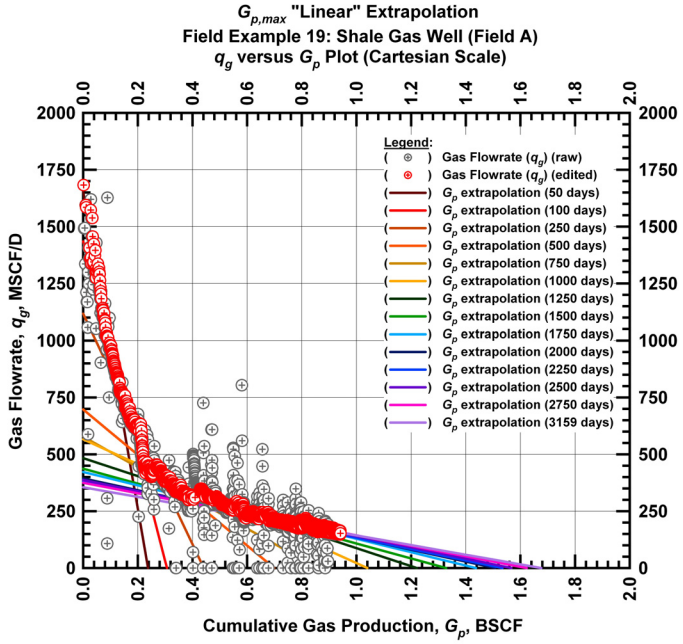

Figure D17 — (Cartesian Plot): Rate Cumulative Plot — flow rate (q_g) versus cumulative production (G_p) and the linear trends fit through the data for field example 19.

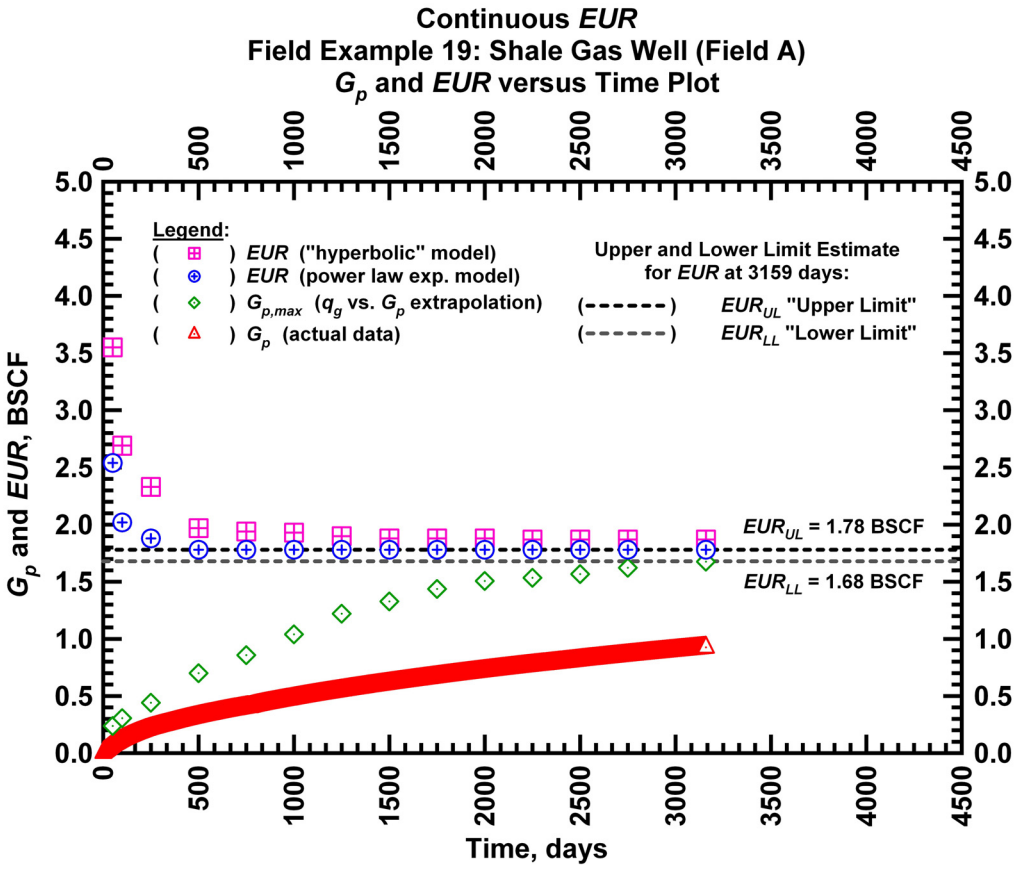

Figure D18 — (Cartesian Plot): *EUR* estimates from model matches and $G_{p,max}$ estimates from extrapolation technique for field example 19.

Table D7 — Analysis results for field example 19 — "hyperbolic" model parameters.

Time Interval, days	q_{gi} (MSCFD)	D_i (D^{-1})	b (dimensionless)	EUR_{hyp} (BSCF)
50	1,682	0.010524	2.7918	3.55
100	2,246	0.035984	2.5700	2.69
250	2,246	0.035984	2.3700	2.33
500	2,491	0.045046	2.1600	1.97
750	2,491	0.046630	2.1600	1.94
1,000	2,474	0.046096	2.1600	1.93
1,250	2,460	0.047000	2.1550	1.90
1,500	2,456	0.047463	2.1549	1.88
1,750	2,456	0.047463	2.1549	1.88
2,000	2,456	0.047465	2.1526	1.88
2,250	2,456	0.046635	2.1388	1.87
2,500	2,456	0.046635	2.1388	1.87
2,750	2,456	0.046635	2.1388	1.87
3,159	2,456	0.046635	2.1388	1.87

Table D8 — Analysis results for field example 19 — power-law exponential model parameters.

Time Interval, days	$\hat{q}_{gi}$ (MSCFD)	$\hat{D}_i$ (D^{-1})	n (dimensionless)	D_∞ (D^{-1})	EUR_{PLE} (BSCF)
50	7,796	1.1380	0.1390	0	2.54
100	39,866	2.3881	0.1010	0	2.02
250	42,133	2.4544	0.1006	0	1.88
500	35,690	2.4051	0.1004	0	1.78
750	35,690	2.4051	0.1004	0	1.78
1,000	35,690	2.4051	0.1004	0	1.78
1,250	35,690	2.4051	0.1004	0	1.78
1,500	35,690	2.4051	0.1004	0	1.78
1,750	35,690	2.4051	0.1004	0	1.78
2,000	35,690	2.4051	0.1004	0	1.78
2,250	35,690	2.4051	0.1004	0	1.78
2,500	35,690	2.4051	0.1004	0	1.78
2,750	35,690	2.4051	0.1004	0	1.78
3,159	35,690	2.4051	0.1004	0	1.78

Table D9 — Analysis results for field example 19 — straight line extrapolation.

Time Interval, days	Slope, 10^{-6} D^{-1}	Intercept, MSCF/D	$G_{p,max}$ (BSCF)
50	6,966	1,654	0.24
100	4,679	1,435	0.31
250	2,532	1,117	0.44
500	997	697	0.70
750	674	578	0.86
1,000	544	566	1.04
1,250	396	483	1.22
1,500	329	437	1.33
1,750	294	423	1.44
2,000	262	394	1.51
2,250	249	382	1.53
2,500	247	387	1.57
2,750	231	375	1.62
3,159	212	355	1.68

Field Example 20

We present the flow rate data and the cumulative production data which spans over 6.8 years for a vertical well producing from a shale gas reservoir in **Fig. D19**. **Fig. D20** presents the "hyperbolic" model matches imposed on the flow rate data along with the *D*- and *b*-parameter trends. In **Fig. D21** we observe that the value of the *b*-parameter as a function of time. The *b*-parameter value decreases from 6.89 to 1.41 during the production history. Every interval is matched with a "hyperbolic" *b*-parameter greater than 1 indicating that boundary-dominated flow has not been established. **Fig. D22** shows the power law exponential model matches imposed on the flow rate data and *D*- and *b*-parameter trends. In **Fig. D23** we show the results of the straight line extrapolation technique, and in **Fig. D24** we present the calculated *EUR* values versus production time. All of the model parameters for this example are presented in **Tables D10, D11, and D12**. The *EUR* of this well should be in between 1.96 BSCF (the "lower" limit given by the straight line extrapolation technique at 2,485 days) and 2.18 BSCF (the "upper" limit given by the power law exponential estimate at 2,485 days).

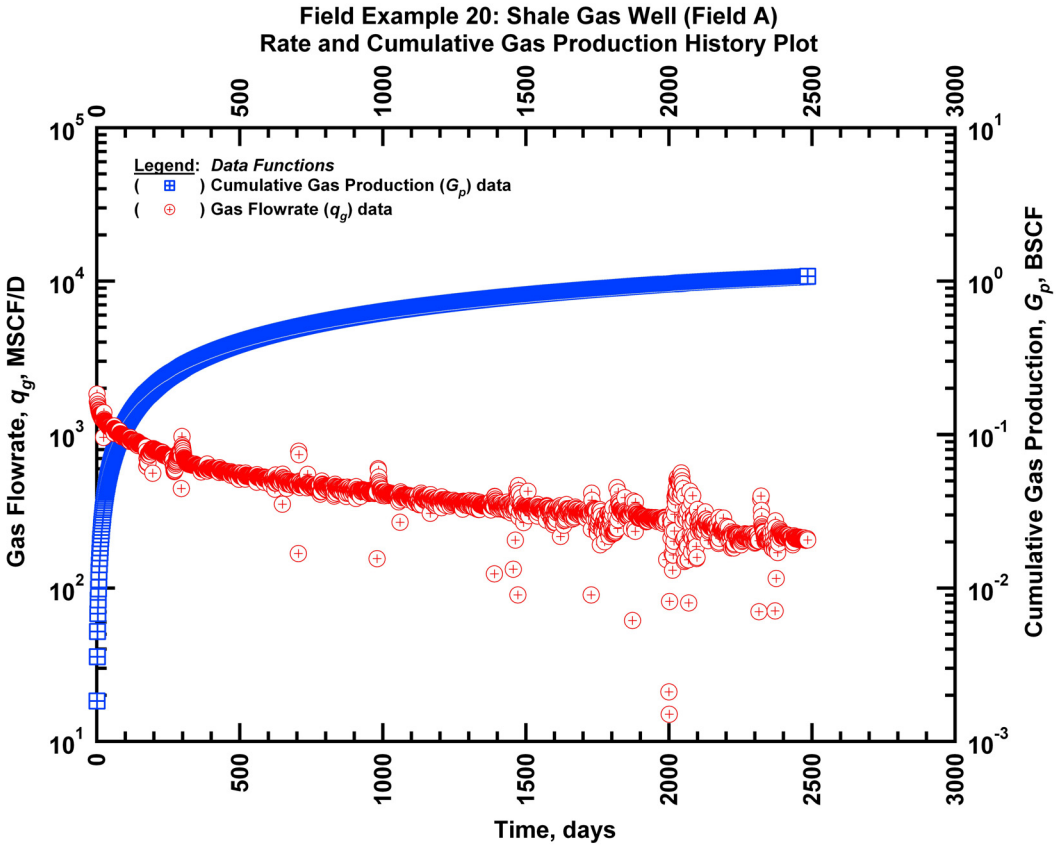

Figure D19 — (Semi-log Plot): Production history plot for field example 20 — flow rate (q_g) and cumulative production (G_p) versus production time.

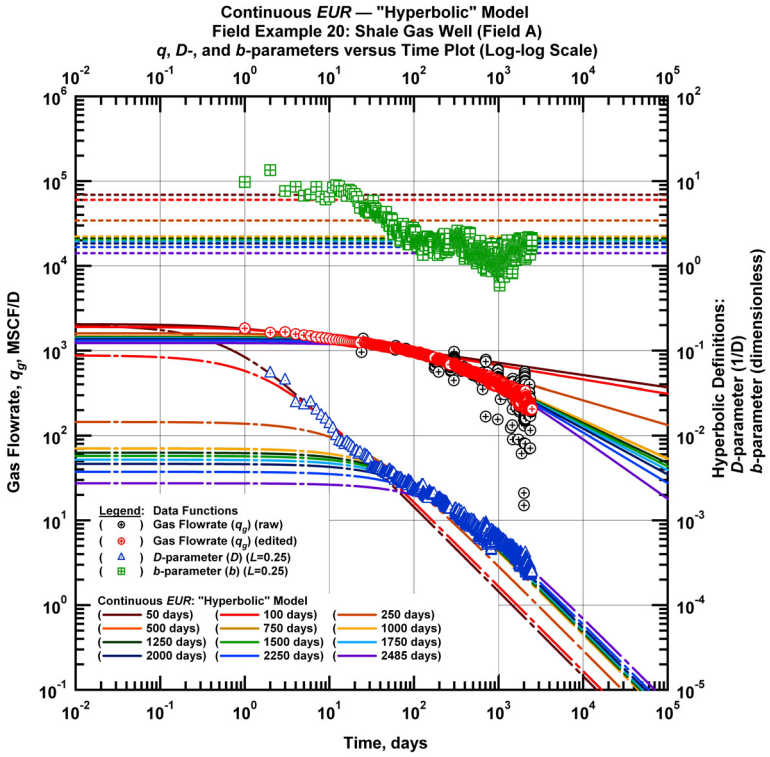

Figure D20 — (Log-log Plot): *qDb* plot — flow rate (q_g), *D*- and *b*-parameters versus production time and "hyperbolic" model matches for field example 20.

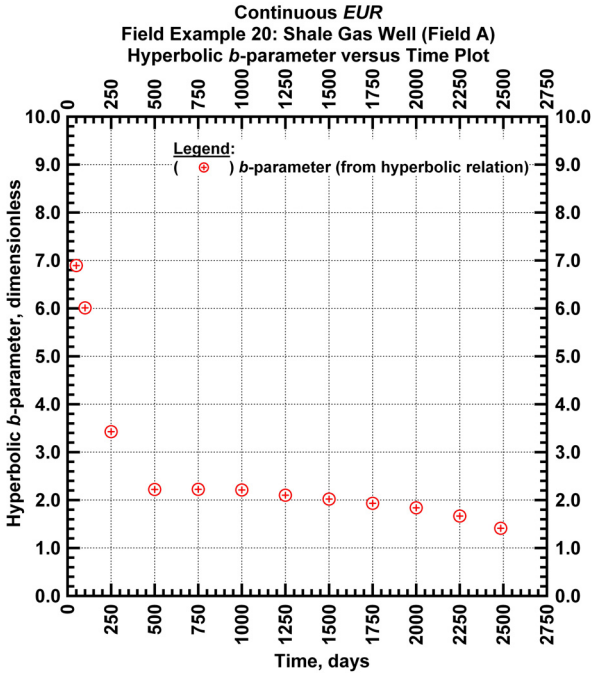

Figure D21 — (Cartesian Plot): Hyperbolic *b*-parameter values obtained from model matches with production data for field example 20.

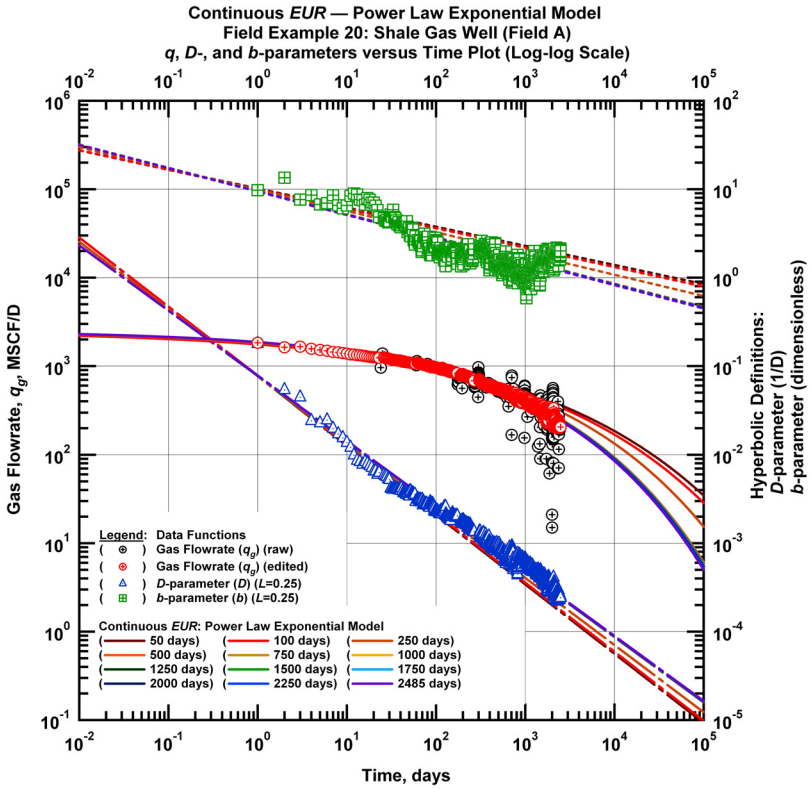

Figure D22 — (Log-log Plot): *qDb* plot — flow rate (q_g), *D*- and *b*-parameters versus production time and power law exponential model matches for field example 20.

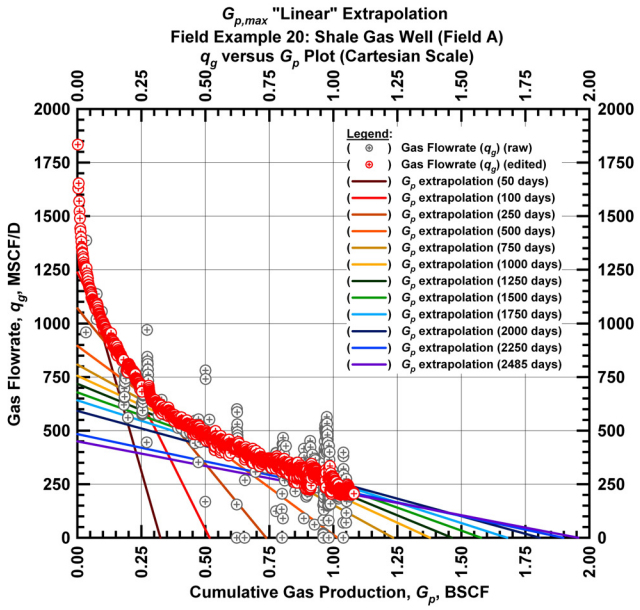

Figure D23 — (Cartesian Plot): Rate Cumulative Plot — flow rate (q_g) versus cumulative production (G_p) and the linear trends fit through the data for field example 20.

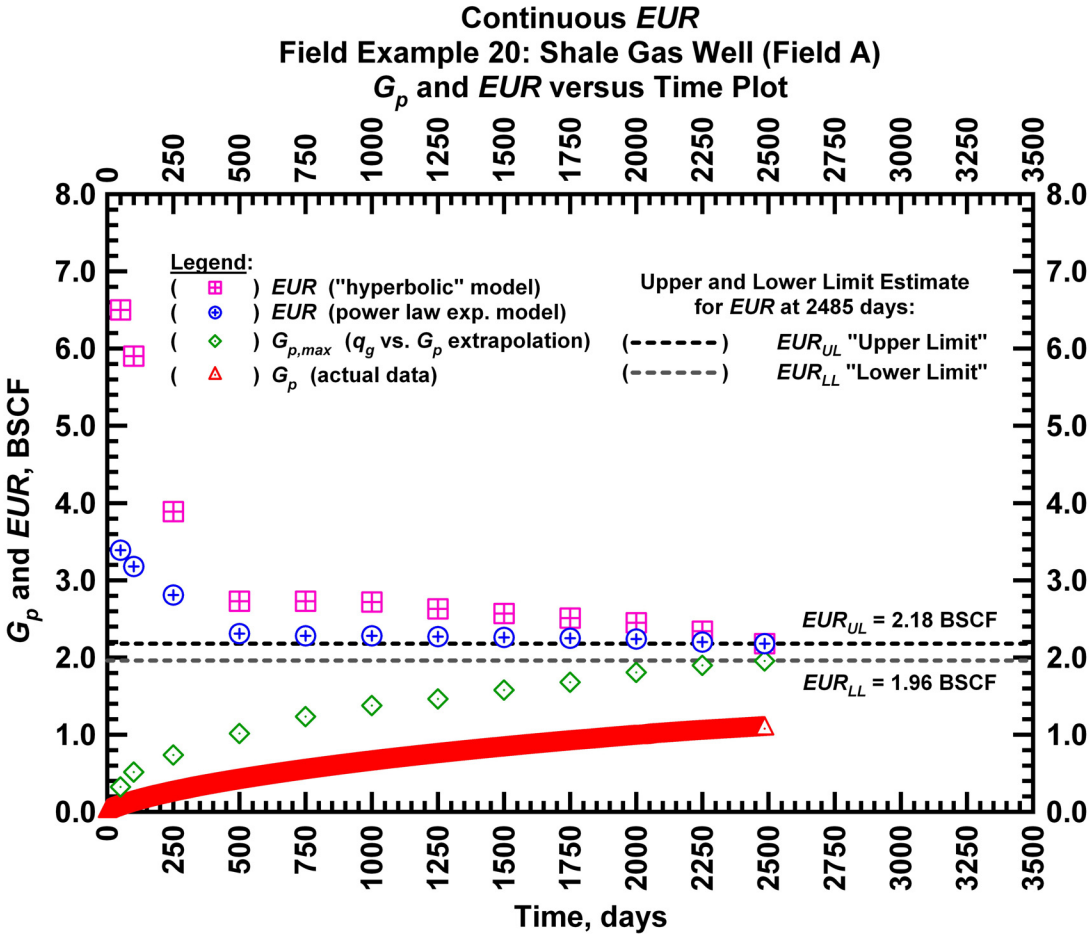

Figure D24 — (Cartesian Plot): *EUR* estimates from model matches and $G_{p,max}$ estimates from extrapolation technique for field example 20.

Table D10 — Analysis results for field example 20 — "hyperbolic" model parameters.

Time Interval, days	q_{gi} (MSCFD)	D_i (D^{-1})	b (dimensionless)	EUR_{hyp} (BSCF)
50	2,049	0.198552	6.892	6.50
100	1,900	0.087887	6.011	5.90
250	1,597	0.014505	3.426	3.89
500	1,473	0.007070	2.222	2.73
750	1,473	0.007072	2.223	2.73
1,000	1,473	0.007033	2.210	2.72
1,250	1,446	0.006292	2.102	2.63
1,500	1,425	0.005767	2.021	2.57
1,750	1,399	0.005198	1.933	2.51
2,000	1,369	0.004643	1.838	2.45
2,250	1,311	0.003741	1.665	2.34
2,485	1,227	0.002738	1.411	2.18

Table D11 — Analysis results for field example 20 — power-law exponential model parameters.

Time Interval, days	$\hat{q}_{gi}$ (MSCFD)	$\hat{D}_i$ (D^{-1})	n (dimensionless)	D_∞ (D^{-1})	EUR_{PLE} (BSCF)
50	2,508	0.3555	0.2162	0	3.39
100	2,508	0.3555	0.2200	0	3.18
250	2,508	0.3202	0.2404	0	2.81
500	2,508	0.2945	0.2621	0	2.31
750	2,508	0.2948	0.2626	0	2.28
1,000	2,508	0.2948	0.2626	0	2.28
1,250	2,508	0.2950	0.2627	0	2.27
1,500	2,508	0.2951	0.2629	0	2.26
1,750	2,508	0.2952	0.2631	0	2.25
2,000	2,508	0.2954	0.2634	0	2.24
2,250	2,508	0.2957	0.2640	0	2.20
2,485	2,508	0.2960	0.2645	0	2.18

Table D12 — Analysis results for field example 20 — straight line extrapolation.

Time Interval, days	Slope, 10^{-6} D^{-1}	Intercept, MSCF/D	$G_{p,max}$ (BSCF)
50	4,186	1,357	0.32
100	2,396	1,237	0.52
250	1,451	1,070	0.74
500	882	896	1.02
750	655	808	1.23
1,000	549	756	1.38
1,250	491	719	1.46
1,500	430	679	1.58
1,750	382	642	1.68
2,000	328	592	1.81
2,250	255	484	1.90
2,485	230	450	1.96

Field Example 21

We present the flow rate data and the cumulative production data which spans almost 3 years for a horizontal well producing from a shale gas reservoir in **Fig. D25**. **Fig. D26** presents the "hyperbolic" model matches imposed on the flow rate data along with the *D*- and *b*-parameter trends. In **Fig. D27** we observe that the value of the *b*-parameter as a function of time. The *b*-parameter value decreases from 3.87 to 2.68 during the production history. Every interval is matched with a "hyperbolic" *b*-parameter greater than 1 indicating that boundary-dominated flow has not been established. **Fig. D28** shows the power law exponential model matches imposed on the flow rate data and *D*- and *b*-parameter trends. In **Fig. D29** we show the results of the straight line extrapolation technique, and in **Fig. D30** we present the calculated *EUR* values versus production time. All of the model parameters for this example are presented in **Tables D13, D14, and D15**. The *EUR* of this well should be in between 2.25 BSCF (the "lower" limit given by the straight line extrapolation technique at 1,071 days) and 3.54 BSCF (the "upper" limit given by the power law exponential estimate at 1,071 days).

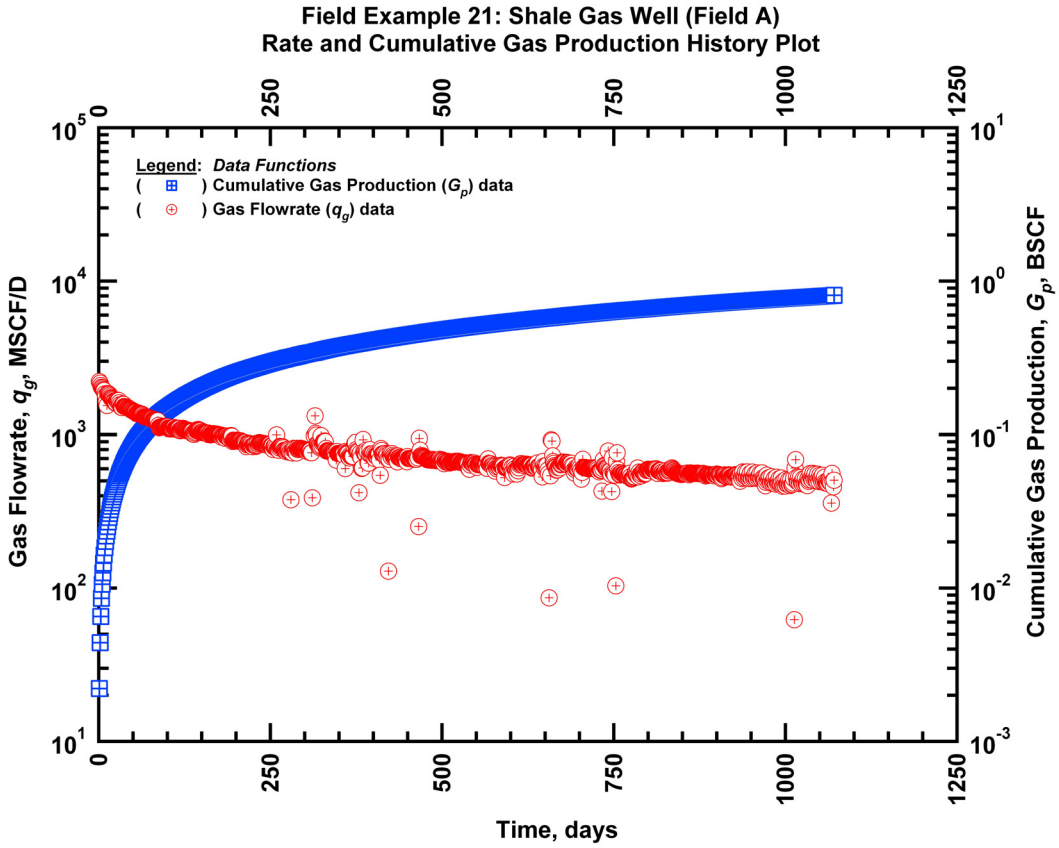

Figure D25 — (Semi-log Plot): Production history plot for field example 21 — flow rate (q_g) and cumulative production (G_p) versus production time.

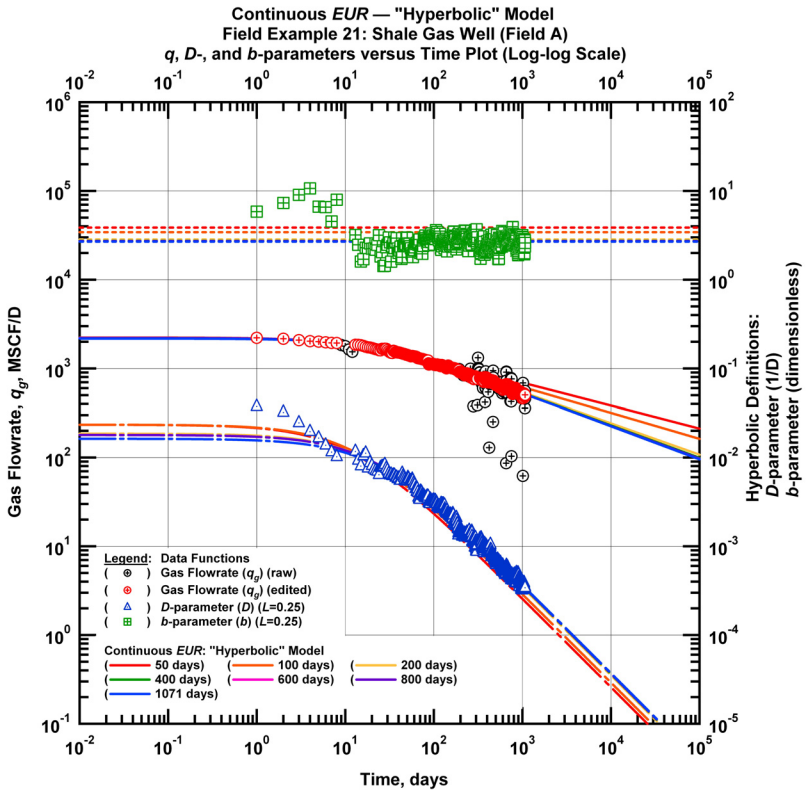

Figure D26 — (Log-log Plot): *qDb* plot — flow rate (q_g), *D*- and *b*-parameters versus production time and "hyperbolic" model matches for field example 21.

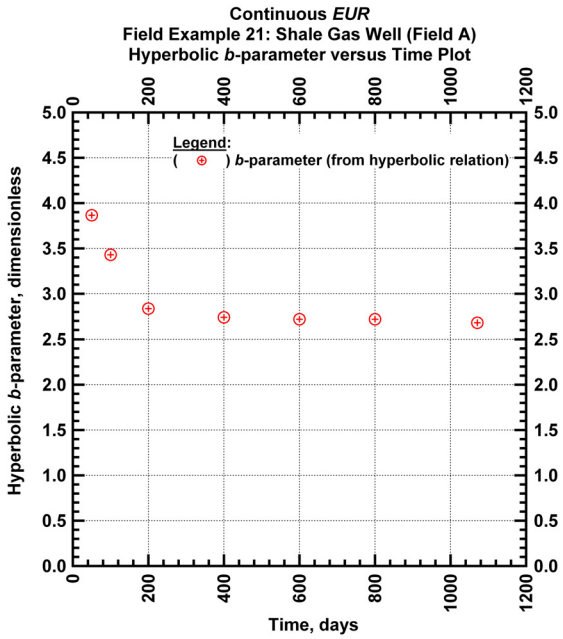

Figure D27 — (Cartesian Plot): Hyperbolic *b*-parameter values obtained from model matches with production data for field example 21.

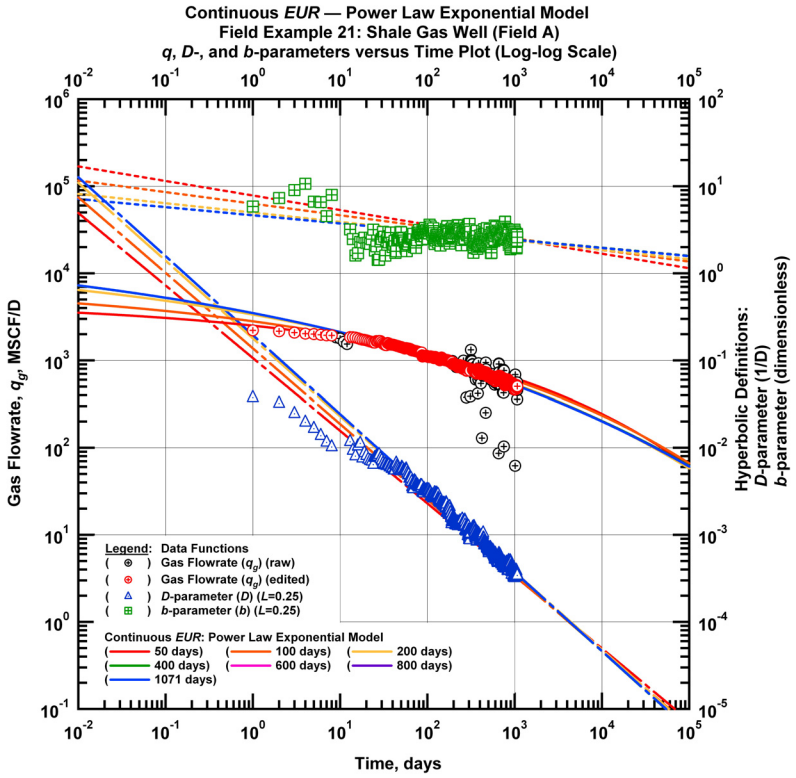

Figure D28 — (Log-log Plot): *qDb* plot — flow rate (q_g), *D*- and *b*-parameters versus production time and power law exponential model matches for field example 21.

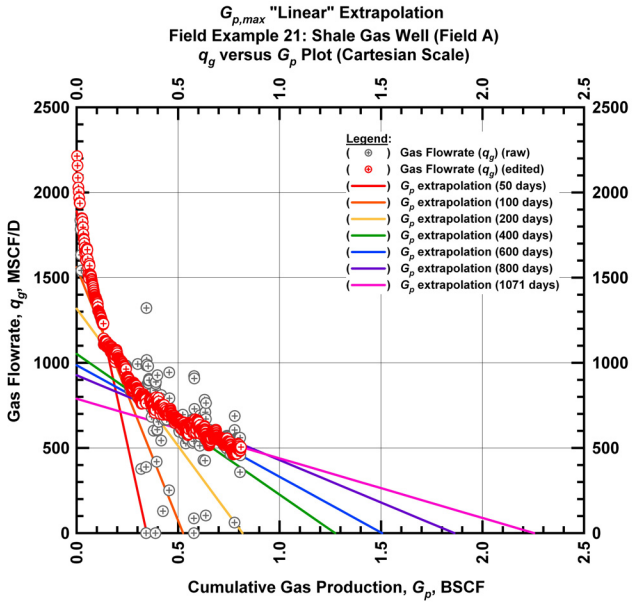

Figure D29 — (Cartesian Plot): Rate Cumulative Plot — flow rate (q_g) versus cumulative production (G_p) and the linear trends fit through the data for field example 21.

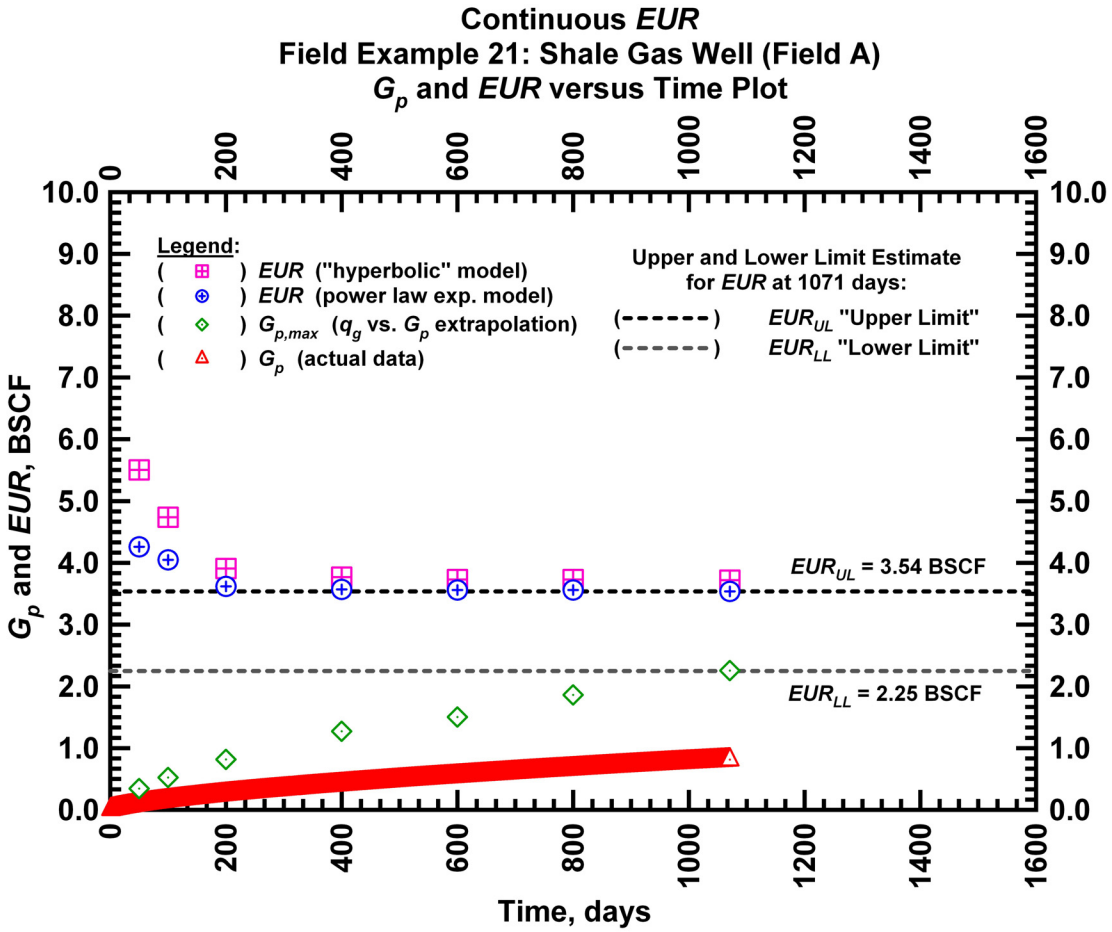

Figure D30 — (Cartesian Plot): *EUR* estimates from model matches and $G_{p,max}$ estimates from extrapolation technique for field example 21.

Table D13 — Analysis results for field example 21 — "hyperbolic" model parameters.

Time Interval, days	q_{gi} (MSCFD)	D_i (D^{-1})	b (dimensionless)	EUR_{hyp} (BSCF)
50	2,230	0.02341	3.866	5.50
100	2,230	0.02341	3.430	4.74
200	2,208	0.01856	2.836	3.91
400	2,208	0.01793	2.740	3.77
600	2,208	0.01793	2.718	3.73
800	2,208	0.01793	2.718	3.73
1071	2,171	0.01626	2.680	3.72

Table D14 — Analysis results for field example 21 — power-law exponential model parameters.

Time Interval, days	$\hat{q}_{gi}$ (MSCFD)	$\hat{D}_i$ (D^{-1})	n (dimensionless)	D_∞ (D^{-1})	EUR_{PLE} (BSCF)
50	4,739	0.637	0.167	0	4.26
100	7,905	1.034	0.133	0	4.05
200	17,875	1.673	0.107	0	3.62
400	28,213	2.090	0.093	0	3.57
600	28,213	2.088	0.094	0	3.56
800	28,213	2.088	0.094	0	3.56
1071	28,213	2.088	0.094	0	3.54

Table D15 — Analysis results for field example 21 — straight line extrapolation.

Time Interval, days	Slope, 10^{-6} D^{-1}	Intercept, MSCF/D	$G_{p,max}$ (BSCF)
50	5,470	1,890	0.35
100	2,976	1,561	0.52
200	1,612	1,318	0.82
400	826	1,052	1.27
600	655	986	1.51
800	498	927	1.86
1071	350	789	2.25

Field Example 22

We present the flow rate data and the cumulative production data which spans almost 1 year for a horizontal well producing from a shale gas reservoir in **Fig. D31**. **Fig. D32** presents the "hyperbolic" model matches imposed on the flow rate data along with the *D*- and *b*-parameter trends. In **Fig. D33** we observe that the value of the *b*-parameter as a function of time. The *b*-parameter value decreases from 6.03 to 2.06 during the production history. Every interval is matched with a "hyperbolic" *b*-parameter greater than 1 indicating that boundary-dominated flow has not been established. **Fig. D34** shows the power law exponential model matches imposed on the flow rate data and *D*- and *b*-parameter trends. In **Fig. D35** we show the results of the straight line extrapolation technique, and in **Fig. D36** we present the calculated *EUR* values versus production time. All of the model parameters for this example are presented in **Tables D16, D17, and D18**. The *EUR* of this well should be in between 1.52 BSCF (the "lower" limit given by the straight line extrapolation technique at 350 days) and 2.50 BSCF (the "upper" limit given by the power law exponential estimate at 350 days).

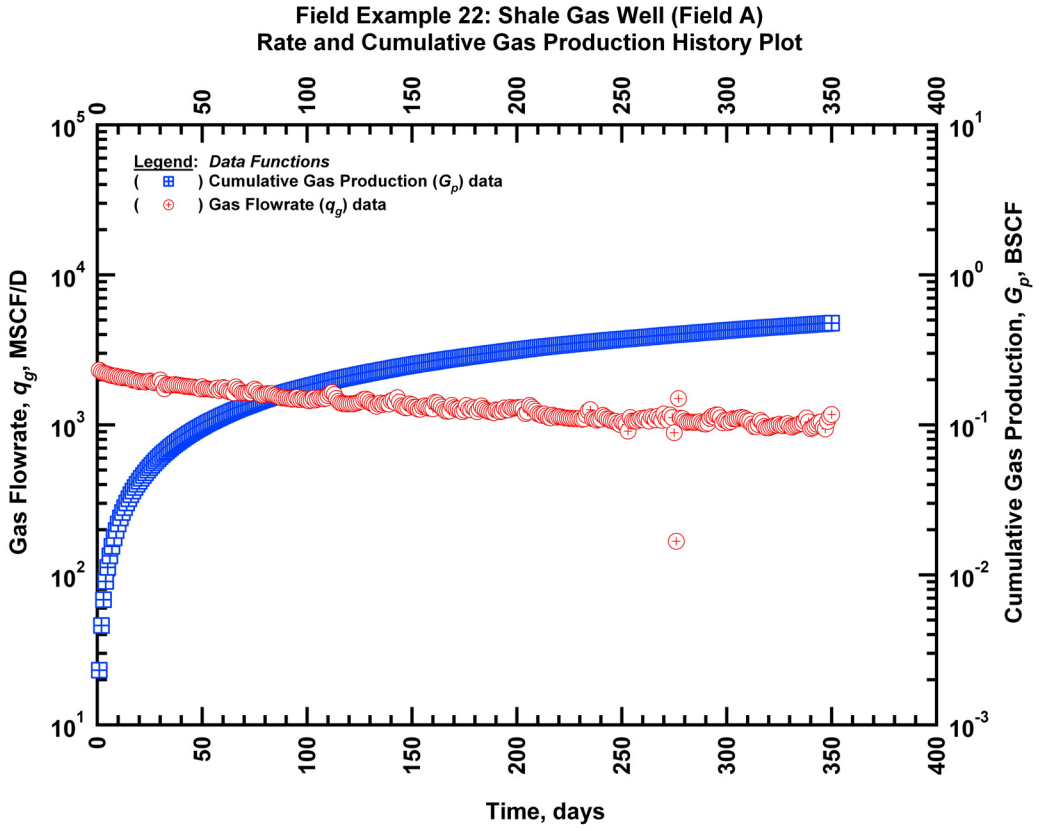

Figure D31 — (Semi-log Plot): Production history plot for field example 22 — flow rate (q_g) and cumulative production (G_p) versus production time.

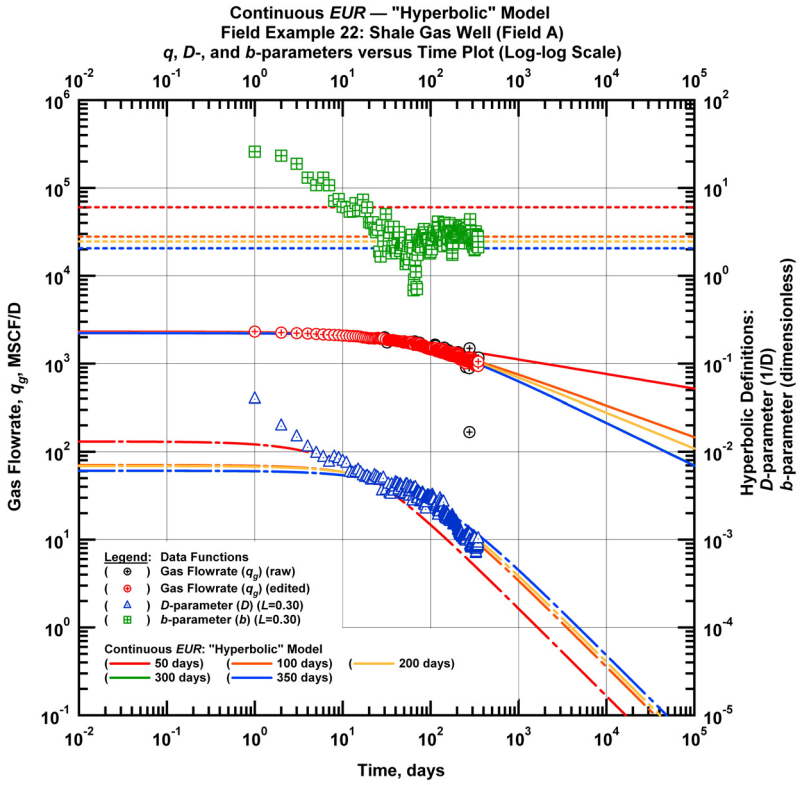

Figure D32 — (Log-log Plot): *qDb* plot — flow rate (q_g), *D*- and *b*-parameters versus production time and "hyperbolic" model matches for field example 22.

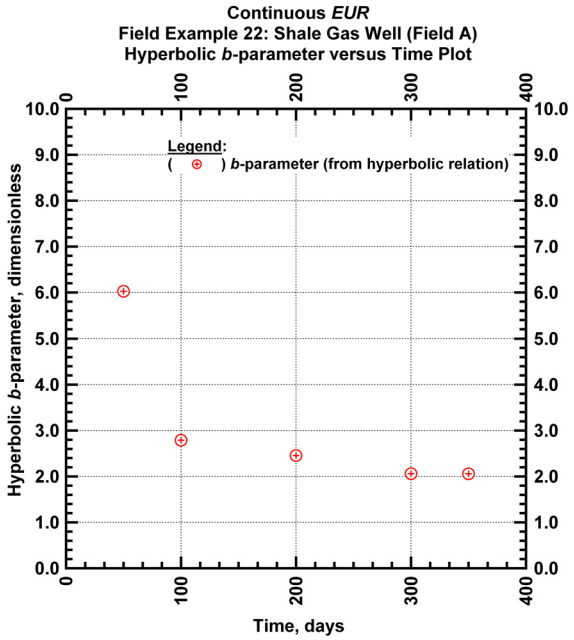

Figure D33 — (Cartesian Plot): Hyperbolic *b*-parameter values obtained from model matches with production data for field example 22.

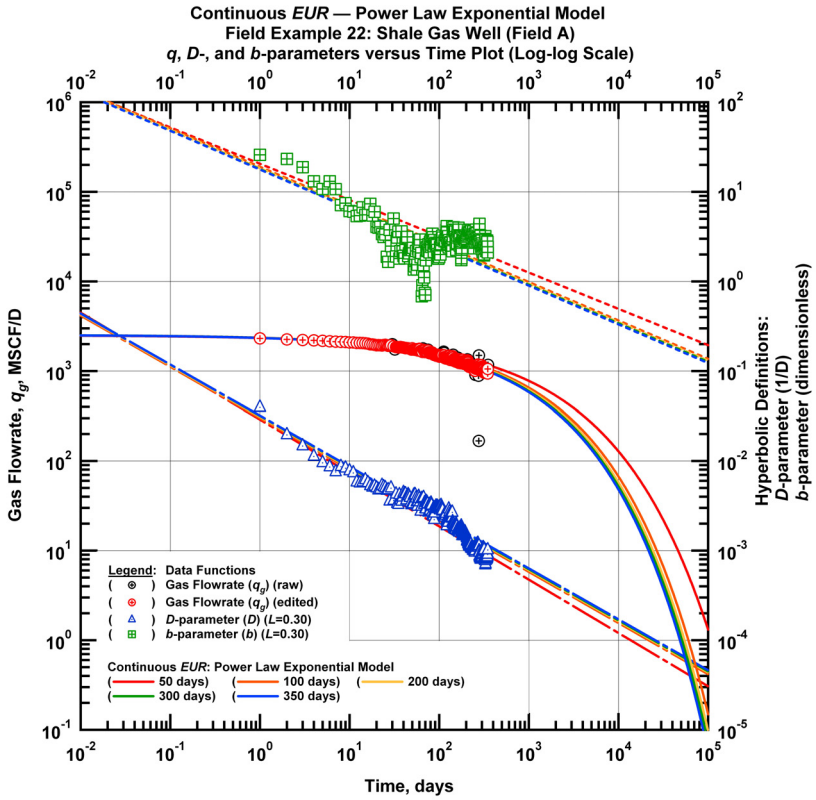

Figure D34 — (Log-log Plot): *qDb* plot — flow rate (q_g), *D*- and *b*-parameters versus production time and power law exponential model matches for field example 22.

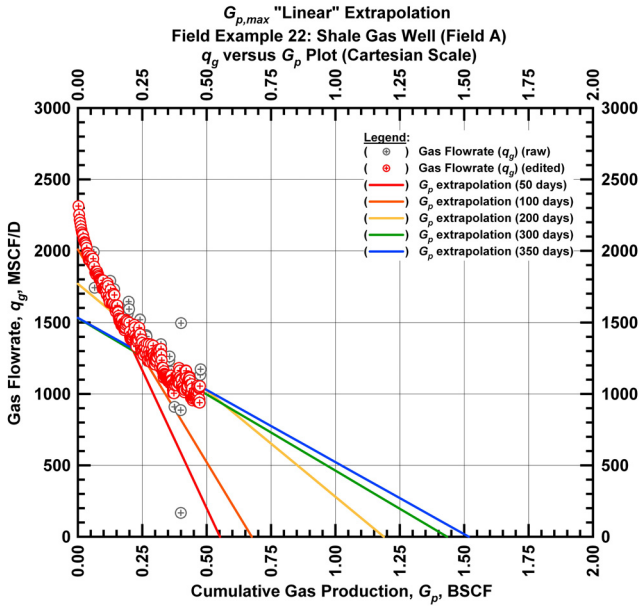

Figure D35 — (Cartesian Plot): Rate Cumulative Plot — flow rate (q_g) versus cumulative production (G_p) and the linear trends fit through the data for field example 22.

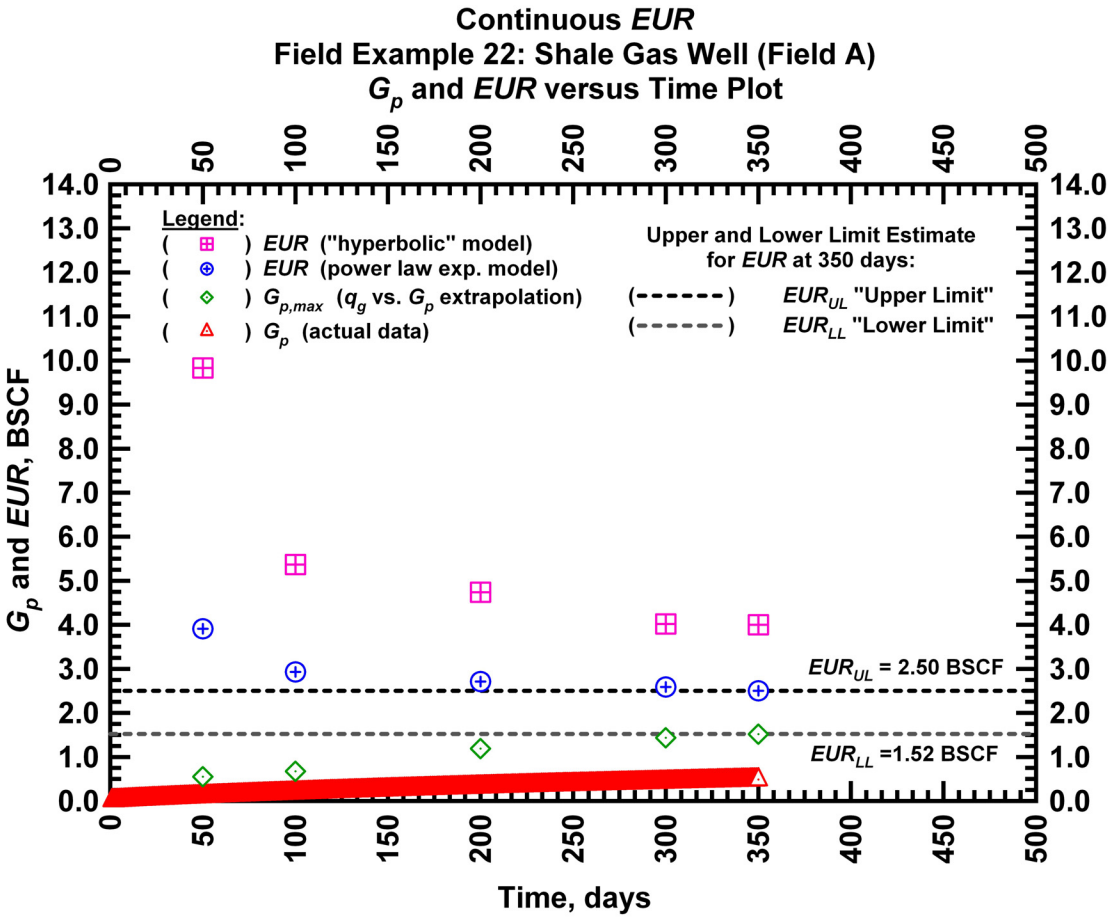

Figure D36 — (Cartesian Plot): *EUR* estimates from model matches and $G_{p,max}$ estimates from extrapolation technique for field example 22.

Table D16 — Analysis results for field example 22 — "hyperbolic" model parameters.

Time Interval, days	q_{gi} (MSCFD)	D_i (D^{-1})	b (dimensionless)	EUR_{hyp} (BSCF)
50	2,306	0.013078	6.025	9.83
100	2,220	0.007044	2.790	5.37
200	2,244	0.006881	2.455	4.74
300	2,224	0.006064	2.060	4.02
350	2,224	0.006084	2.057	4.00

Table D17 — Analysis results for field example 22 — power-law exponential model parameters.

Time Interval, days	$\hat{q}_{gi}$ (MSCFD)	$\hat{D}_i$ (D^{-1})	n (dimensionless)	D_∞ (D^{-1})	EUR_{PLE} (BSCF)
50	2,508	0.0714	0.4049	0	3.91
100	2,525	0.0699	0.4288	0	2.93
200	2,525	0.0724	0.4295	0	2.71
300	2,525	0.0740	0.4300	0	2.59
350	2,520	0.0741	0.4320	0	2.50

Table D18 — Analysis results for field example 22 — straight line extrapolation.

Time Interval, days	Slope, 10^{-6} D^{-1}	Intercept, MSCF/D	$G_{p,max}$ (BSCF)
50	3,868	2,133	0.55
100	2,974	2,009	0.68
200	1,489	1,769	1.19
300	1,068	1,531	1.43
350	1,010	1,533	1.52

Field Example 23

We present the flow rate data and the cumulative production data which spans almost 2.5 years for a horizontal well producing from a shale gas reservoir in **Fig. D37**. **Fig. D38** presents the "hyperbolic" model matches imposed on the flow rate data along with the *D*- and *b*-parameter trends. In **Fig. D39** we observe that the value of the *b*-parameter as a function of time. The *b*-parameter value decreases from 4.57 to 2.18 during the production history. Every interval is matched with a "hyperbolic" *b*-parameter greater than 1 indicating that boundary-dominated flow has not been established. **Fig. D40** shows the power law exponential model matches imposed on the flow rate data and *D*- and *b*-parameter trends. In **Fig. D41** we show the results of the straight line extrapolation technique, and in **Fig. D42** we present the calculated *EUR* values versus production time. All of the model parameters for this example are presented in **Tables D19, D20, and D21**. The *EUR* of this well should be in between 1.91 BSCF (the "lower" limit given by the straight line extrapolation technique at 899 days) and 2.77 BSCF (the "upper" limit given by the power law exponential estimate at 899 days).

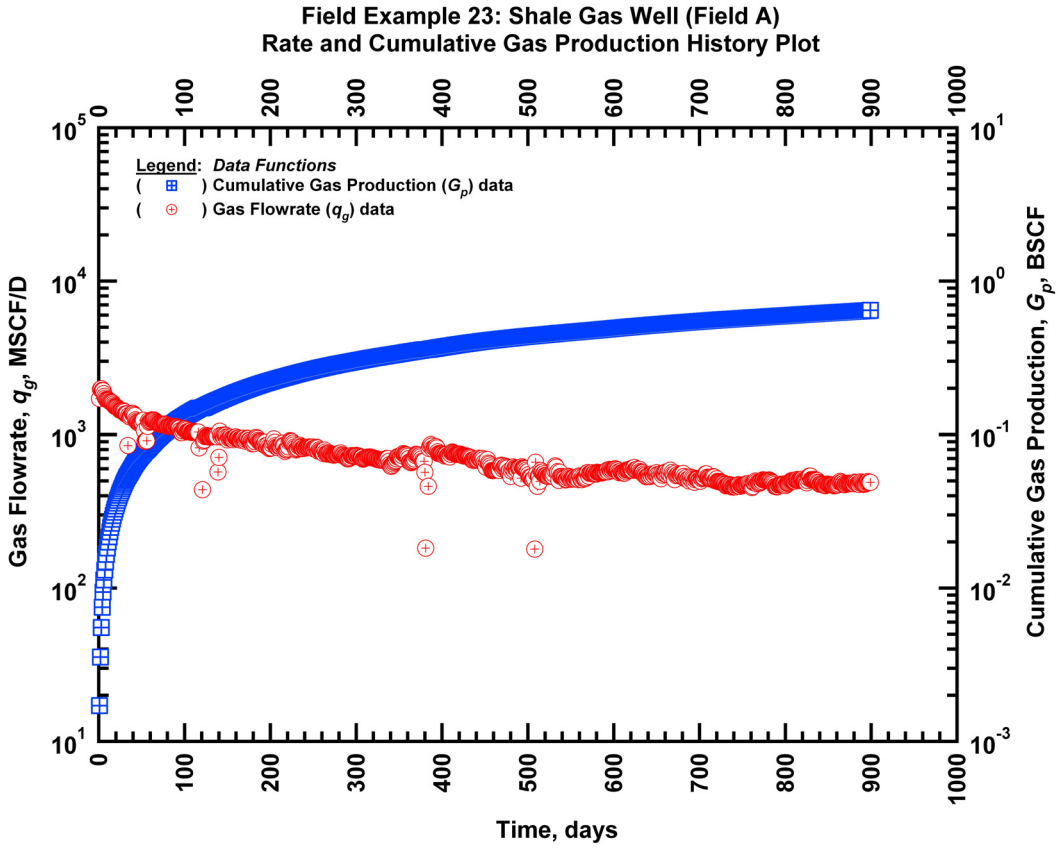

Figure D37 — (Semi-log Plot): Production history plot for field example 23 — flow rate (q_g) and cumulative production (G_p) versus production time.

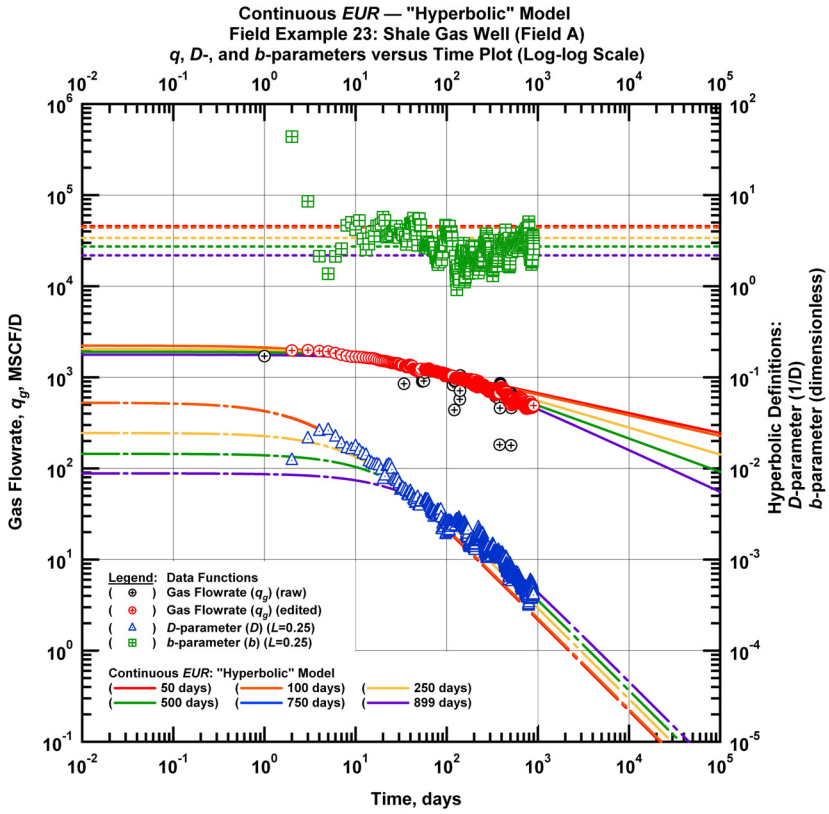

Figure D38 — (Log-log Plot): qDb plot — flow rate (q_g), D- and b-parameters versus production time and "hyperbolic" model matches for field example 23.

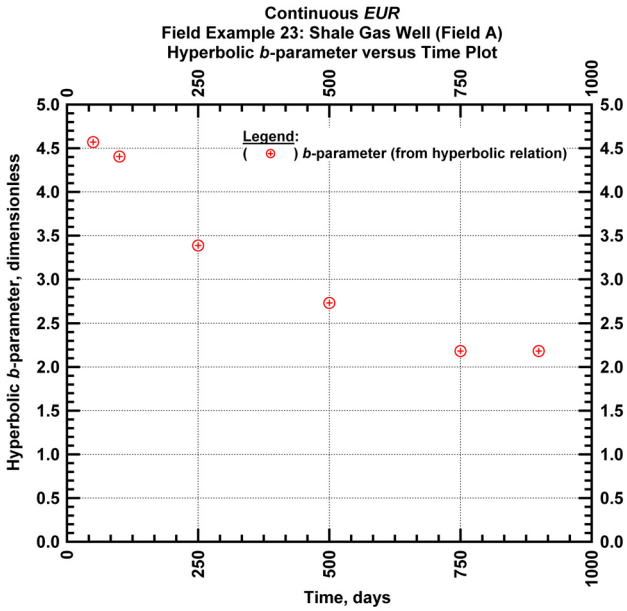

Figure D39 — (Cartesian Plot): Hyperbolic b-parameter values obtained from model matches with production data for field example 23.

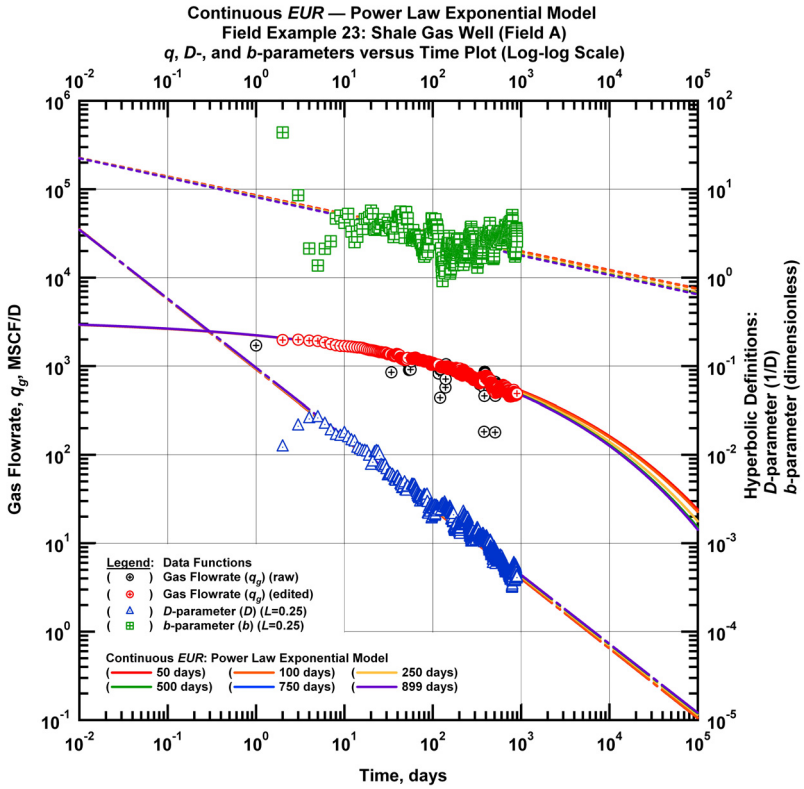

Figure D40 — (Log-log Plot): *qDb* plot — flow rate (q_g), *D*- and *b*-parameters versus production time and power law exponential model matches for field example 23.

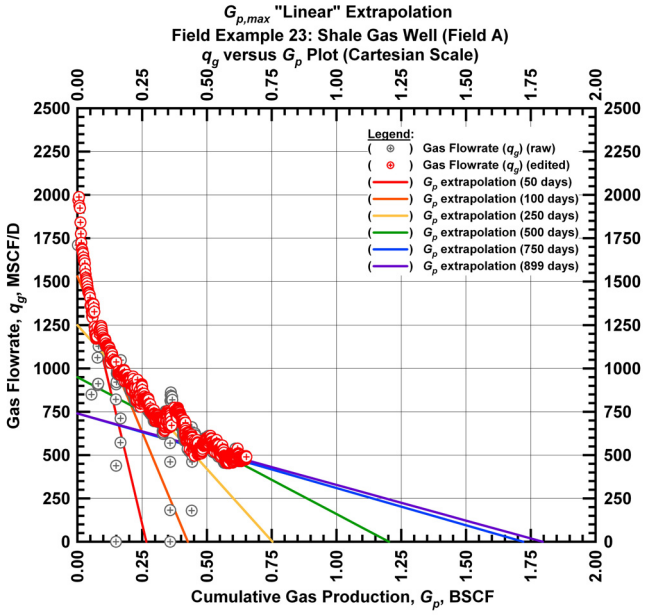

Figure D41 — (Cartesian Plot): Rate Cumulative Plot — flow rate (q_g) versus cumulative production (*Gp*) and the linear trends fit through the data for field example 23.

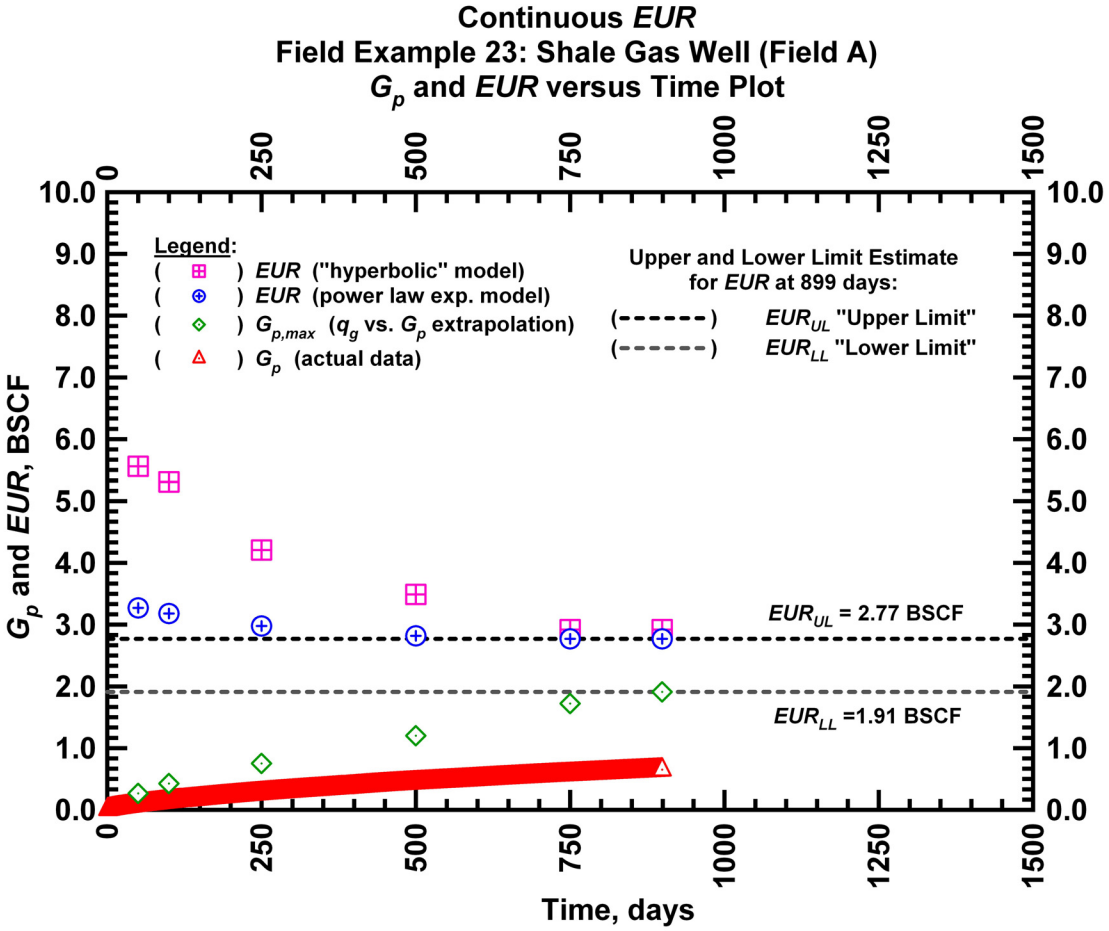

Figure D42 — (Cartesian Plot): *EUR* estimates from model matches and $G_{p,max}$ estimates from extrapolation technique for field example 23.

Table D19 — Analysis results for field example 23 — "hyperbolic" model parameters.

Time Interval, days	q_{gi} (MSCFD)	D_i (D^{-1})	b (dimensionless)	EUR_{hyp} (BSCF)
50	2,226	0.05272	4.570	5.56
100	2,226	0.05272	4.405	5.31
250	2,041	0.02450	3.386	4.21
500	1,907	0.01448	2.729	3.49
750	1,773	0.00883	2.182	2.92
899	1,773	0.00883	2.182	2.92

Table D20 — Analysis results for field example 23 — power-law exponential model parameters.

Time Interval, days	$\hat{q}_{gi}$ (MSCFD)	$\hat{D}_i$ (D^{-1})	n (dimensionless)	D_∞ (D^{-1})	EUR_{PLE} (BSCF)
50	3,448	0.436	0.211	0	3.27
100	3,448	0.441	0.211	0	3.18
250	3,448	0.435	0.217	0	2.98
500	3,448	0.436	0.219	0	2.82
750	3,448	0.436	0.220	0	2.77
899	3,448	0.436	0.220	0	2.77

Table D21 — Analysis results for field example 23 — straight line extrapolation.

Time Interval, days	Slope, 10^{-6} D^{-1}	Intercept, MSCF/D	$G_{p,max}$ (BSCF)
50	6,310	1,680	0.27
100	3,590	1,530	0.43
250	1,660	1,250	0.75
500	790	950	1.20
750	430	740	1.72
899	412	740	1.91

Field Example 24

We present the flow rate data and the cumulative production data which spans over 2.5 years for a horizontal well producing from a shale gas reservoir in **Fig. D43**. **Fig. D44** presents the "hyperbolic" model matches imposed on the flow rate data along with the *D*- and *b*-parameter trends. In **Fig. D45** we observe that the value of the *b*-parameter as a function of time. The *b*-parameter value decreases from 2.60 to 1.85 during the production history. Every interval is matched with a "hyperbolic" *b*-parameter greater than 1 indicating that boundary-dominated flow has not been established. **Fig. D46** shows the power law exponential model matches imposed on the flow rate data and *D*- and *b*-parameter trends. In **Fig. D47** we show the results of the straight line extrapolation technique, and in **Fig. D48** we present the calculated *EUR* values versus production time. All of the model parameters for this example are presented in **Tables D22, D23, and D24**. The *EUR* of this well should be in between 1.87 BSCF (the "lower" limit given by the straight line extrapolation technique at 919 days) and 2.94 BSCF (the "upper" limit given by the power law exponential estimate at 919 days).

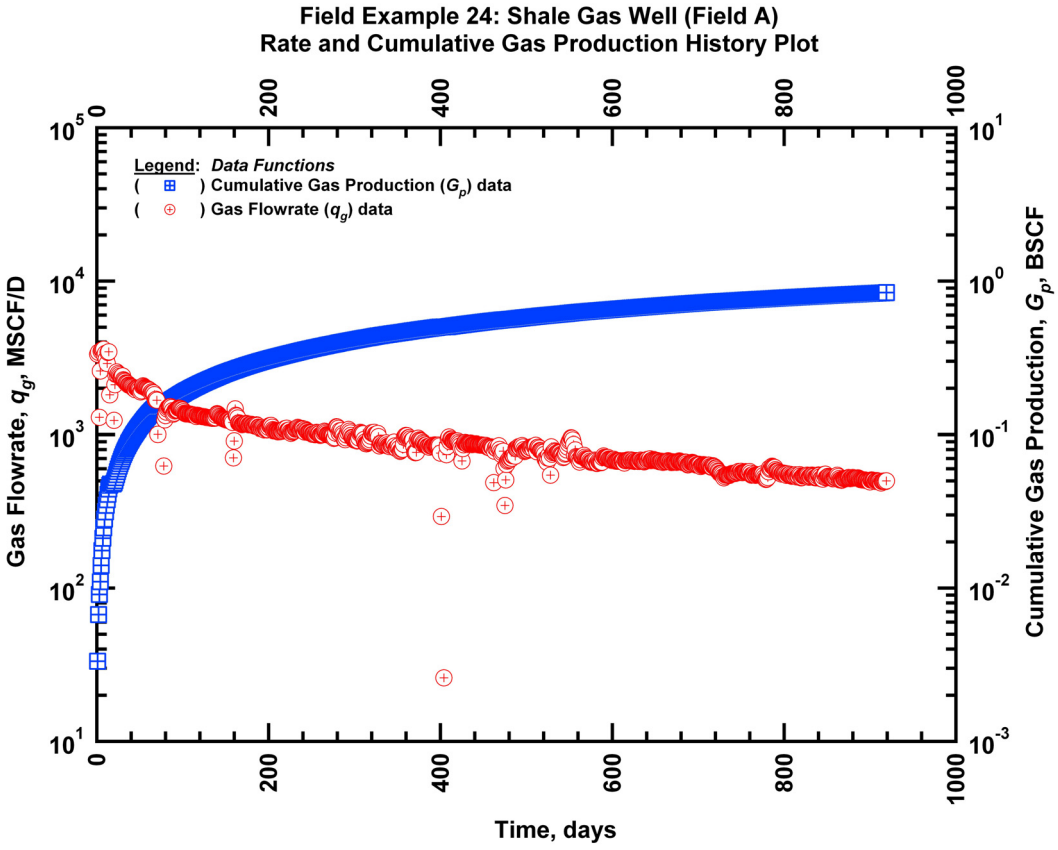

Figure D43 — (Semi-log Plot): Production history plot for field example 24 — flow rate (q_g) and cumulative production (G_p) versus production time.

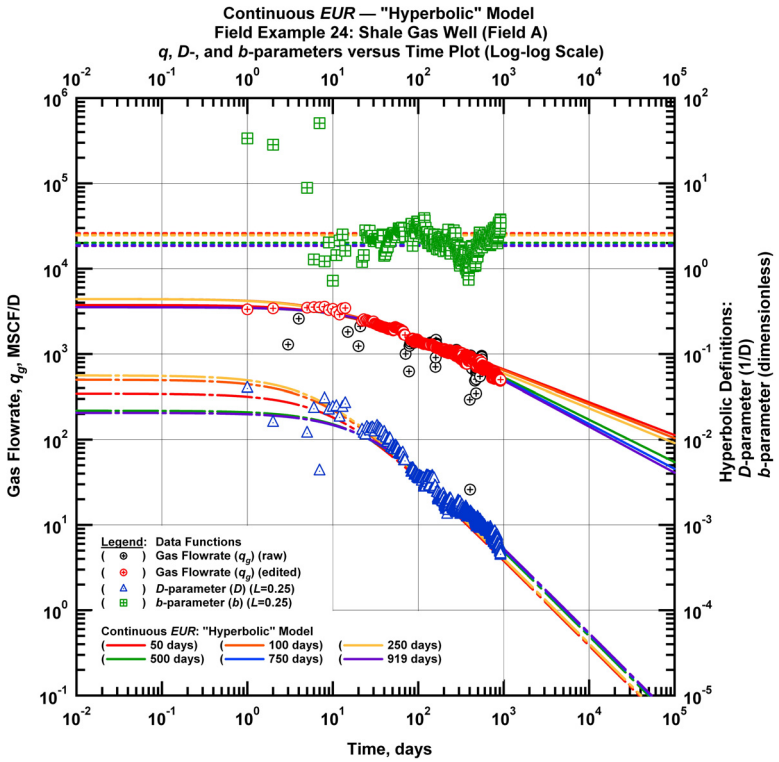

Figure D44 — (Log-log Plot): *qDb* plot — flow rate (q_g), *D*- and *b*-parameters versus production time and "hyperbolic" model matches for field example 24.

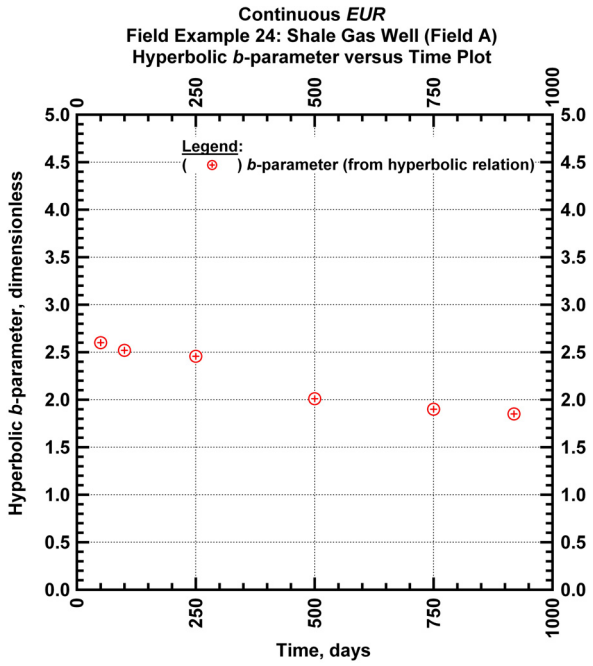

Figure D45 — (Cartesian Plot): Hyperbolic *b*-parameter values obtained from model matches with production data for field example 24.

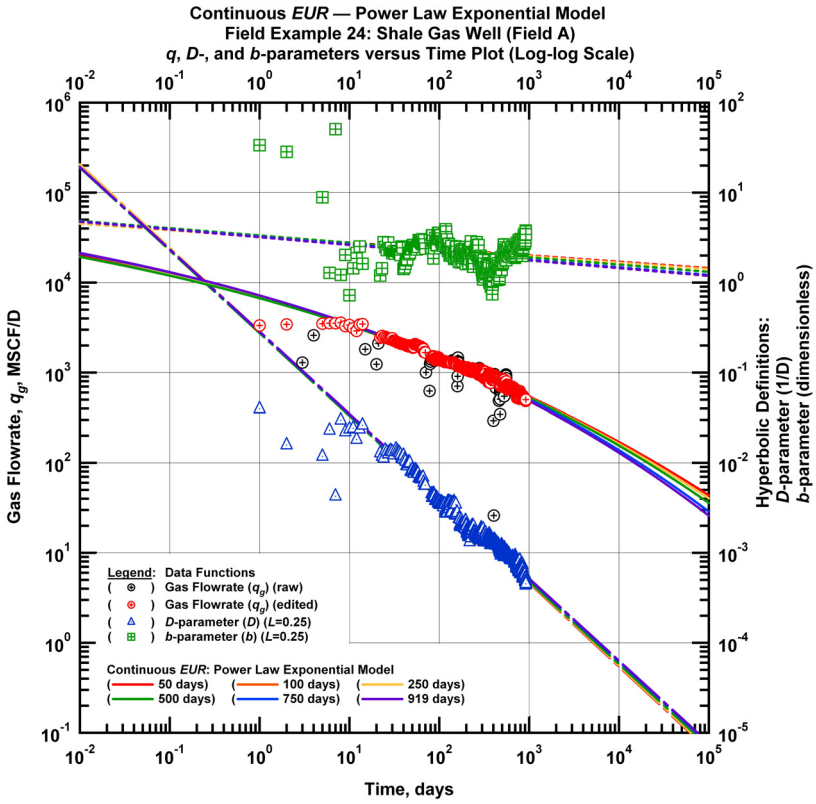

Figure D46 — (Log-log Plot): *qDb* plot — flow rate (q_g), *D*- and *b*-parameters versus production time and power law exponential model matches for field example 24.

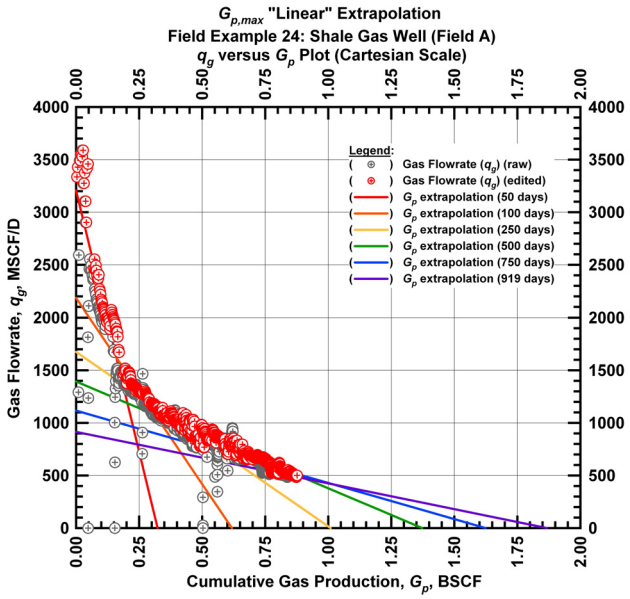

Figure D47 — (Cartesian Plot): Rate Cumulative Plot — flow rate (q_g) versus cumulative production (G_p) and the linear trends fit through the data for field example 24.

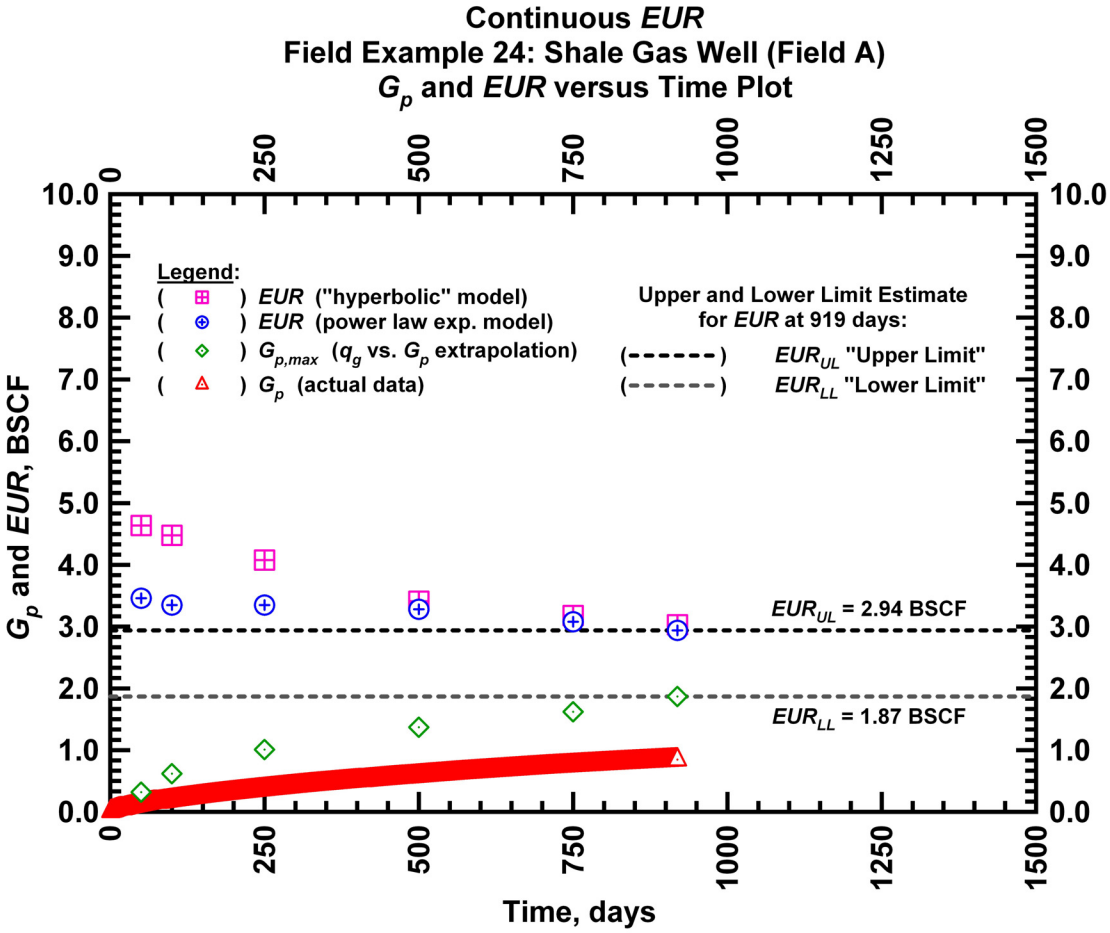

Figure D48 — (Cartesian Plot): *EUR* estimates from model matches and $G_{p,max}$ estimates from extrapolation technique for field example 24.

Table D22 — Analysis results for field example 24 — "hyperbolic" model parameters.

Time Interval, days	q_{gi} (MSCFD)	D_i (D^{-1})	b (dimensionless)	EUR_{hyp} (BSCF)
50	3,746	0.03456	2.600	4.64
100	4,404	0.05000	2.520	4.48
250	4,404	0.05612	2.457	4.08
500	3,531	0.02179	2.010	3.41
750	3,531	0.02057	1.900	3.18
919	3,531	0.02057	1.850	3.03

Table D23 — Analysis results for field example 24 — power-law exponential model parameters.

Time Interval, days	$\hat{q}_{gi}$ (MSCFD)	$\hat{D}_i$ (D^{-1})	n (dimensionless)	D_∞ (D^{-1})	EUR_{PLE} (BSCF)
50	369,460	3.999	0.071	0	3.46
100	369,460	3.983	0.072	0	3.35
250	369,460	3.983	0.072	0	3.35
500	200,000	3.396	0.081	0	3.28
750	200,000	3.326	0.085	0	3.08
919	200,000	3.326	0.086	0	2.94

Table D24 — Analysis results for field example 24 — straight line extrapolation.

Time Interval, days	Slope, 10^{-6} D^{-1}	Intercept, MSCF/D	$G_{p,max}$ (BSCF)
50	9,920	3,206	0.32
100	3,535	2,185	0.62
250	1,659	1,675	1.01
500	1,015	1,394	1.37
750	688	1,117	1.62
919	490	915	1.87

Field Example 25

We present the flow rate data and the cumulative production data which spans almost 1.4 years for a horizontal well producing from a shale gas reservoir in **Fig. D49**. **Fig. D50** presents the "hyperbolic" model matches imposed on the flow rate data along with the *D*- and *b*-parameter trends. In **Fig. D51** we observe that the value of the *b*-parameter as a function of time. The *b*-parameter value decreases from 4.13 to 2.57 during the production history. Every interval is matched with a "hyperbolic" *b*-parameter greater than 1 indicating that boundary-dominated flow has not been established. **Fig. D52** shows the power law exponential model matches imposed on the flow rate data and *D*- and *b*-parameter trends. In **Fig. D53** we show the results of the straight line extrapolation technique, and in **Fig. D54** we present the calculated *EUR* values versus production time. All of the model parameters for this example are presented in **Tables D25, D26, and D27**. The *EUR* of this well should be in between 1.10 BSCF (the "lower" limit given by the straight line extrapolation technique at 504 days) and 2.73 BSCF (the "upper" limit given by the power law exponential estimate at 504 days).

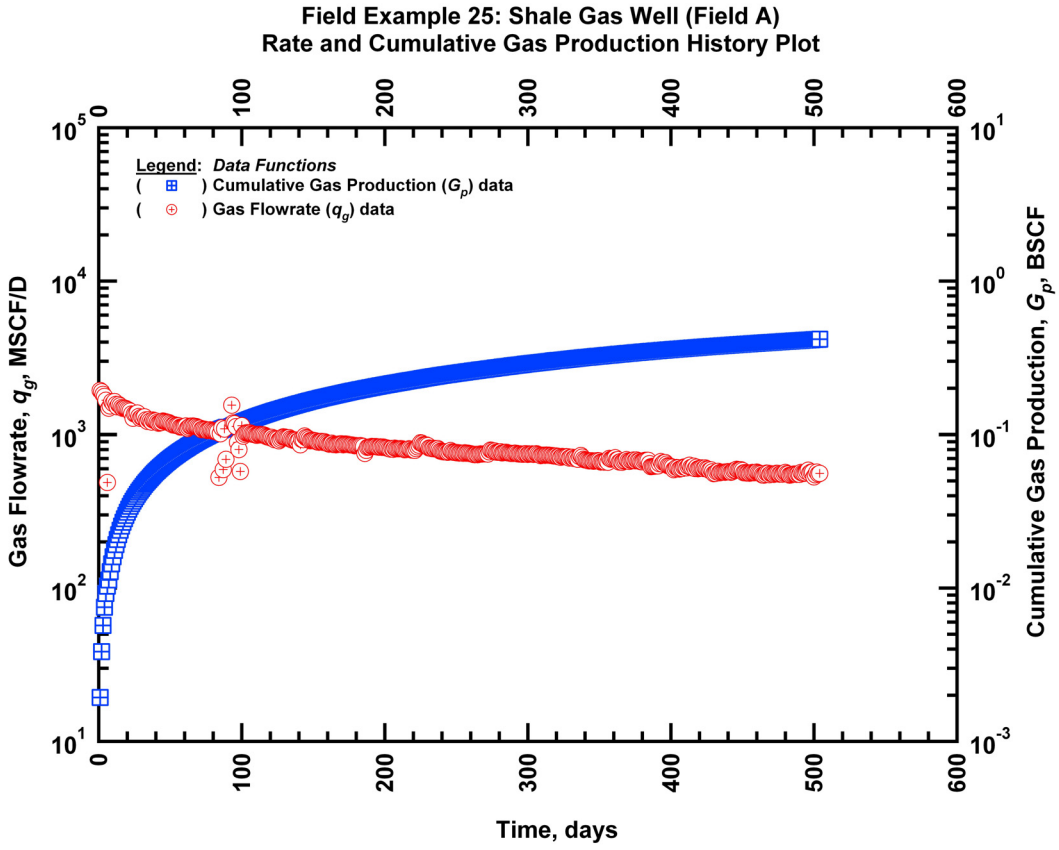

Figure D49 — (Semi-log Plot): Production history plot for field example 25 — flow rate (q_g) and cumulative production (G_p) versus production time.

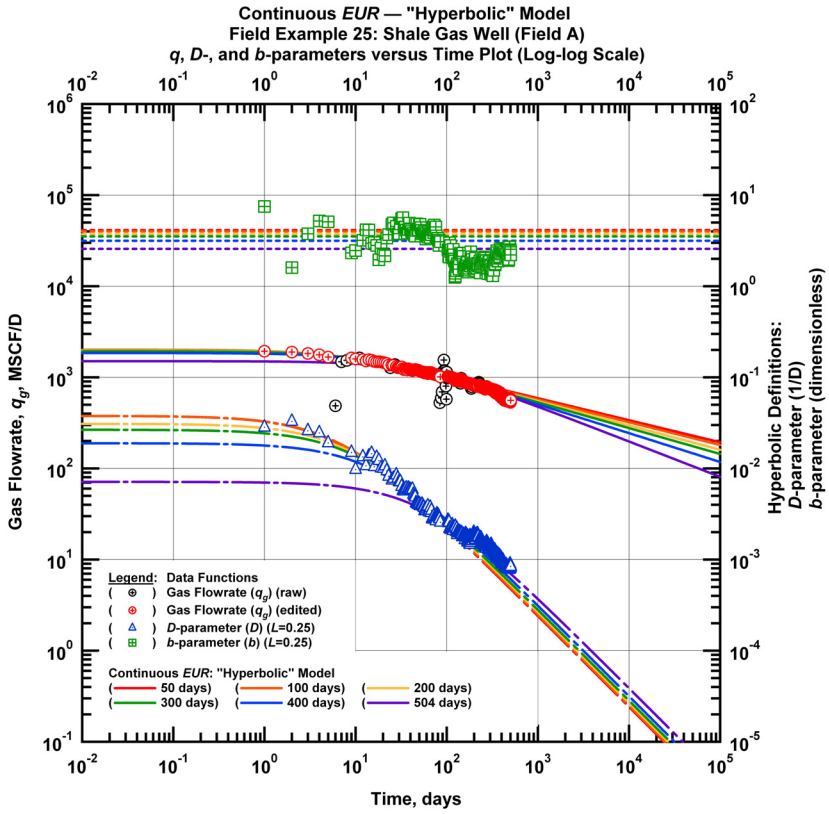

Figure D50 — (Log-log Plot): qDb plot — flow rate (q_g), D- and b-parameters versus production time and "hyperbolic" model matches for field example 25.

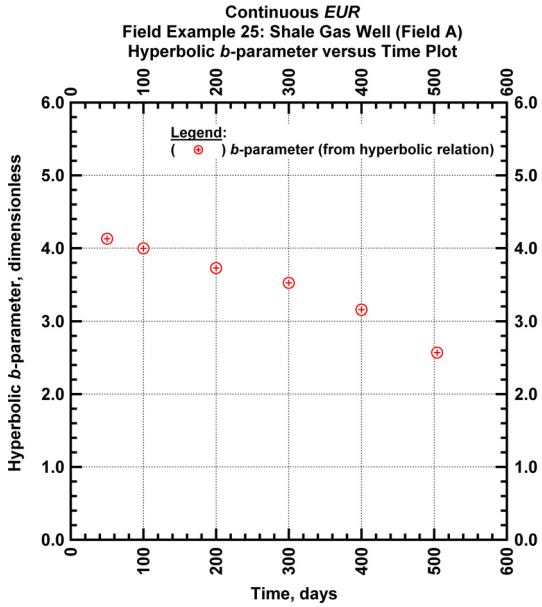

Figure D51 — (Cartesian Plot): Hyperbolic b-parameter values obtained from model matches with production data for field example 25.

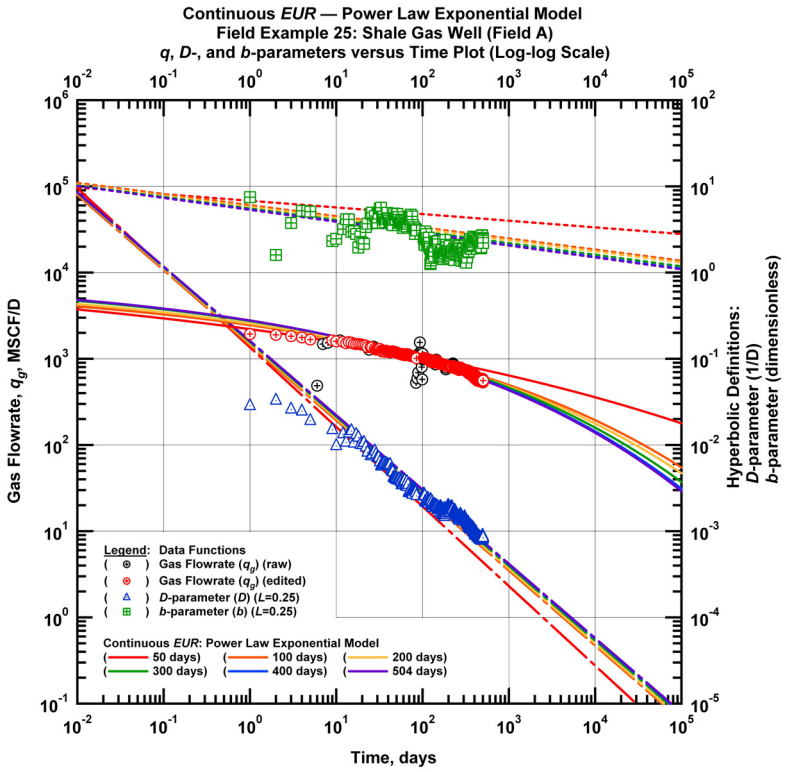

Figure D52 — (Log-log Plot): *qDb* plot — flow rate (q_g), *D*- and *b*-parameters versus production time and power law exponential model matches for field example 25.

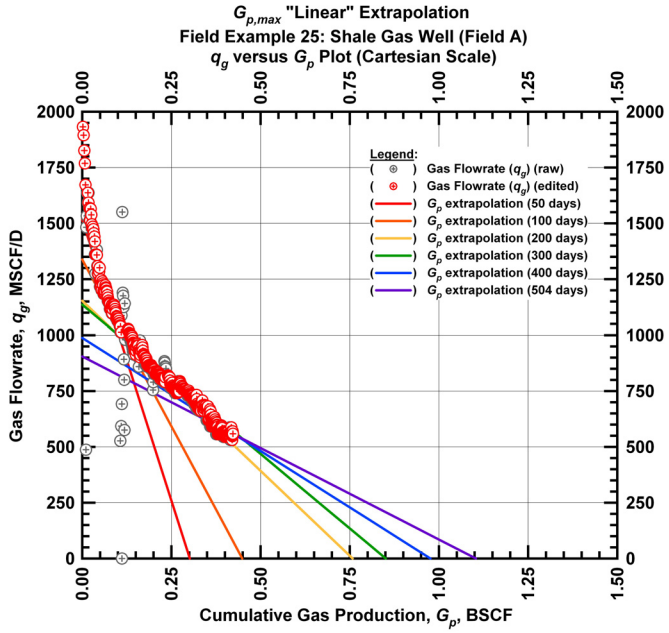

Figure D53 — (Cartesian Plot): Rate Cumulative Plot — flow rate (q_g) versus cumulative production (G_p) and the linear trends fit through the data for field example 25.

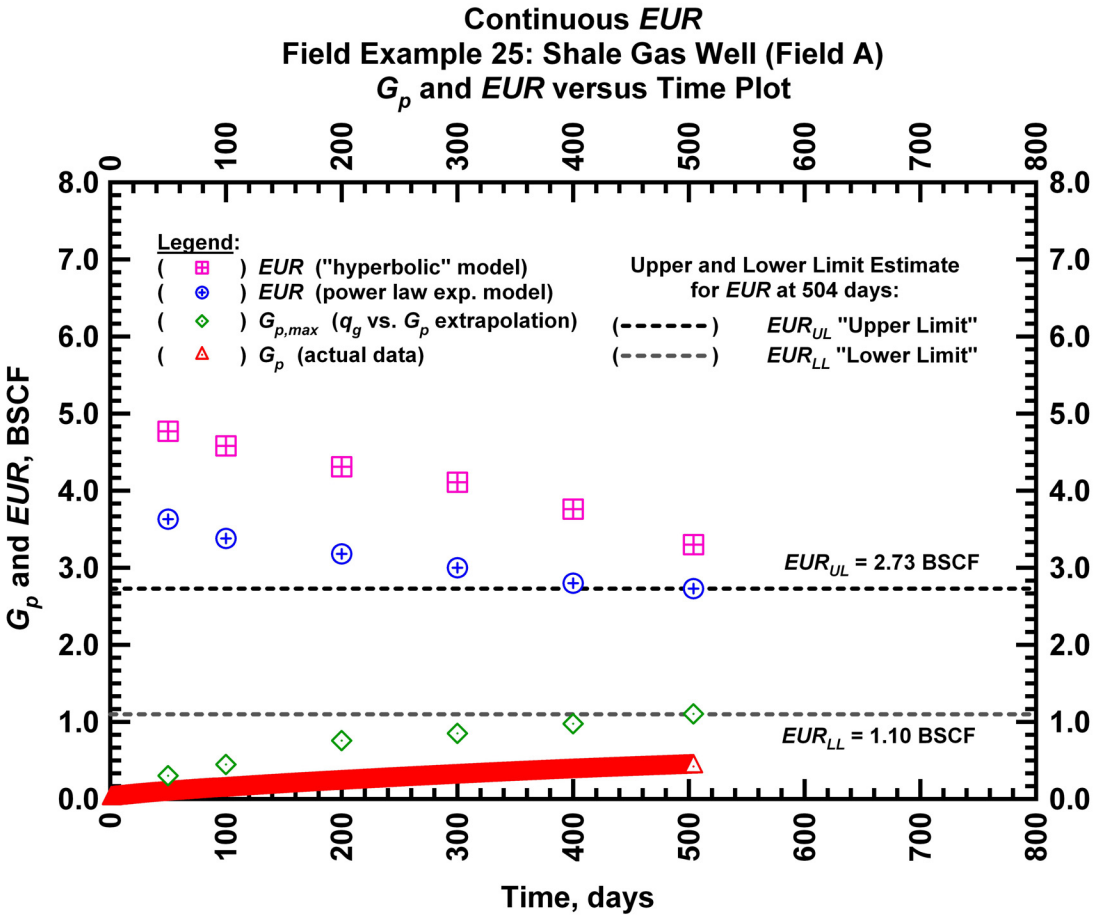

Figure D54 — (Cartesian Plot): *EUR* estimates from model matches and $G_{p,max}$ estimates from extrapolation technique for field example 25.

Table D25 — Analysis results for field example 25 — "hyperbolic" model parameters.

Time Interval, days	q_{gi} (MSCFD)	D_i (D^{-1})	b (dimensionless)	EUR_{hyp} (BSCF)
50	2,007	0.03773	4.130	4.77
100	2,007	0.03773	3.997	4.58
200	1,966	0.03087	3.727	4.31
300	1,934	0.02659	3.523	4.11
400	1,850	0.01890	3.156	3.76
504	1,504	0.00713	2.570	3.30

Table D26 — Analysis results for field example 25 — power-law exponential model parameters.

Time Interval, days	$\hat{q}_{gi}$ (MSCFD)	$\hat{D}_i$ (D^{-1})	n (dimensionless)	D_∞ (D^{-1})	EUR_{PLE} (BSCF)
50	12,826	1.7600	0.077	0	3.63
100	7,480	1.1132	0.129	0	3.38
200	8,240	1.1701	0.129	0	3.18
300	8,830	1.1695	0.134	0	3.00
400	8,953	1.1695	0.137	0	2.80
504	8,953	1.1695	0.138	0	2.73

Table D27 — Analysis results for field example 25 — straight line extrapolation.

Time Interval, days	Slope, 10^{-6} D^{-1}	Intercept, MSCF/D	$G_{p,max}$ (BSCF)
50	5,031	1,517	0.30
100	2,982	1,338	0.45
200	1,521	1,153	0.76
300	1,335	1,136	0.85
400	1,012	988	0.98
504	820	905	1.10

Field Example 26

We present the flow rate data and the cumulative production data which spans almost 1.4 years for a horizontal well producing from a shale gas reservoir in **Fig. D55**. **Fig. D56** presents the "hyperbolic" model matches imposed on the flow rate data along with the *D*- and *b*-parameter trends. In **Fig. D57** we observe that the value of the *b*-parameter as a function of time. The *b*-parameter value decreases from 4.86 to 2.01 during the production history. Every interval is matched with a "hyperbolic" *b*-parameter greater than 1 indicating that boundary-dominated flow has not been established. **Fig. D58** shows the power law exponential model matches imposed on the flow rate data and *D*- and *b*-parameter trends. In **Fig. D59** we show the results of the straight line extrapolation technique, and in **Fig. D60** we present the calculated *EUR* values versus production time. All of the model parameters for this example are presented in **Tables D28, D29, and D30**. The *EUR* of this well should be in between 1.06 BSCF (the "lower" limit given by the straight line extrapolation technique at 502 days) and 2.60 BSCF (the "upper" limit given by the power law exponential estimate at 502 days).

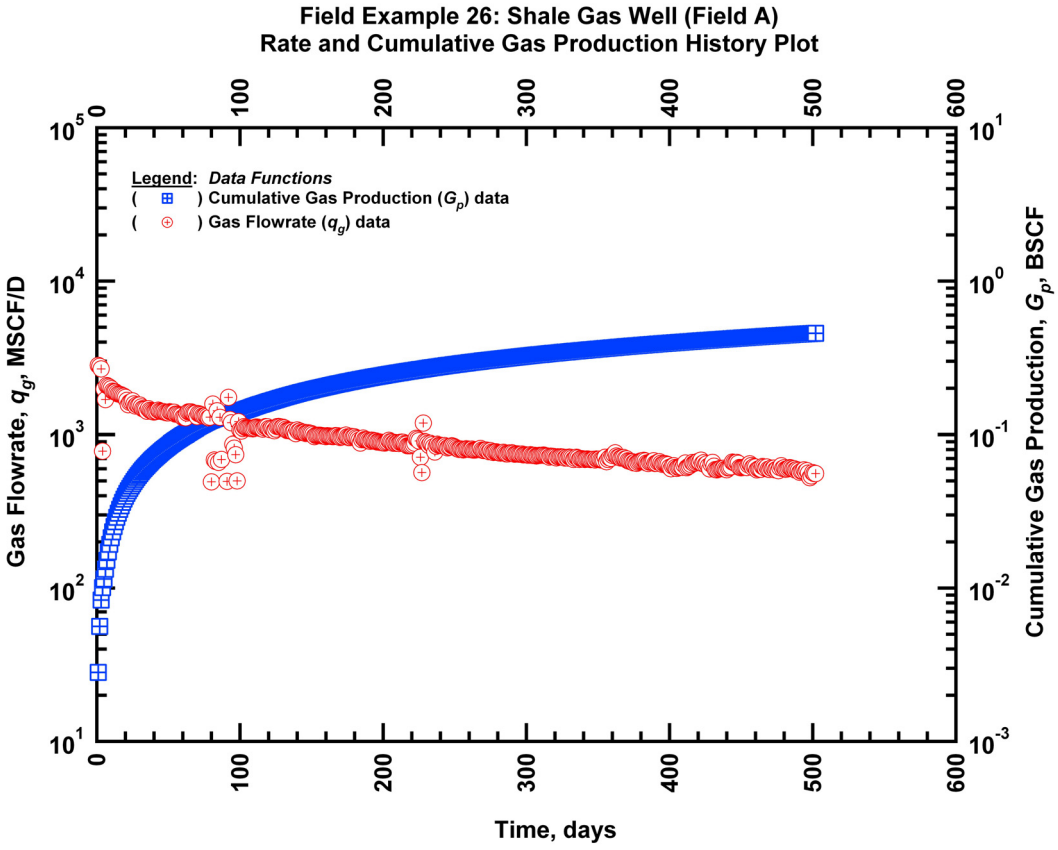

Figure D55 — (Semi-log Plot): Production history plot for field example 26 — flow rate (q_g) and cumulative production (G_p) versus production time.

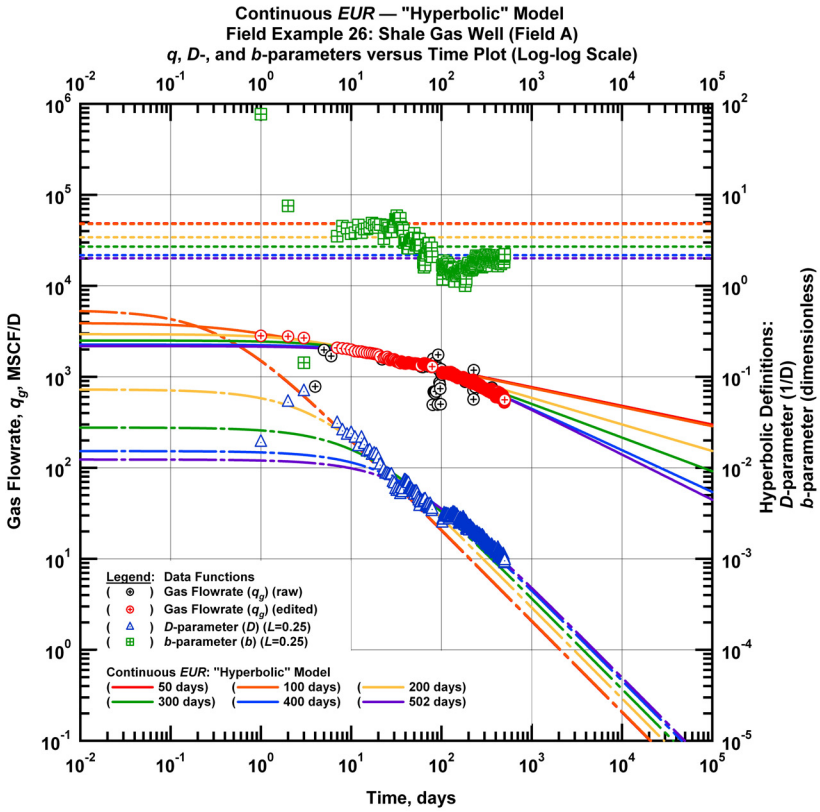

Figure D56 — (Log-log Plot): *qDb* plot — flow rate (q_g), *D*- and *b*-parameters versus production time and "hyperbolic" model matches for field example 26.

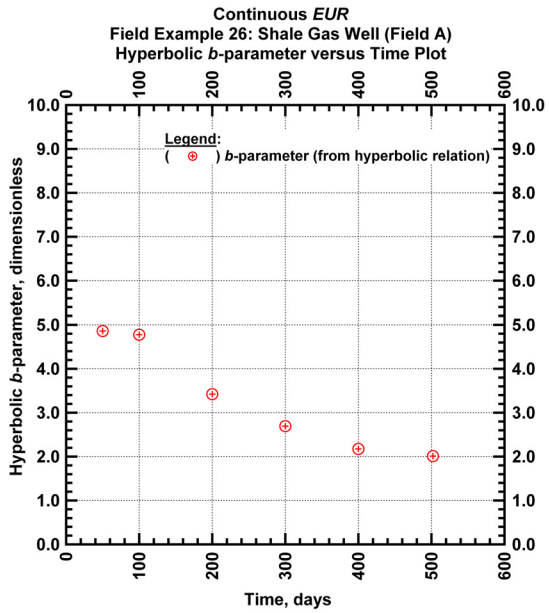

Figure D57 — (Cartesian Plot): Hyperbolic *b*-parameter values obtained from model matches with production data for field example 26.

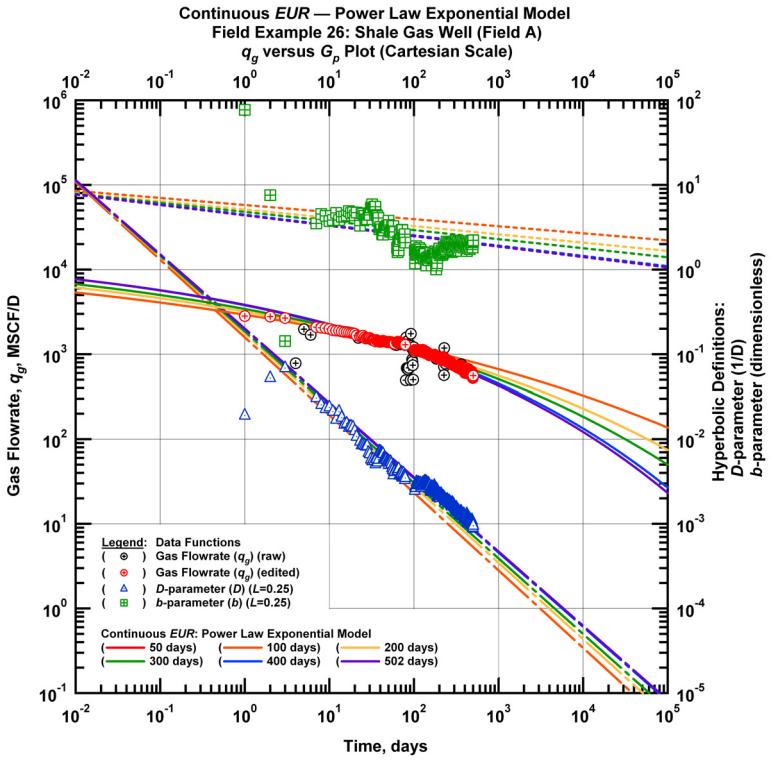

Figure D58 — (Log-log Plot): *qDb* plot — flow rate (q_g), *D*- and *b*-parameters versus production time and power law exponential model matches for field example 26.

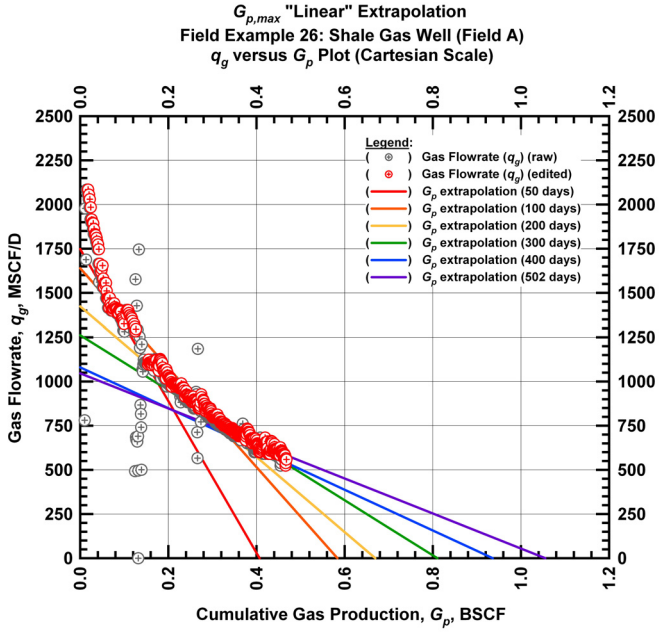

Figure D59 — (Cartesian Plot): Rate Cumulative Plot — flow rate (q_g) versus cumulative production (G_p) and the linear trends fit through the data for field example 26.

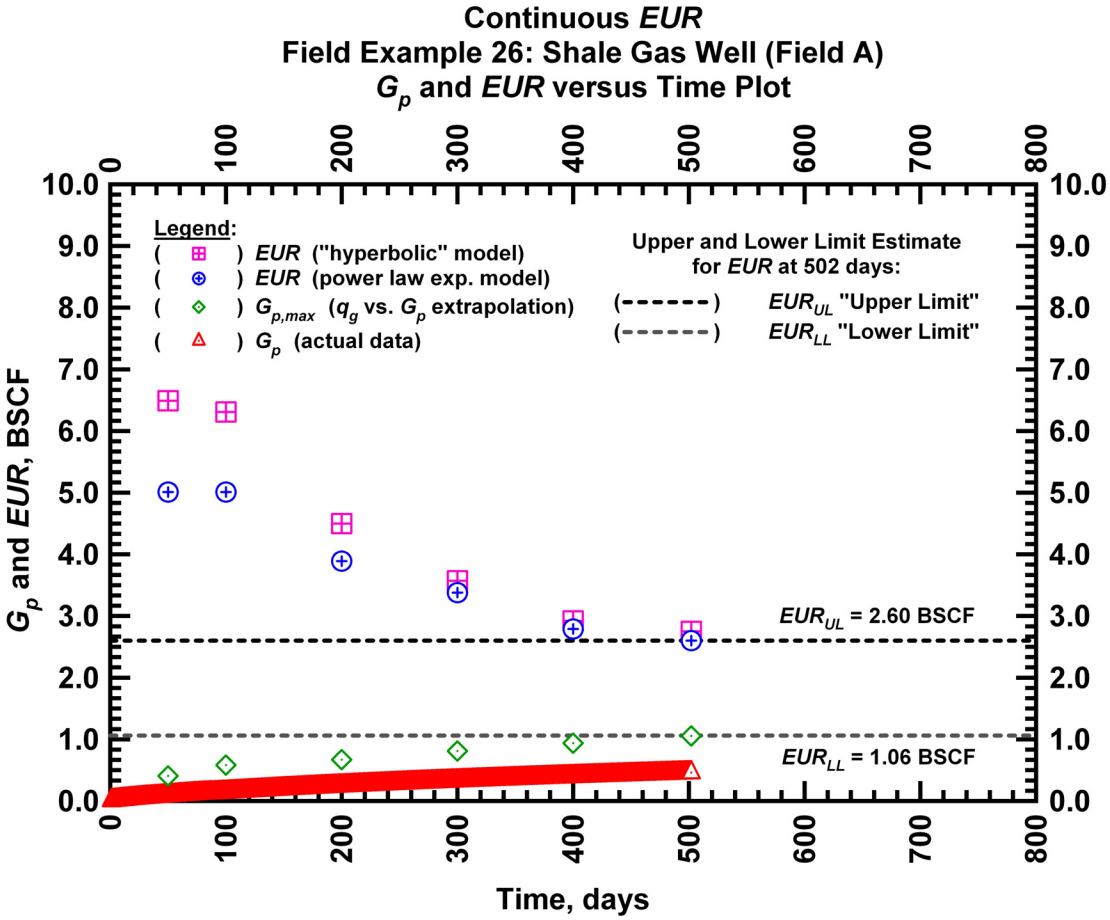

Figure D60 — (Cartesian Plot): *EUR* estimates from model matches and $G_{p,max}$ estimates from extrapolation technique for field example 26.

Table D28 — Analysis results for field example 26 — "hyperbolic" model parameters.

Time Interval, days	q_{gi} (MSCFD)	D_i (D^{-1})	b (dimensionless)	EUR_{hyp} (BSCF)
50	3,899	0.542519	4.860	6.49
100	3,899	0.542519	4.777	6.31
200	2,942	0.072588	3.423	4.50
300	2,507	0.027685	2.694	3.57
400	2,260	0.015262	2.175	2.92
502	2,175	0.012321	2.010	2.75

Table D29 — Analysis results for field example 26 — power-law exponential model parameters.

Time Interval, days	$\hat{q}_{gi}$ (MSCFD)	$\hat{D}_i$ (D^{-1})	n (dimensionless)	D_∞ (D^{-1})	EUR_{PLE} (BSCF)
50	19,422	1.893	0.0836	0	5.01
100	19,422	1.893	0.0836	0	5.01
200	19,422	1.806	0.0977	0	3.89
300	19,422	1.737	0.1072	0	3.38
400	19,422	1.623	0.1217	0	2.79
502	19,422	1.634	0.1230	0	2.60

Table D30 — Analysis results for field example 26 — straight line extrapolation.

Time Interval, days	Slope, 10^{-6} D^{-1}	Intercept, MSCF/D	$G_{p,max}$ (BSCF)
50	4,295	1,748	0.41
100	2,808	1,639	0.58
200	2,125	1,423	0.67
300	1,557	1,262	0.81
400	1,154	1,080	0.94
502	991	1,046	1.06

APPENDIX E
EXAMPLES FROM FIELD B

Field Example 27

We present the flow rate data and the cumulative production data which spans almost 1 year for a horizontal well producing from a shale gas reservoir in **Fig. E1**. **Fig. E2** presents the "hyperbolic" model matches imposed on the flow rate data along with the *D*- and *b*-parameter trends. In **Fig. E3** we observe that the value of the *b*-parameter as a function of time. The *b*-parameter value decreases from 1.66 to 1.53 during the production history. Every interval is matched with a "hyperbolic" *b*-parameter greater than 1 indicating that boundary-dominated flow has not been established. **Fig. E4** shows the power law exponential model matches imposed on the flow rate data and *D*- and *b*-parameter trends. In **Fig. E5** we show the results of the straight line extrapolation technique, and in **Fig. E6** we present the calculated *EUR* values versus production time. All of the model parameters for this example are presented in **Tables E1, E2, and E3**. The *EUR* of this well should be in between 0.94 BSCF (the "lower" limit given by the straight line extrapolation technique at 301 days) and 1.80 BSCF (the "upper" limit given by the power law exponential estimate at 301 days).

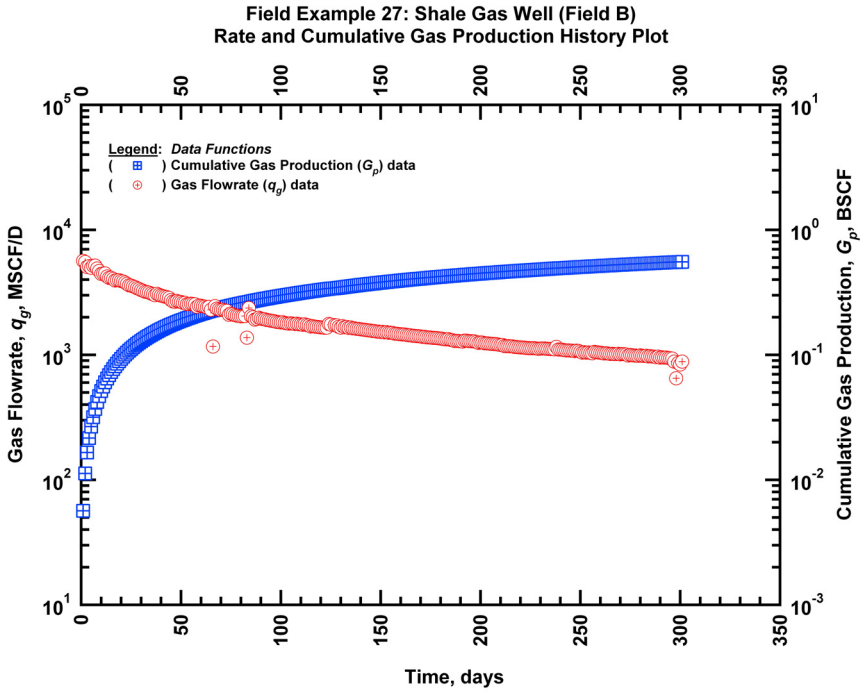

Figure E1 — (Semi-log Plot): Production history plot for field example 27 — flow rate (q_g) and cumulative production (G_p) versus production time.

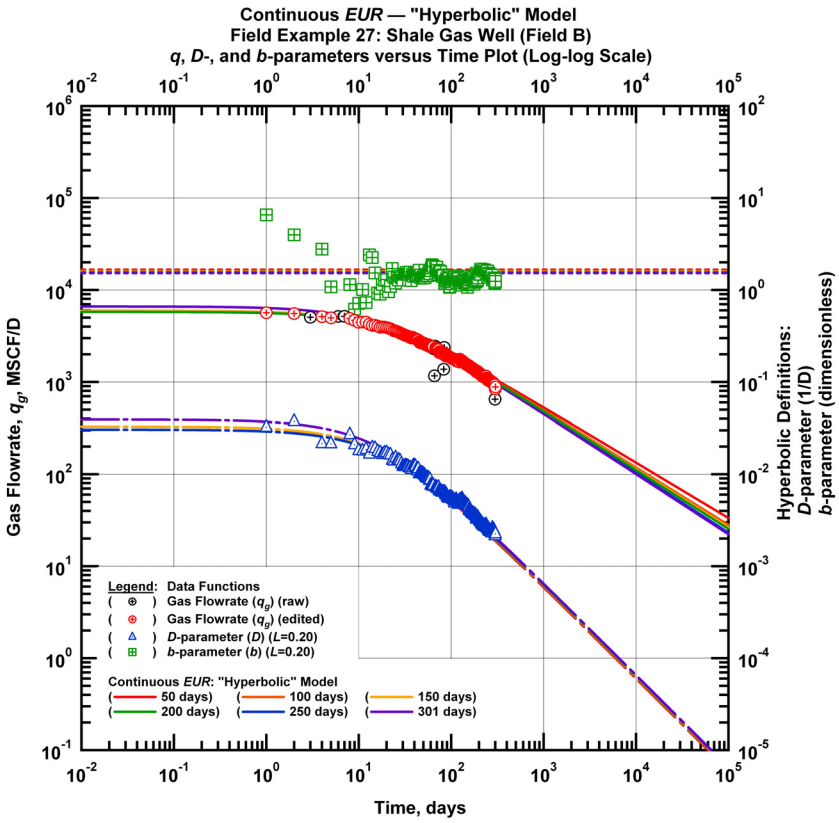

Figure E2 — (Log-log Plot): *qDb* plot — flow rate (q_g), *D*- and *b*-parameters versus production time and "hyperbolic" model matches for field example 27.

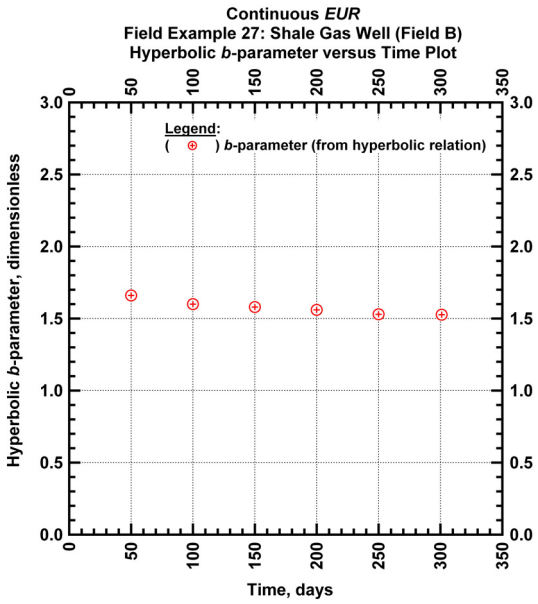

Figure E3 — (Cartesian Plot): Hyperbolic *b*-parameter values obtained from model matches with production data for field example 27.

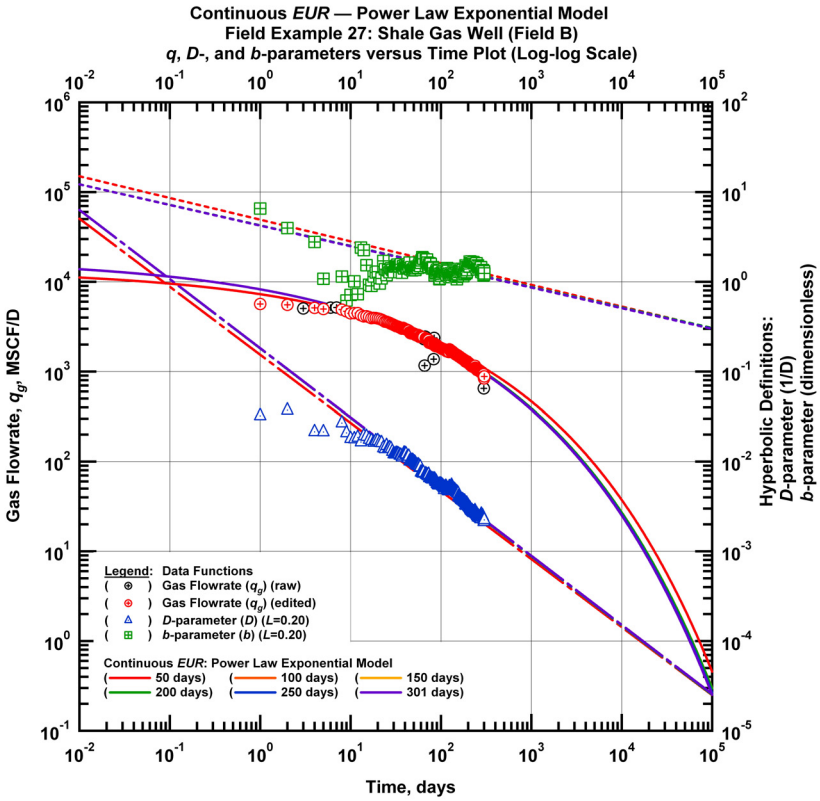

Figure E4 — (Log-log Plot): *qDb* plot — flow rate (q_g), *D*- and *b*-parameters versus production time and power law exponential model matches for field example 27.

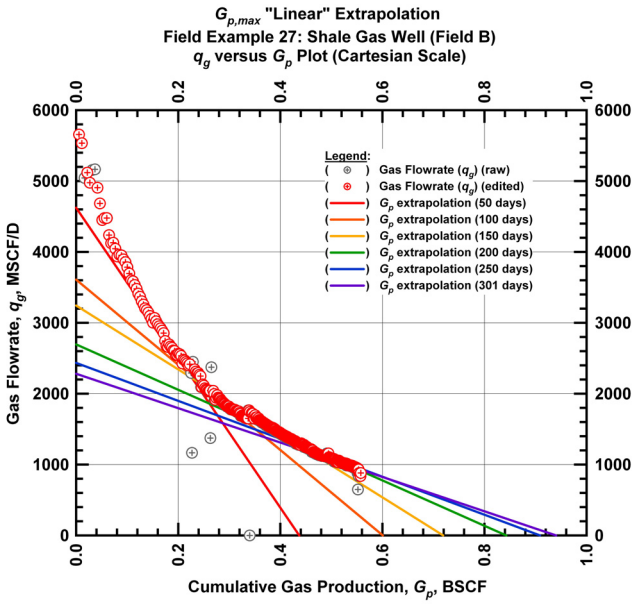

Figure E5 — (Cartesian Plot): Rate Cumulative Plot — flow rate (q_g) versus cumulative production (G_p) and the linear trends fit through the data for field example 27.

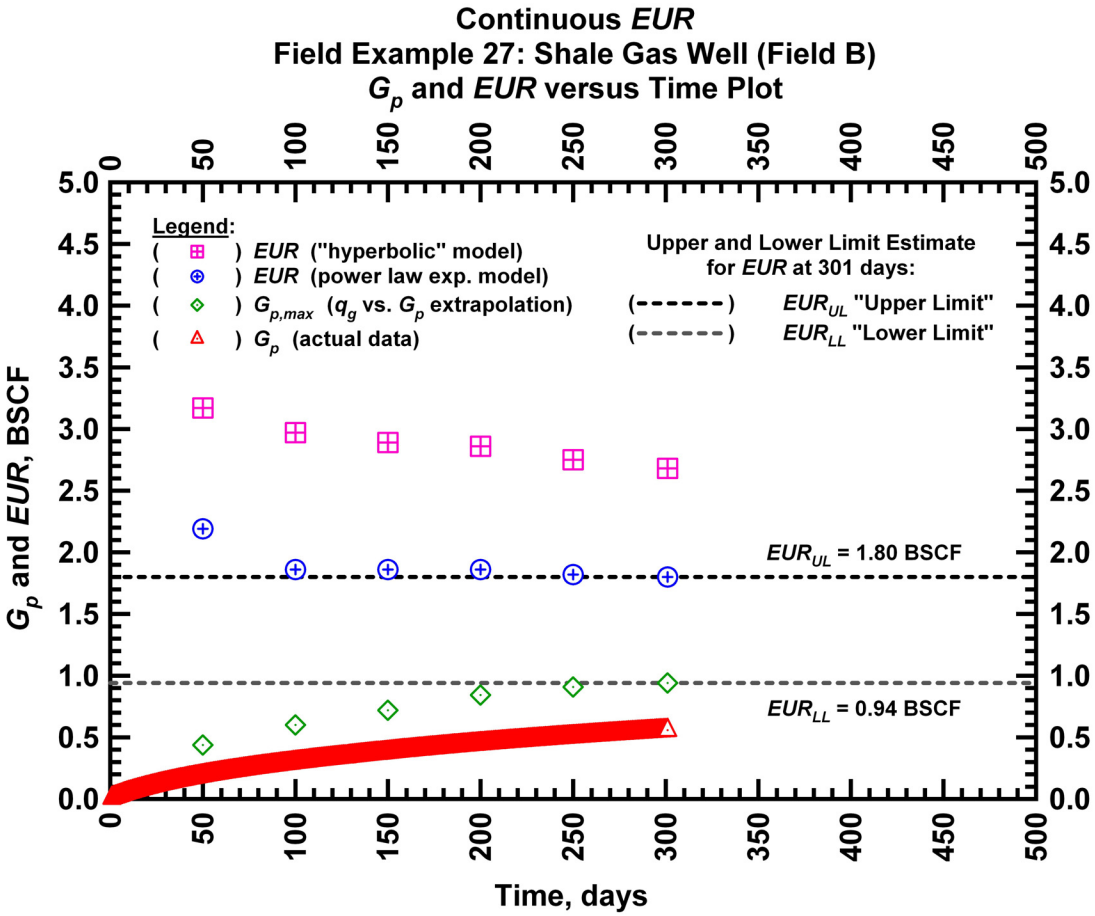

Figure E6 — (Cartesian Plot): *EUR* estimates from model matches and $G_{p,max}$ estimates from extrapolation technique for field example 27.

Table E1 — Analysis results for field example 27 — "hyperbolic" model parameters.

Time Interval, days	q_{gi} (MSCFD)	D_i (D^{-1})	b (dimensionless)	EUR_{hyp} (BSCF)
50	5,951	0.032861	1.660	3.17
100	5,951	0.032861	1.600	2.97
150	5,951	0.032861	1.579	2.89
200	5,777	0.030443	1.560	2.86
250	5,777	0.030443	1.530	2.75
301	6,610	0.039146	1.527	2.68

Table E2 — Analysis results for field example 27 — power lawexponential model parameters.

Time Interval, days	$\hat{q}_{gi}$ (MSCFD)	$\hat{D}_i$ (D^{-1})	n (dimensionless)	D_∞ (D^{-1})	EUR_{PLE} (BSCF)
50	13,745	0.6359	0.2420	0	2.19
100	18,200	0.7918	0.2287	0	1.86
150	18,200	0.7918	0.2287	0	1.86
200	18,200	0.7917	0.2288	0	1.86
250	18,200	0.7919	0.2296	0	1.82
301	18,200	0.7920	0.2300	0	1.80

Table E3 — Analysis results for field example 27 — straight line extrapolation.

Time Interval, days	Slope, 10^{-6} D^{-1}	Intercept, MSCF/D	Gp,max (BSCF)
50	10,580	4,624	0.44
100	6,008	3,609	0.60
150	4,512	3,244	0.72
200	3,198	2,695	0.84
250	2,679	2,435	0.91
301	2,426	2,281	0.94

Field Example 28

We present the flow rate data and the cumulative production data which spans almost 1 year for a horizontal well producing from a shale gas reservoir in **Fig. E7**. **Fig. E8** presents the "hyperbolic" model matches imposed on the flow rate data along with the *D*- and *b*-parameter trends. In **Fig. E9** we observe that the value of the *b*-parameter as a function of time. The *b*-parameter value decreases from 4.45 to 1.19 during the production history. Every interval is matched with a "hyperbolic" *b*-parameter greater than 1 indicating that boundary-dominated flow has not been established. **Fig. E10** shows the power law exponential model matches imposed on the flow rate data and *D*- and *b*-parameter trends. In **Fig. E11** we show the results of the straight line extrapolation technique, and in **Fig. E12** we present the calculated *EUR* values versus production time. All of the model parameters for this example are presented in **Tables E4, E5, and E6**. The *EUR* of this well should be in between 1.24 BSCF (the "lower" limit given by the straight line extrapolation technique at 313 days) and 2.02 BSCF (the "upper" limit given by the power law exponential estimate at 313 days).

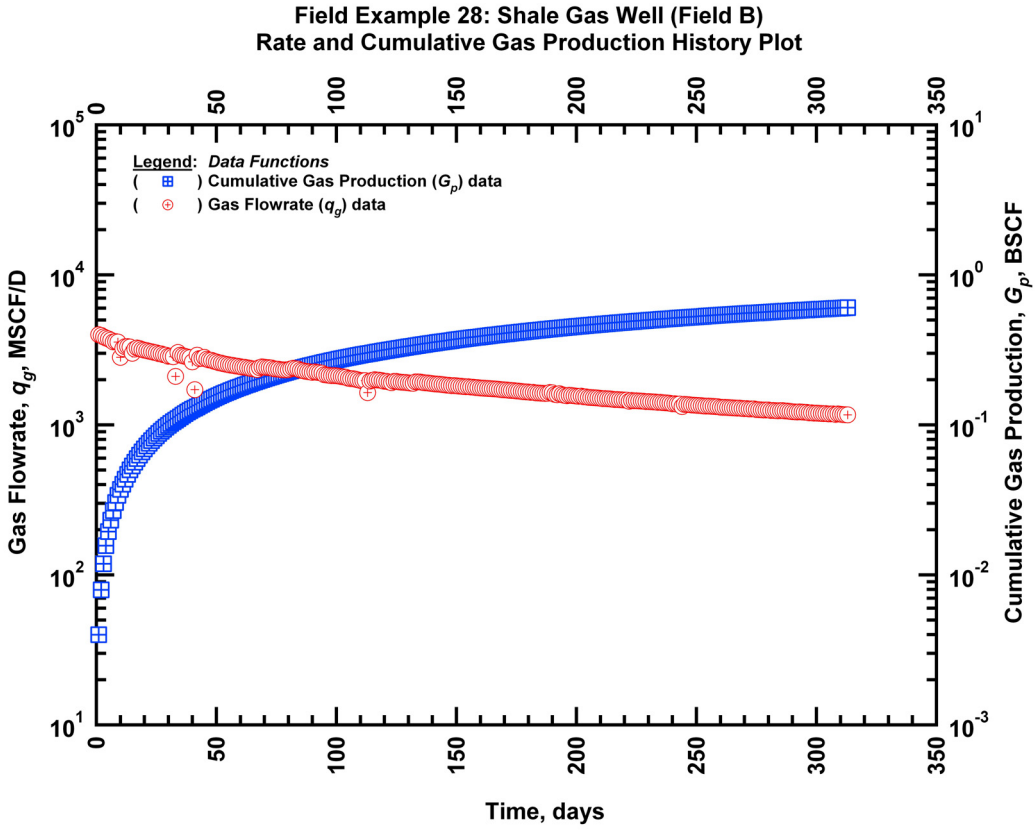

Figure E7 — (Semi-log Plot): Production history plot for field example 28 — flow rate (q_g) and cumulative production (G_p) versus production time.

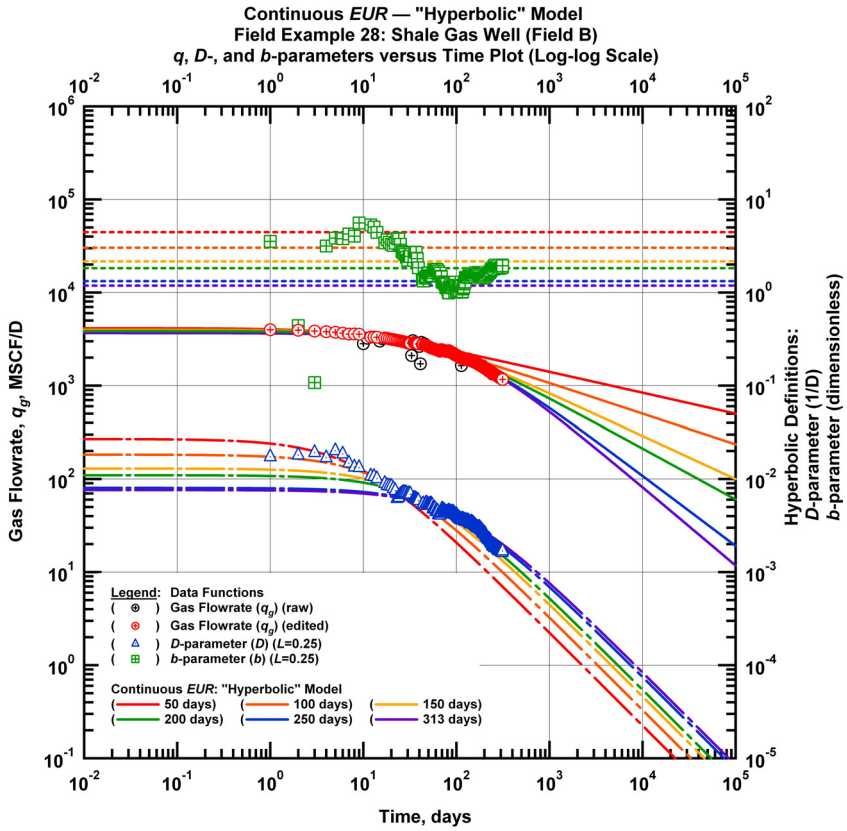

Figure E8 — (Log-log Plot): *qDb* plot — flow rate (q_g), *D*- and *b*-parameters versus production time and "hyperbolic" model matches for field example 28.

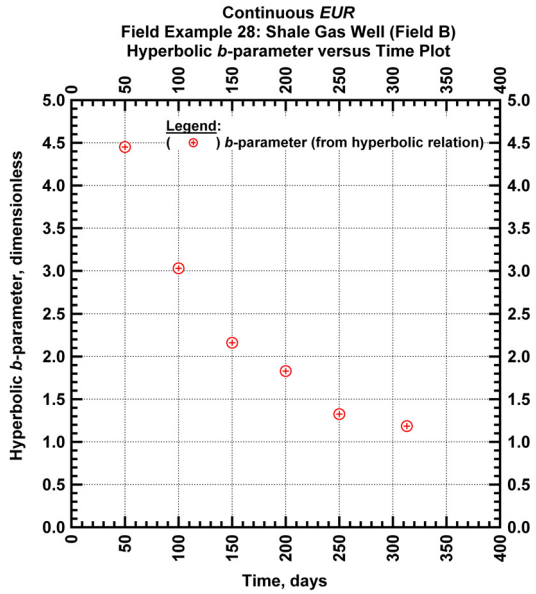

Figure E9 — (Cartesian Plot): Hyperbolic *b*-parameter values obtained from model matches with production data for field example 28.

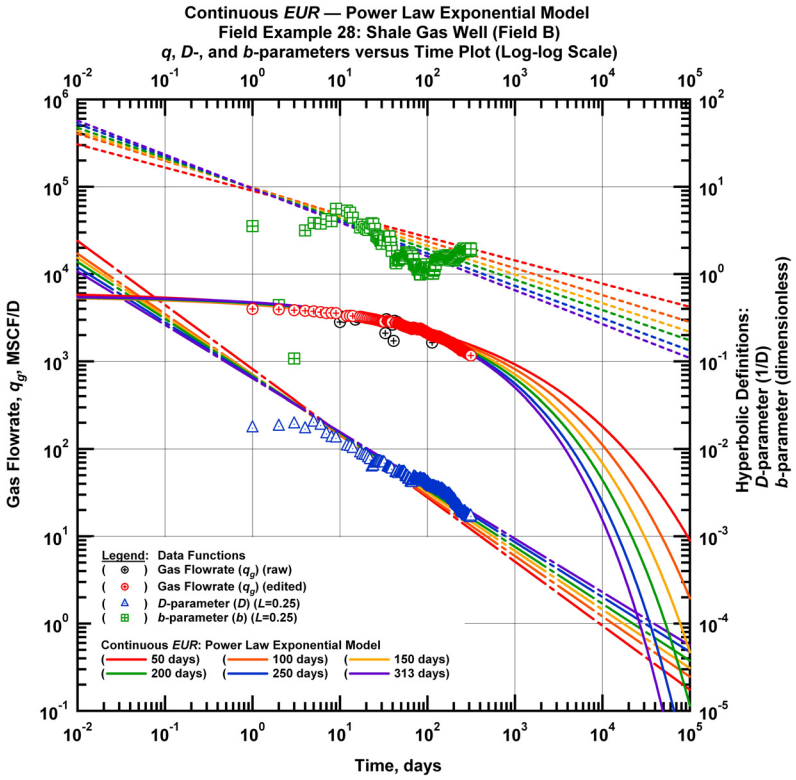

Figure E10 — (Log-log Plot): *qDb* plot — flow rate (q_g), *D*- and *b*-parameters versus production time and power law exponential model matches for field example 28.

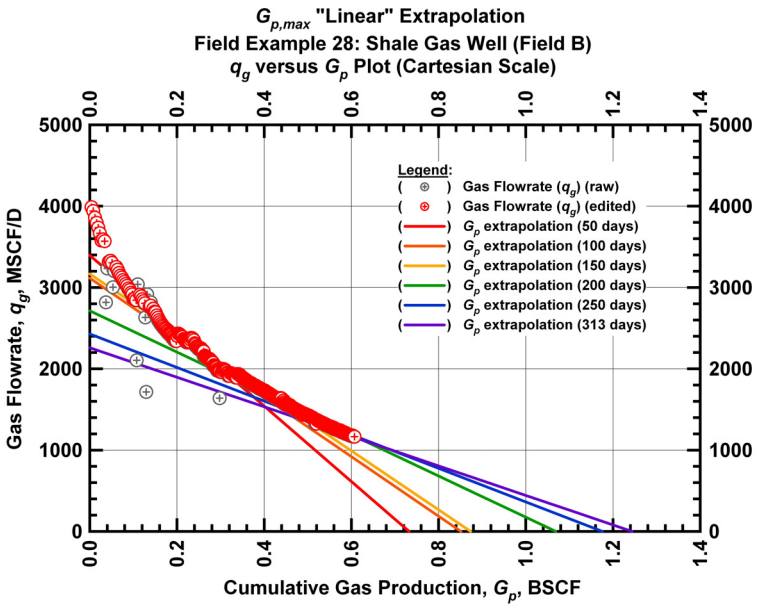

Figure E11 — (Cartesian Plot): Rate Cumulative Plot — flow rate (q_g) versus cumulative production (G_p) and the linear trends fit through the data for field example 28.

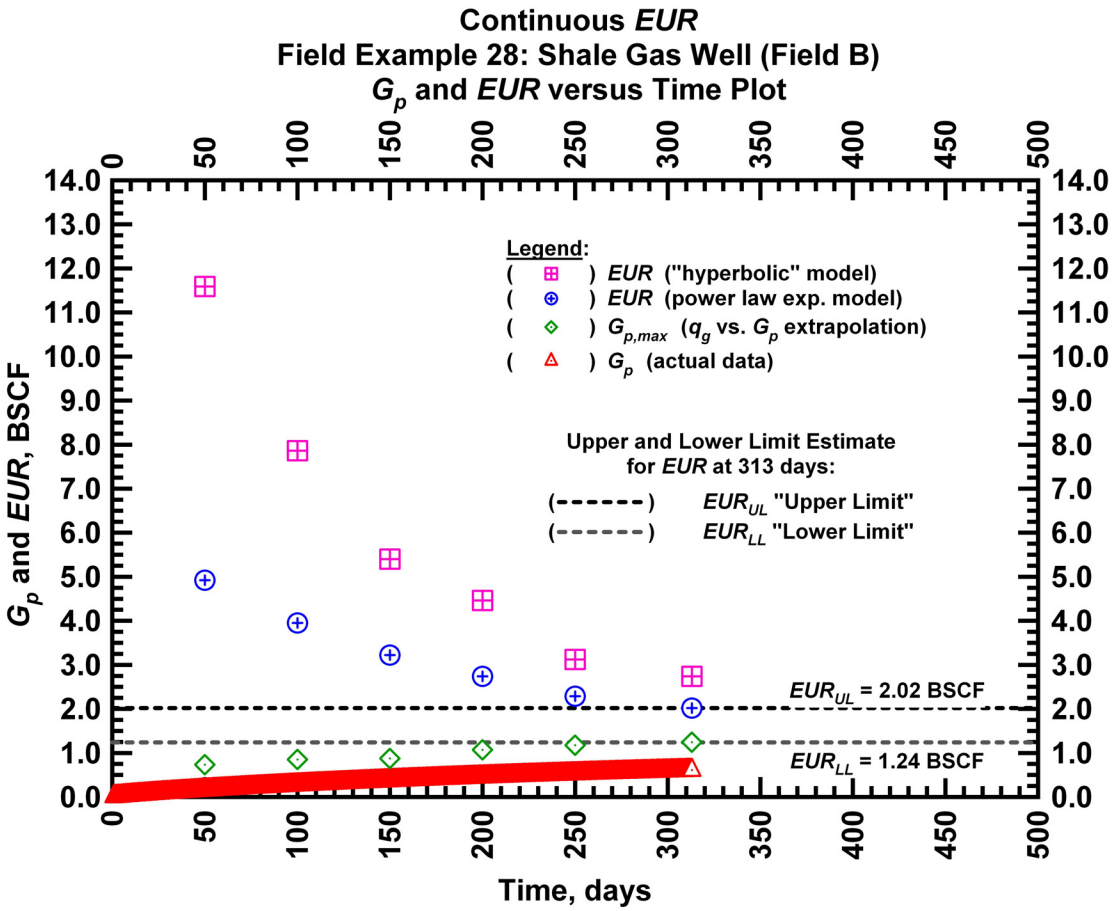

Figure E12 — (Cartesian Plot): *EUR* estimates from model matches and $G_{p,max}$ estimates from extrapolation technique for field example 28.

Table E4 — Analysis results for field example 28 — "hyperbolic" model parameters.

Time Interval, days	q_{gi} (MSCFD)	D_i (D^{-1})	b (dimensionless)	EUR_{hyp} (BSCF)
50	4,131	0.026888	4.4509	11.59
100	4,038	0.018284	3.0297	7.86
150	3,922	0.012959	2.1619	5.40
200	3,852	0.010986	1.8292	4.46
250	3,669	0.008028	1.3260	3.12
313	3,669	0.007614	1.1851	2.74

Table E5 — Analysis results for field example 28 — power lawexponential model parameters.

Time Interval, days	$\hat{q}_{gi}$ (MSCFD)	$\hat{D}_i$ (D^{-1})	n (dimensionless)	D_∞ (D^{-1})	EUR_{PLE} (BSCF)
50	6,336	0.3069	0.2660	0	4.92
100	5,594	0.2297	0.3080	0	3.95
150	5,594	0.2130	0.3288	0	3.22
200	5,594	0.1964	0.3480	0	2.74
250	5,594	0.1778	0.3712	0	2.29
313	5,594	0.1649	0.3884	0	2.02

Table E6 — Analysis results for field example 28 — straight line extrapolation.

Time Interval, days	Slope, 10^{-6} D^{-1}	Intercept, MSCF/D	Gp,max (BSCF)
50	4,635	3,395	0.73
100	3,659	3,115	0.85
150	3,626	3,167	0.87
200	2,538	2,713	1.07
250	2,066	2,429	1.18
313	1,816	2,259	1.24

Field Example 29

We present the flow rate data and the cumulative production data which spans almost 0.75 years for a horizontal well producing from a shale gas reservoir in **Fig. E13**. **Fig. E14** presents the "hyperbolic" model matches imposed on the flow rate data along with the *D*- and *b*-parameter trends. In **Fig. E15** we observe that the value of the *b*-parameter as a function of time. The *b*-parameter value decreases to 1.35 during the production history. Every interval is matched with a "hyperbolic" *b*-parameter greater than 1 indicating that boundary-dominated flow has not been established. **Fig. E16** shows the power law exponential model matches imposed on the flow rate data and *D*- and *b*-parameter trends. In **Fig. E17** we show the results of the straight line extrapolation technique, and in **Fig. E18** we present the calculated *EUR* values versus production time. All of the model parameters for this example are presented in **Tables E7, E8, and E9**. The *EUR* of this well should be in between 1.86 BSCF (the "lower" limit given by the straight line extrapolation technique at 272 days) and 2.56 BSCF (the "upper" limit given by the power law exponential estimate at 272 days).

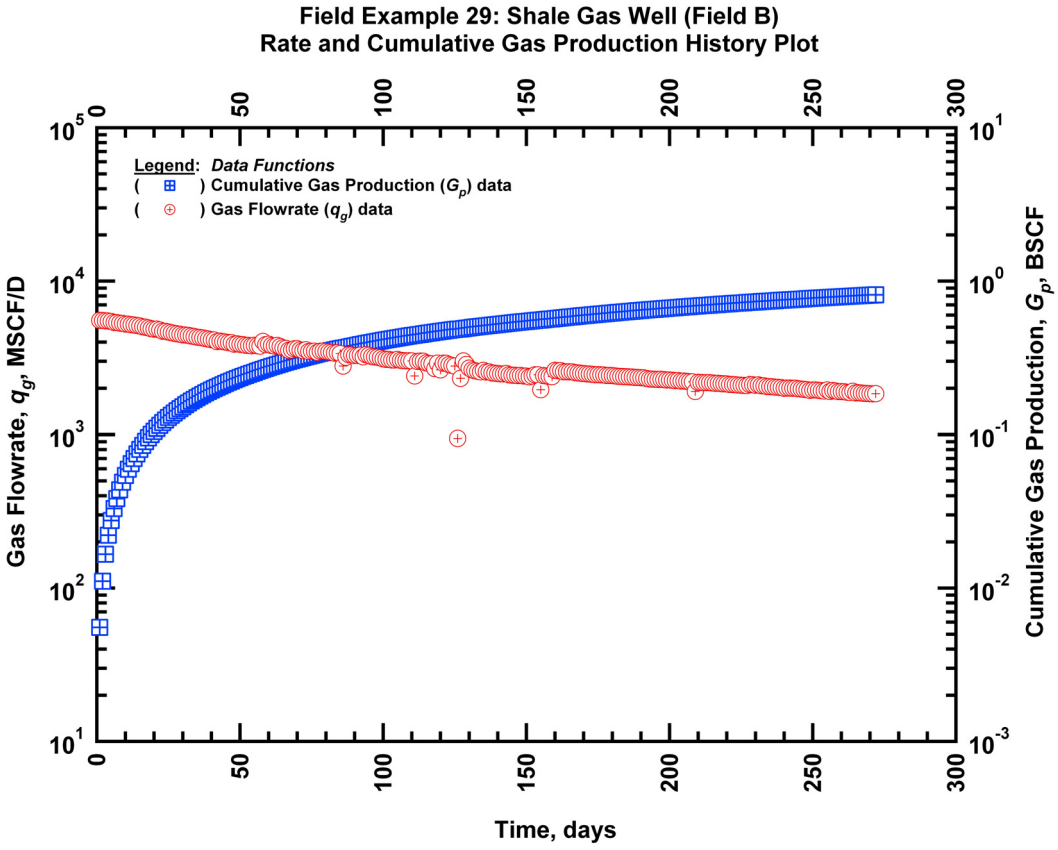

Figure E13 — (Semi-log Plot): Production history plot for field example 29 — flow rate (q_g) and cumulative production (G_p) versus production time.

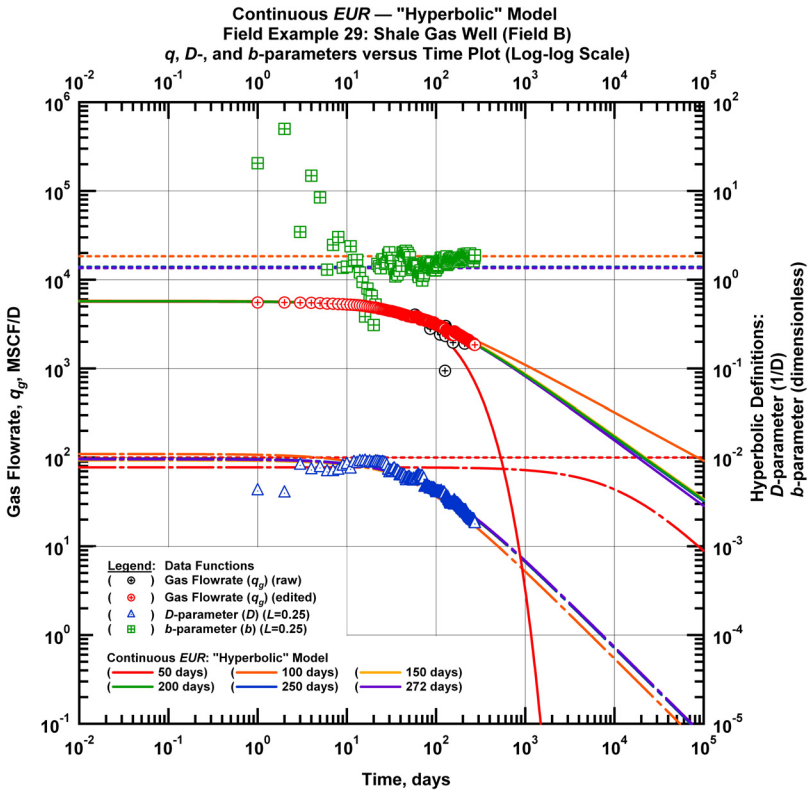

Figure E14 — (Log-log Plot): *qDb* plot — flow rate (q_g), *D*- and *b*-parameters versus production time and "hyperbolic" model matches for field example 29.

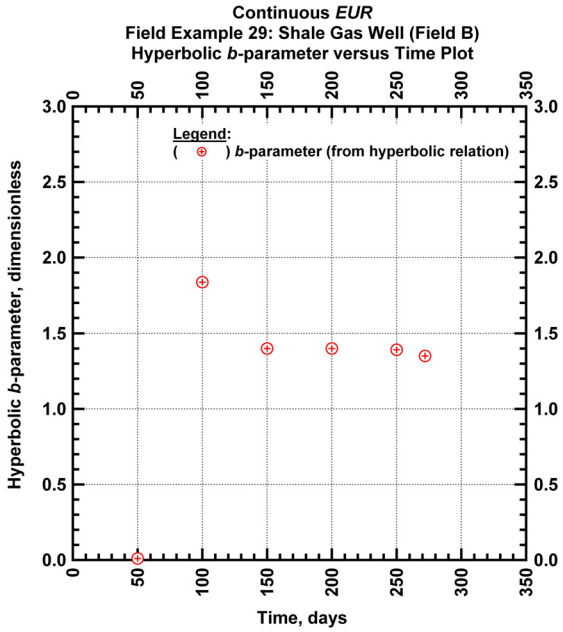

Figure E15 — (Cartesian Plot): Hyperbolic *b*-parameter values obtained from model matches with production data for field example 29.

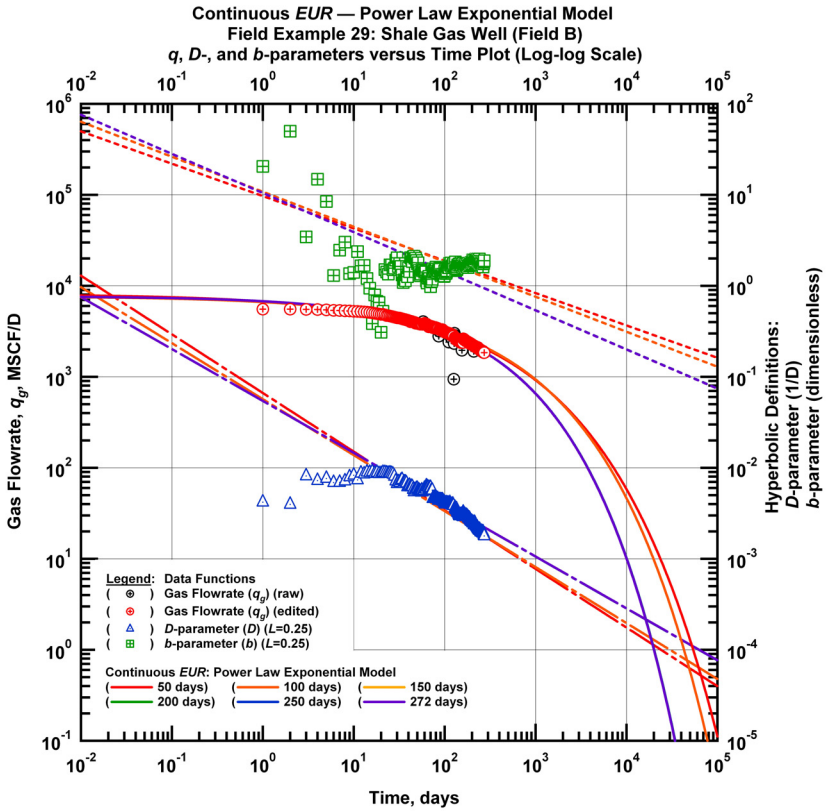

Figure E16 — (Log-log Plot): *qDb* plot — flow rate (q_g), *D*- and *b*-parameters versus production time and power law exponential model matches for field example 29.

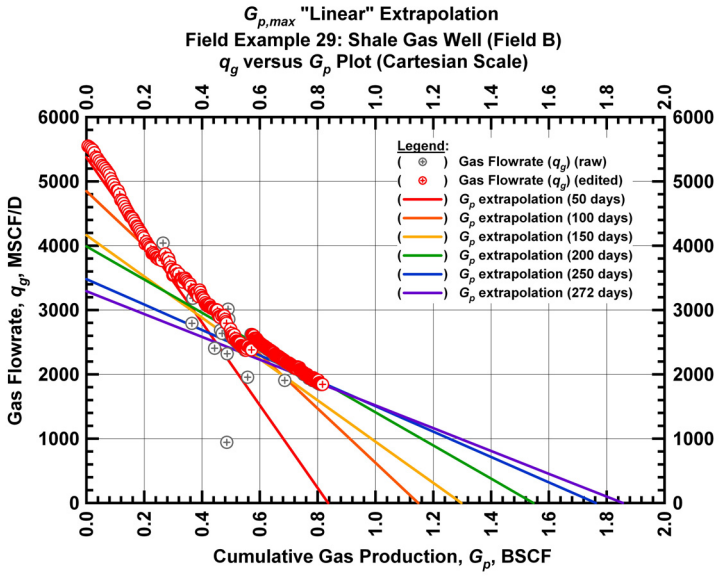

Figure E17 — (Cartesian Plot): Rate Cumulative Plot — flow rate (q_g) versus cumulative production (G_p) and the linear trends fit through the data for field example 29.

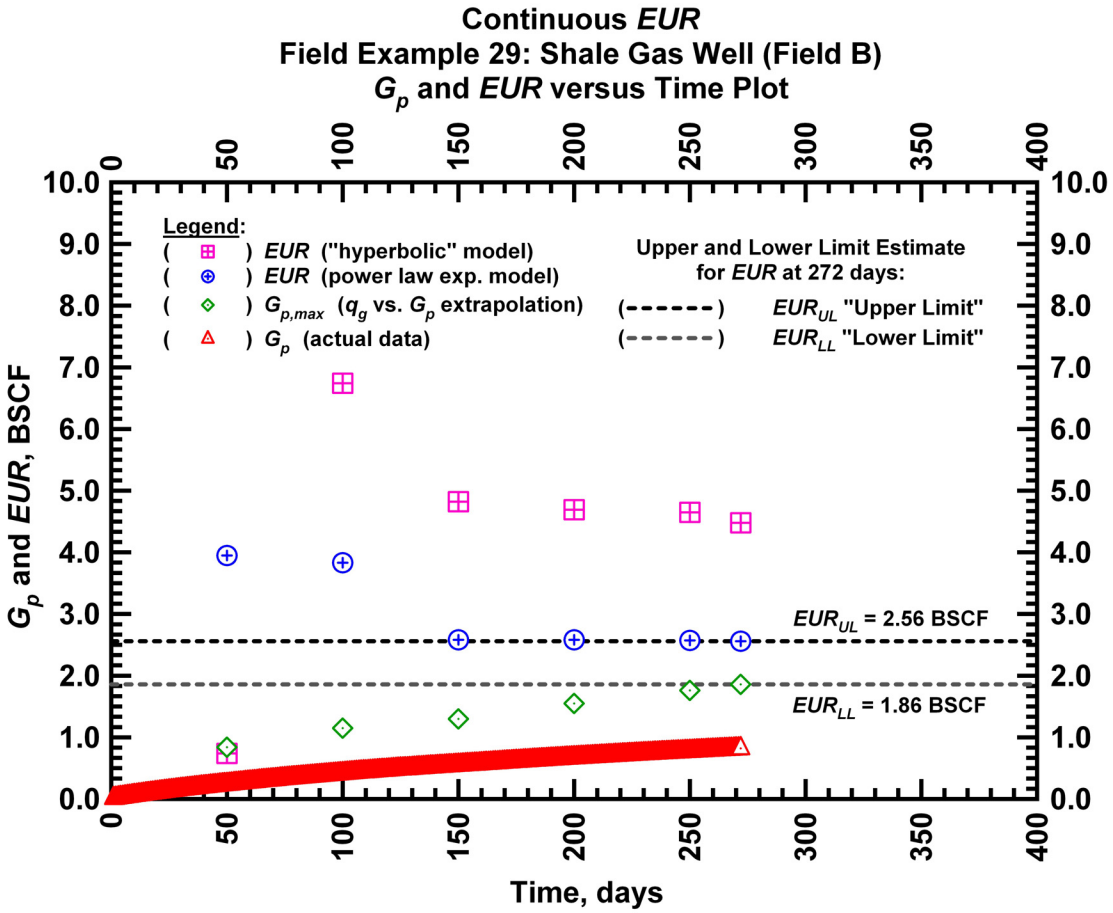

Figure E18 — (Cartesian Plot): *EUR* estimates from model matches and $G_{p,max}$ estimates from extrapolation technique for field example 29.

Table E7 — Analysis results for field example 29 — "hyperbolic" model parameters.

Time Interval, days	q_{gi} (MSCFD)	D_i (D^{-1})	b (dimensionless)	EUR_{hyp} (BSCF)
50	5,665	0.007762	0.010	0.74
100	5,770	0.010949	1.837	6.74
150	5,713	0.009289	1.400	4.82
200	5,713	0.009678	1.400	4.69
250	5,713	0.009685	1.392	4.65
272	5,713	0.009531	1.351	4.48

Table E8 — Analysis results for field example 29 — power lawexponential model parameters.

Time Interval, days	$\hat{q}_{gi}$ (MSCFD)	$\hat{D}_i$ (D^{-1})	n (dimensionless)	D_∞ (D^{-1})	EUR_{PLE} (BSCF)
50	8,127	0.1869	0.3555	0	3.95
100	7,689	0.1478	0.3847	0	3.83
150	7,689	0.1265	0.4297	0	2.58
200	7,689	0.1265	0.4297	0	2.58
250	7,689	0.1264	0.4299	0	2.57
272	7,689	0.1265	0.4300	0	2.56

Table E9 — Analysis results for field example 29 — straight line extrapolation.

Time Interval, days	Slope, 10^{-6} D^{-1}	Intercept, MSCF/D	Gp,max (BSCF)
50	6,425	5,375	0.84
100	4,222	4,847	1.15
150	3,210	4,164	1.30
200	2,580	3,990	1.55
250	1,975	3,480	1.76
272	1,774	3,292	1.86

Field Example 30

We present the flow rate data and the cumulative production data which spans almost 0.6 years for a horizontal well producing from a shale gas reservoir in **Fig. E19**. **Fig. E20** presents the "hyperbolic" model matches imposed on the flow rate data along with the *D*- and *b*-parameter trends. In **Fig. E21** we observe that the value of the *b*-parameter as a function of time. The *b*-parameter value decreases from 1.80 to 1.40 during the production history. Every interval is matched with a "hyperbolic" *b*-parameter greater than 1 indicating that boundary-dominated flow has not been established. **Fig. E22** shows the power law exponential model matches imposed on the flow rate data and *D*- and *b*-parameter trends. In **Fig. E23** we show the results of the straight line extrapolation technique, and in **Fig. E24** we present the calculated *EUR* values versus production time. All of the model parameters for this example are presented in **Tables E10, E11, and E12**. The *EUR* of this well should be in between 1.05 BSCF (the "lower" limit given by the straight line extrapolation technique at 207 days) and 1.71 BSCF (the "upper" limit given by the power law exponential estimate at 207 days).

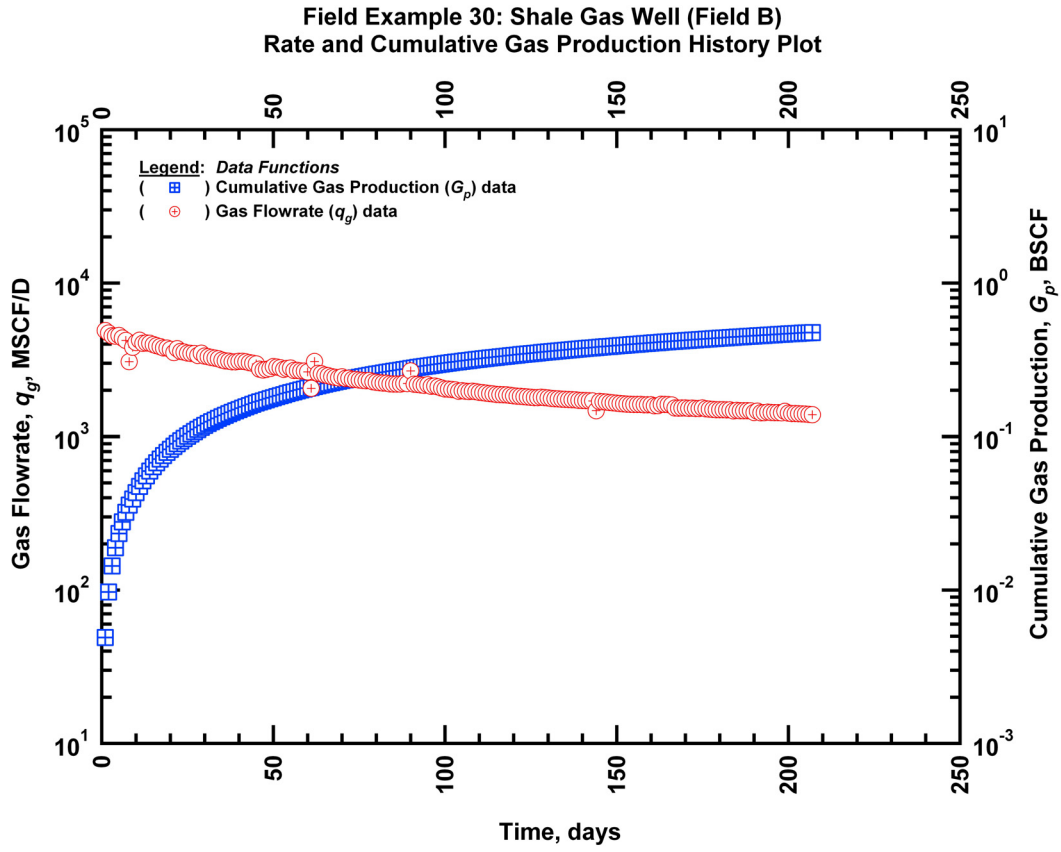

Figure E19 — (Semi-log Plot): Production history plot for field example 30 — flow rate (q_g) and cumulative production (G_p) versus production time.

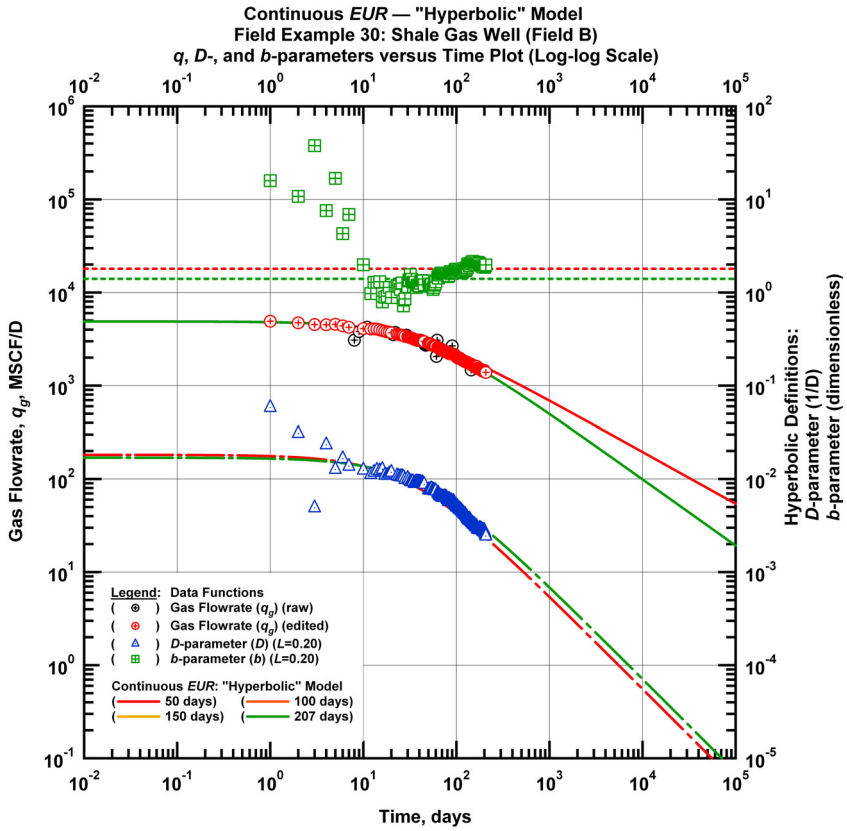

Figure E20 — (Log-log Plot): *qDb* plot — flow rate (q_g), *D*- and *b*-parameters versus production time and "hyperbolic" model matches for field example 30.

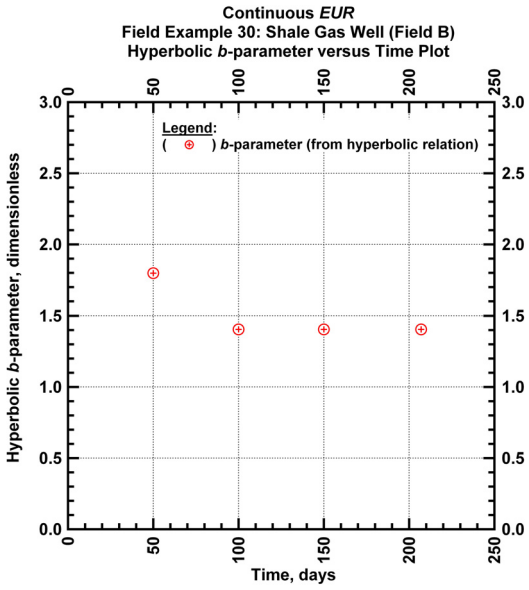

Figure E21 — (Cartesian Plot): Hyperbolic *b*-parameter values obtained from model matches with production data for field example 30.

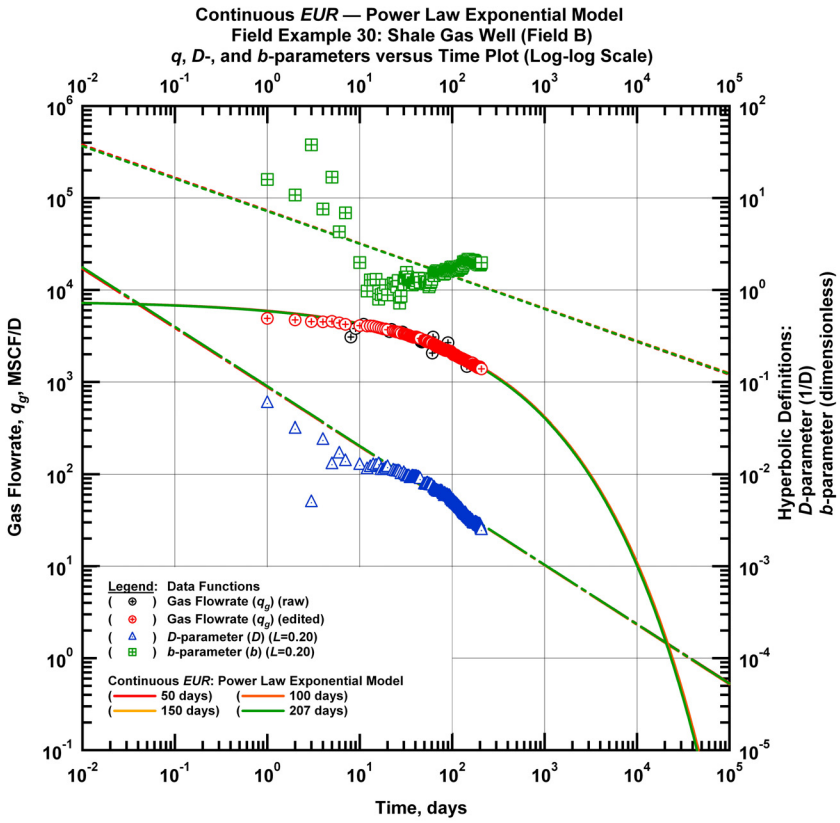

Figure E22 — (Log-log Plot): *qDb* plot — flow rate (q_g), *D*- and *b*-parameters versus production time and power law exponential model matches for field example 30.

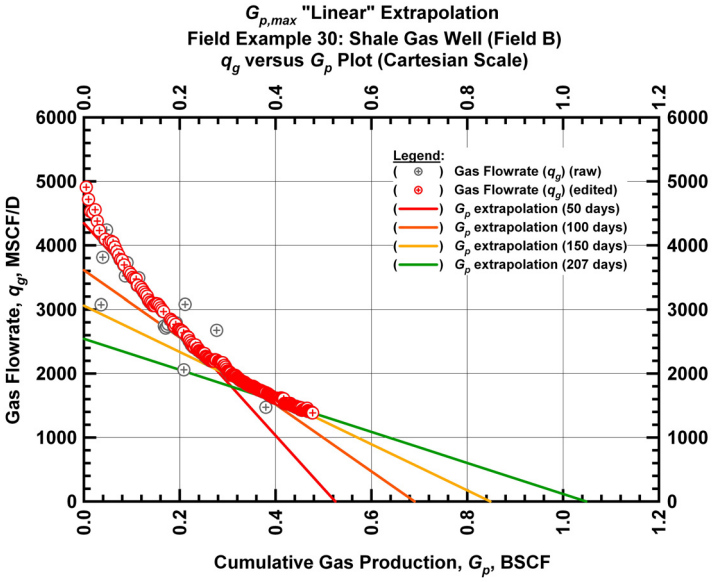

Figure E23 — (Cartesian Plot): Rate Cumulative Plot — flow rate (q_g) versus cumulative production (G_p) and the linear trends fit through the data for field example 30.

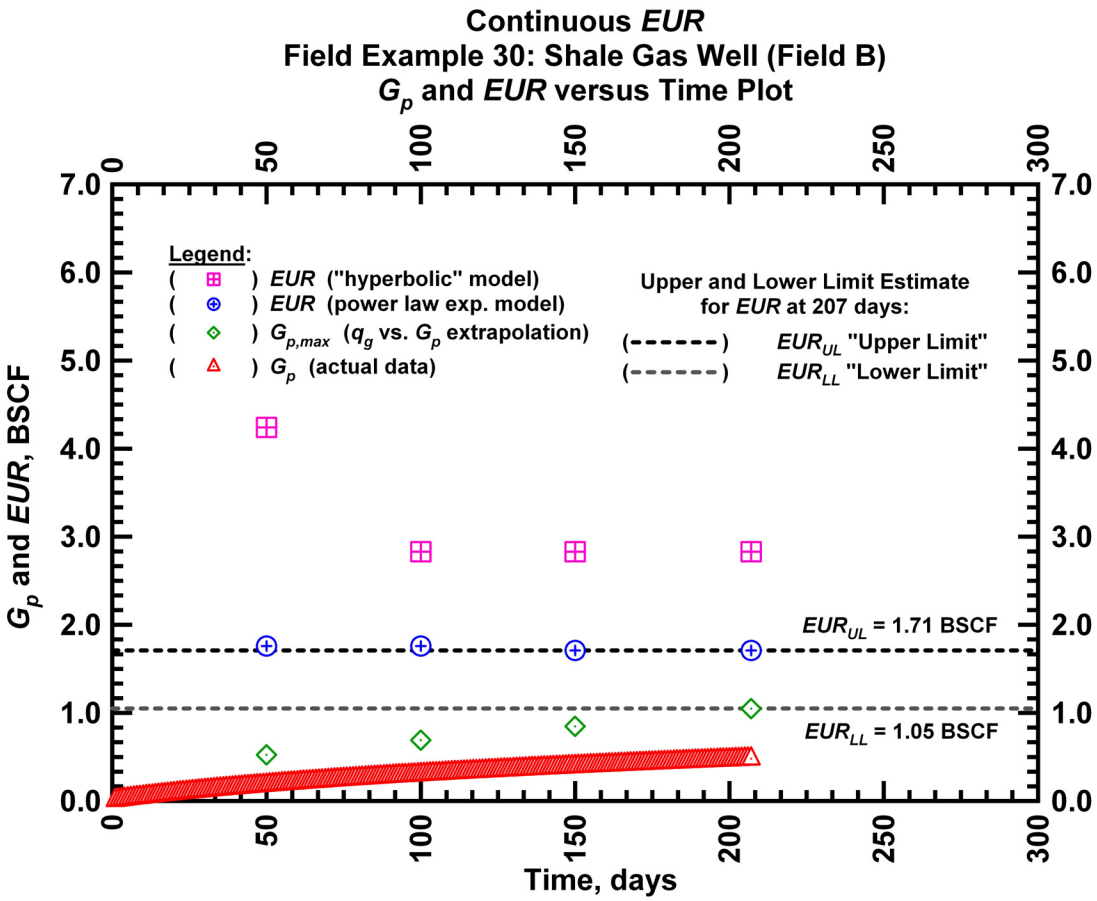

Figure E24 — (Cartesian Plot): *EUR* estimates from model matches and $G_{p,max}$ estimates from extrapolation technique for field example 30.

Table E10 — Analysis results for field example 30 — "hyperbolic" model parameters.

Time Interval, days	q_{gi} (MSCFD)	D_i (D^{-1})	b (dimensionless)	EUR_{hyp} (BSCF)
50	4,885	0.018193	1.7977	4.24
100	4,885	0.016938	1.4046	2.83
150	4,885	0.016938	1.4046	2.83
207	4,885	0.016938	1.4046	2.83

Table E11 — Analysis results for field example 30 — power lawexponential model parameters.

Time Interval, days	$\hat{q}_{gi}$ (MSCFD)	$\hat{D}_i$ (D^{-1})	n (dimensionless)	D_∞ (D^{-1})	EUR_{PLE} (BSCF)
50	7,584	0.2461	0.357	0	1.76
100	7,584	0.2532	0.353	0	1.76
150	7,584	0.2540	0.354	0	1.71
207	7,584	0.2540	0.354	0	1.71

Table E12 — Analysis results for field example 30 — straight line extrapolation.

Time Interval, days	Slope, 10^{-6} D^{-1}	Intercept, MSCF/D	Gp,max (BSCF)
50	8,282	4,345	0.52
100	5,233	3,611	0.69
150	3,608	3,060	0.85
207	2,426	2,543	1.05

Field Example 31

We present the flow rate data and the cumulative production data which spans almost 0.5 years for a horizontal well producing from a shale gas reservoir in **Fig. E25**. **Fig. E26** presents the "hyperbolic" model matches imposed on the flow rate data along with the *D*- and *b*-parameter trends. In **Fig. E27** we observe that the value of the *b*-parameter as a function of time. The *b*-parameter value decreases from 3.48 to 1.24 during the production history. Every interval is matched with a "hyperbolic" *b*-parameter greater than 1 indicating that boundary-dominated flow has not been established. **Fig. E28** shows the power law exponential model matches imposed on the flow rate data and *D*- and *b*-parameter trends. In **Fig. E29** we show the results of the straight line extrapolation technique, and in **Fig. E30** we present the calculated *EUR* values versus production time. All of the model parameters for this example are presented in **Tables E13, E14, and E15**. The *EUR* of this well should be in between 0.77 BSCF (the "lower" limit given by the straight line extrapolation technique at 171 days) and 2.01 BSCF (the "upper" limit given by the power law exponential estimate at 171 days).

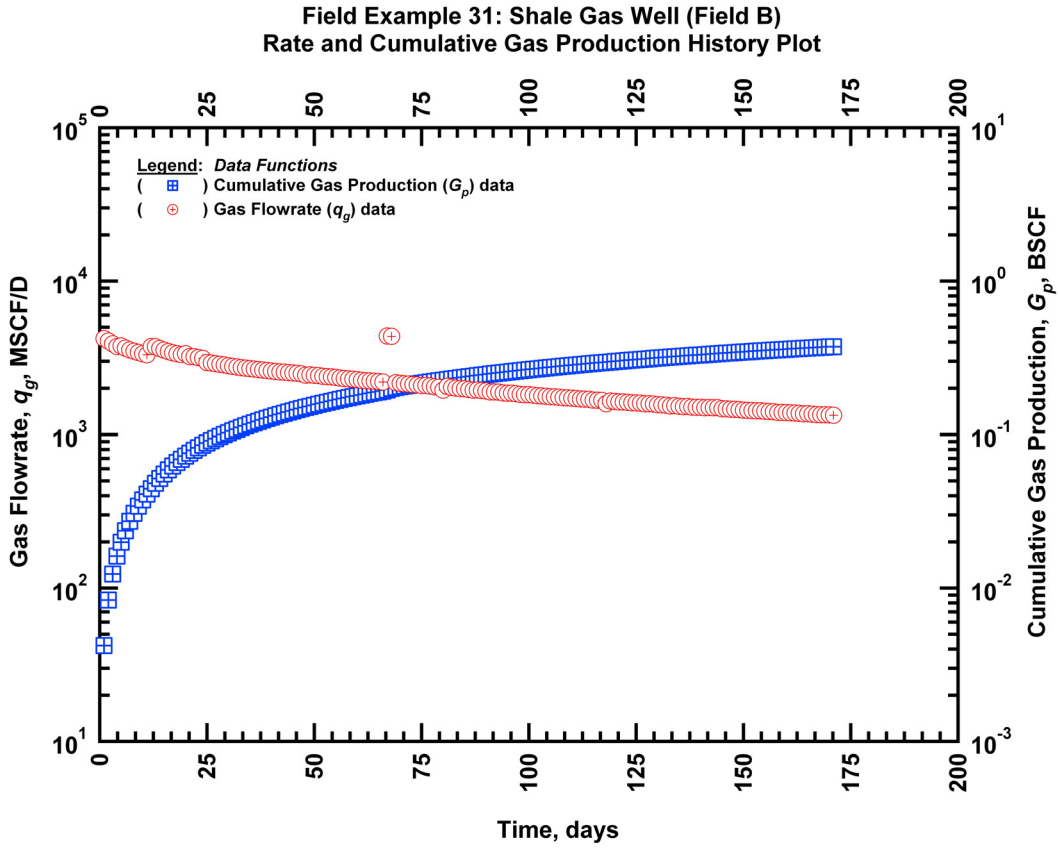

Figure E25 — (Semi-log Plot): Production history plot for field example 31 — flow rate (q_g) and cumulative production (G_p) versus production time.

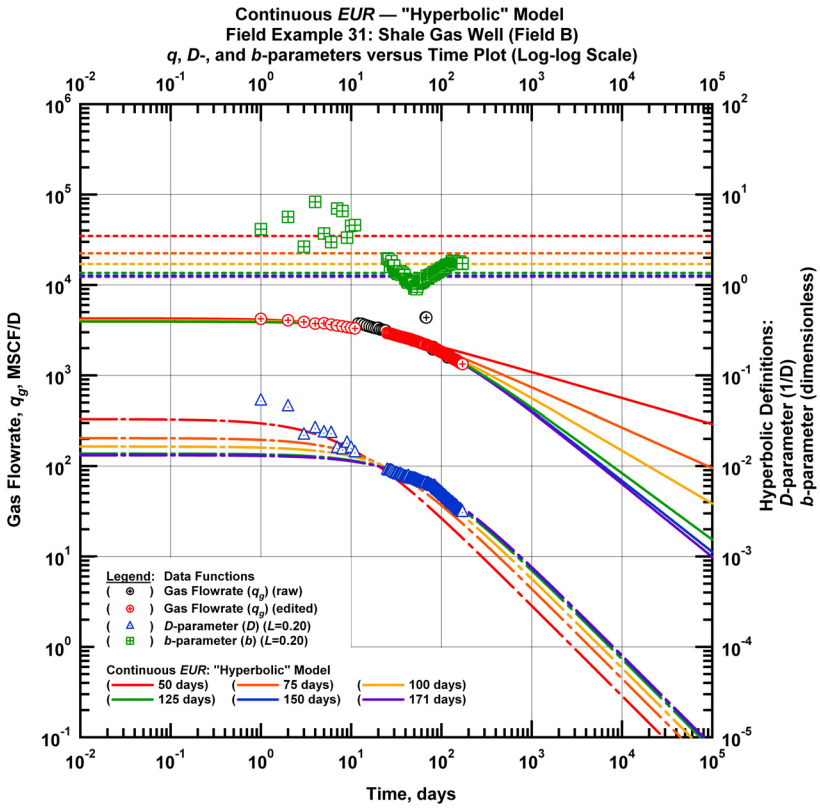

Figure E26 — (Log-log Plot): *qDb* plot — flow rate (q_g), *D*- and *b*-parameters versus production time and "hyperbolic" model matches for field example 31.

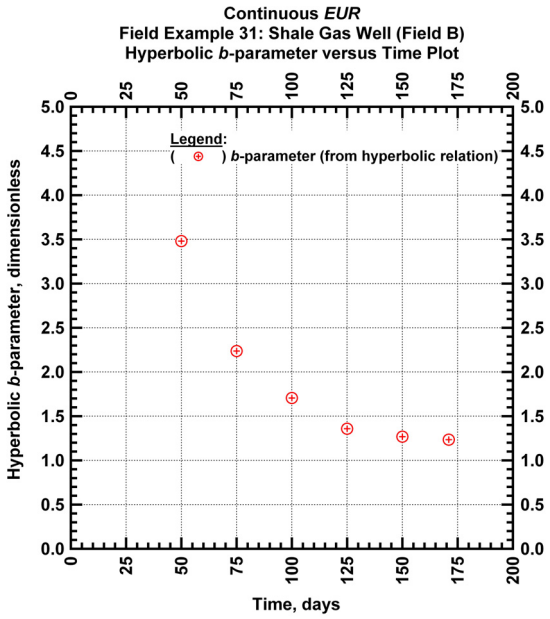

Figure E27 — (Cartesian Plot): Hyperbolic *b*-parameter values obtained from model matches with production data for field example 31.

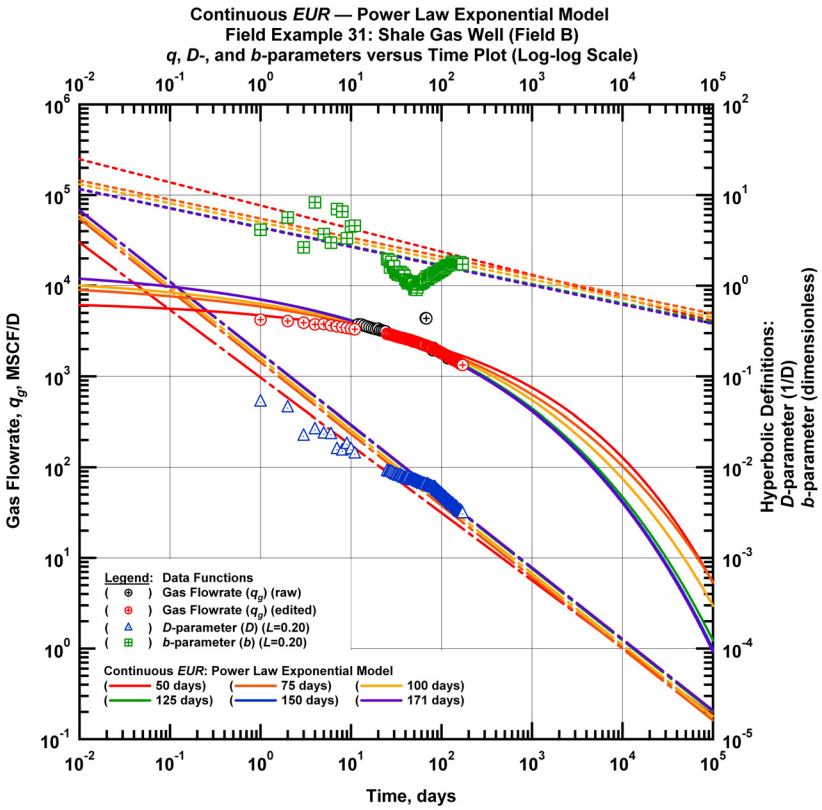

Figure E28 — (Log-log Plot): *qDb* plot — flow rate (q_g), *D*- and *b*-parameters versus production time and power law exponential model matches for field example 31.

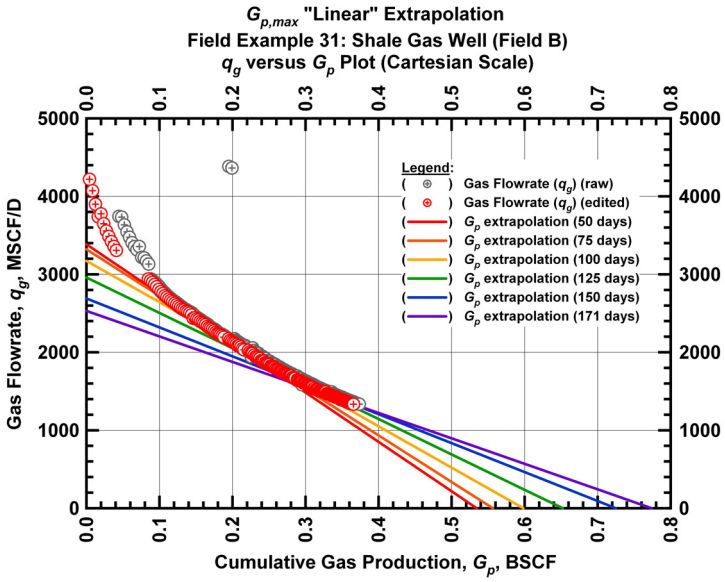

Figure E29 — (Cartesian Plot): Rate Cumulative Plot — flow rate (q_g) versus cumulative production (G_p) and the linear trends fit through the data for field example 31.

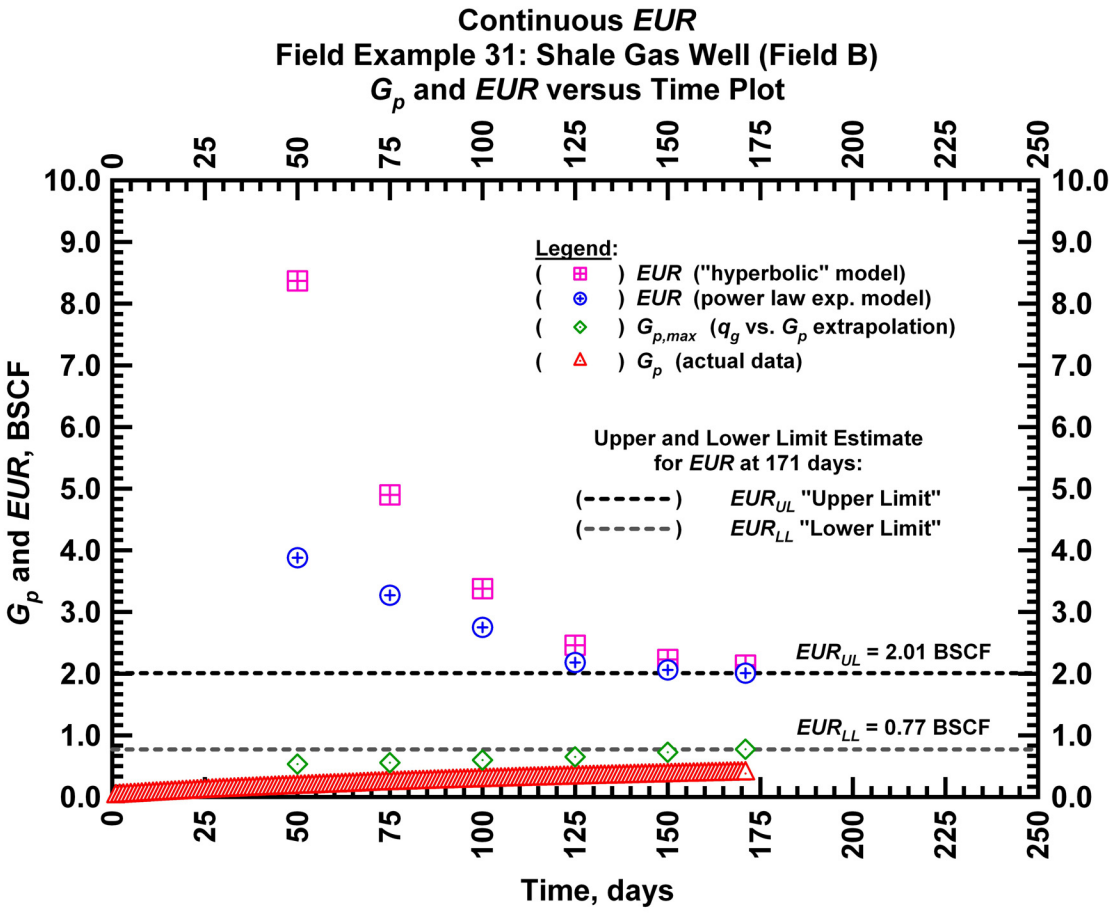

Figure E30 — (Cartesian Plot): *EUR* estimates from model matches and $G_{p,max}$ estimates from extrapolation technique for field example 31.

Table E13 — Analysis results for field example 31 — "hyperbolic" model parameters.

Time Interval, days	q_{gi} (MSCFD)	D_i (D^{-1})	b (dimensionless)	EUR_{hyp} (BSCF)
50	4,260	0.033052	3.4802	8.37
75	4,105	0.020364	2.2372	4.90
100	4,032	0.016444	1.7063	3.38
125	3,936	0.013732	1.3575	2.46
150	3,936	0.013326	1.2686	2.23
171	3,936	0.013157	1.2350	2.14

Table E14 — Analysis results for field example 31 — power law exponential model parameters.

Time Interval, days	$\hat{q}_{gi}$ (MSCFD)	$\hat{D}_i$ (D^{-1})	n (dimensionless)	D_∞ (D^{-1})	EUR_{PLE} (BSCF)
50	6,884	0.381	0.255	0	3.88
75	11,643	0.684	0.210	0	3.27
100	13,370	0.750	0.210	0	2.75
125	16,452	0.847	0.210	0	2.18
150	16,452	0.847	0.212	0	2.06
171	16,452	0.853	0.212	0	2.01

Table E15 — Analysis results for field example 31 — straight line extrapolation.

Time Interval, days	Slope, 10^{-6} D^{-1}	Intercept, MSCF/D	*Gp,max* (BSCF)
50	6,335	3,385	0.53
75	5,967	3,321	0.56
100	5,304	3,173	0.60
125	4,537	2,959	0.65
150	3,711	2,690	0.72
171	3,270	2,531	0.77

Field Example 32

We present the flow rate data and the cumulative production data which spans over 0.6 years for a horizontal well producing from a shale gas reservoir in **Fig. E31**. **Fig. E32** presents the "hyperbolic" model matches imposed on the flow rate data along with the *D*- and *b*-parameter trends. In **Fig. E33** we observe that the value of the *b*-parameter as a function of time. The *b*-parameter value decreases from 3.94 to 2.41 during the production history. Every interval is matched with a "hyperbolic" *b*-parameter greater than 1 indicating that boundary-dominated flow has not been established. **Fig. E34** shows the power law exponential model matches imposed on the flow rate data and *D*- and *b*-parameter trends. In **Fig. E35** we show the results of the straight line extrapolation technique, and in **Fig. E36** we present the calculated *EUR* values versus production time. All of the model parameters for this example are presented in **Tables E16, E17, and E18**. The *EUR* of this well should be in between 0.36 BSCF (the "lower" limit given by the straight line extrapolation technique at 222 days) and 1.54 BSCF (the "upper" limit given by the power law exponential estimate at 222 days).

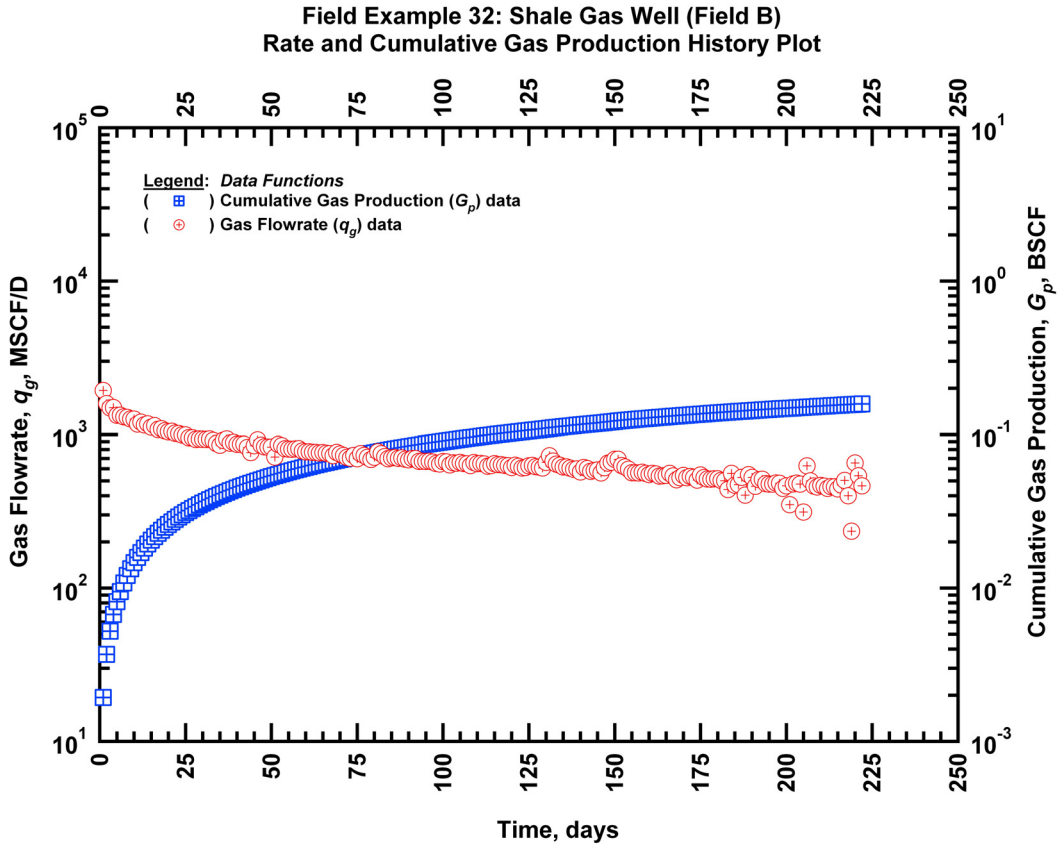

Figure E31 — (Semi-log Plot): Production history plot for field example 32 — flow rate (q_g) and cumulative production (G_p) versus production time.

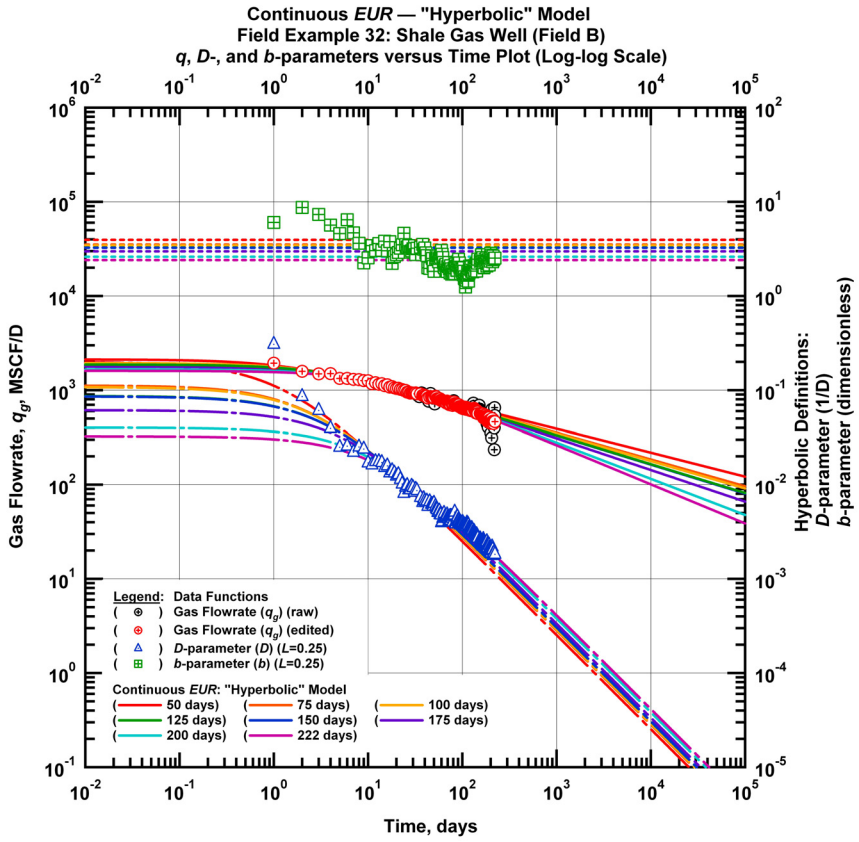

Figure E32 — (Log-log Plot): qDb plot — flow rate (q_g), D- and b-parameters versus production time and "hyperbolic" model matches for field example 32.

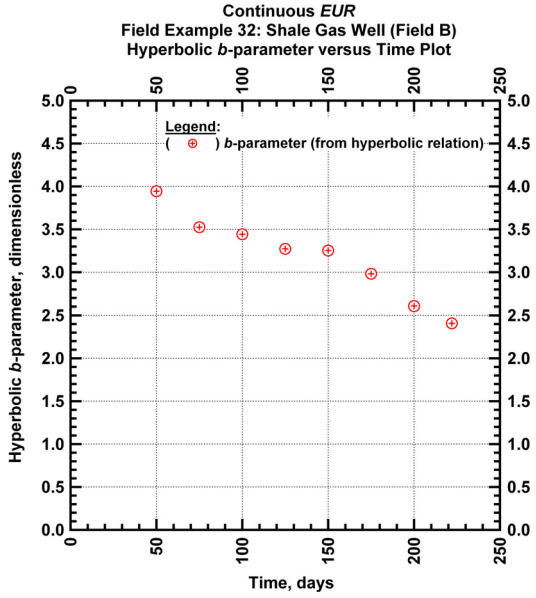

Figure E33 — (Cartesian Plot): Hyperbolic b-parameter values obtained from model matches with production data for field example 32.

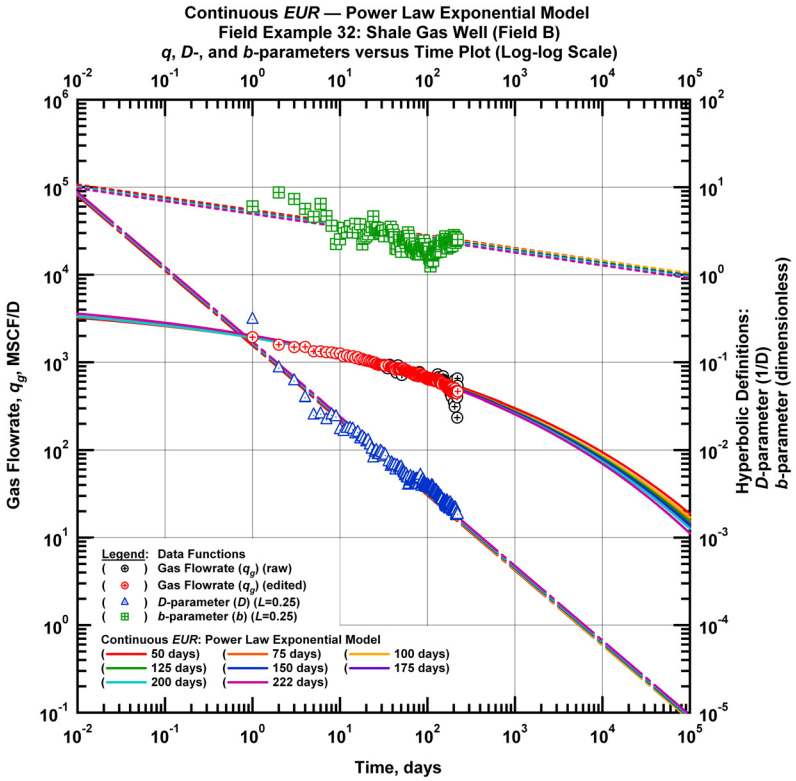

Figure E34 — (Log-log Plot): *qDb* plot — flow rate (q_g), *D*- and *b*-parameters versus production time and power law exponential model matches for field example 32.

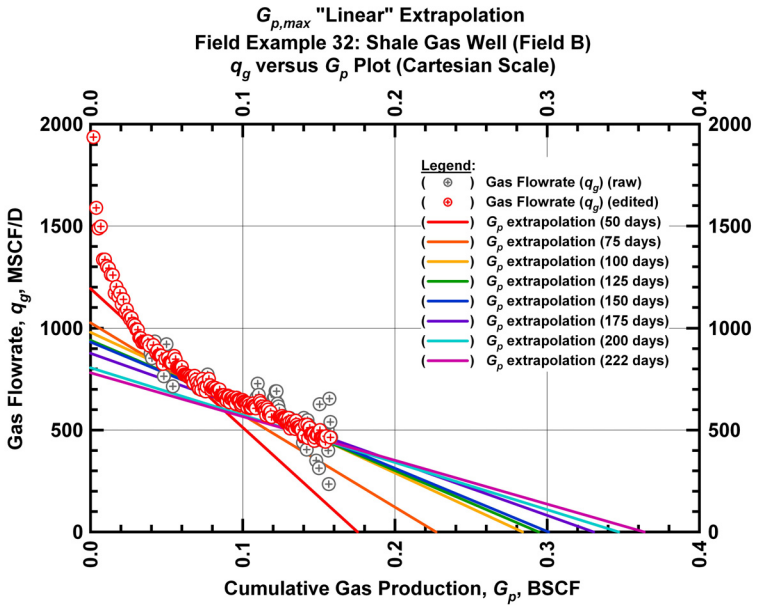

Figure E35 — (Cartesian Plot): Rate Cumulative Plot — flow rate (q_g) versus cumulative production (G_p) and the linear trends fit through the data for field example 32.

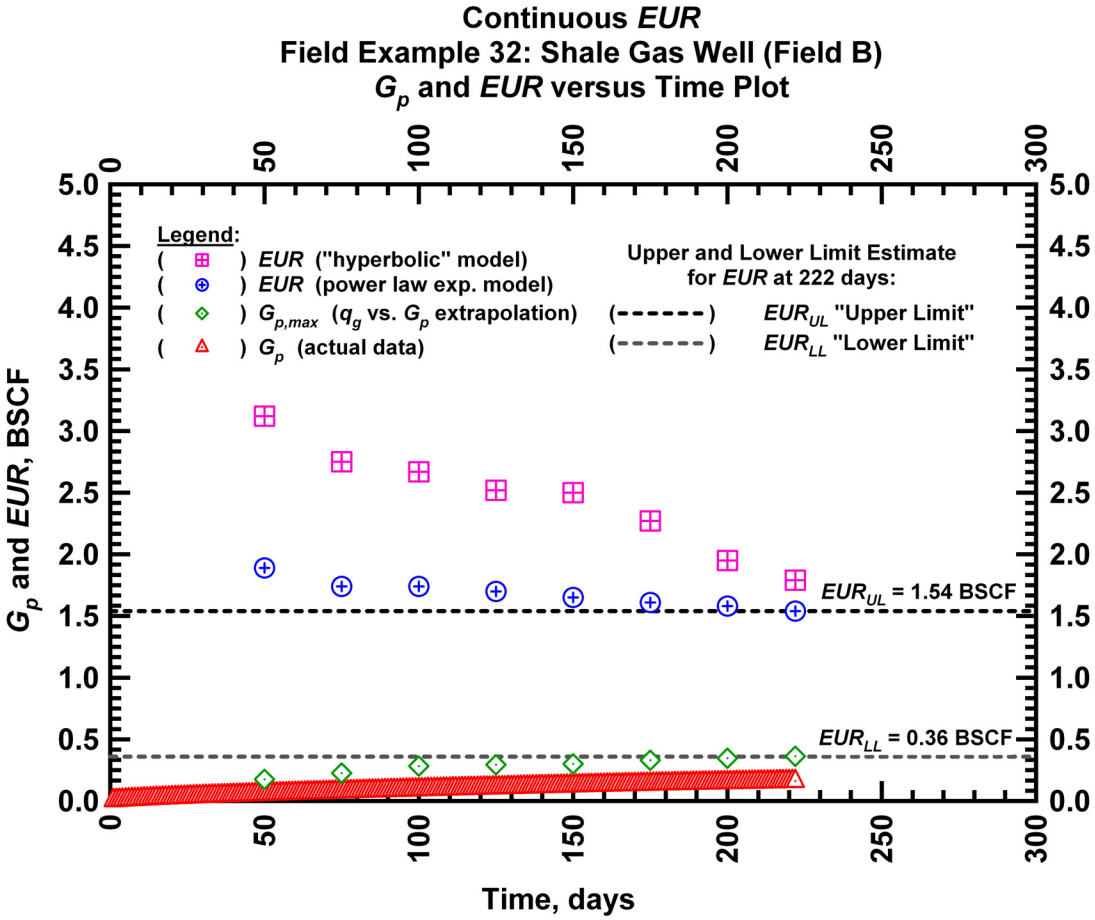

Figure E36 — (Cartesian Plot): *EUR* estimates from model matches and $G_{p,max}$ estimates from extrapolation technique for field example 32.

Table E16 — Analysis results for field example 32 — "hyperbolic" model parameters.

Time Interval, days	q_{gi} (MSCFD)	D_i (D^{-1})	b (dimensionless)	EUR_{hyp} (BSCF)
50	2,119	0.199097	3.944	3.12
75	1,938	0.112024	3.525	2.75
100	1,938	0.107850	3.443	2.67
125	1,872	0.086724	3.273	2.52
150	1,872	0.085785	3.252	2.50
175	1,777	0.061385	2.981	2.27
200	1,661	0.040139	2.607	1.95
222	1,605	0.032476	2.407	1.79

Table E17 — Analysis results for field example 32 — power lawexponential model parameters.

Time Interval, days	$\hat{q}_{gi}$ (MSCFD)	$\hat{D}_i$ (D^{-1})	n (dimensionless)	D_∞ (D^{-1})	EUR_{PLE} (BSCF)
50	5,594	1.074	0.145	0	1.89
75	5,995	1.132	0.144	0	1.74
100	6,163	1.176	0.140	0	1.74
125	5,913	1.126	0.145	0	1.70
150	5,913	1.126	0.146	0	1.65
175	5,913	1.126	0.147	0	1.61
200	5,913	1.131	0.147	0	1.58
222	6,513	1.172	0.147	0	1.54

Table E18 — Analysis results for field example 32 — straight line extrapolation.

Time Interval, days	Slope, 10^{-6} D^{-1}	Intercept, MSCF/D	*Gp,max* (BSCF)
50	6,801	1,193	0.18
75	4,525	1,027	0.23
100	3,453	980	0.28
125	3,197	941	0.29
150	3,097	932	0.30
175	2,653	877	0.33
200	2,323	806	0.35
222	2,147	781	0.36

Field Example 33

We present the flow rate data and the cumulative production data which spans over 1 year for a horizontal well producing from a shale gas reservoir for a horizontal well producing from a shale gas reservoir in **Fig. E37**. **Fig. E38** presents the "hyperbolic" model matches imposed on the flow rate data along with the *D*- and *b*-parameter trends. In **Fig. E39** we observe that the value of the *b*-parameter as a function of time. The *b*-parameter value decreases from 1.94 to 1.29 during the production history. Every interval is matched with a "hyperbolic" *b*-parameter greater than 1 indicating that boundary-dominated flow has not been established. **Fig. E40** shows the power law exponential model matches imposed on the flow rate data and *D*- and *b*-parameter trends. In **Fig. E41** we show the results of the straight line extrapolation technique, and in **Fig. E42** we present the calculated *EUR* values versus production time. All of the model parameters for this example are presented in **Tables E19, E20, and E21**. The *EUR* of this well should be in between 3.20 BSCF (the "lower" limit given by the straight line extrapolation technique at 373 days) and 5.85 BSCF (the "upper" limit given by the power law exponential estimate at 373 days).

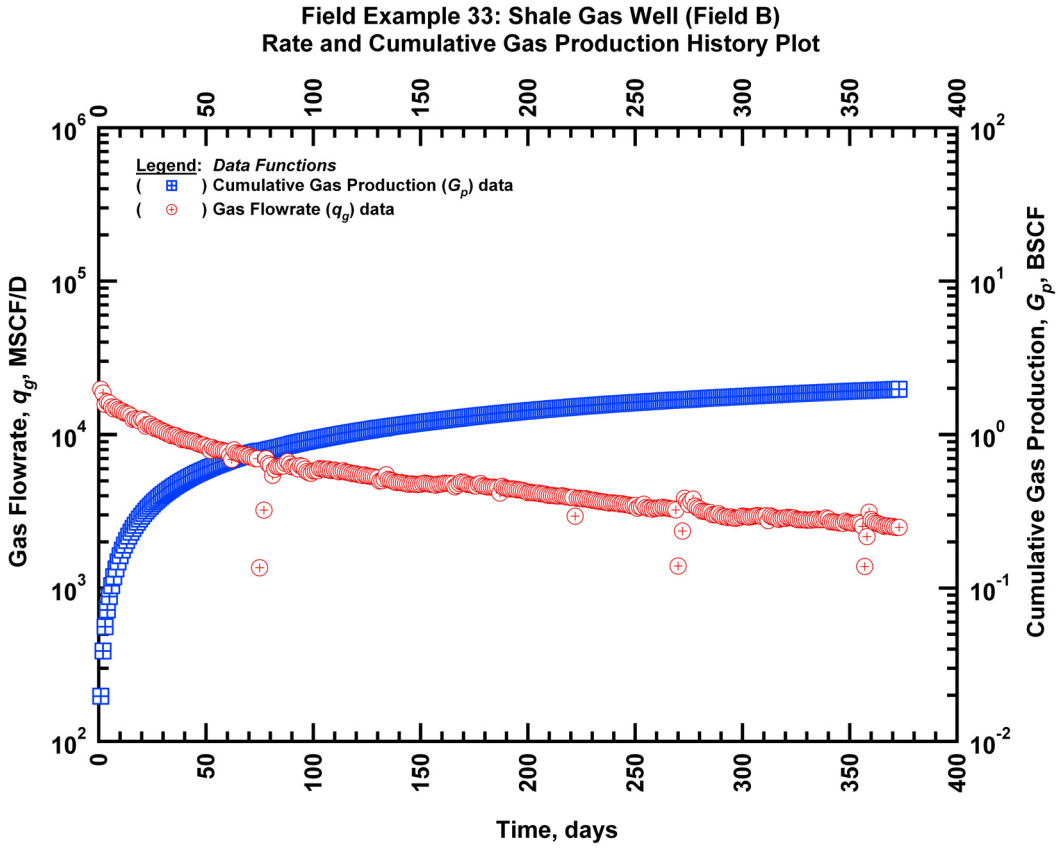

Figure E37 — (Semi-log Plot): Production history plot for field example 33 — flow rate (q_g) and cumulative production (G_p) versus production time.

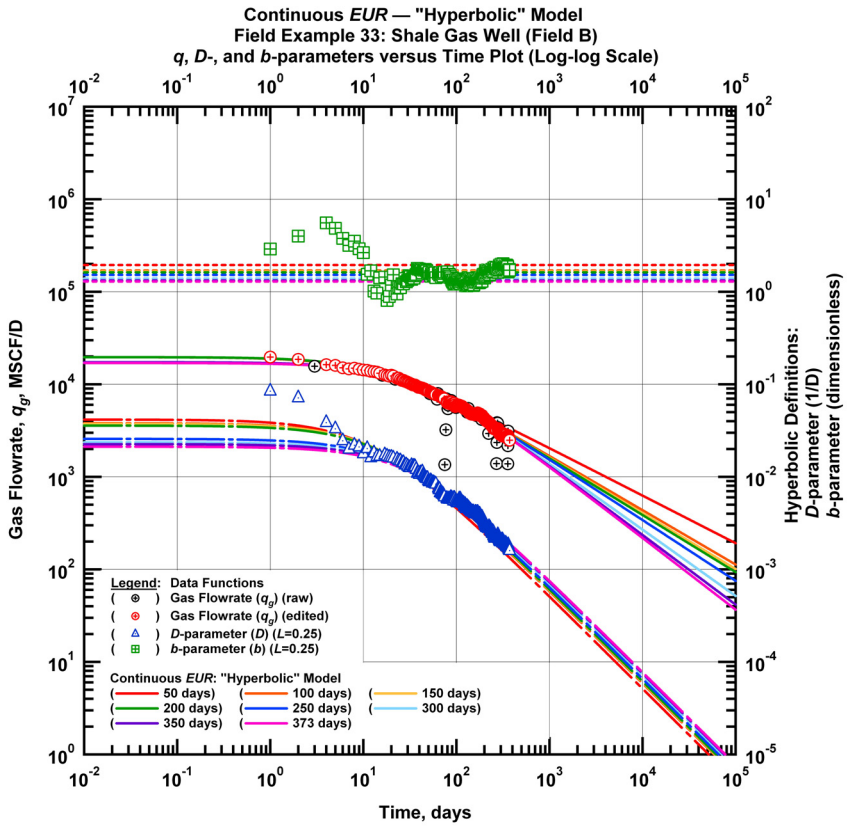

Figure E38 — (Log-log Plot): *qDb* plot — flow rate (q_g), *D*- and *b*-parameters versus production time and "hyperbolic" model matches for field example 33.

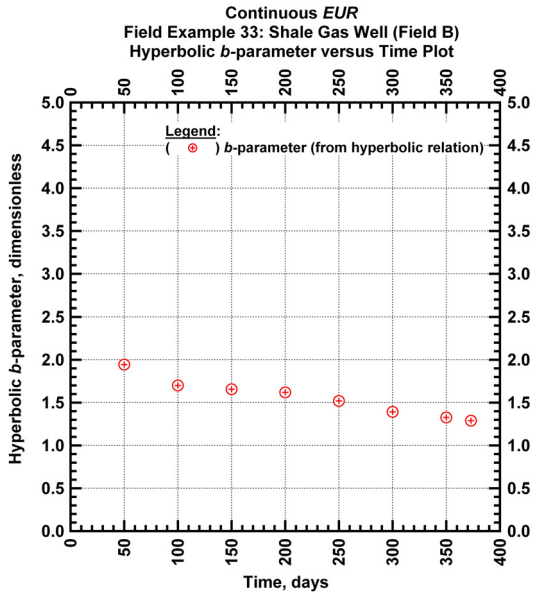

Figure E39 — (Cartesian Plot): Hyperbolic *b*-parameter values obtained from model matches with production data for field example 33.

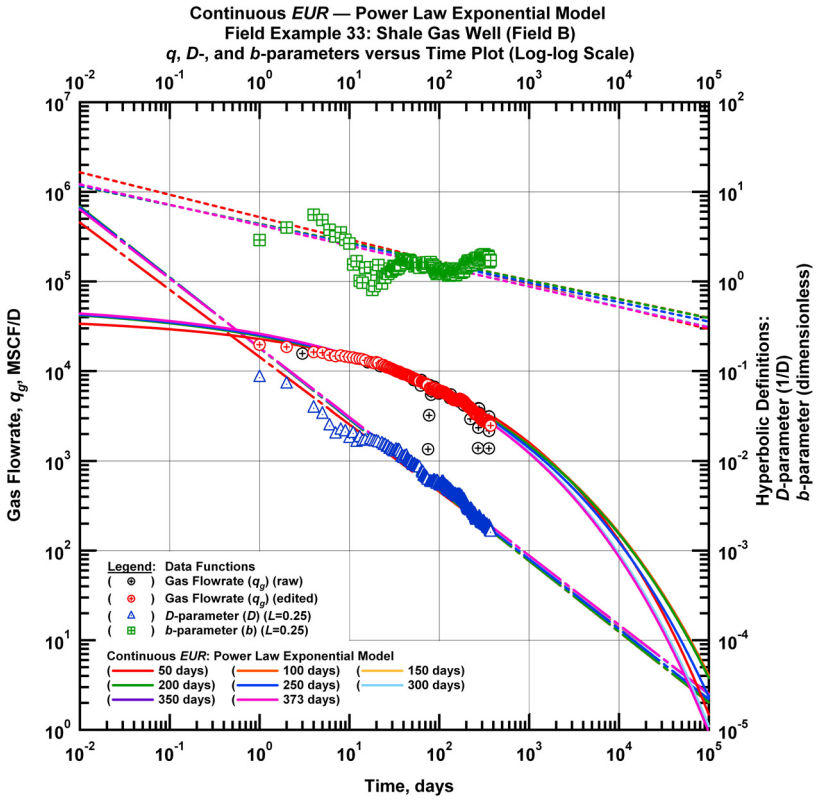

Figure E40 — (Log-log Plot): *qDb* plot — flow rate (q_g), *D*- and *b*-parameters versus production time and power law exponential model matches for field example 33.

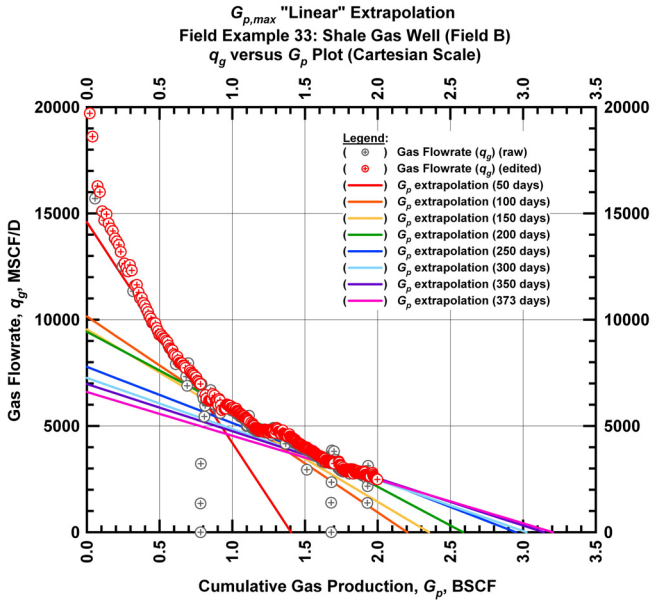

Figure E41 — (Cartesian Plot): Rate Cumulative Plot — flow rate (q_g) versus cumulative production (G_p) and the linear trends fit through the data for field example 33.

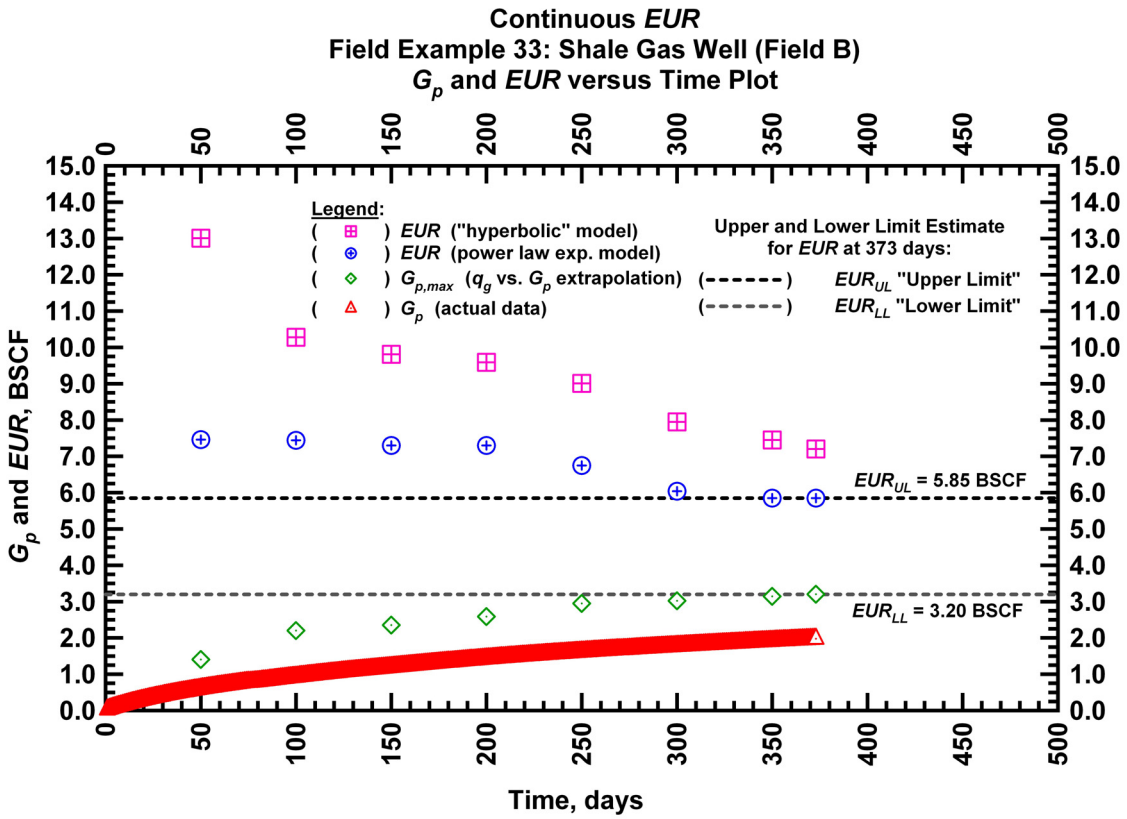

Figure E42 — (Cartesian Plot): *EUR* estimates from model matches and $G_{p,max}$ estimates from extrapolation technique for field example 33.

Table E19 — Analysis results for field example 33 — "hyperbolic" model parameters.

Time Interval, days	q_{gi} (MSCFD)	D_i (D^{-1})	b (dimensionless)	EUR_{hyp} (BSCF)
50	19,654	0.0416	1.9437	13.01
100	19,654	0.0380	1.7000	10.28
150	19,654	0.0373	1.6556	9.81
200	19,654	0.0358	1.6200	9.59
250	17,330	0.0257	1.5201	9.01
300	17,330	0.0237	1.3925	7.95
350	17,330	0.0226	1.3270	7.45
373	17,000	0.0212	1.2889	7.20

Table E20 — Analysis results for field example 33 — power lawexponential model parameters.

Time Interval, days	$\hat{q}_{gi}$ (MSCFD)	$\hat{D}_i$ (D^{-1})	n (dimensionless)	D_∞ (D^{-1})	EUR_{PLE} (BSCF)
50	40,421	0.5744	0.2500	0	7.46
100	57,911	0.8556	0.2097	0	7.44
150	57,911	0.8558	0.2103	0	7.30
200	57,911	0.8558	0.2103	0	7.30
250	57,911	0.8323	0.2170	0	6.75
300	57,911	0.7977	0.2269	0	6.04
350	57,911	0.7980	0.2281	0	5.85
373	57,911	0.7980	0.2281	0	5.85

Table E21 — Analysis results for field example 33 — straight line extrapolation.

Time Interval, days	Slope, 10^{-6} D^{-1}	Intercept, MSCF/D	*Gp,max* (BSCF)
50	10,385	14,588	1.40
100	4,608	10,153	2.20
150	4,056	9,544	2.35
200	3,646	9,434	2.59
250	2,636	7,779	2.95
300	2,401	7,260	3.02
350	2,219	6,973	3.14
373	2,059	6,599	3.20

Field Example 34

We present the flow rate data and the cumulative production data which spans almost 0.55 years for a horizontal well producing from a shale gas reservoir in **Fig. E43**. **Fig. E44** presents the "hyperbolic" model matches imposed on the flow rate data along with the *D*- and *b*-parameter trends. In **Fig. E45** we observe that the value of the *b*-parameter as a function of time. The *b*-parameter value decreases from 1.78 to 1.15 during the production history. Every interval is matched with a "hyperbolic" *b*-parameter greater than 1 indicating that boundary-dominated flow has not been established. **Fig. E46** shows the power law exponential model matches imposed on the flow rate data and *D*- and *b*-parameter trends. In **Fig. E47** we show the results of the straight line extrapolation technique, and in **Fig. E48** we present the calculated *EUR* values versus production time. All of the model parameters for this example are presented in **Tables E22, E23, and E24**. The *EUR* of this well should be in between 4.56 BSCF (the "lower" limit given by the straight line extrapolation technique at 206 days) and 9.44 BSCF (the "upper" limit given by the power law exponential estimate at 206 days).

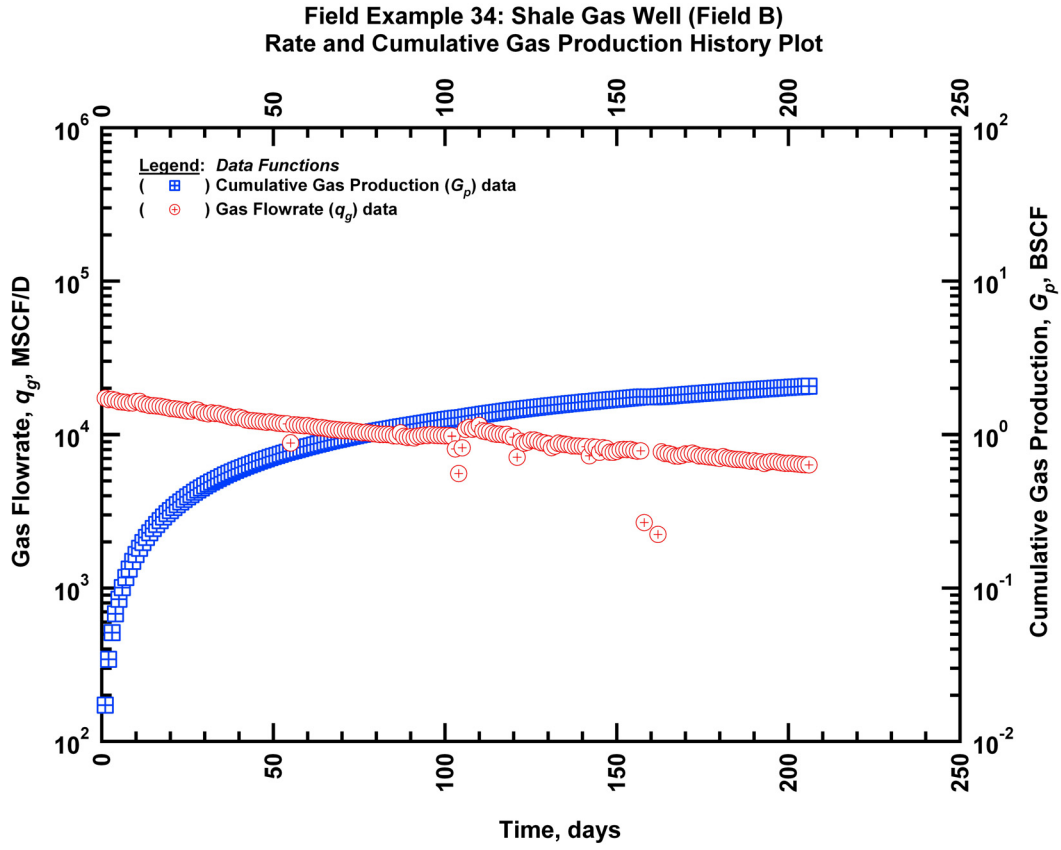

Figure E43 — (Semi-log Plot): Production history plot for field example 34 — flow rate (q_g) and cumulative production (G_p) versus production time.

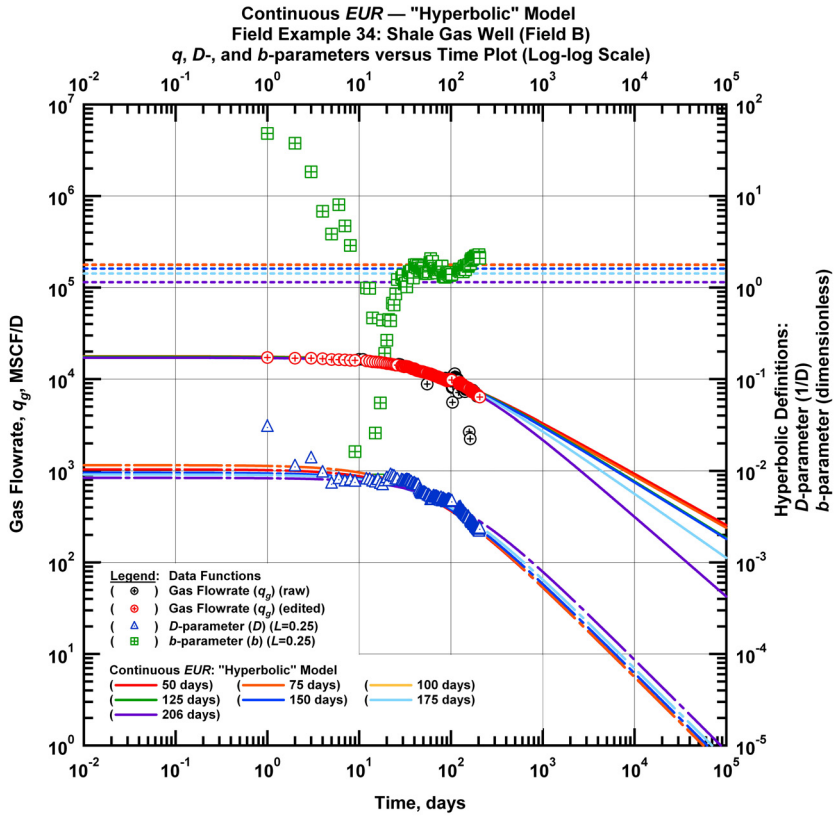

Figure E44 — (Log-log Plot): qDb plot — flow rate (q_g), D- and b-parameters versus production time and "hyperbolic" model matches for field example 34.

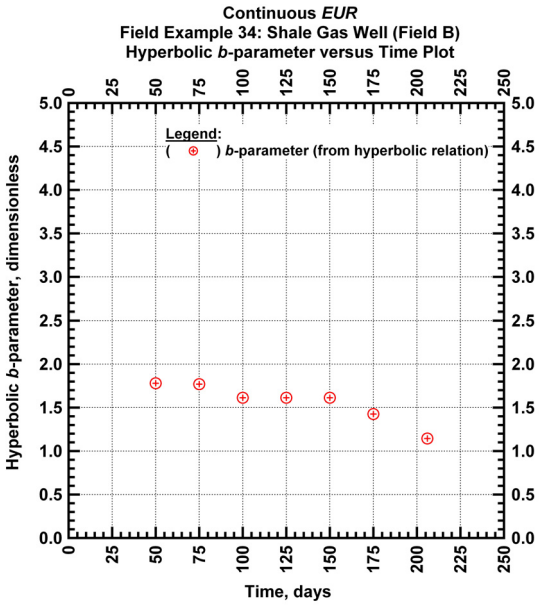

Figure E45 — (Cartesian Plot): Hyperbolic b-parameter values obtained from model matches with production data for field example 34.

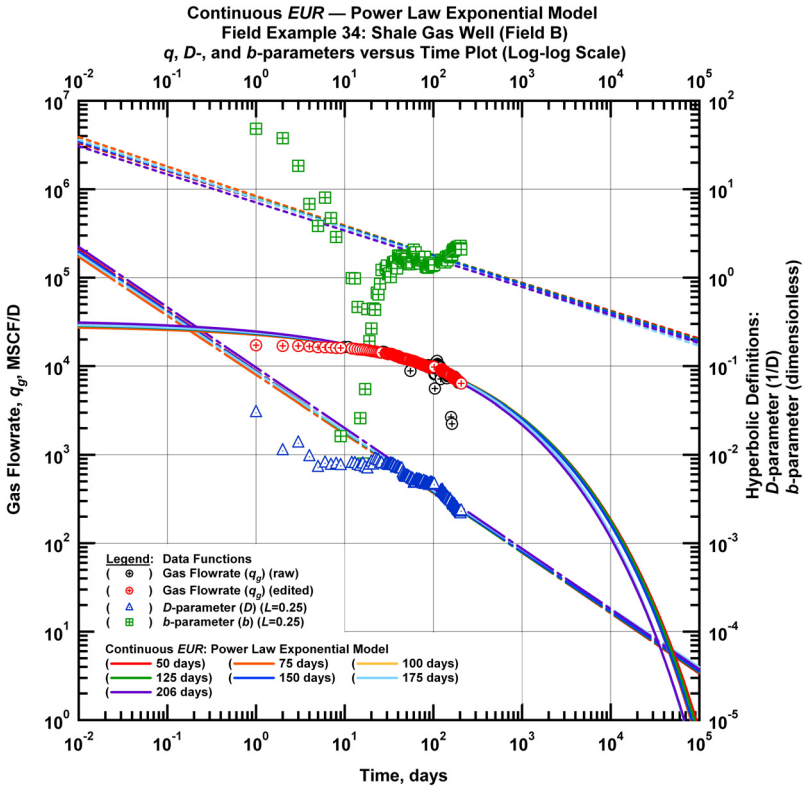

Figure E46 — (Log-log Plot): *qDb* plot — flow rate (q_g), *D*- and *b*-parameters versus production time and power law exponential model matches for field example 34.

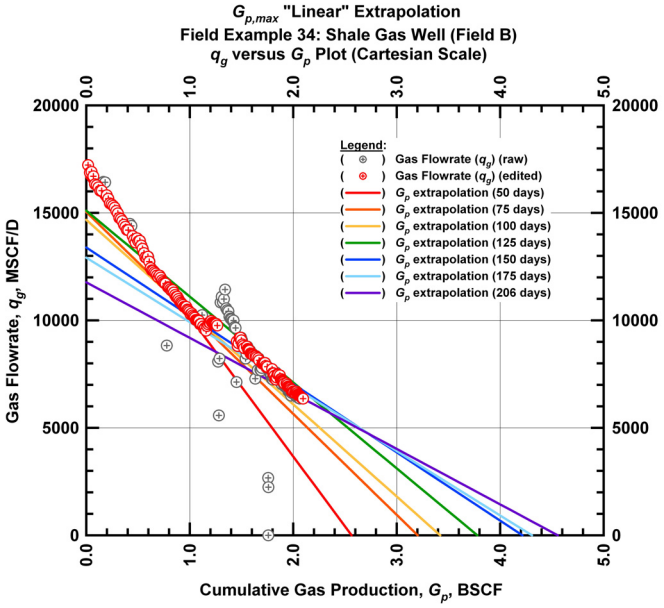

Figure E47 — (Cartesian Plot): Rate Cumulative Plot — flow rate (q_g) versus cumulative production (G_p) and the linear trends fit through the data for field example 34.

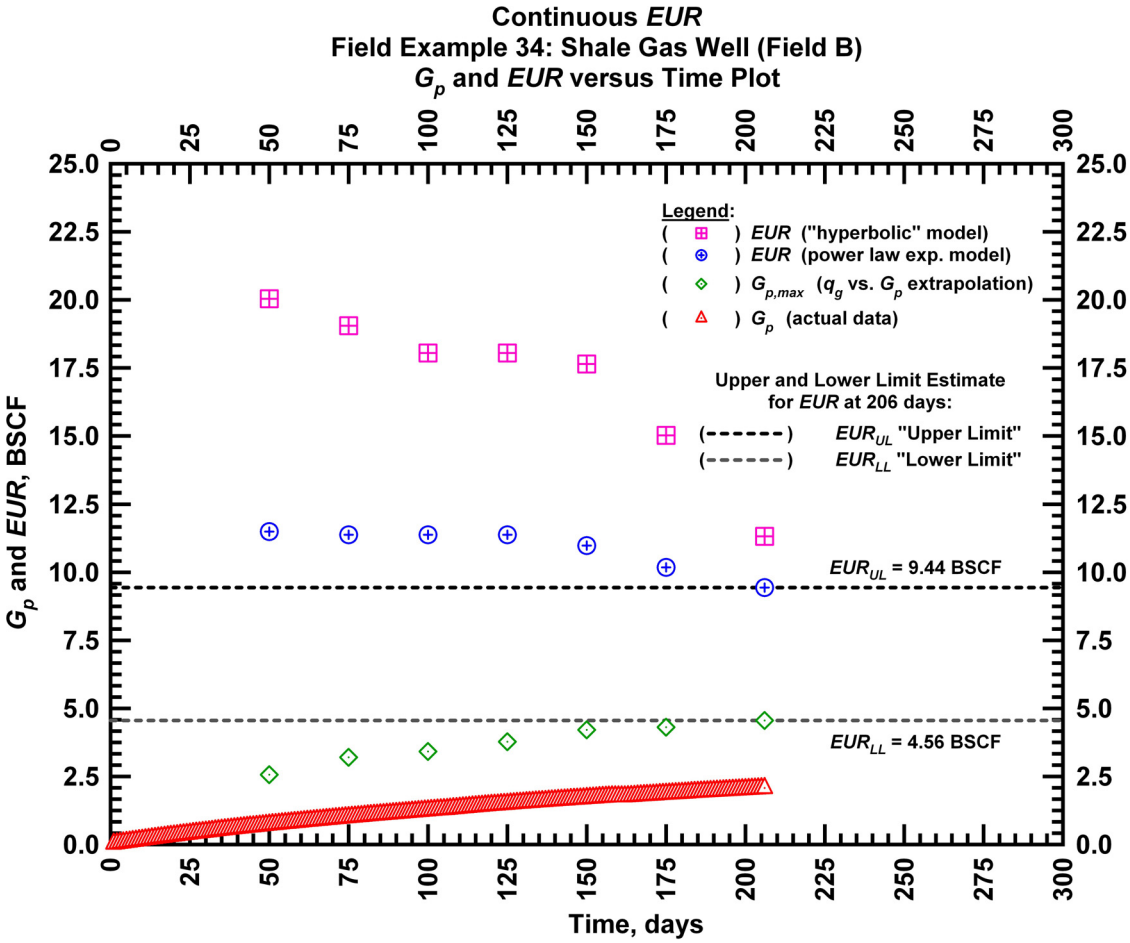

Figure E48 — (Cartesian Plot): *EUR* estimates from model matches and $G_{p,max}$ estimates from extrapolation technique for field example 34.

Table E22 — Analysis results for field example 34 — "hyperbolic" model parameters.

Time Interval, days	q_{gi} (MSCFD)	D_i (D^{-1})	b (dimensionless)	EUR_{hyp} (BSCF)
50	17,508	0.010375	1.780	20.04
75	17,752	0.011563	1.770	19.05
100	17,508	0.009556	1.613	18.05
125	17,508	0.009556	1.613	18.05
150	17,115	0.009556	1.613	17.64
175	17,115	0.009114	1.426	15.02
206	17,115	0.008399	1.145	11.32

Table E23 — Analysis results for field example 34 — power lawexponential model parameters.

Time Interval, days	$\hat{q}_{gi}$ (MSCFD)	$\hat{D}_i$ (D^{-1})	n (dimensionless)	D_∞ (D^{-1})	EUR_{PLE} (BSCF)
50	31,081	0.279	0.316	0	11.50
75	28,606	0.239	0.333	0	11.38
100	30,233	0.267	0.321	0	11.38
125	30,233	0.267	0.321	0	11.38
150	30,654	0.270	0.322	0	10.98
175	30,654	0.256	0.333	0	10.18
206	33,306	0.303	0.318	0	9.44

Table E24 — Analysis results for field example 34 — straight line extrapolation.

Time Interval, days	Slope, 10^{-6} D^{-1}	Intercept, MSCF/D	*Gp,max* (BSCF)
50	6,499	16,665	2.56
75	4,696	15,042	3.20
100	4,290	14,675	3.42
125	3,996	15,102	3.78
150	3,177	13,392	4.22
175	2,999	12,918	4.31
206	2,583	11,770	4.56

APPENDIX F
EXAMPLES FROM FIELD C

Field Example 35

We present the flow rate data and the cumulative production data which spans almost 0.7 years for a horizontal well producing from a shale gas reservoir in **Fig. F1**. **Fig. F2** presents the "hyperbolic" model matches imposed on the flow rate data along with the *D*- and *b*-parameter trends. In **Fig. F3** we observe that the value of the *b*-parameter as a function of time. The *b*-parameter value is stable around 2.8 during the production history. Every interval is matched with a "hyperbolic" *b*-parameter greater than 1 indicating that boundary-dominated flow has not been established. **Fig. F4** shows the power law exponential model matches imposed on the flow rate data and *D*- and *b*-parameter trends. In **Fig. F5** we show the results of the straight line extrapolation technique, and in **Fig. F6** we present the calculated *EUR* values versus production time. All of the model parameters for this example are presented in **Tables F1, F2, and F3**. The *EUR* of this well should be in between 1.77 BSCF (the "lower" limit given by the straight line extrapolation technique at 255 days) and 5.93 BSCF (the "upper" limit given by the power law exponential estimate at 255 days).

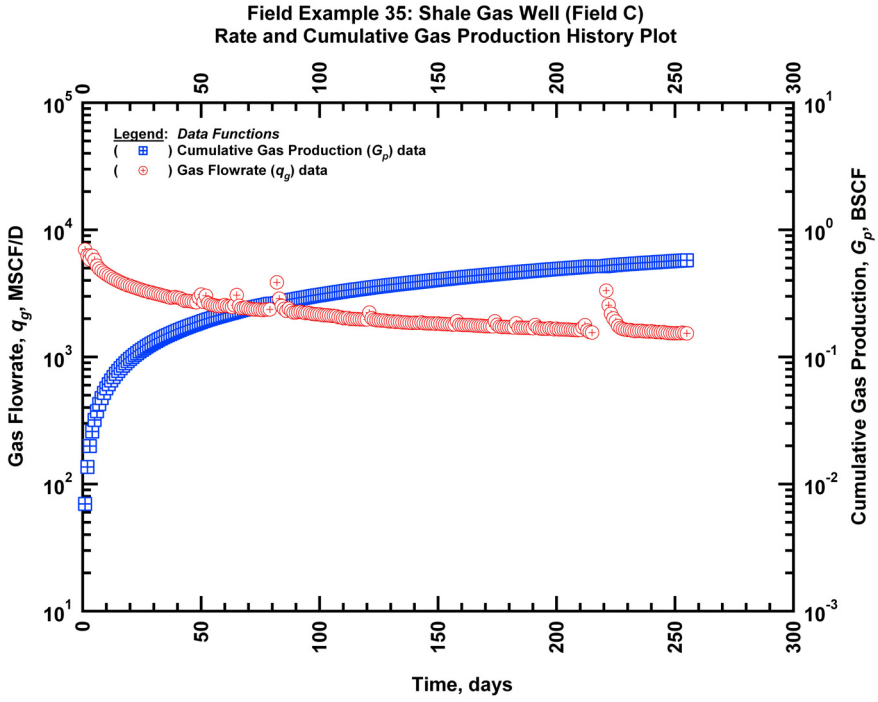

Figure F1 — (Semi-log Plot): Production history plot for field example 35 — flow rate (q_g) and cumulative production (G_p) versus production time.

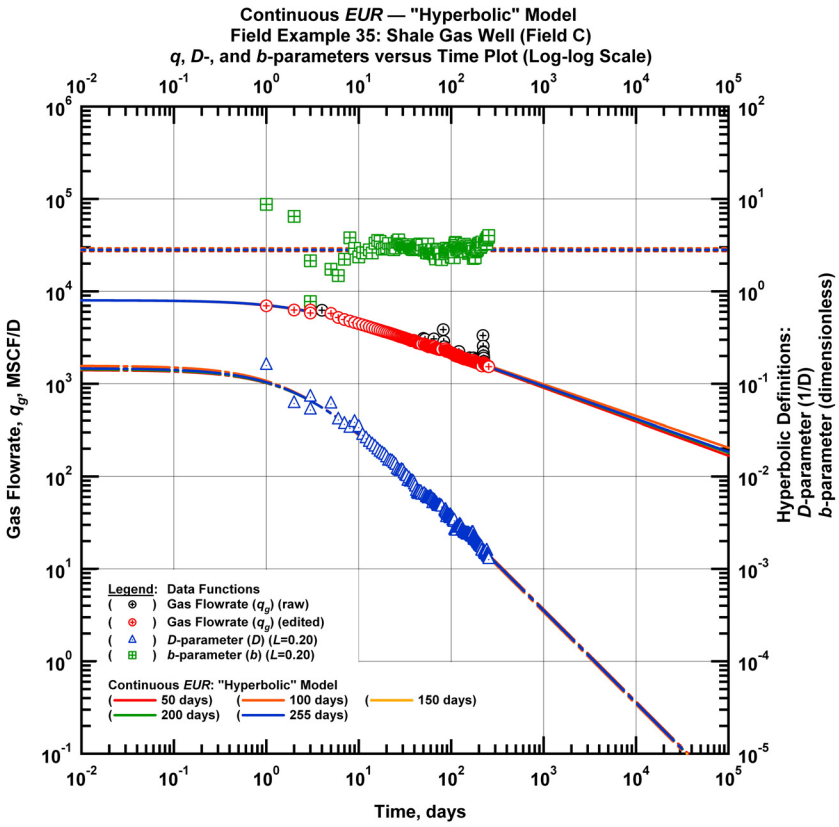

Figure F2 — (Log-log Plot): *qDb* plot — flow rate (q_g), *D*- and *b*-parameters versus production time and "hyperbolic" model matches for field example 35.

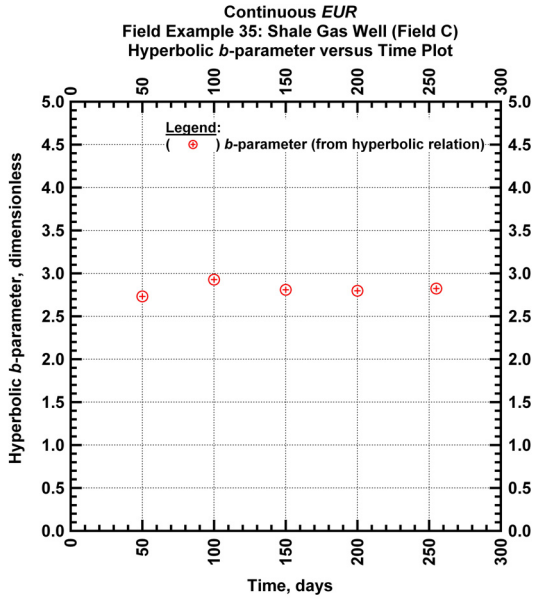

Figure F3 — (Cartesian Plot): Hyperbolic *b*-parameter values obtained from model matches with production data for field example 35.

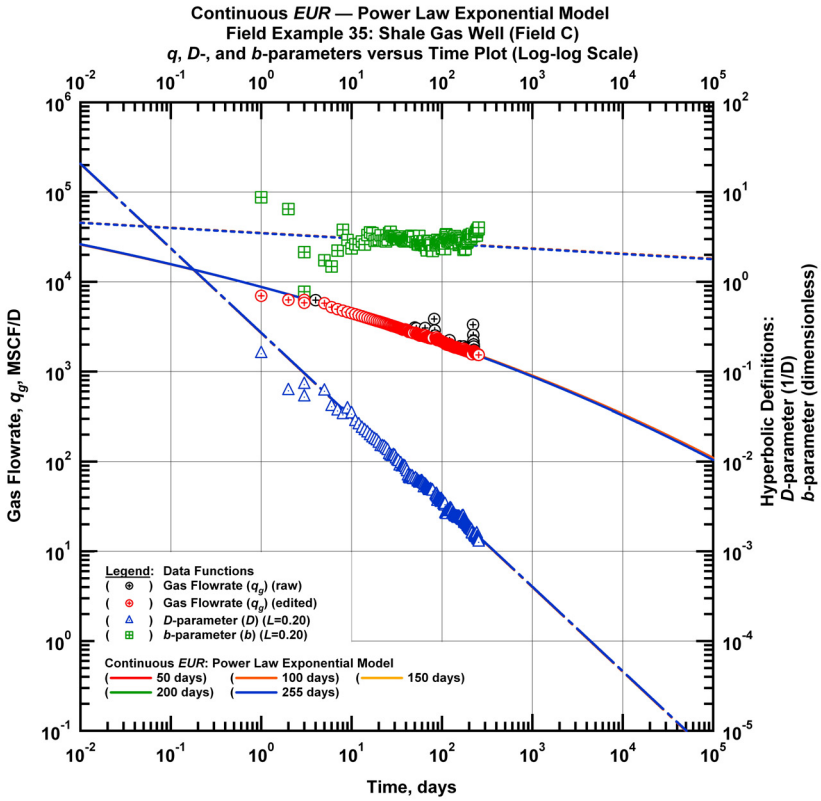

Figure F4 — (Log-log Plot): *qDb* plot — flow rate (q_g), *D*- and *b*-parameters versus production time and power law exponential model matches for field example 35.

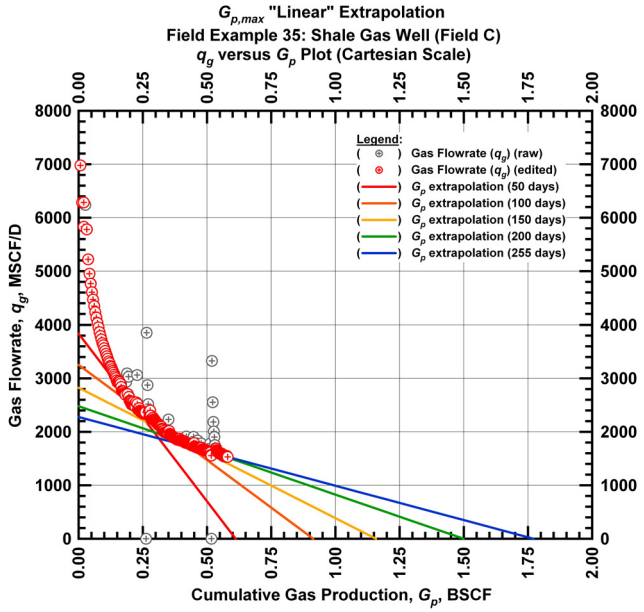

Figure F5 — (Cartesian Plot): Rate Cumulative Plot — flow rate (q_g) versus cumulative production (G_p) and the linear trends fit through the data for field example 35.

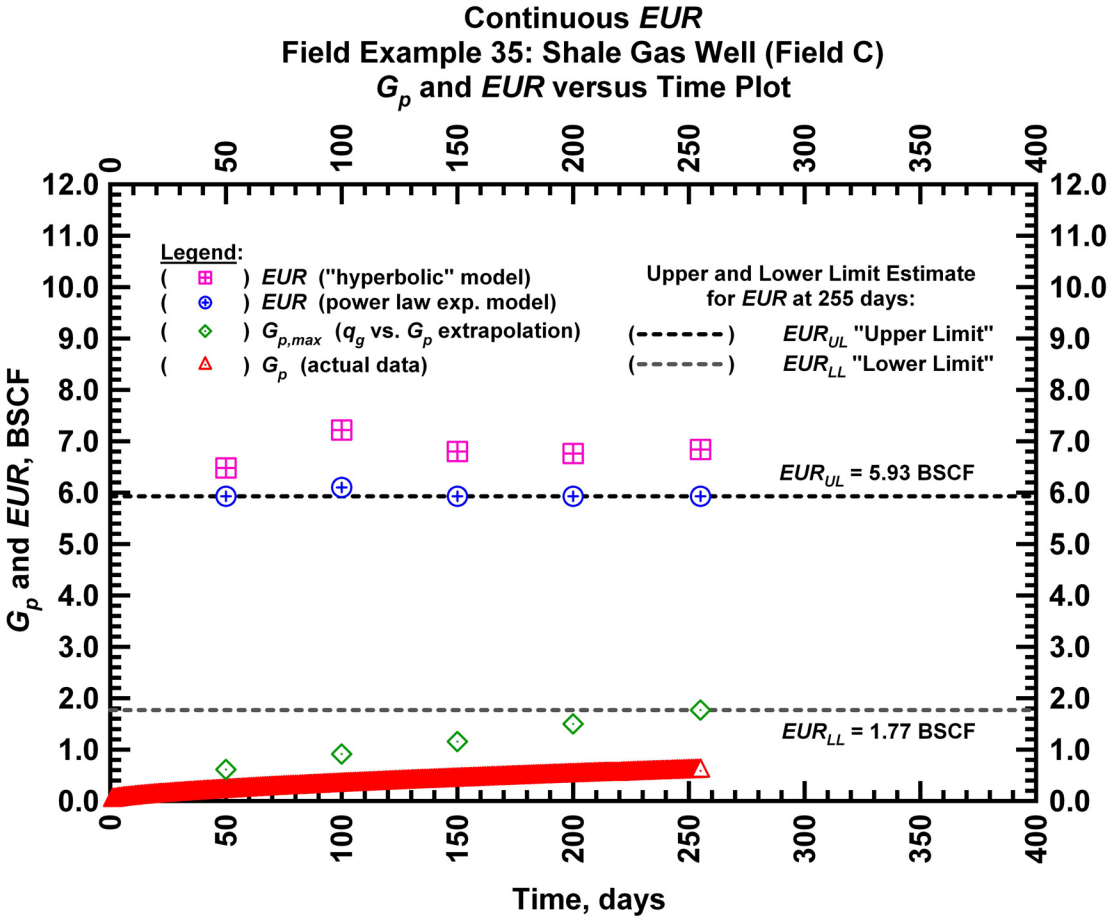

Figure F6 — (Cartesian Plot): *EUR* estimates from model matches and $G_{p,max}$ estimates from extrapolation technique for field example 35.

Table F1 — Analysis results for field example 35 — "hyperbolic" model parameters.

Time Interval, days	q_{gi} (MSCFD)	D_i (D^{-1})	b (dimensionless)	EUR_{hyp} (BSCF)
50	8,000	0.140843	2.7323	6.48
100	8,000	0.156611	2.9276	7.22
150	8,000	0.145182	2.8091	6.80
200	8,000	0.143877	2.7963	6.76
255	8,000	0.146903	2.8223	6.84

Table F2 — Analysis results for field example 35 — power law exponential model parameters.

Time Interval, days	$\hat{q}_{gi}$ (MSCFD)	$\hat{D}_i$ (D^{-1})	n (dimensionless)	D_∞ (D^{-1})	EUR_{PLE} (BSCF)
50	933,190	4.6666	0.0575	0	5.93
100	933,190	4.6666	0.0575	0	6.10
150	933,190	4.6666	0.0580	0	5.93
200	933,190	4.6666	0.0580	0	5.93
255	933,190	4.6666	0.0580	0	5.93

Table F3 — Analysis results for field example 35 — straight line extrapolation.

Time Interval, days	Slope, 10^{-6} D^{-1}	Intercept, MSCF/D	$G_{p,max}$ (BSCF)
50	6,271	3,835	0.61
100	3,561	3,253	0.91
150	2,440	2,825	1.16
200	1,654	2,480	1.50
255	1,286	2,278	1.77

Field Example 36

We present the flow rate data and the cumulative production data which spans almost 0.8 years for a horizontal well producing from a shale gas reservoir in **Fig. F7**. **Fig. F8** presents the "hyperbolic" model matches imposed on the flow rate data along with the *D*- and *b*-parameter trends. In **Fig. F9** we observe that the value of the *b*-parameter as a function of time. The *b*-parameter value decreases from 4.6 to 2.7 during the production history. Every interval is matched with a "hyperbolic" *b*-parameter greater than 1 indicating that boundary-dominated flow has not been established. **Fig. F10** shows the power law exponential model matches imposed on the flow rate data and *D*- and *b*-parameter trends. In **Fig. F11** we show the results of the straight line extrapolation technique, and in **Fig. F12** we present the calculated *EUR* values versus production time. All of the model parameters for this example are presented in **Tables F4, F5, and F6**. The *EUR* of this well should be in between 3.51 BSCF (the "lower" limit given by the straight line extrapolation technique at 286 days) and 6.81 BSCF (the "upper" limit given by the power law exponential estimate at 286 days).

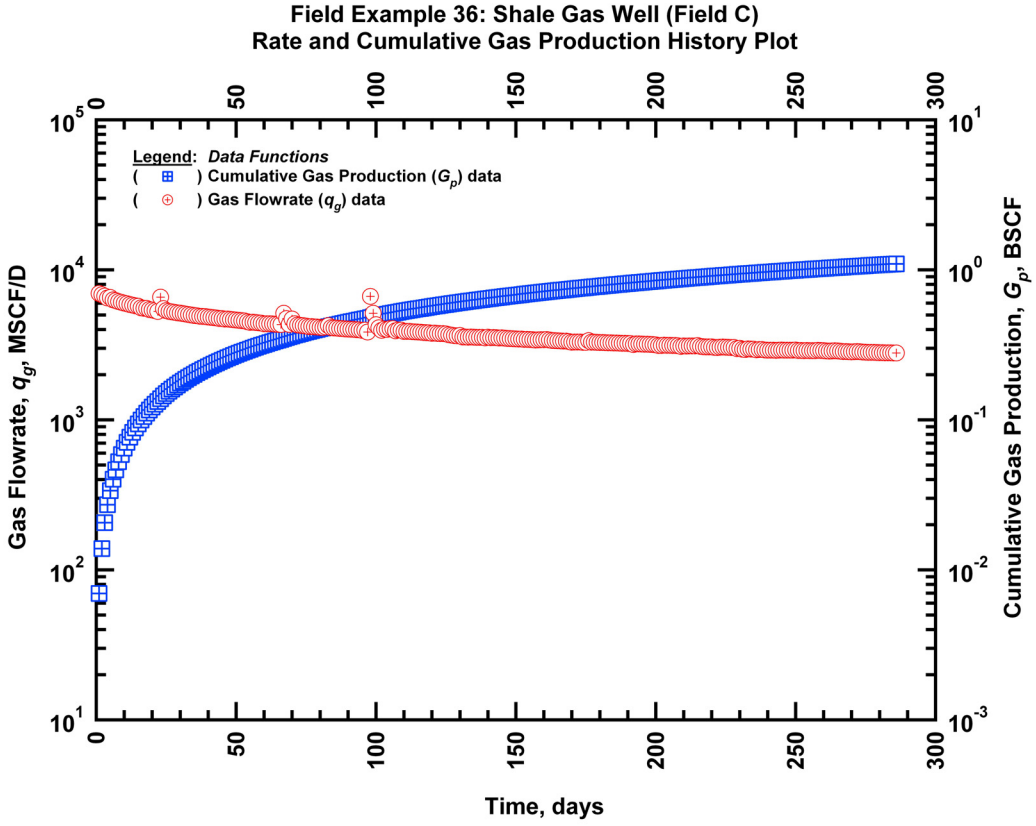

Figure F7 — (Semi-log Plot): Production history plot for field example 36 — flow rate (q_g) and cumulative production (G_p) versus production time.

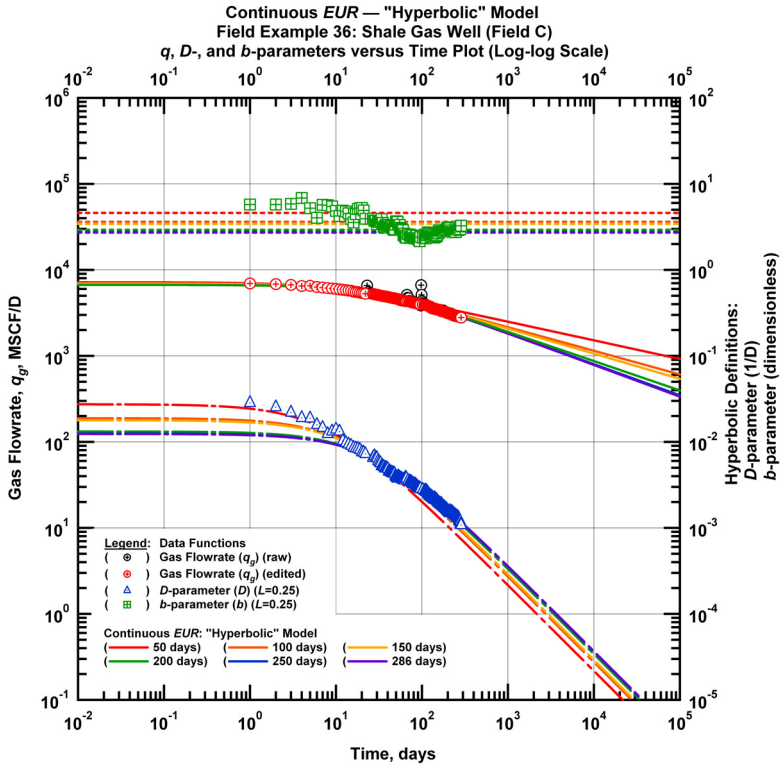

Figure F8 — (Log-log Plot): *qDb* plot — flow rate (q_g), *D*- and *b*-parameters versus production time and "hyperbolic" model matches for field example 36.

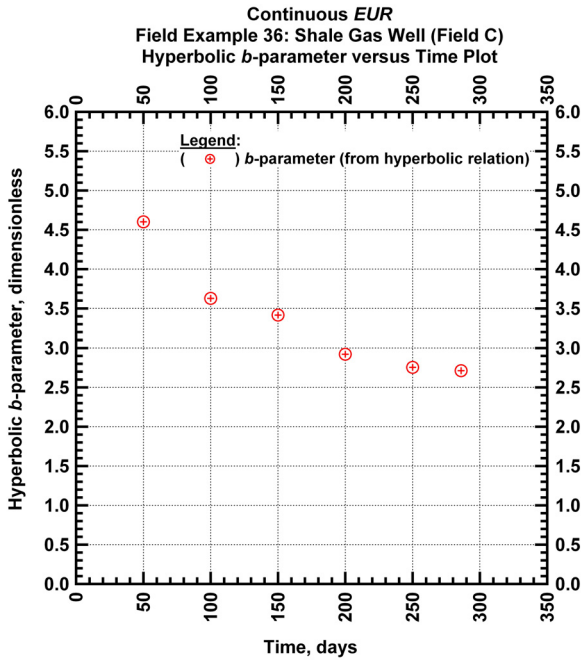

Figure F9 — (Cartesian Plot): Hyperbolic *b*-parameter values obtained from model matches with production data for field example 36.

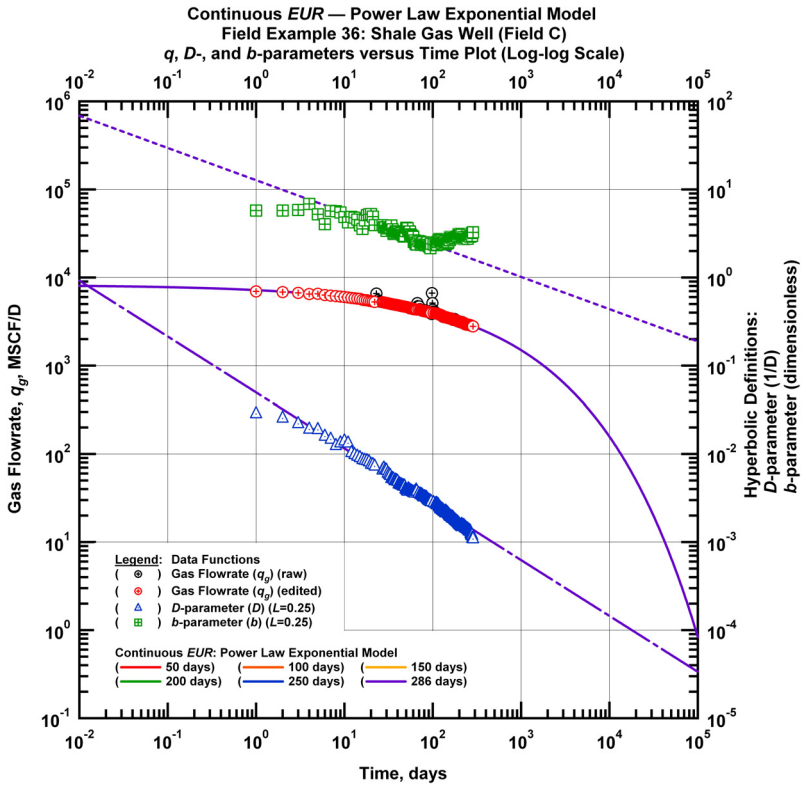

Figure F10 — (Log-log Plot): *qDb* plot — flow rate (q_g), *D*- and *b*-parameters versus production time and power law exponential model matches for field example 36.

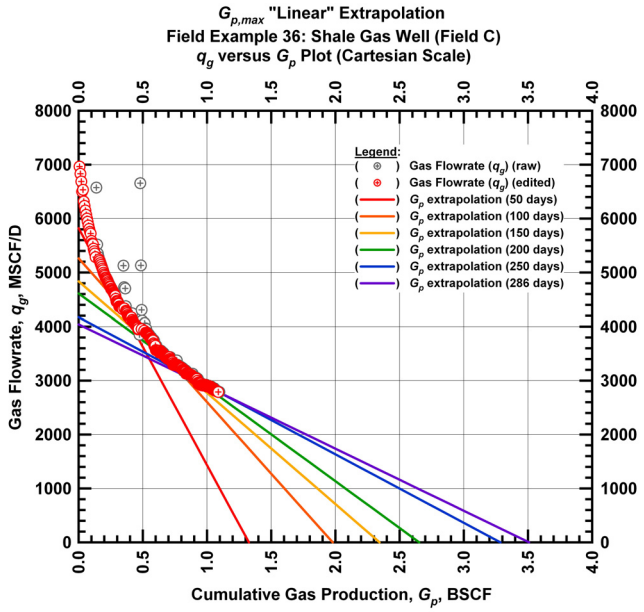

Figure F11 — (Cartesian Plot): Rate Cumulative Plot — flow rate (q_g) versus cumulative production (G_p) and the linear trends fit through the data for field example 36.

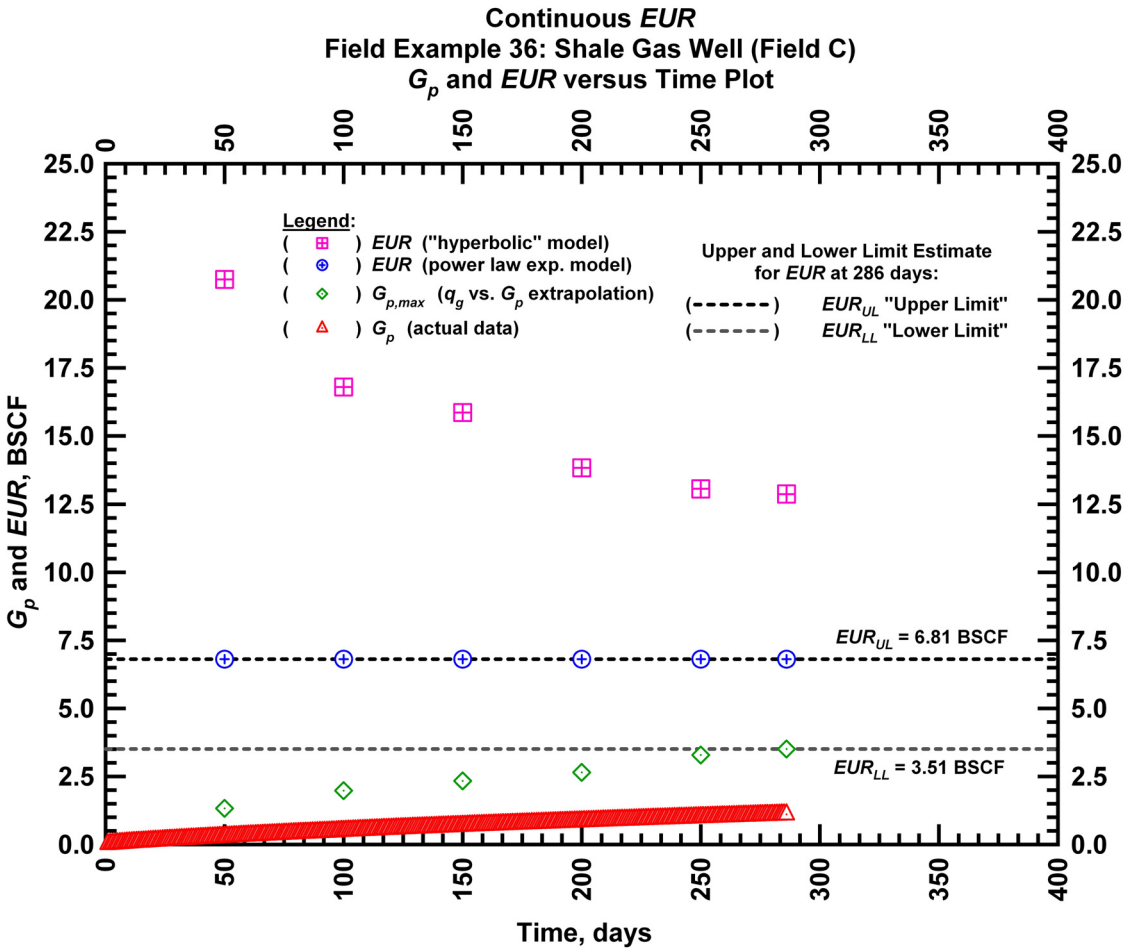

Figure F12 — (Cartesian Plot): *EUR* estimates from model matches and $G_{p,max}$ estimates from extrapolation technique for field example 36.

Table F4 — Analysis results for field example 36 — "hyperbolic" model parameters.

Time Interval, days	q_{gi} (MSCFD)	D_i (D^{-1})	b (dimensionless)	EUR_{hyp} (BSCF)
50	7,161	0.02740	4.601	20.75
100	6,941	0.01887	3.628	16.80
150	6,941	0.01784	3.415	15.86
200	6,698	0.01321	2.921	13.83
250	6,698	0.01254	2.754	13.06
286	6,698	0.01236	2.712	12.87

Table F5 — Analysis results for field example 36 — power law exponential model parameters.

Time Interval, days	$\hat{q}_{gi}$ (MSCFD)	$\hat{D}_i$ (D^{-1})	n (dimensionless)	D_∞ (D^{-1})	EUR_{PLE} (BSCF)
50	8,240	0.136	0.366	0	6.81
100	8,240	0.136	0.366	0	6.81
150	8,240	0.136	0.366	0	6.81
200	8,240	0.136	0.366	0	6.81
250	8,240	0.136	0.366	0	6.81
286	8,240	0.136	0.366	0	6.81

Table F6 — Analysis results for field example 36 — straight line extrapolation.

Time Interval, days	Slope, 10^{-6} D^{-1}	Intercept, MSCF/D	$G_{p,max}$ (BSCF)
50	4,390	5,821	1.33
100	2,659	5,262	1.98
150	2,063	4,836	2.34
200	1,738	4,611	2.65
250	1,270	4,173	3.29
286	1,152	4,042	3.51

Field Example 37

We present the flow rate data and the cumulative production data which spans over 1.5 years for a horizontal well producing from a shale gas reservoir in **Fig. F13**. **Fig. F14** presents the "hyperbolic" model matches imposed on the flow rate data along with the *D*- and *b*-parameter trends. In **Fig. F15** we observe that the value of the *b*-parameter as a function of time. The *b*-parameter value decreases from 4.2 to 2.4 during the production history. Every interval is matched with a "hyperbolic" *b*-parameter greater than 1 indicating that boundary-dominated flow has not been established. **Fig. F16** shows the power law exponential model matches imposed on the flow rate data and *D*- and *b*-parameter trends. In **Fig. F17** we show the results of the straight line extrapolation technique, and in **Fig. F18** we present the calculated *EUR* values versus production time. All of the model parameters for this example are presented in **Tables F7, F8, and F9**. The *EUR* of this well should be in between 3.87 BSCF (the "lower" limit given by the straight line extrapolation technique at 553 days) and 6.24 BSCF (the "upper" limit given by the power law exponential estimate at 553 days).

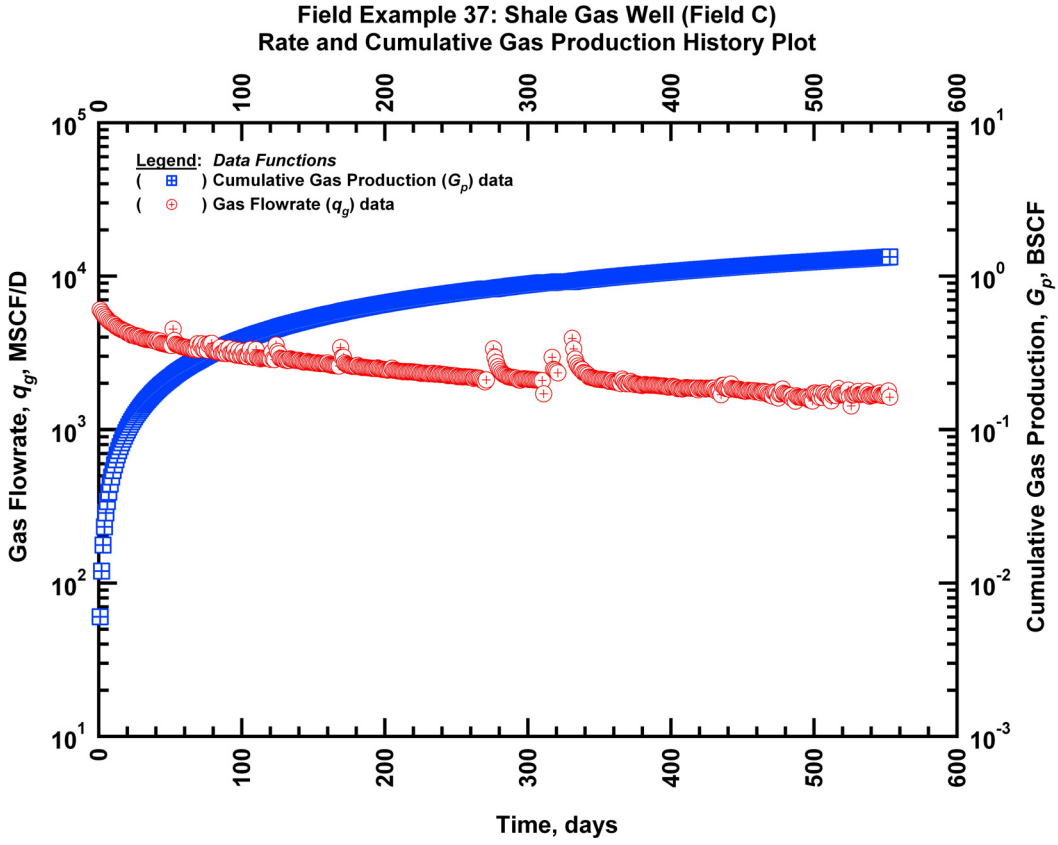

Figure F13 — (Semi-log Plot): Production history plot for field example 37 — flow rate (q_g) and cumulative production (G_p) versus production time.

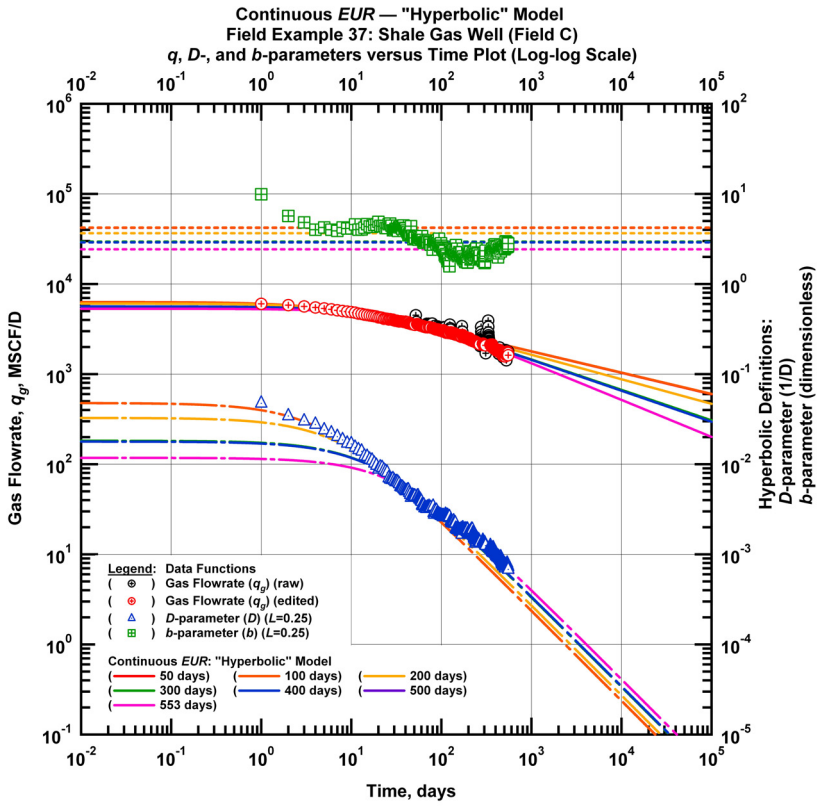

Figure F14 — (Log-log Plot): *qDb* plot — flow rate (q_g), *D*- and *b*-parameters versus production time and "hyperbolic" model matches for field example 37.

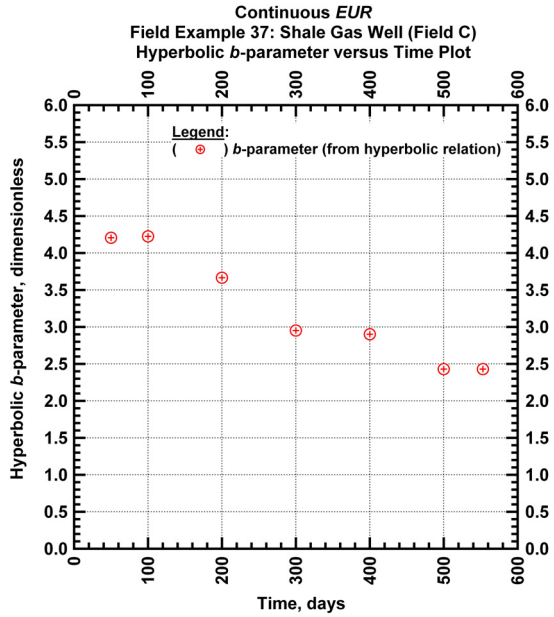

Figure F15 — (Cartesian Plot): Hyperbolic *b*-parameter values obtained from model matches with production data for field example 37.

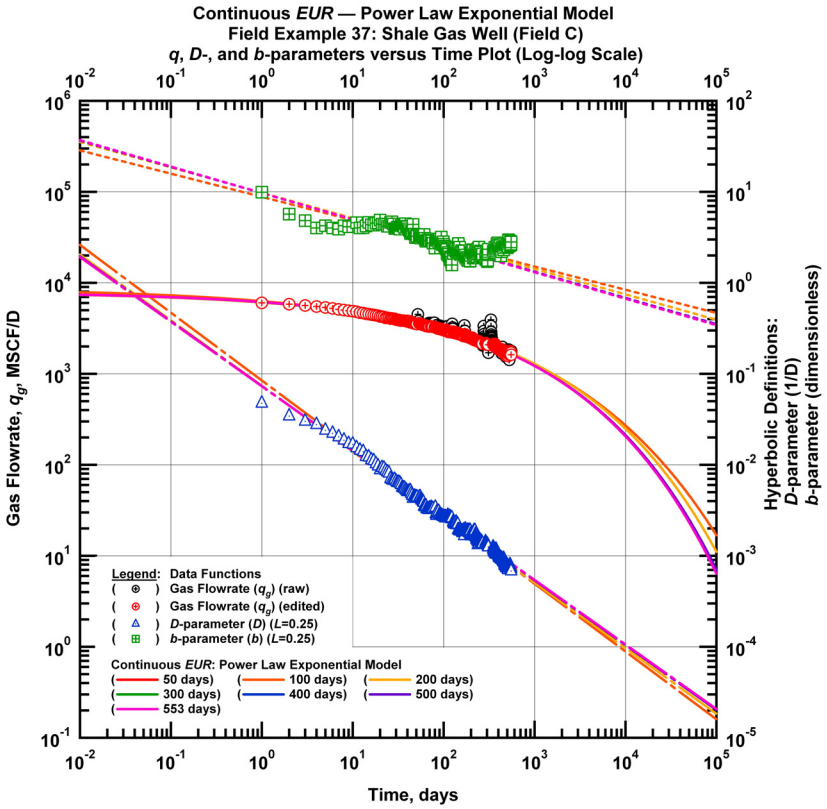

Figure F16 — (Log-log Plot): *qDb* plot — flow rate (q_g), *D*- and *b*-parameters versus production time and power law exponential model matches for field example 37.

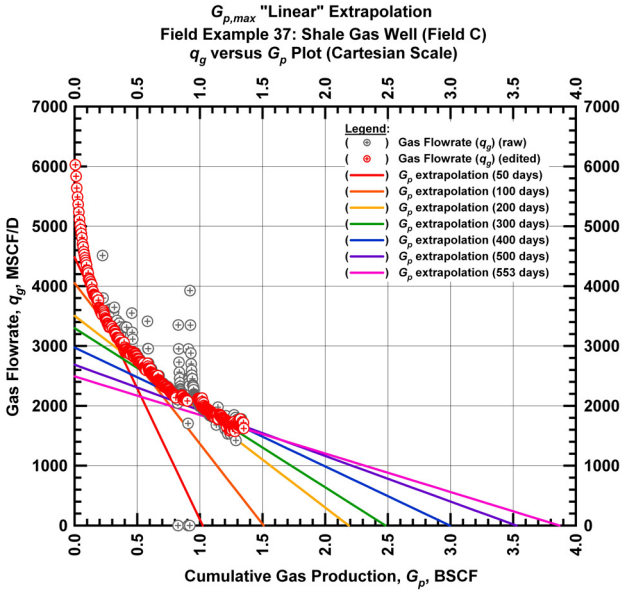

Figure F17 — (Cartesian Plot): Rate Cumulative Plot — flow rate (q_g) versus cumulative production (G_p) and the linear trends fit through the data for field example 37.

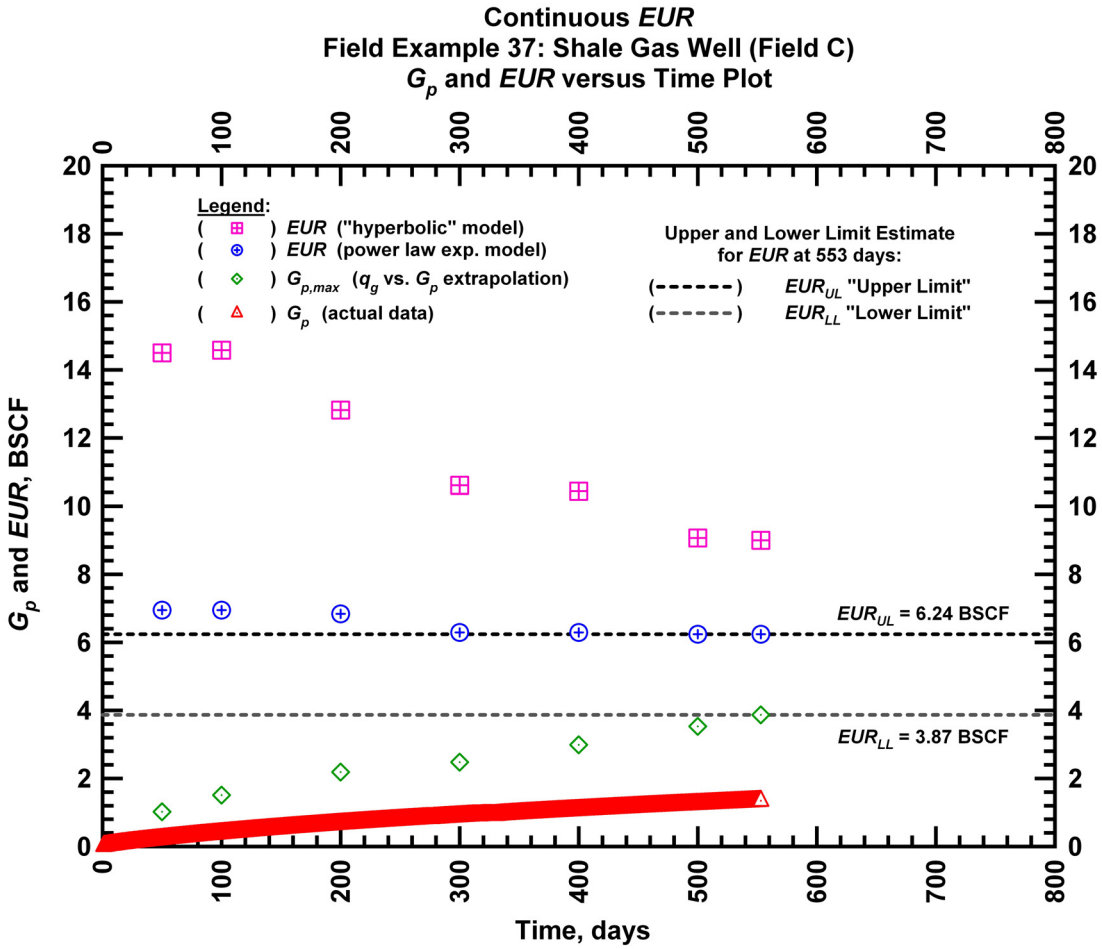

Figure F18 — (Cartesian Plot): *EUR* estimates from model matches and $G_{p,max}$ estimates from extrapolation technique for field example 37.

Table F7 — Analysis results for field example 37 — "hyperbolic" model parameters.

Time Interval, days	q_{gi} (MSCFD)	D_i (D^{-1})	b (dimensionless)	EUR_{hyp} (BSCF)
50	6,308	0.047757	4.2060	14.50
100	6,308	0.047782	4.2245	14.58
200	6,065	0.032676	3.6661	12.82
300	5,635	0.018212	2.9515	10.61
400	5,635	0.017825	2.9021	10.44
500	5,320	0.011775	2.4293	9.07
553	5,320	0.011775	2.4293	9.00

Table F8 — Analysis results for field example 37 — power law exponential model parameters.

Time Interval, days	$\hat{q}_{gi}$ (MSCFD)	$\hat{D}_i$ (D^{-1})	n (dimensionless)	D_∞ (D^{-1})	EUR_{PLE} (BSCF)
50	8,754	0.3314	0.2552	0	6.95
100	8,754	0.3314	0.2552	0	6.95
200	7,912	0.2641	0.2792	0	6.84
300	7,912	0.2537	0.2889	0	6.29
400	7,912	0.2537	0.2889	0	6.29
500	7,905	0.2550	0.2880	0	6.24
553	7,905	0.2511	0.2906	0	6.24

Table F9 — Analysis results for field example 37 — straight line extrapolation.

Time Interval, days	Slope, 10^{-6} D^{-1}	Intercept, MSCF/D	$G_{p,max}$ (BSCF)
50	4,384	4,482	1.02
100	2,683	4,048	1.51
200	1,601	3,503	2.19
300	1,329	3,297	2.48
400	993	2,974	2.99
500	762	2,687	3.53
553	644	2,492	3.87

Field Example 38

We present the flow rate data and the cumulative production data which spans almost 1 year for a horizontal well producing from a shale gas reservoir in **Fig. F19**. **Fig. F20** presents the "hyperbolic" model matches imposed on the flow rate data along with the *D*- and *b*-parameter trends. In **Fig. F21** we observe that the value of the *b*-parameter as a function of time. The *b*-parameter value decreases from 2.74 to 2.27 during the production history. Every interval is matched with a "hyperbolic" *b*-parameter greater than 1 indicating that boundary-dominated flow has not been established. **Fig. F22** shows the power law exponential model matches imposed on the flow rate data and *D*- and *b*-parameter trends. In **Fig. F23** we show the results of the straight line extrapolation technique, and in **Fig. F24** we present the calculated *EUR* values versus production time. All of the model parameters for this example are presented in **Tables F10, F11, and F12**. The *EUR* of this well should be in between 1.98 BSCF (the "lower" limit given by the straight line extrapolation technique at 320 days) and 5.32 BSCF (the "upper" limit given by the power law exponential estimate at 320 days).

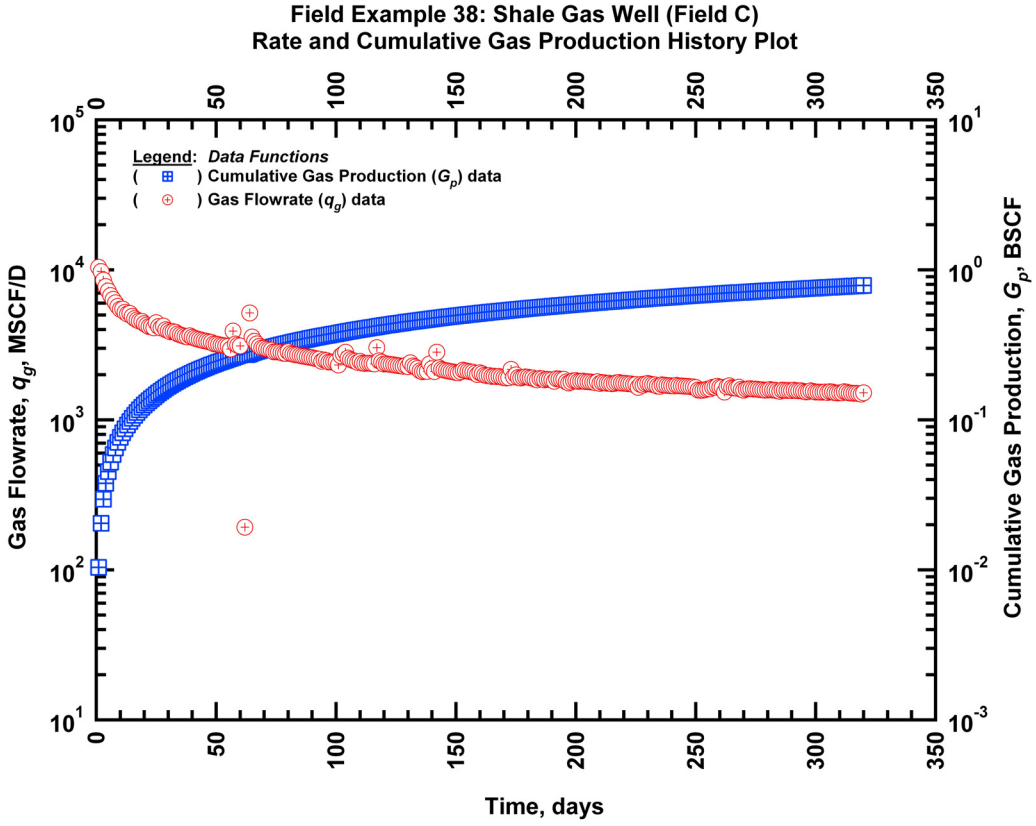

Figure F19 — (Semi-log Plot): Production history plot for field example 38 — flow rate (q_g) and cumulative production (G_p) versus production time.

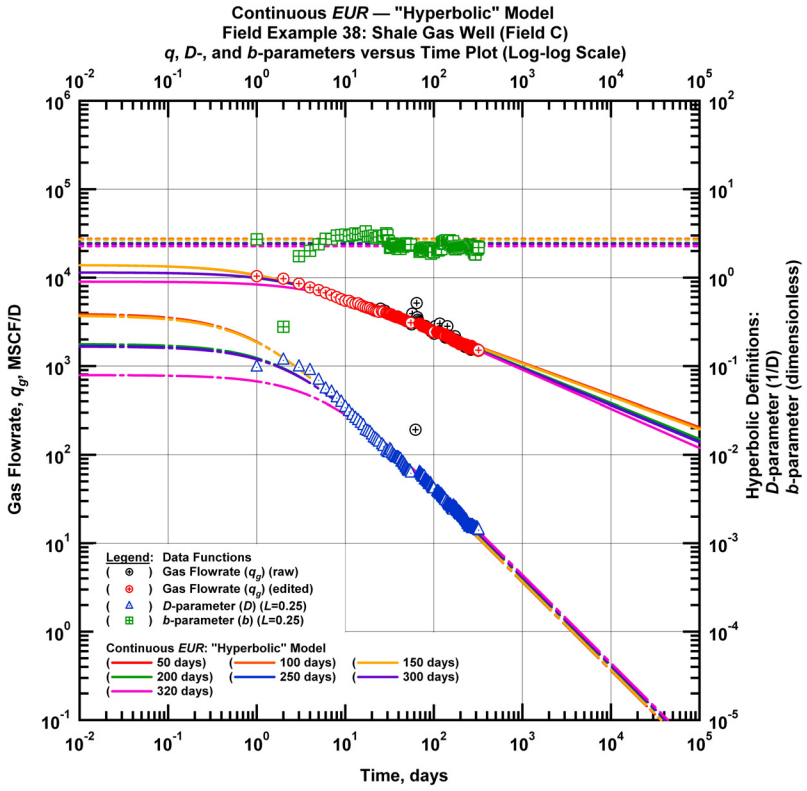

Figure F20 — (Log-log Plot): *qDb* plot — flow rate (q_g), *D*- and *b*-parameters versus production time and "hyperbolic" model matches for field example 38.

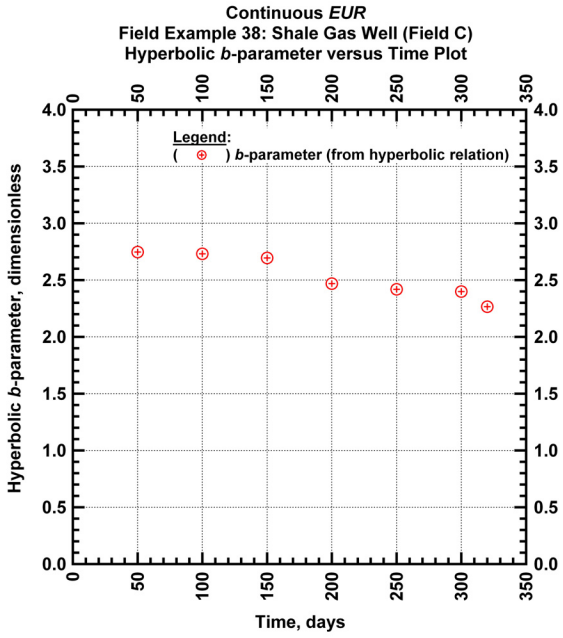

Figure F21 — (Cartesian Plot): Hyperbolic *b*-parameter values obtained from model matches with production data for field example 38.

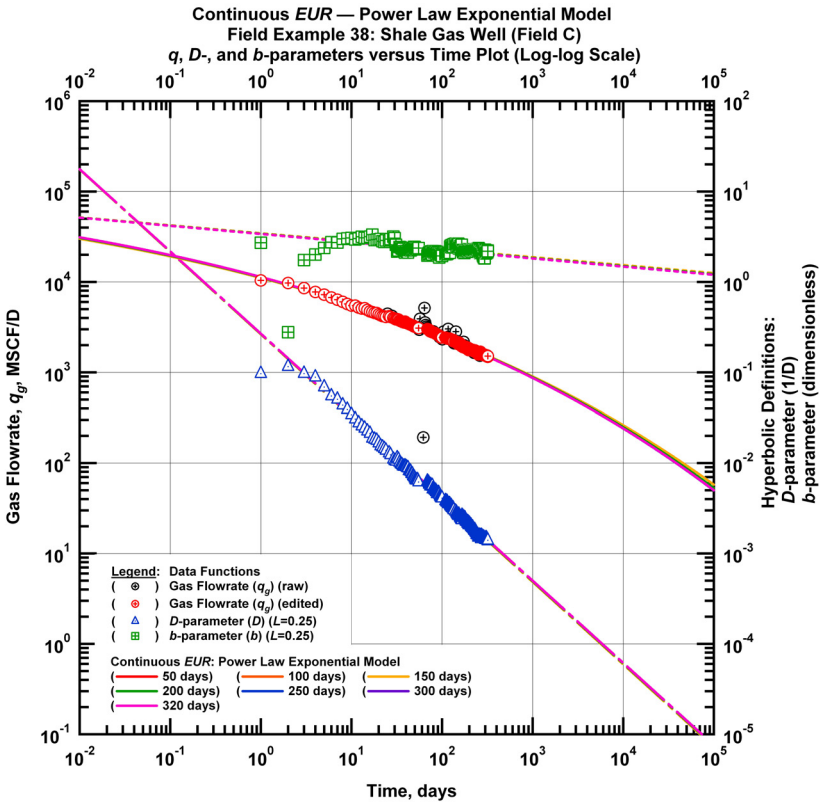

Figure F22 — (Log-log Plot): *qDb* plot — flow rate (q_g), *D*- and *b*-parameters versus production time and power law exponential model matches for field example 38.

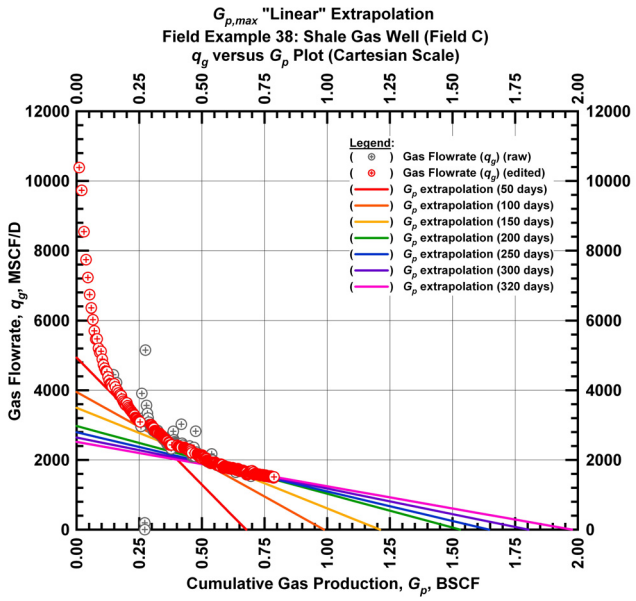

Figure F23 — (Cartesian Plot): Rate Cumulative Plot — flow rate (q_g) versus cumulative production (G_p) and the linear trends fit through the data for field example 38.

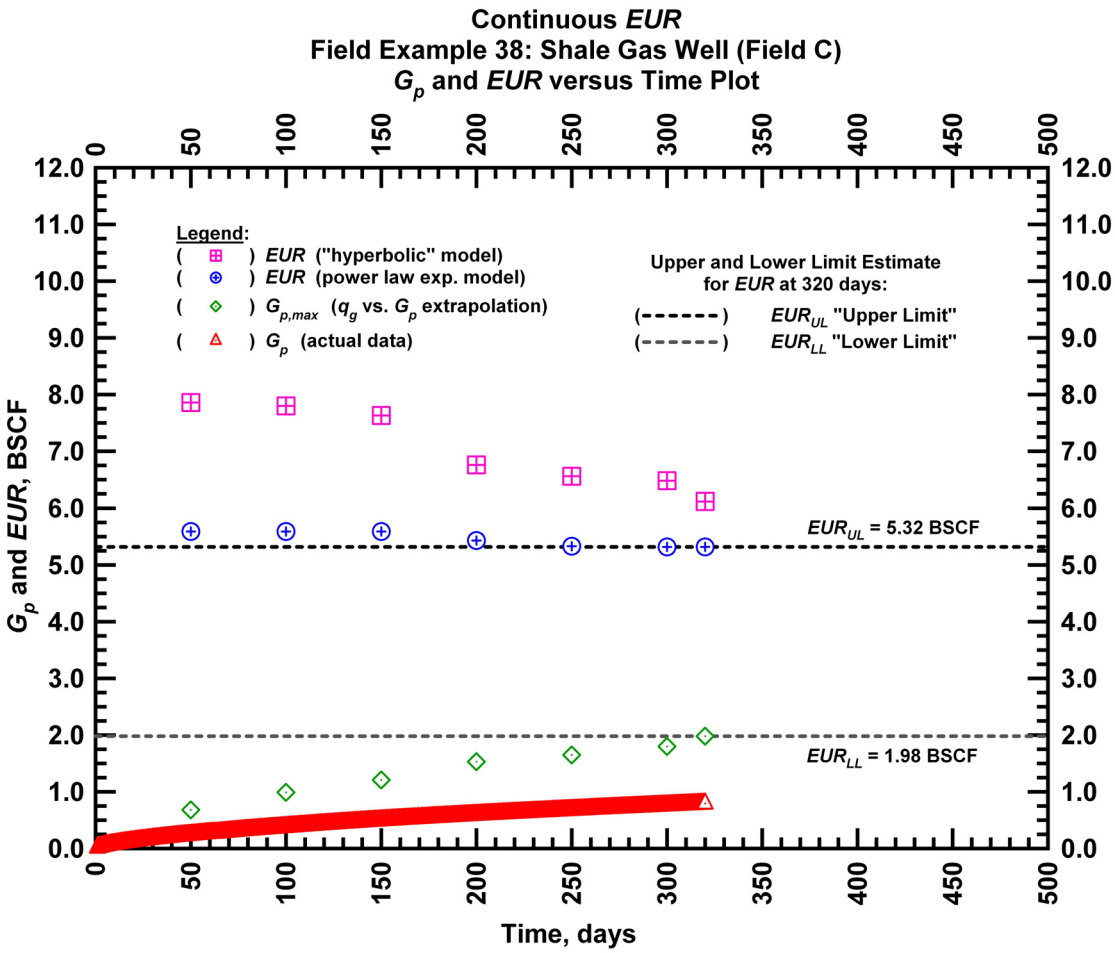

Figure F24 — (Cartesian Plot): *EUR* estimates from model matches and $G_{p,max}$ estimates from extrapolation technique for field example 38.

Table F10 — Analysis results for field example 38 — "hyperbolic" model parameters.

Time Interval, days	q_{gi} (MSCFD)	D_i (D^{-1})	b (dimensionless)	EUR_{hyp} (BSCF)
50	13,863	0.3891	2.7469	7.86
100	13,863	0.3836	2.7316	7.80
150	13,863	0.3711	2.6946	7.63
200	11,441	0.1772	2.4685	6.76
250	11,441	0.1696	2.4190	6.56
300	11,441	0.1663	2.3987	6.48
320	9,000	0.0791	2.2654	6.12

Table F11 — Analysis results for field example 38 — power law exponential model parameters.

Time Interval, days	$\hat{q}_{gi}$ (MSCFD)	$\hat{D}_i$ (D^{-1})	n (dimensionless)	D_∞ (D^{-1})	EUR_{PLE} (BSCF)
50	221,486	2.9966	0.0880	0	5.59
100	221,486	2.9966	0.0880	0	5.59
150	221,486	2.9966	0.0880	0	5.59
200	221,486	2.9801	0.0894	0	5.43
250	221,486	2.9716	0.0902	0	5.33
300	221,486	2.9707	0.0903	0	5.32
320	221,486	2.9715	0.0902	0	5.32

Table F12 — Analysis results for field example 38 — straight line extrapolation.

Time Interval, days	Slope, 10^{-6} D^{-1}	Intercept, MSCF/D	$G_{p,max}$ (BSCF)
50	7,292	4,936	0.68
100	4,003	3,951	0.99
150	2,888	3,497	1.21
200	1,944	2,974	1.53
250	1,699	2,796	1.65
300	1,467	2,645	1.80
320	1,274	2,518	1.98

Field Example 39

We present the flow rate data and the cumulative production data which spans almost 1 year for a horizontal well producing from a shale gas reservoir in **Fig. F25**. **Fig. F26** presents the "hyperbolic" model matches imposed on the flow rate data along with the *D*- and *b*-parameter trends. In **Fig. F27** we observe that the value of the *b*-parameter as a function of time. The *b*-parameter value decreases from 3.1 to 2.2 during the production history. Every interval is matched with a "hyperbolic" *b*-parameter greater than 1 indicating that boundary-dominated flow has not been established. **Fig. F28** shows the power law exponential model matches imposed on the flow rate data and *D*- and *b*-parameter trends. In **Fig. F29** we show the results of the straight line extrapolation technique, and in **Fig. F30** we present the calculated *EUR* values versus production time. All of the model parameters for this example are presented in **Tables F13, F14, and F15**. The *EUR* of this well should be in between 1.20 BSCF (the "lower" limit given by the straight line extrapolation technique at 305 days) and 2.47 BSCF (the "upper" limit given by the power law exponential estimate at 305 days).

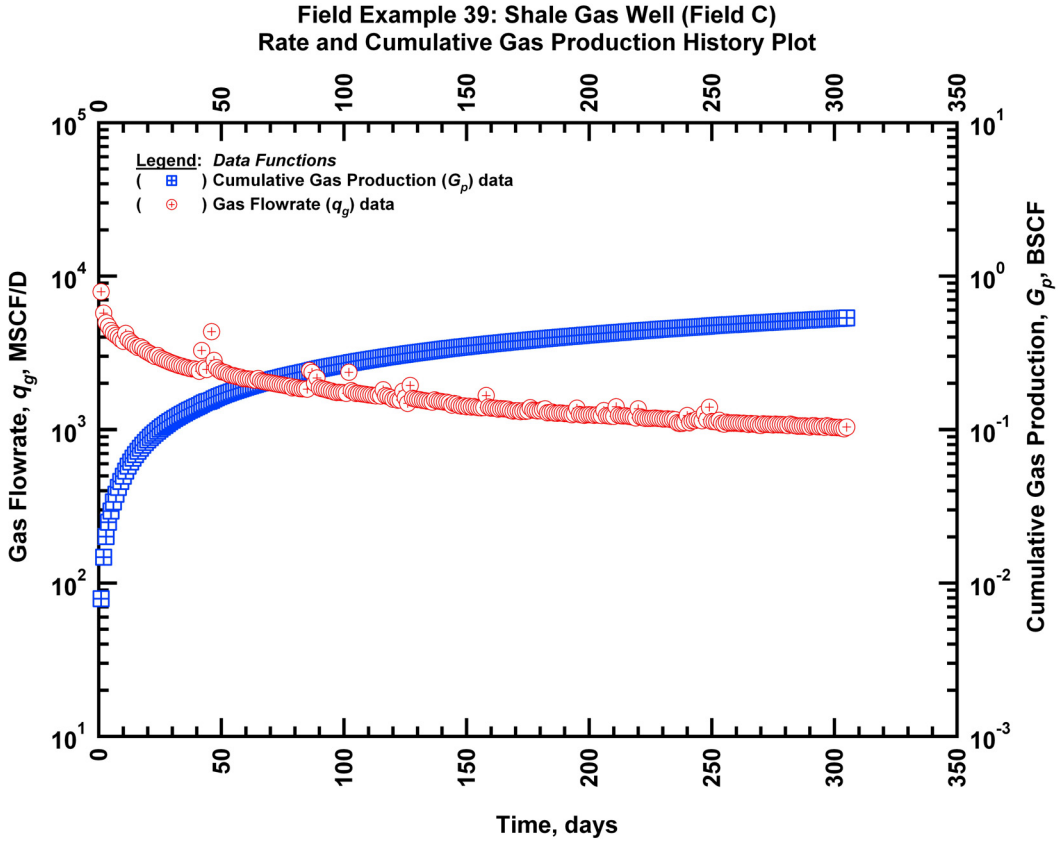

Figure F25 — (Semi-log Plot): Production history plot for field example 39 — flow rate (q_g) and cumulative production (G_p) versus production time.

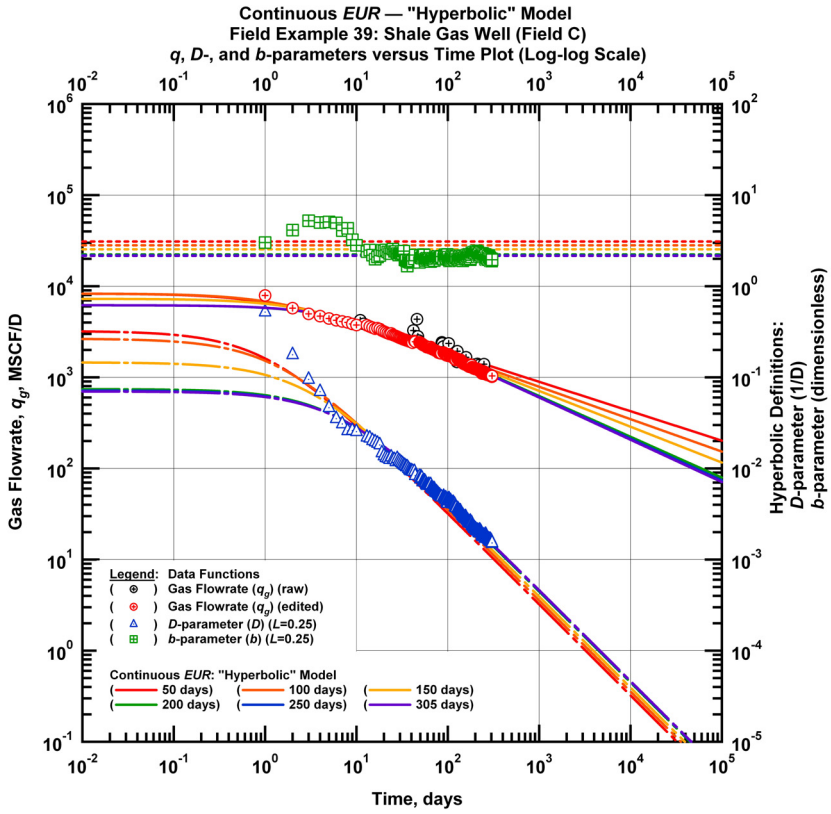

Figure F26 — (Log-log Plot): *qDb* plot — flow rate (q_g), *D*- and *b*-parameters versus production time and "hyperbolic" model matches for field example 39.

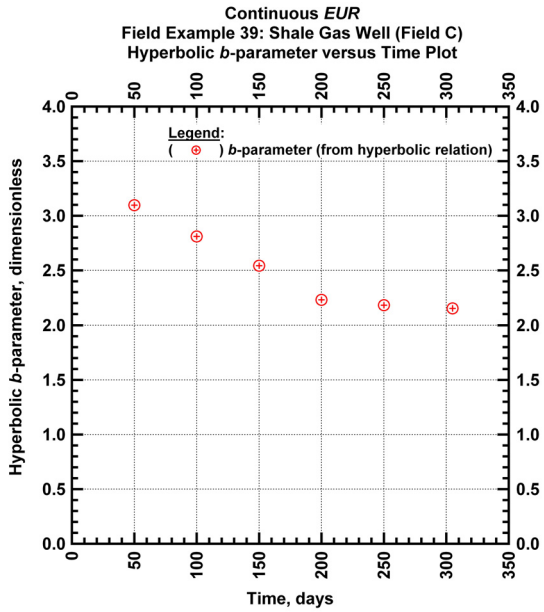

Figure F27 — (Cartesian Plot): Hyperbolic *b*-parameter values obtained from model matches with production data for field example 39.

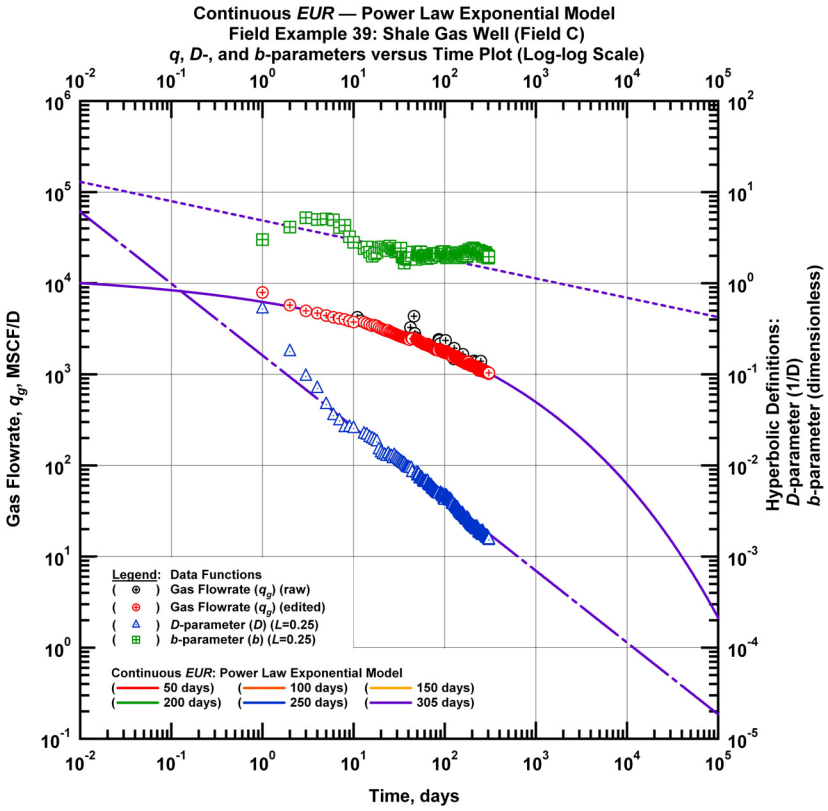

Figure F28 — (Log-log Plot): qDb plot — flow rate (q_g), D- and b-parameters versus production time and power law exponential model matches for field example 39.

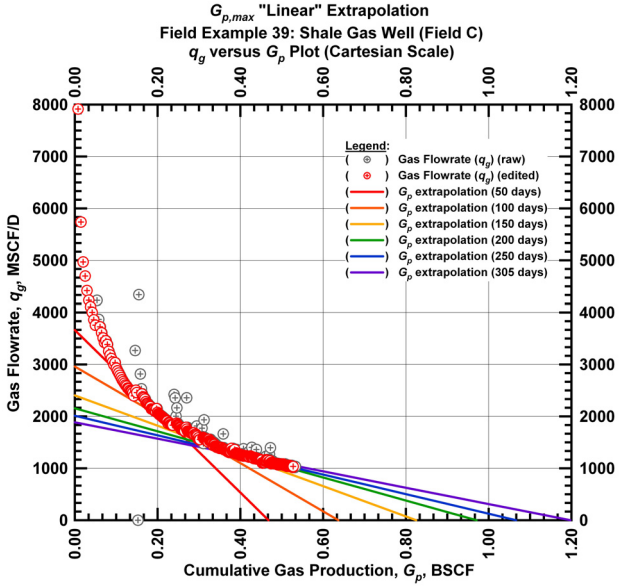

Figure F29 — (Cartesian Plot): Rate Cumulative Plot — flow rate (q_g) versus cumulative production (G_p) and the linear trends fit through the data for field example 39.

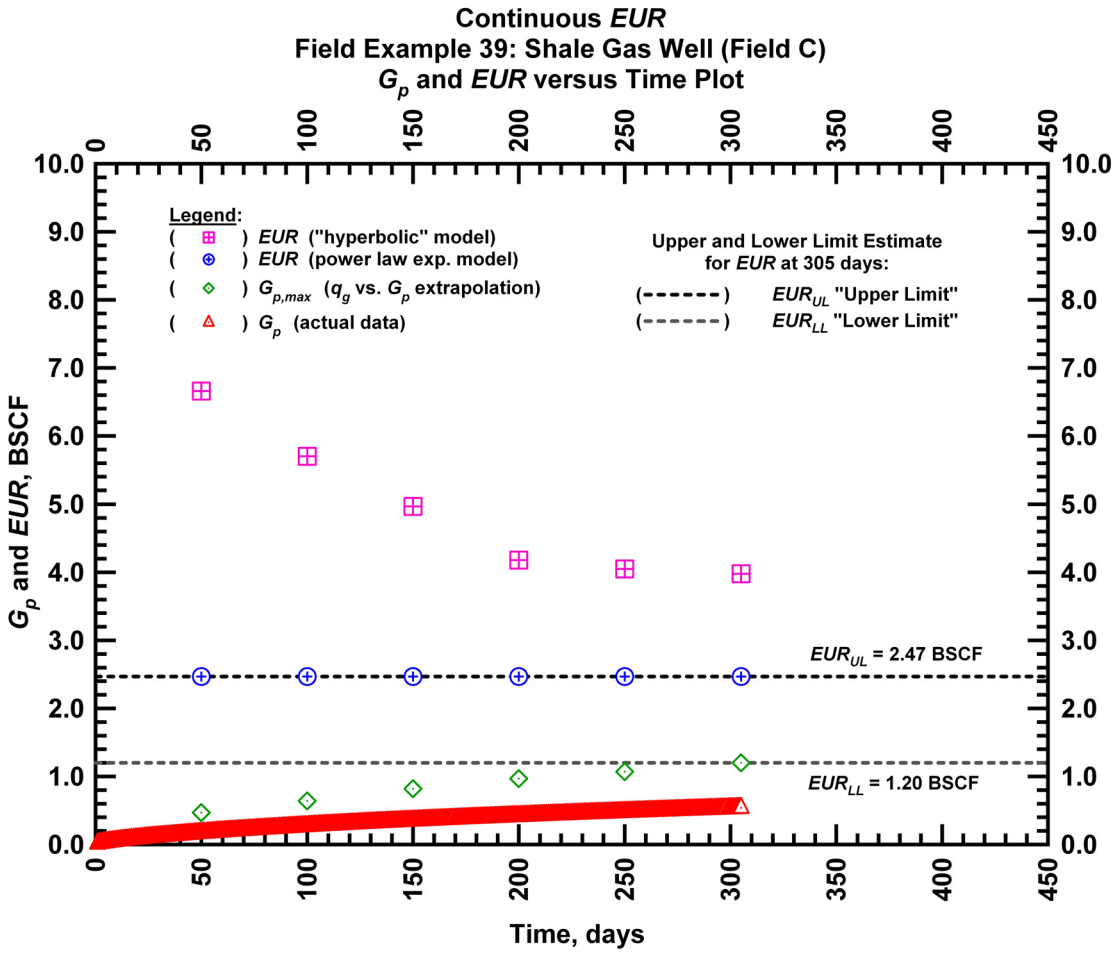

Figure F30 — (Cartesian Plot): *EUR* estimates from model matches and $G_{p,max}$ estimates from extrapolation technique for field example 39.

Table F13 — Analysis results for field example 39 — "hyperbolic" model parameters.

Time Interval, days	q_{gi} (MSCFD)	D_i (D^{-1})	b (dimensionless)	EUR_{hyp} (BSCF)
50	8,303	0.3221	3.0972	6.66
100	8,303	0.2655	2.8101	5.70
150	7,275	0.1459	2.5428	4.97
200	6,190	0.0743	2.2302	4.18
250	6,190	0.0716	2.1815	4.05
305	6,190	0.0700	2.1524	3.98

Table F14 — Analysis results for field example 39 — power law exponential model parameters.

Time Interval, days	$\hat{q}_{gi}$ (MSCFD)	$\hat{D}_i$ (D^{-1})	n (dimensionless)	D_∞ (D^{-1})	EUR_{PLE} (BSCF)
50	13,370	0.7617	0.212	0	2.47
100	13,370	0.7617	0.212	0	2.47
150	13,370	0.7617	0.212	0	2.47
200	13,370	0.7617	0.212	0	2.47
250	13,370	0.7617	0.212	0	2.47
305	13,370	0.7617	0.212	0	2.47

Table F15 — Analysis results for field example 39 — straight line extrapolation.

Time Interval, days	Slope, 10^{-6} D^{-1}	Intercept, MSCF/D	$G_{p,max}$ (BSCF)
50	7,826	3,663	0.47
100	4,649	2,960	0.64
150	2,916	2,405	0.82
200	2,221	2,156	0.97
250	1,887	2,012	1.07
305	1,575	1,886	1.20

Field Example 40

We present the flow rate data and the cumulative production data which spans almost 0.6 years for a horizontal well producing from a shale gas reservoir in **Fig. F31**. **Fig. F32** presents the "hyperbolic" model matches imposed on the flow rate data along with the *D*- and *b*-parameter trends. In **Fig. F33** we observe that the value of the *b*-parameter as a function of time. The *b*-parameter value is relatively stable around 2.46 for the entire production history. Every interval is matched with a "hyperbolic" *b*-parameter greater than 1 indicating that boundary-dominated flow has not been established. **Fig. F34** shows the power law exponential model matches imposed on the flow rate data and *D*- and *b*-parameter trends. In **Fig. F35** we show the results of the straight line extrapolation technique, and in **Fig. F36** we present the calculated *EUR* values versus production time. All of the model parameters for this example are presented in **Tables F16, F17, and F18**. The *EUR* of this well should be in between 1.35 BSCF (the "lower" limit given by the straight line extrapolation technique at 218 days) and 2.67 BSCF (the "upper" limit given by the power law exponential estimate at 218 days).

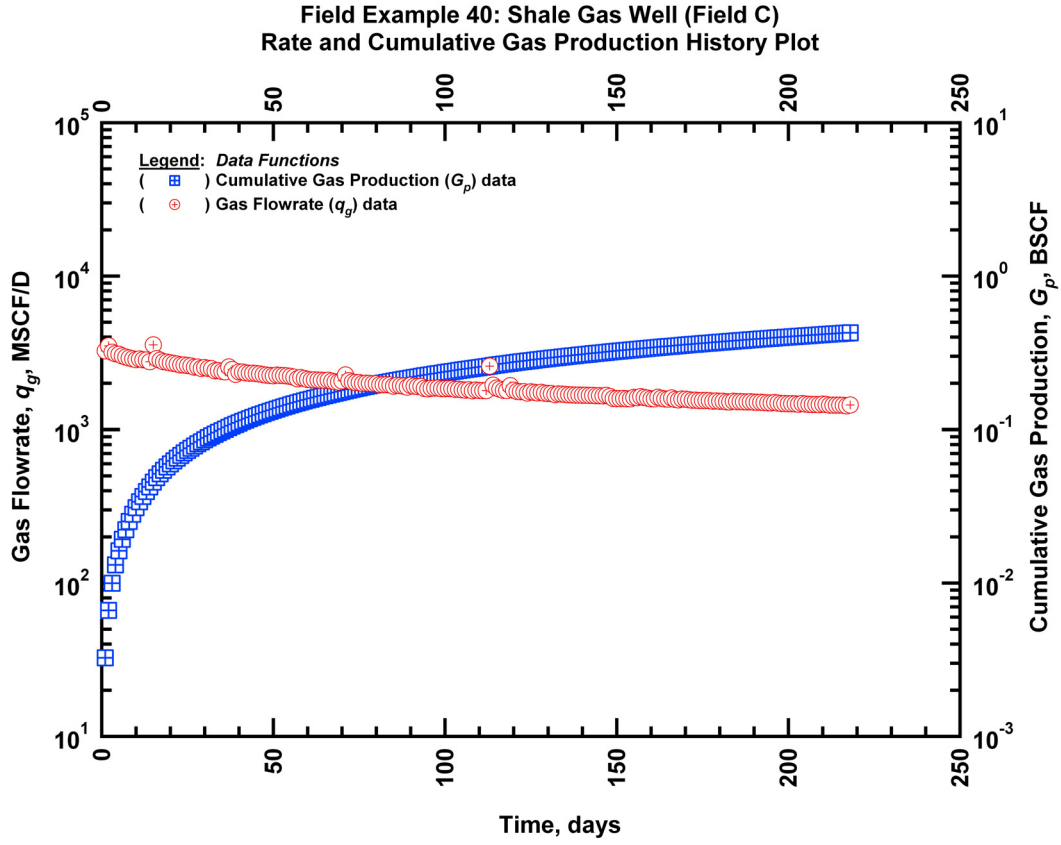

Figure F31 — (Semi-log Plot): Production history plot for field example 40 — flow rate (q_g) and cumulative production (G_p) versus production time.

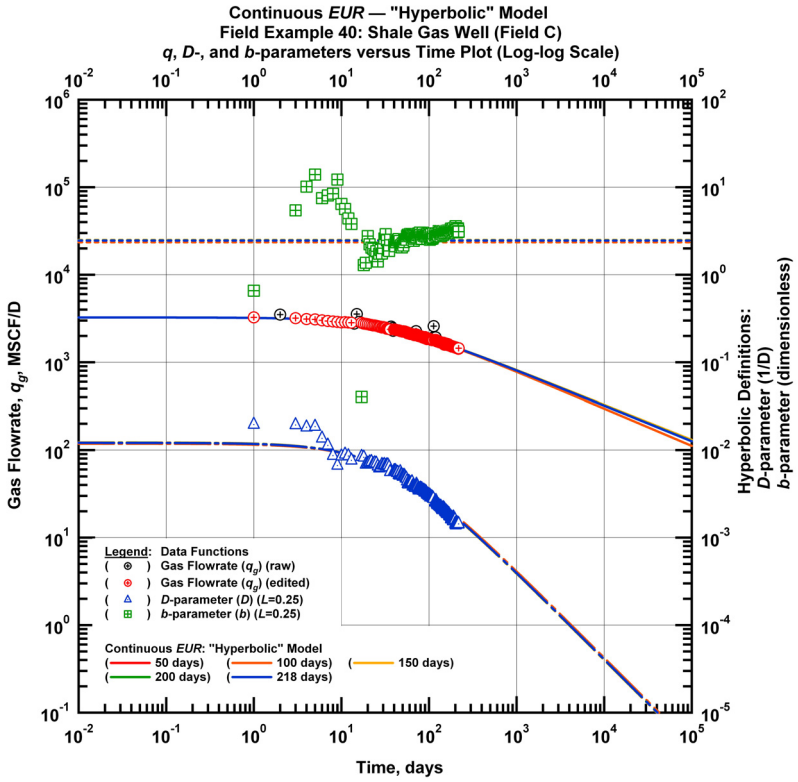

Figure F32 — (Log-log Plot): *qDb* plot — flow rate (q_g), *D*- and *b*-parameters versus production time and "hyperbolic" model matches for field example 40.

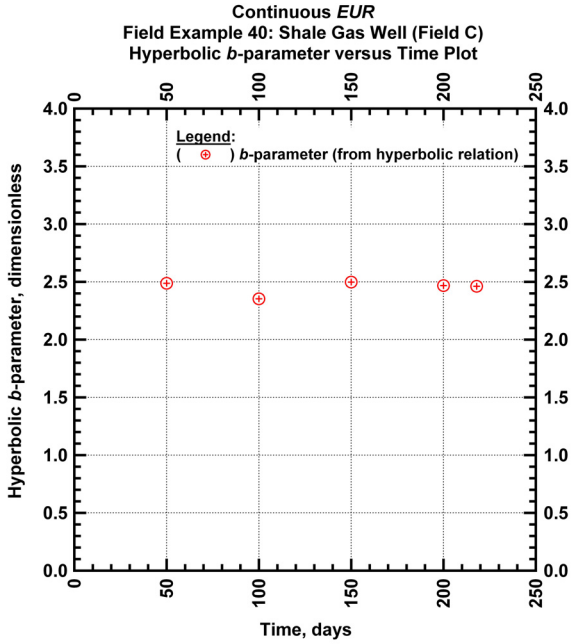

Figure F33 — (Cartesian Plot): Hyperbolic *b*-parameter values obtained from model matches with production data for field example 40.

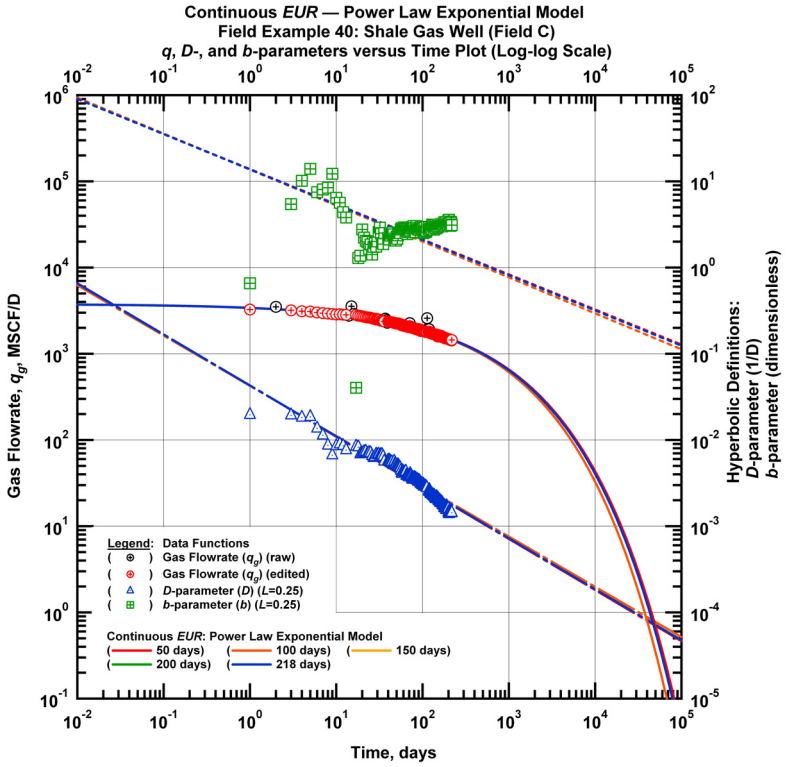

Figure F34 — (Log-log Plot): *qDb* plot — flow rate (q_g), *D*- and *b*-parameters versus production time and power law exponential model matches for field example 40.

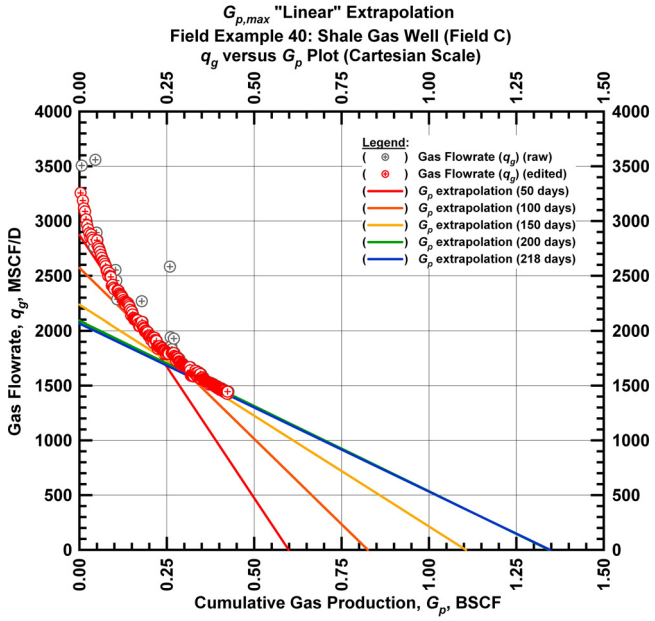

Figure F35 — (Cartesian Plot): Rate Cumulative Plot — flow rate (q_g) versus cumulative production (G_p) and the linear trends fit through the data for field example 40.

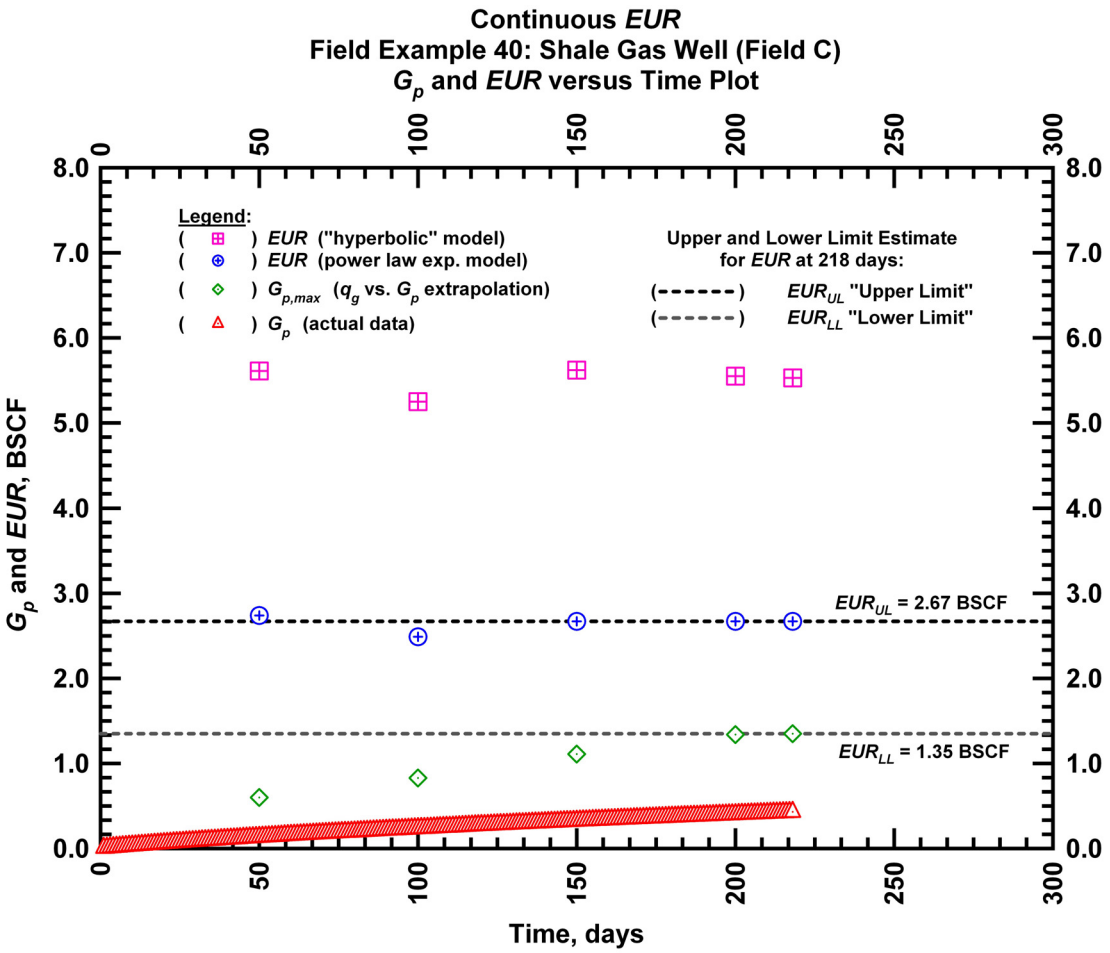

Figure F36 — (Cartesian Plot): *EUR* estimates from model matches and $G_{p,max}$ estimates for field example 40.

Table F16 — Analysis results for field example 40 — "hyperbolic" model parameters.

Time Interval, days	q_{gi} (MSCFD)	D_i (D^{-1})	b (dimensionless)	EUR_{hyp} (BSCF)
50	3,249	0.01	2.49	5.61
100	3,249	0.01	2.35	5.25
150	3,249	0.01	2.50	5.62
200	3,249	0.01	2.47	5.55
218	3,249	0.01	2.46	5.53

Table F17 — Analysis results for field example 40 — power law exponential model parameters.

Time Interval, days	$\hat{q}_{gi}$ (MSCFD)	$\hat{D}_i$ (D^{-1})	n (dimensionless)	D_∞ (D^{-1})	EUR_{PLE} (BSCF)
50	3,776	0.1052	0.407	0	2.74
100	3,776	0.1020	0.417	0	2.49
150	3,776	0.1049	0.409	0	2.67
200	3,776	0.1049	0.409	0	2.67
218	3,776	0.1049	0.409	0	2.67

Table F18 — Analysis results for field example 40 — straight line extrapolation.

Time Interval, days	Slope, 10^{-6} D^{-1}	Intercept, MSCF/D	$G_{p,max}$ (BSCF)
50	4,798	2,872	0.60
100	3,117	2,572	0.83
150	2,022	2,236	1.11
200	1,557	2,092	1.34
218	1,535	2,067	1.35

APPENDIX G
EXAMPLES FROM FIELD D

Field Example 41

We present the flow rate data and the cumulative production data which spans almost 2 years for a vertical well producing from a shale gas reservoir in **Fig. G1**. **Fig. G2** presents the "hyperbolic" model matches imposed on the flow rate data along with the *D*- and *b*-parameter trends. In **Fig. G3** we observe that the value of the *b*-parameter as a function of time. The *b*-parameter value decreases from 2.87 to 2.31 during the production history. Every interval is matched with a "hyperbolic" *b*-parameter greater than 1 indicating that boundary-dominated flow has not been established. **Fig. G4** shows the power law exponential model matches imposed on the flow rate data and *D*- and *b*-parameter trends. In **Fig. G5** we show the results of the straight line extrapolation technique, and in **Fig. G6** we present the calculated *EUR* values versus production time. All of the model parameters for this example are presented in **Tables G1, G2, and G3**. The *EUR* of this well should be in between 0.13 BSCF (the "lower" limit given by the straight line extrapolation technique at 728 days) and 0.20 BSCF (the "upper" limit given by the power law exponential estimate at 728 days).

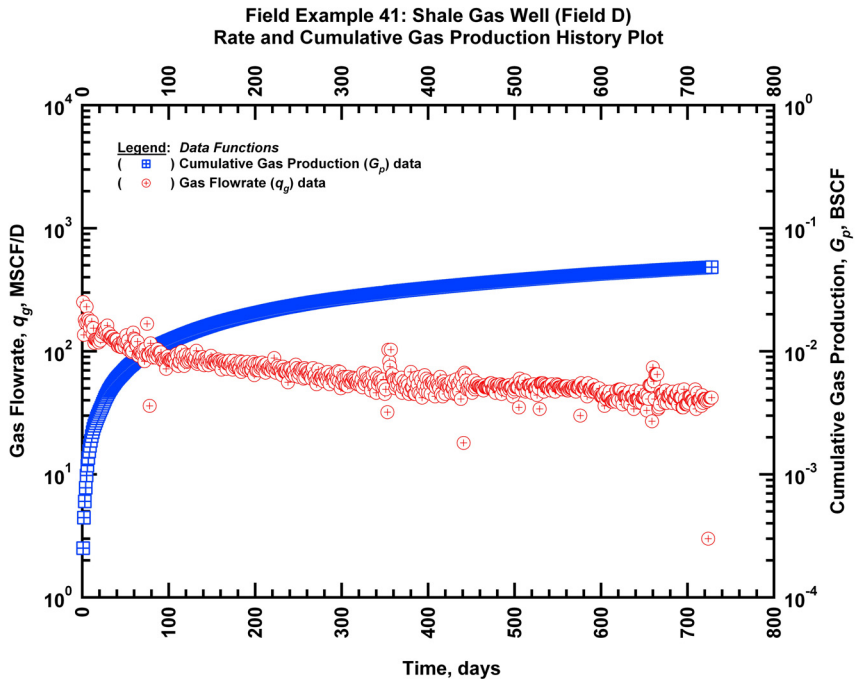

Figure G1 — (Semi-log Plot): Production history plot for field example 41 — flow rate (q_g) and cumulative production (G_p) versus production time.

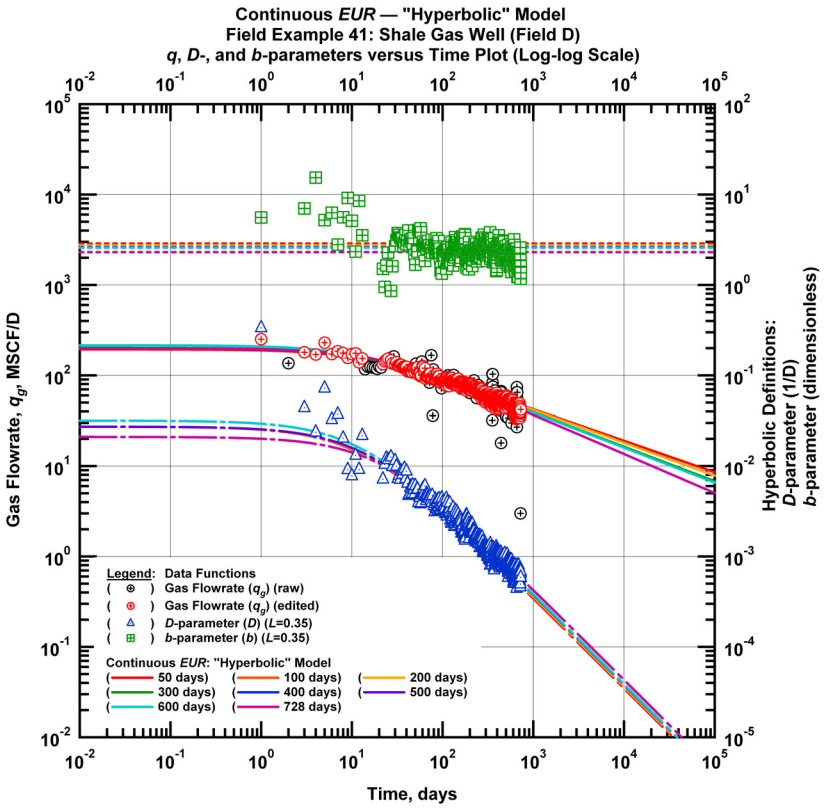

Figure G2 — (Log-log Plot): *qDb* plot — flow rate (q_g), *D*- and *b*-parameters versus production time and "hyperbolic" model matches for field example 41.

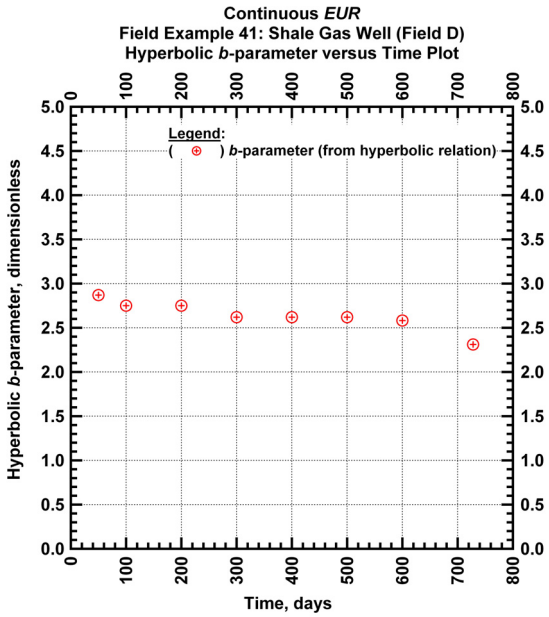

Figure G3 — (Cartesian Plot): Hyperbolic *b*-parameter values obtained from model matches with production data for field example 41.

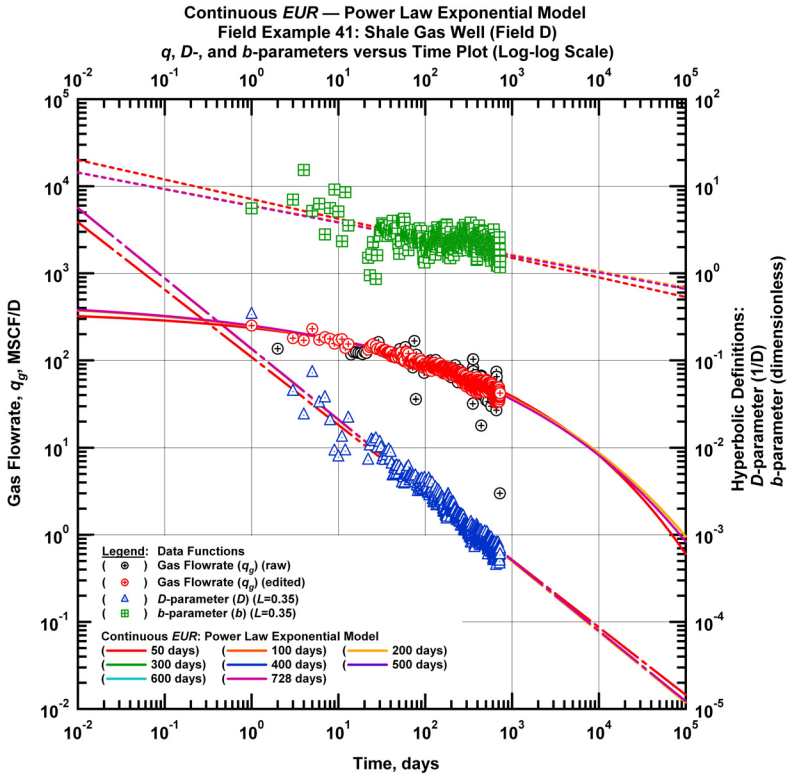

Figure G4 — (Log-log Plot): *qDb* plot — flow rate (q_g), *D*- and *b*-parameters versus production time and power law exponential model matches for field example 41.

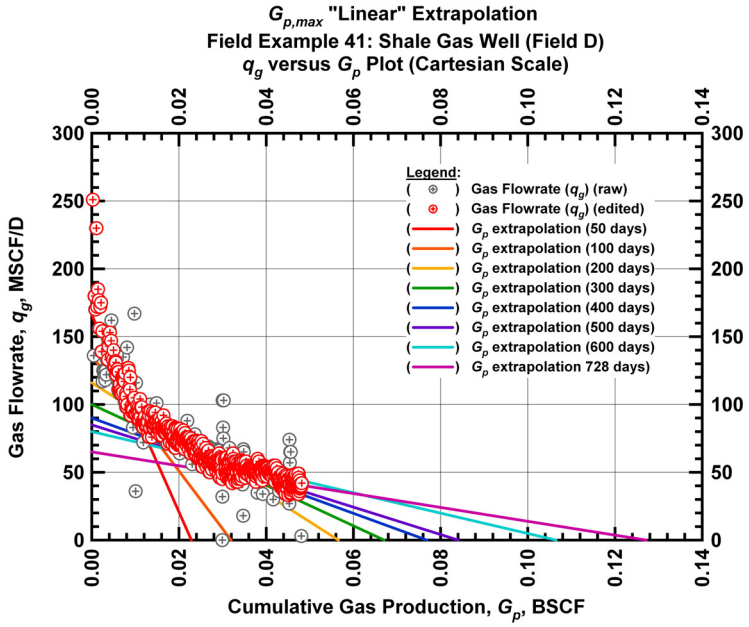

Figure G5 — (Cartesian Plot): Rate Cumulative Plot — flow rate (q_g) versus cumulative production (G_p) and the linear trends fit through the data for field example 41.

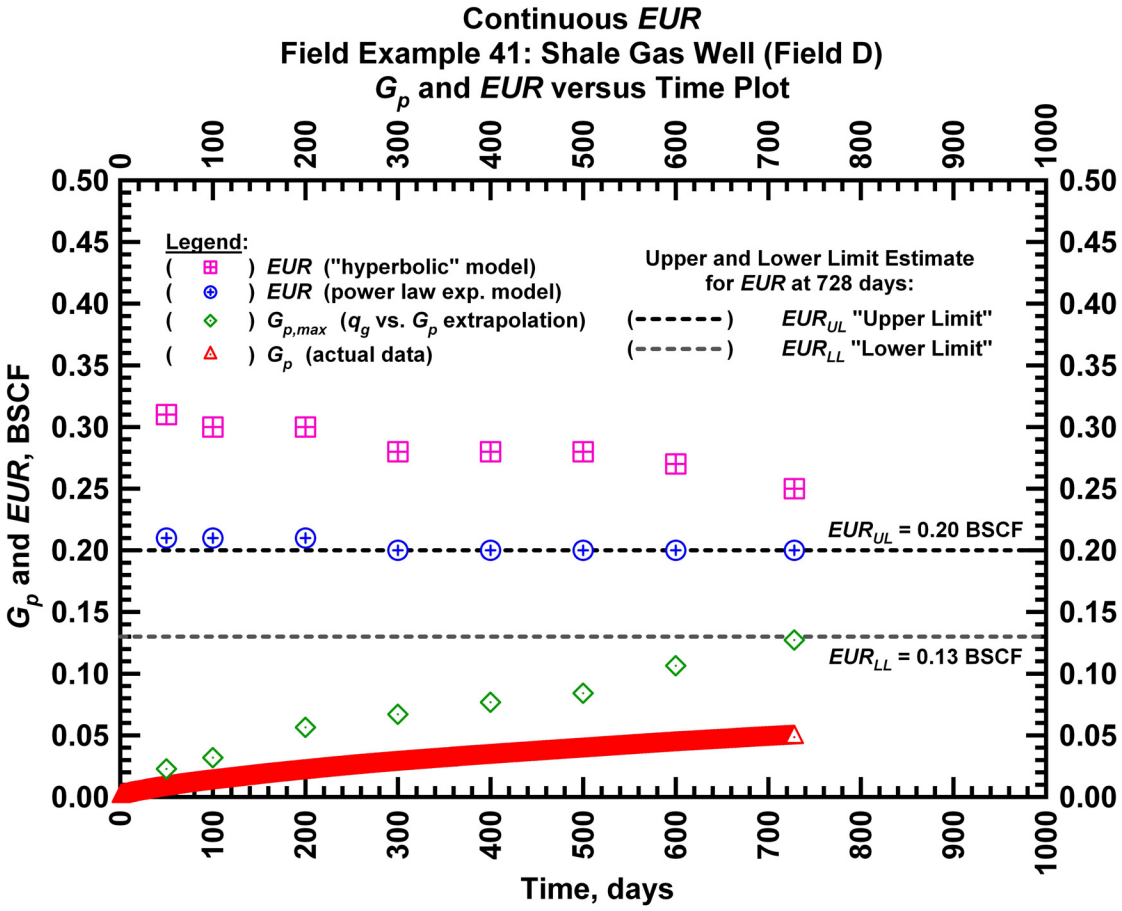

Figure G6 — (Cartesian Plot): *EUR* estimates from model matches and $G_{p,max}$ estimates from extrapolation technique for field example 41.

Table G1 — Analysis results for field example 41 — "hyperbolic" model parameters.

Time Interval, days	q_{gi} (MSCFD)	D_i (D^{-1})	b (dimensionless)	EUR_{hyp} (BSCF)
50	194	0.027254	2.87	0.31
100	201	0.027254	2.75	0.30
200	201	0.027254	2.75	0.30
300	201	0.027254	2.62	0.28
400	201	0.027254	2.62	0.28
500	201	0.027254	2.62	0.28
600	215	0.031791	2.58	0.27
728	198	0.021017	2.31	0.25

Table G2 — Analysis results for field example 41 — power law exponential model parameters.

Time Interval, days	$\hat{q}_{gi}$ (MSCFD)	$\hat{D}_i$ (D^{-1})	n (dimensionless)	D_∞ (D^{-1})	EUR_{PLE} (BSCF)
50	382	0.4840	0.225	0	0.21
100	504	0.7117	0.189	0	0.21
200	504	0.7117	0.189	0	0.21
300	511	0.7117	0.191	0	0.20
400	511	0.7117	0.191	0	0.20
500	511	0.7117	0.191	0	0.20
600	511	0.7117	0.191	0	0.20
728	511	0.7117	0.191	0	0.20

Table G3 — Analysis results for field example 41 — straight line extrapolation.

Time Interval, days	Slope, 10^{-6} D^{-1}	Intercept, MSCF/D	$G_{p,max}$ (BSCF)
50	7,267	166	0.02
100	4,257	136	0.03
200	2,051	116	0.06
300	1,491	100	0.07
400	1,171	90	0.08
500	1,011	85	0.08
600	751	80	0.11
728	511	65	0.13

Field Example 42

We present the flow rate data and the cumulative production data which spans almost 1 year for a horizontal well producing from a shale gas reservoir in **Fig. G7**. **Fig. G8** presents the "hyperbolic" model matches imposed on the flow rate data along with the *D*- and *b*-parameter trends. In **Fig. G9** we observe that the value of the *b*-parameter as a function of time. The *b*-parameter value decreases from 4.13 to 2.51 during the production history. Every interval is matched with a "hyperbolic" *b*-parameter greater than 1 indicating that boundary-dominated flow has not been established. **Fig. G10** shows the power law exponential model matches imposed on the flow rate data and *D*- and *b*-parameter trends. In **Fig. G11** we show the results of the straight line extrapolation technique, and in **Fig. G12** we present the calculated *EUR* values versus production time. All of the model parameters for this example are presented in **Tables G4, G5, and G6**. The *EUR* of this well should be in between 1.35 BSCF (the "lower" limit given by the straight line extrapolation technique at 331 days) and 2.86 BSCF (the "upper" limit given by the power law exponential estimate at 331 days).

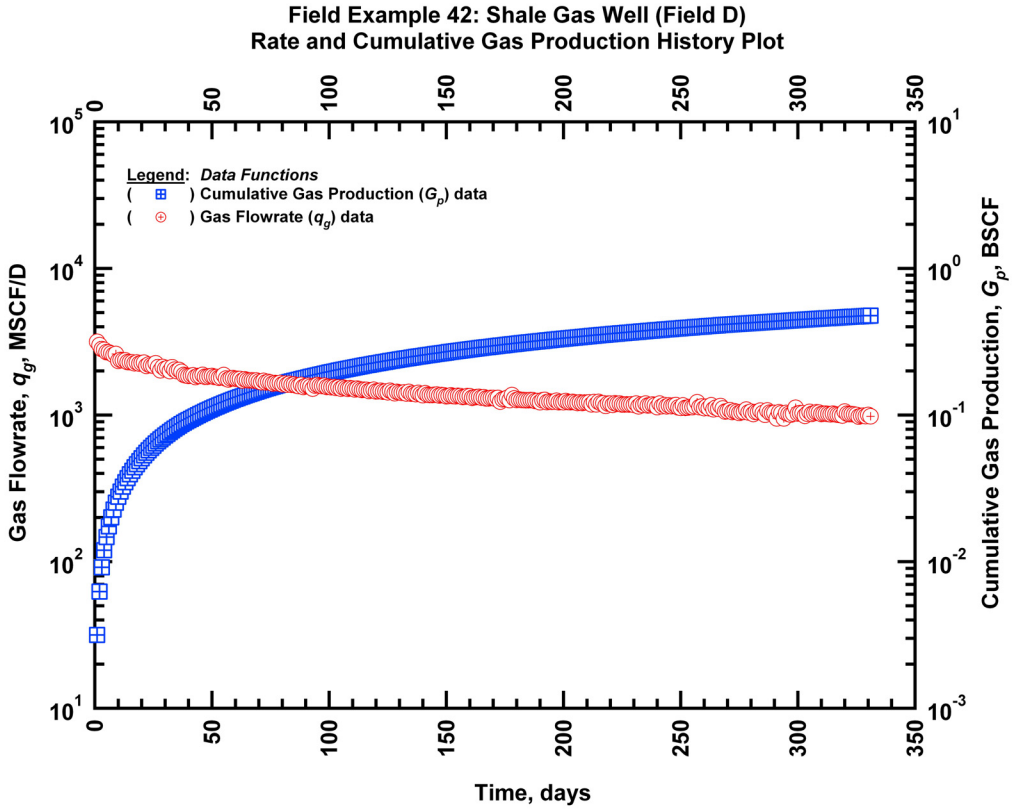

Figure G7 — (Semi-log Plot): Production history plot for field example 42 — flow rate (q_g) and cumulative production (G_p) versus production time.

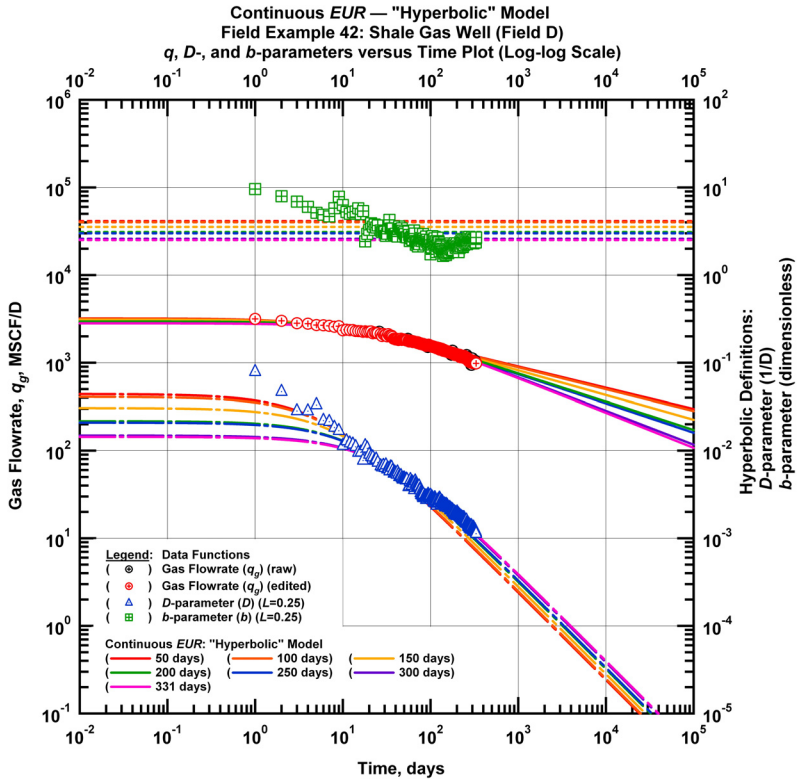

Figure G8 — (Log-log Plot): *qDb* plot — flow rate (q_g), *D*- and *b*-parameters versus production time and "hyperbolic" model matches for field example 42.

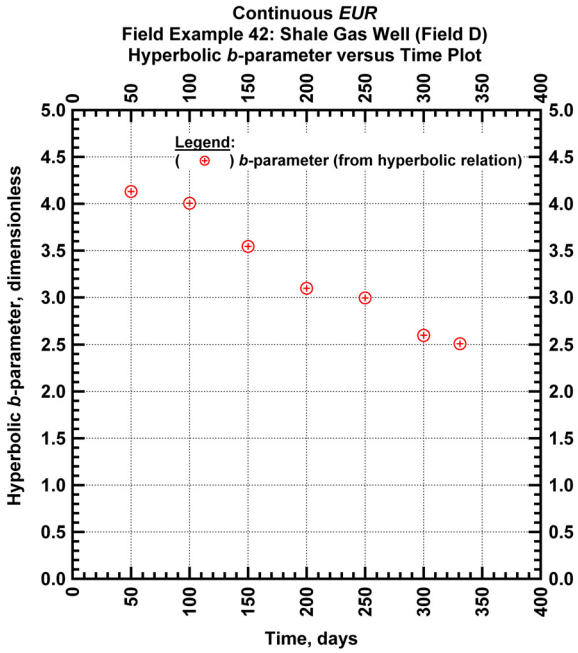

Figure G9 — (Cartesian Plot): Hyperbolic *b*-parameter values obtained from model matches with production data for field example 42.

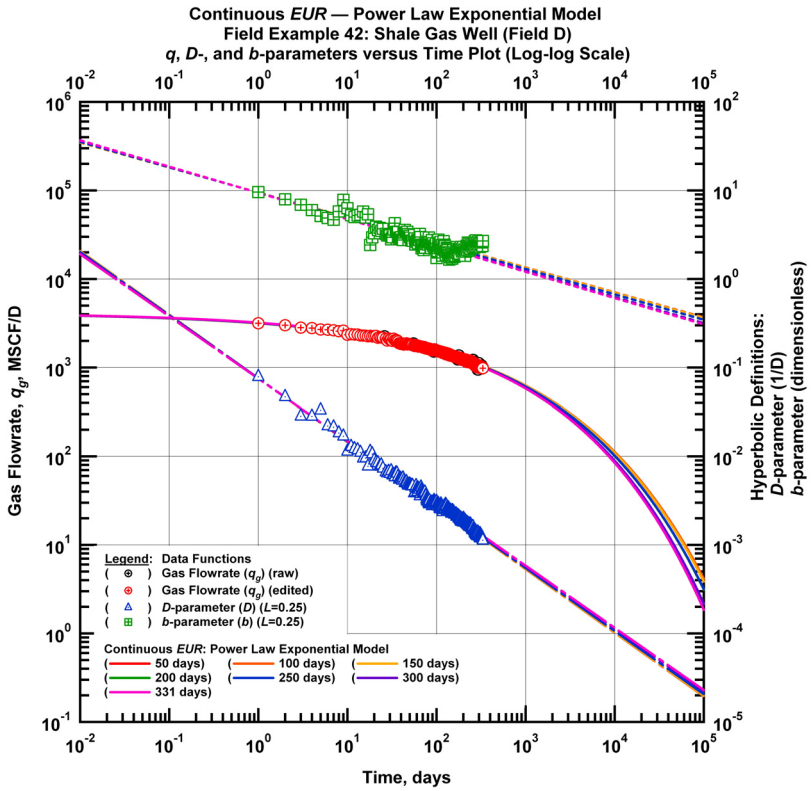

Figure G10 — (Log-log Plot): *qDb* plot — flow rate (q_g), *D*- and *b*-parameters versus production time and power law exponential model matches for field example 42.

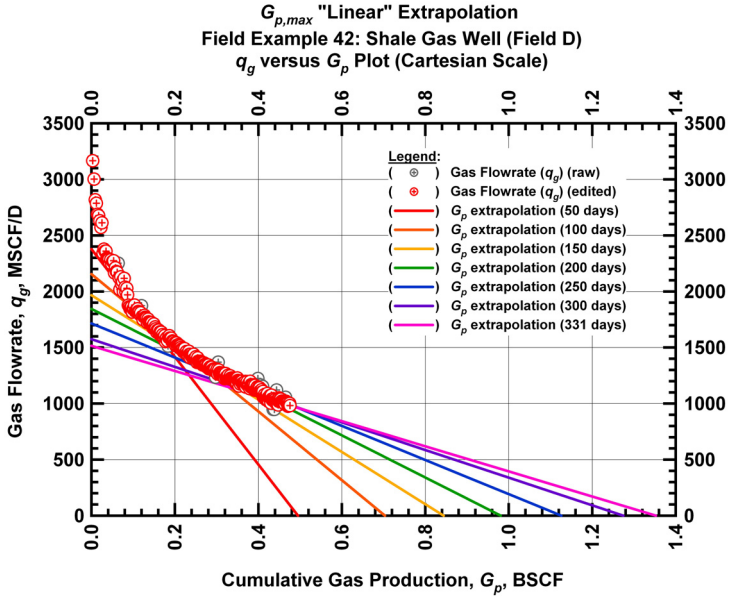

Figure G11 — (Cartesian Plot): Rate Cumulative Plot — flow rate (q_g) versus cumulative production (G_p) and the linear trends fit through the data for field example 42.

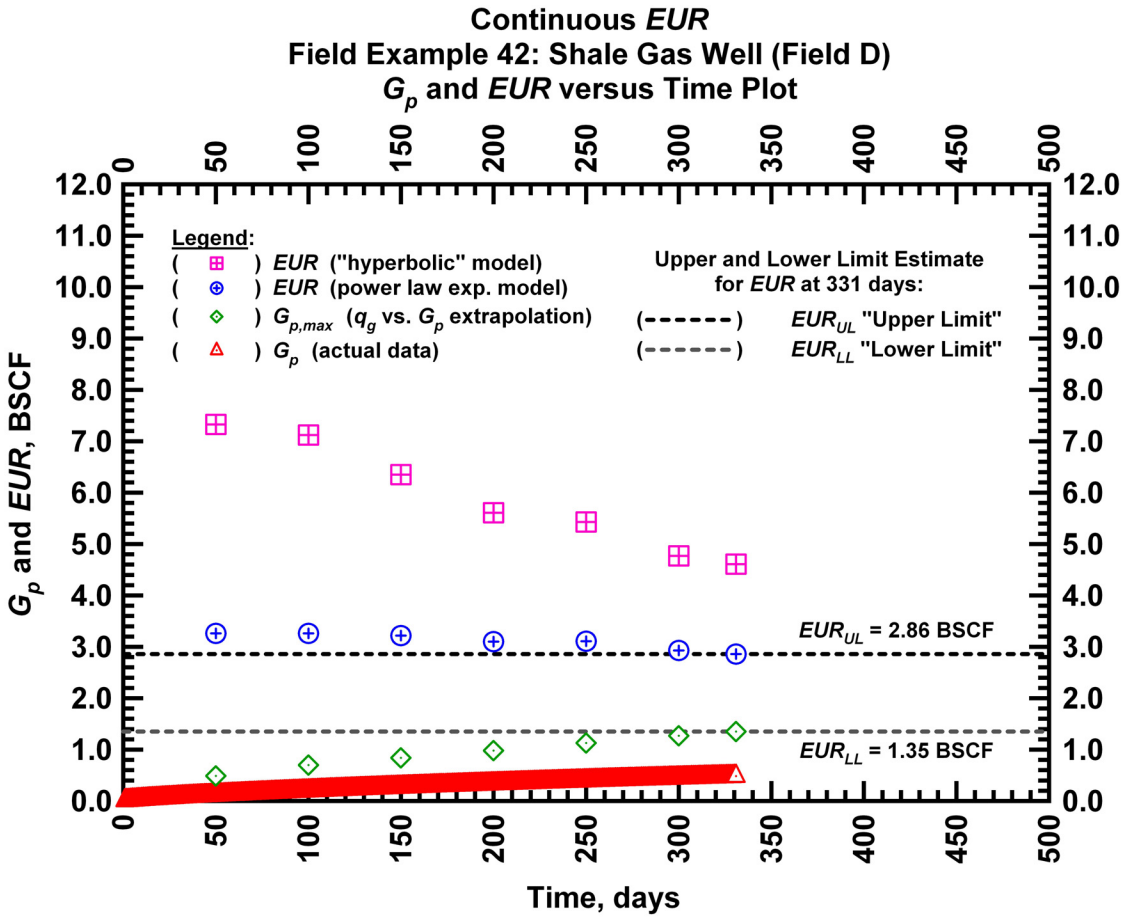

Figure G12 — (Cartesian Plot): *EUR* estimates from model matches and $G_{p,max}$ estimates from extrapolation technique for field example 42.

Table G4 — Analysis results for field example 42 — "hyperbolic" model parameters.

Time Interval, days	q_{gi} (MSCFD)	D_i (D^{-1})	b (dimensionless)	EUR_{hyp} (BSCF)
50	3,200	0.044021	4.1296	7.33
100	3,178	0.040960	4.0056	7.12
150	3,084	0.030510	3.5441	6.35
200	2,954	0.021652	3.0974	5.61
250	2,954	0.020845	2.9953	5.43
300	2,815	0.014874	2.5958	4.77
331	2,815	0.014356	2.5087	4.61

Table G5 — Analysis results for field example 42 — power law exponential model parameters.

Time Interval, days	$\hat{q}_{gi}$ (MSCFD)	$\hat{D}_i$ (D^{-1})	n (dimensionless)	D_∞ (D^{-1})	EUR_{PLE} (BSCF)
50	4,127	0.2686	0.2820	0	3.26
100	4,127	0.2686	0.2820	0	3.26
150	4,127	0.2671	0.2834	0	3.22
200	4,127	0.2631	0.2873	0	3.10
250	4,127	0.2634	0.2870	0	3.11
300	4,127	0.2551	0.2943	0	2.93
331	4,127	0.2519	0.2972	0	2.86

Table G6 — Analysis results for field example 42 — straight line extrapolation.

Time Interval, days	Slope, 10^{-6} D^{-1}	Intercept, MSCF/D	$G_{p,max}$ (BSCF)
50	4,805	2,378	0.49
100	3,062	2,154	0.70
150	2,329	1,966	0.84
200	1,881	1,845	0.98
250	1,523	1,715	1.13
300	1,235	1,574	1.27
331	1,120	1,515	1.35

APPENDIX H
EXAMPLE FROM FIELD E

Field Example 43

We present the flow rate data and the cumulative production data which spans almost 1 year for a vertical well producing from a shale gas reservoir in **Fig. H1**. **Fig. H2** presents the "hyperbolic" model matches imposed on the flow rate data along with the *D*- and *b*-parameter trends. In **Fig. H3** we observe that the value of the *b*-parameter as a function of time. The *b*-parameter value stabilizes around 2.8 after 350 days of production. Every interval is matched with a "hyperbolic" *b*-parameter greater than 1 indicating that boundary-dominated flow has not been established. **Fig. H4** shows the power law exponential model matches imposed on the flow rate data and *D*- and *b*-parameter trends. In **Fig. H5** we show the results of the straight line extrapolation technique, and in **Fig. H6** we present the calculated *EUR* values versus production time. All of the model parameters for this example are presented in **Tables H1, H2, and H3**. The *EUR* of this well should be in between 0.20 BSCF (the "lower" limit given by the straight line extrapolation technique at 350 days) and 0.49 BSCF (the "upper" limit given by the power law exponential estimate at 350 days).

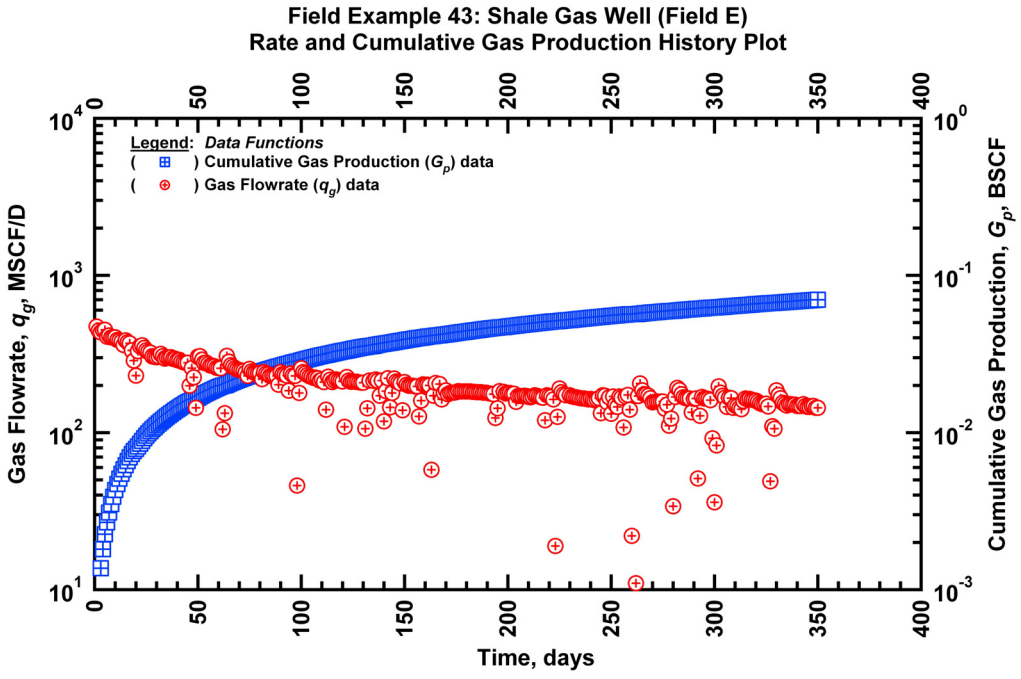

Figure H1 — (Semi-log Plot): Production history plot for field example 43 — flow rate (q_g) and cumulative production (G_p) versus production time.

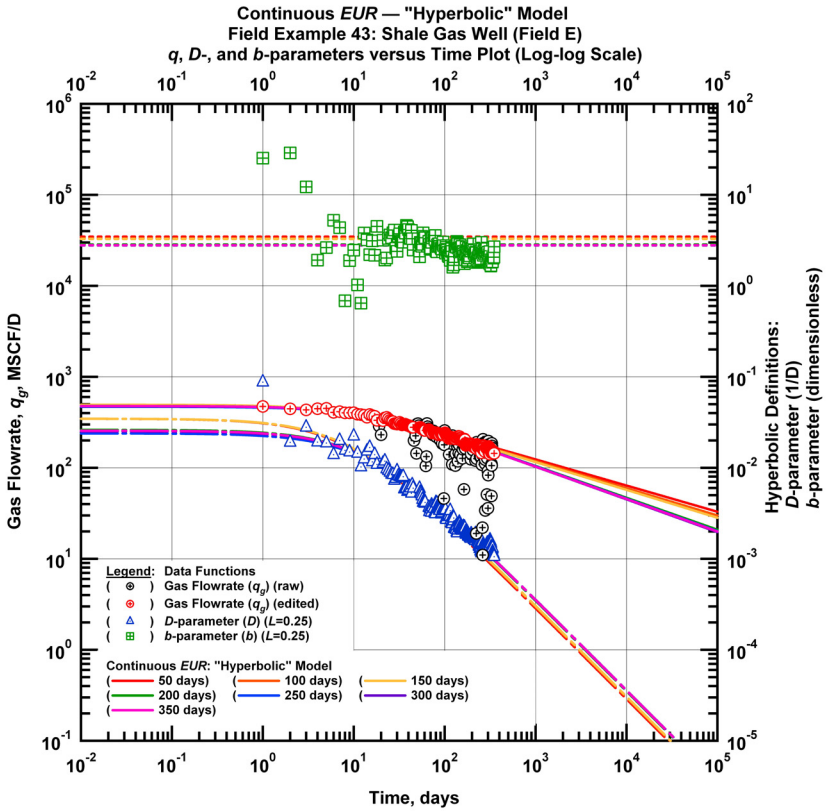

Figure H2 — (Log-log Plot): *qDb* plot — flow rate (q_g), *D*- and *b*-parameters versus production time and "hyperbolic" model matches for field example 43.

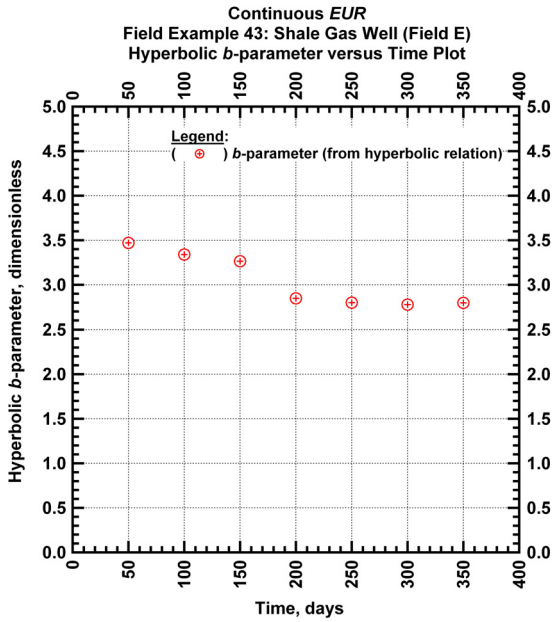

Figure H3 — (Cartesian Plot): Hyperbolic *b*-parameter values obtained from model matches with production data for field example 43.

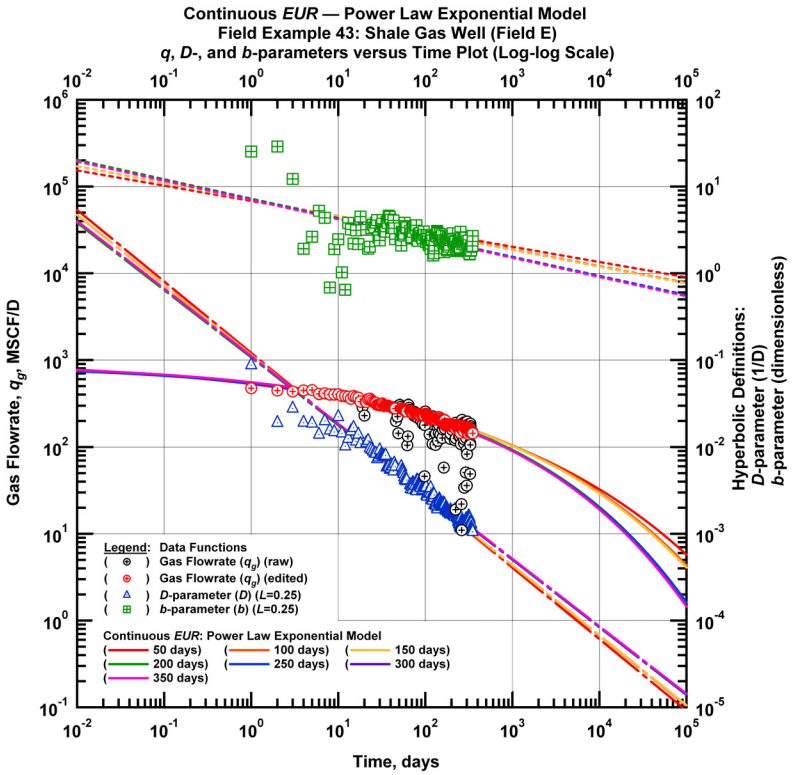

Figure H4 — (Log-log Plot): *qDb* plot — flow rate (q_g), *D*- and *b*-parameters versus production time and power law exponential model matches for field example 43.

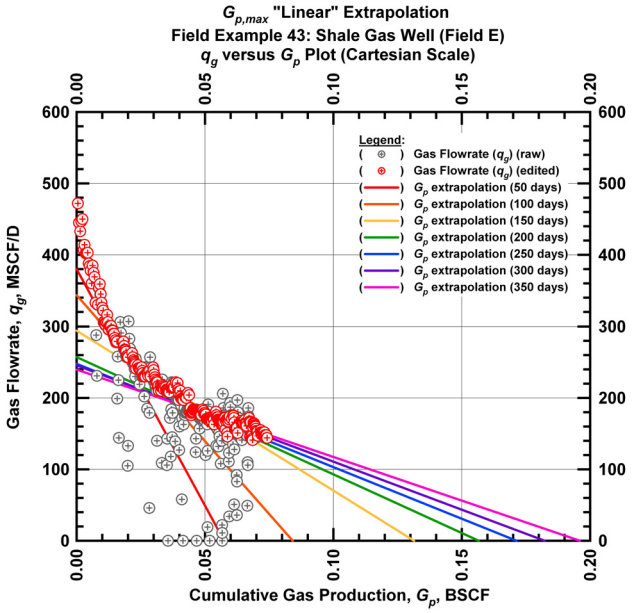

Figure H5 — (Cartesian Plot): Rate Cumulative Plot — flow rate (q_g) versus cumulative production (G_p) and the linear trends fit through the data for field example 43.

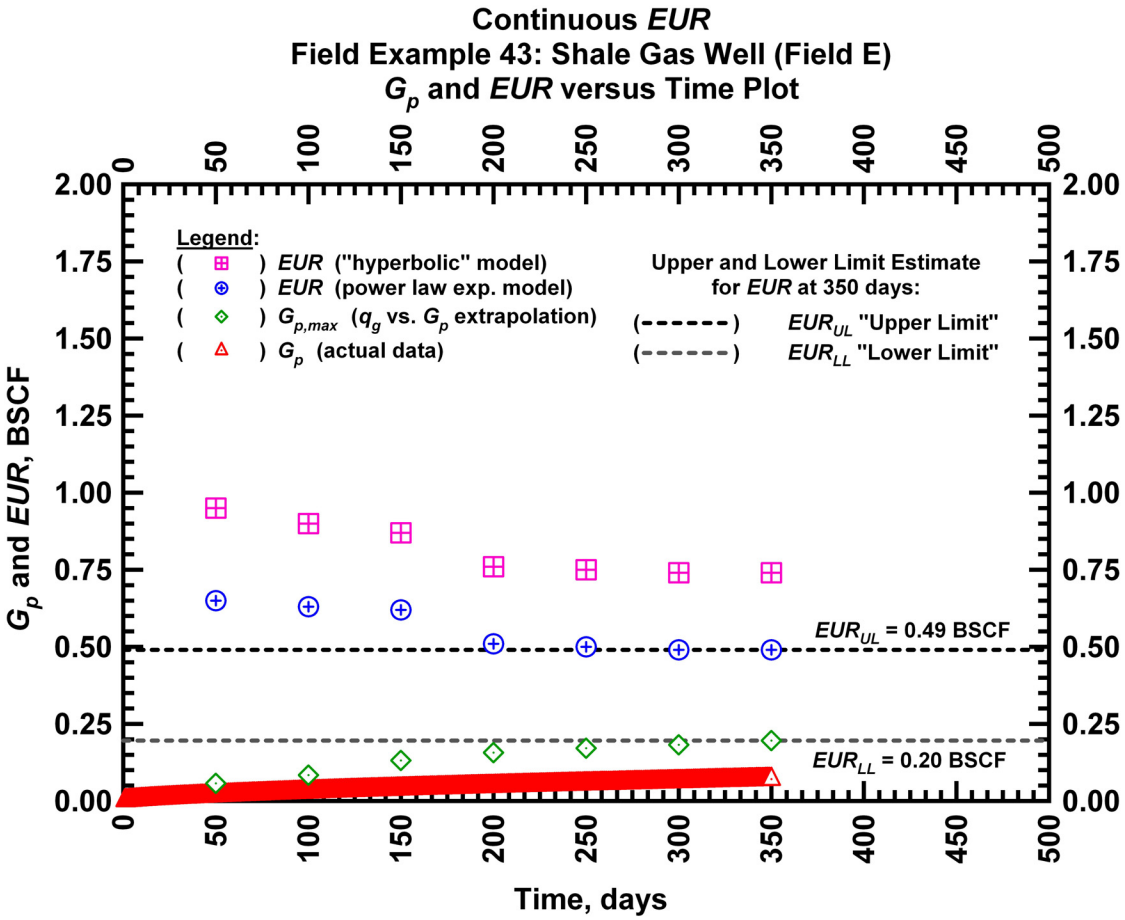

Figure H6 — (Cartesian Plot): *EUR* estimates from model matches and $G_{p,max}$ estimates from extrapolation technique for field example 43.

Table H1 — Analysis results for field example 43 — "hyperbolic" model parameters.

Time Interval, days	q_{gi} (MSCFD)	D_i (D^{-1})	b (dimensionless)	EUR_{hyp} (BSCF)
50	493	0.034625	3.470	0.95
100	493	0.034625	3.340	0.90
150	493	0.034625	3.264	0.87
200	478	0.026118	2.848	0.76
250	469	0.023899	2.800	0.75
300	476	0.025158	2.777	0.74
350	477	0.025589	2.797	0.74

Table H2 — Analysis results for field example 43 — power law exponential model parameters.

Time Interval, days	$\hat{q}_{gi}$ (MSCFD)	$\hat{D}_i$ (D^{-1})	n (dimensionless)	D_∞ (D^{-1})	EUR_{PLE} (BSCF)
50	1,050	0.686	0.176	0	0.65
100	979	0.594	0.192	0	0.63
150	979	0.594	0.193	0	0.62
200	877	0.478	0.224	0	0.51
250	889	0.501	0.220	0	0.50
300	914	0.501	0.222	0	0.49
350	914	0.501	0.222	0	0.49

Table H3 — Analysis results for field example 43 — straight line extrapolation.

Time Interval, days	Slope, 10^{-6} D^{-1}	Intercept, MSCF/D	$G_{p,max}$ (BSCF)
50	6,618	380	0.06
100	4,080	343	0.08
150	2,239	294	0.13
200	1,643	257	0.16
250	1,447	248	0.17
300	1,347	246	0.18
350	1,223	240	0.20

VITA

Name:	Stephanie Marie Currie
Mailing Address:	3116 TAMU — 507 Richardson Building College Station, TX 77843
E-mail Address:	stephaniemariecurrie@gmail.com
Education:	Texas A&M University, College Station, Texas, USA M.S., Petroleum Engineering August 2010
	Texas A&M University, College Station, Texas, USA B.S., Petroleum Engineering May 2008
Affiliations:	Society of Petroleum Engineers